Title
Synthesis of Coralloidolide B, Coralloidolide C, a Photochemical Synthesis of Intricarene, and Progress Towards the Synthesis of Bielschowskysin

Author
Kimbrough, Thomas James

Publication Date
2011

Peer reviewed|Thesis/dissertation

Synthesis of Coralloidolide B, Coralloidolide C, a Photochemical Synthesis of Intricarene, and Progress Towards the Synthesis of Bielschowskysin

by

Thomas James Kimbrough

A dissertation submitted in partial satisfaction of the

requirements for the degree of

Doctor of Philosophy

in

Chemistry

in the

Graduate Division

of the

University of California, Berkeley

Committee in charge:

Professor Dirk Trauner, Co-Chair
Professor Richmond Sarpong, Co-Chair
Professor Dean Toste
Professor David Presti

Fall 2011

Abstract

Synthesis of Coralloidolide B, Coralloidolide C,
a Photochemical Synthesis of Intricarene,
and Progress Towards the Synthesis of
Bielschowskysin

by
Thomas James Kimbrough
Doctor of Philosophy in Chemistry
University of California, Berkeley
Professor Dirk Trauner, Co-Chair
Professor Richmond Sarpong, Co-Chair

The total synthesis and synthetic efforts towards several diterpene natural products are described. The syntheses of the furanocembranoids coralloidolide B and coralloidolide C were both achieved in a single step from coralloidolide E. The furanocembranoid bipinnatin J was used in a model system to explore the conditions necessary to effect a transannular [2+2] cycloaddition in assembling the pentacyclic core of bielschowskysin. Two distinct strategies were evaluated as part of this model system for their effectiveness in synthesizing the cyclobutane ring of bielschowskysin. Progress was also made towards synthesizing a macrocyclic precursor of bielschowskysin. Numerous selective oxidations of the furanocembranoid carbon framework were discovered which should find utility in the synthesis of other members of this family of diterpenes. Several novel transformations of furanocembranoid derivatives are described, along with a synthesis of the furanocembranoid intricarene through photochemical means.

To my parents, for their endless love and support,

without which none of this would be possible.

Table of Contents

Chapter 1

Furanocembranoids – Background

1.1 Introduction

The oceans contain a rich diversity of natural products that possess a remarkable multitude of structures and bioactivities. One of the veins that has been mined by natural product chemists is the Anthozoa class of animals which includes sea corals and anemones. As animals, these organisms metabolize sugars and oxygen to obtain energy, releasing water and carbon dioxide as by-products. They are also known to produce a variety of secondary metabolites. Many species within the subclass Octocorallia have proven to be ample sources for a family of macrocyclic diterpenoids known as the furanocembranoids.[1] The furanocembranoids have drawn attention from both synthetic and natural product chemists due to their attractive molecular architectures and interesting biological activities. Given the scarce quantities of material available to scientists from these animals and the increasing ecological threat posed by rising ocean acidity, there exists a strong motivation to design synthetic routes to these intriguing molecular targets.

1.2 Structural Classification, Isolation and Biological Activity

The furanocembranoid family is comprised of a diverse array of carbon frameworks featuring varying degrees of oxygenation. The most common members of the family – the furanocembranoids proper – feature a 14-membered macrocyclic ring that often incorporates a furan, a butenolide, and an isopropylidene moiety, exemplified by rubifolide (**1.1**) in Figure 1.1.

Figure 1.1 Rubifolide.

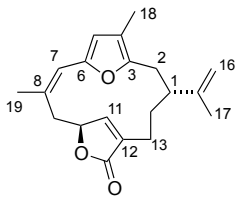

rubifolide (**1.1**)

In terms of oxidation patterns, the $\Delta^{7,8}$, $\Delta^{11,12}$ and $\Delta^{15,16}$ alkenes are known to frequently undergo oxidation to the epoxide (and subsequent reactions). Carbons C2 and C13 can be hydroxylated and are often fitted with acetoxy groups. The methyl groups at C17 and C18 can attain all possible oxidation states, but the C19 methyl has never been found oxidized in nature. Interestingly, when the C18 methyl is oxidized to any extent, the macrocycle is never oxidized at C2. The furan often displays a rich oxidation chemistry as well, e.g. oxidation to the enedione, the dihydroxyfuran, or the bis-epoxide.

In terms of established configurations, the $\Delta^{7,8}$ double bond is known to be either (*E*) or (*Z*). However epoxidation seems to occur almost exclusively with (*E*)-configured alkenes. The isopropylidene moiety is typically (*R*)-configured at C1, but there is a small number of furanocembranoids known with the opposite configuration.

The structures of bipinnatins A-Q highlight the variety of oxidation states that members of this family can attain (Figure 1.2). Bipinnatins A-J were isolated from *Pseudopterogorgia bipinnata*[2], while bipinnatins K-Q were derived from *Pseudopterogorgia kallos.*[3] Amongst these, bipinnatin J (**1.11**) possesses the simplest oxidation pattern, bearing only a hydroxy at C2 in addition to the typical furan and butenolide. Rubifolide (**1.1**) differs from bipinnatin J (**1.11**) only by the lack of oxidation at C2. Interestingly, rubifolide has never been isolated from any *Pseudopterogorgia* species. This natural product was isolated from the coral *Gersemia rubiformis* and from the skin extracts of the dendronotid nudibranch *Tochuina tetraquetra*, along with pukalide (**1.20**).[4] It may be, however, that rubifolide exists transiently in *Pseudopterogorgia sp.* but is quickly shuttled into the various oxidative manifolds. Bipinnatin K displays an unusual methoxy group at C7, and it was suggested by the isolationists that this could be an artifact from methanolysis of a highly reactive furanyl epoxide moiety. Bipinnatin P (**1.17**) bears an atypical (*Z*)-configured epoxide – the only natural example discovered to date.

Figure 1.2 Selection of regular and oxidized furanocembranoids.

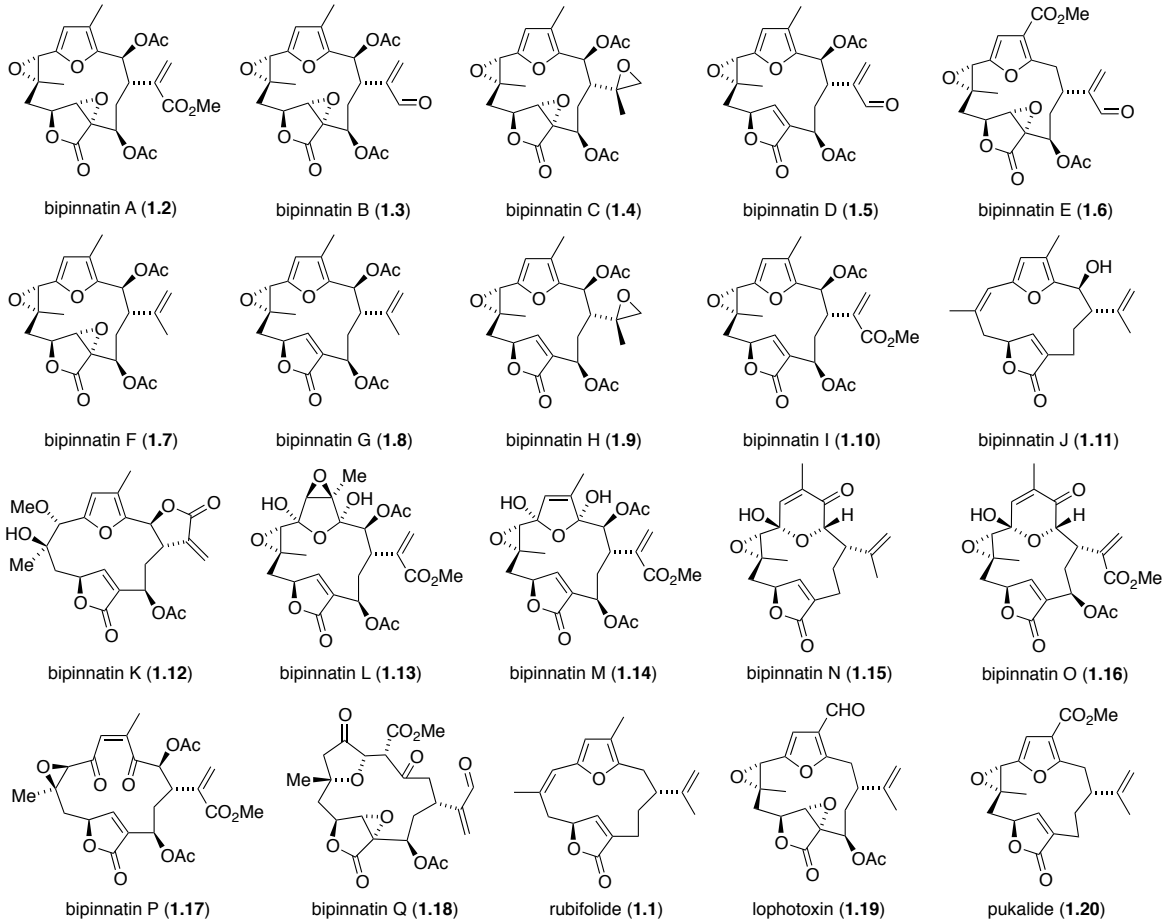

In addition to their diverse and complex structures, many of the furanocembranoids have been demonstrated to possess remarkable biological activities. Lophotoxin (**1.19**), for example, is the oldest known and most intensely studied of the group. This natural product was initially isolated by Fenical *et al.* in 1981[5] from several pacific gorgonians of the genus Lophogorgia. Lophotoxin acts an irreversible inhibitor of the nicotinic acetylcholine receptor, functioning as a

neuromuscular toxin.[6] Abramson and co-workers have reported detailed studies on lophotoxin (**1.19**) and related natural products in their interactions with the nicotinic acetylcholine receptor.[7] Amongst the bipinnatins, members A, B, D, H and I all showed strong cytotoxic action against tumor and cancer cell lines.[2,7b]

Besides the canonical 14-membered macrocyclic furanocembranoids, there exist two other major classes of compounds with rearranged skeletons that can be said to belong to the larger family of natural products. The pseudopteranes possess a rearranged 12-membered ring that features an additional isopropylidene substituent in addition to the usual furan and butenolide moieties, epitomized by kallolide A (Figure 1.3). The gersolanes by contrast feature an isomeric skeleton with a characteristic bicyclo[11.1.0]tetradecane ring system, epitomized by pinnatin A. While the selection presented in Figure 1.3 is not comprehensive, the variety of oxidation states that these compounds can achieve is evident. Amongst the pseudopteranes, kallolide A (**1.21**) – isolated from *Pseudopterogorgia bipinnata* and *P. kallos* - has shown potent anti-inflammatory activity.[8] Pseudopterolide (**1.25**), isolated from *Pseudopterogorgia acerosa,* has shown interesting cytotoxic activity by inhibiting overall cell division in fertilized urchin eggs without interfering in nuclear division, thus bearing similarity to cytochalasin D.[9] Pinnatins A-E and gersolide from the gersolane class were isolated from the corals *Pseudopterogorgia bipinnata* and *P. kallos* (Figure 1.4).[10] Pinnatins A (**1.26**) and B (**1.27**) have showed potent biological activity against several cancer cells, including renal, ovarian and breast.[10b]

Figure 1.3 Selection of pseudopteranes and gersolanes.

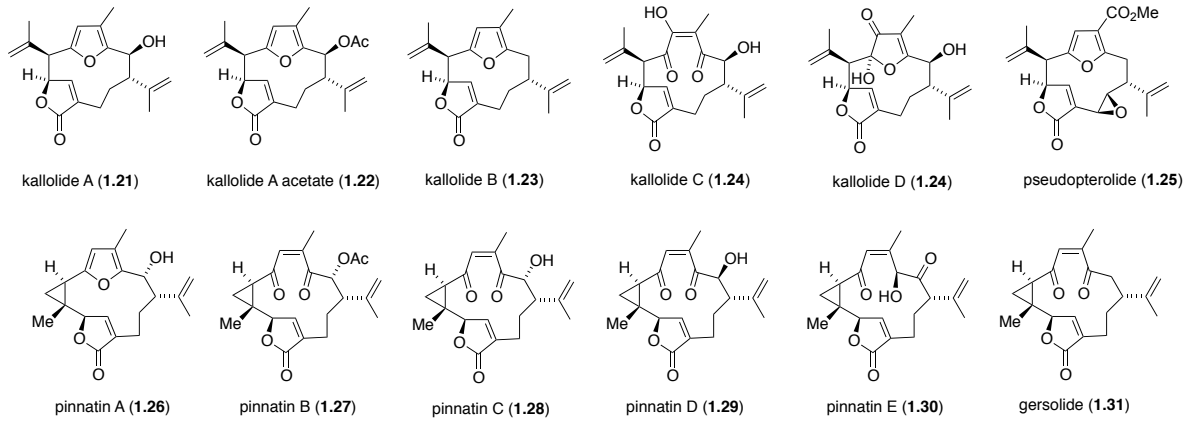

The six members of the coralloidolide subclass emerged from a harvest of the coral *Alcyonium coralloides.*[11] (Figure 1.4) From a structural standpoint, coralloidolides A (**1.32**) and E (**1.36**) can be viewed as typical furanocembranoids, featuring an epoxidized butenolide moiety in both compounds and a furan oxidized to the enedione in coralloidolide E. Coralloidolides B (**1.33**) and D (**1.35**) retain the overall oxidation state of coralloidolide E (**1.36**) but both incorporate a water molecule into their respective structures. Coralloidolides C (**1.34**) and F (**1.37**) each feature a rearranged skeleton with an additional carbon-carbon bond. To date the coralloidolides have not been screened for biological activity.

Figure 1.4 Coralloidolides A-F.

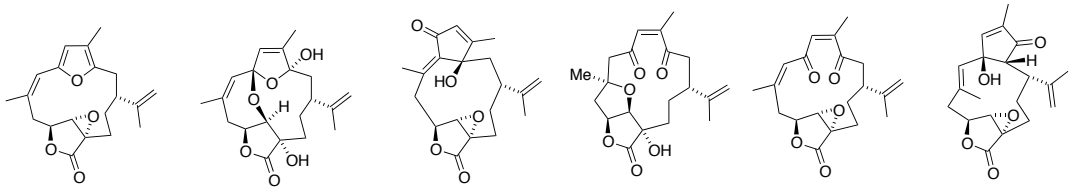

coralloidolide A (**1.32**) coralloidolide B (**1.33**) coralloidolide C (**1.34**) coralloidolide D (**1.35**) coralloidolide E (**1.36**) coralloidolide F (**1.37**)

The subgroup of furanocembranoids that includes members with rearranged polycyclic skeletons comprises a diverse array of structures that in some cases bear little resemblance to the parent compounds in the family. Coralloidolides C (**1.34**) and F (**1.37**) belong to this class. Also amongst this group, bielschowskysin (**1.38**) was first isolated from *Pseudopterogorgia kallos* in 2004 by Rodriguez, *et al.*[12] (Figure 1.5). The molecule features an unprecedented tricyclo[9.3.0.$0^{2,10}$]tetradecane ring system containing a cyclobutane ring and eleven stereocenters, seven of which are contiguous. It exhibits both antimalarial activity and potent anticancer activity. The cyclobutanol providencin (**1.39**) and the pentacyclic natural product intricarene (**1.40**) were also isolated from *P. kallos*.[13] Both compounds displayed mild cytotoxic activity. Verrillin (**1.41**), yet to be tested for activity, was isolated from *Pseudopterogorgia bipinnata.*[14] The tetracyclic diterpene mandapamate (**1.42**) was isolated from the coral *Sinularia dissecta*[15], while the related diastereomeric natural products isomandapamate (**1.43**) and bishomoisomandapamate (**1.44**) were found in *Sinularia maxima.*[16] A gorgonian coral of the genus *Plumarella* yielded the structurally similar tetra- and pentacyclic compounds plumarellic acid ethyl ester (**1.45**) and plumarellide (**1.46**)[17]. From this related group, only plumarellide (**1.46**) and plumarellic acid ethyl ester (**1.45**) have been examined for biological activity, with both compounds showing moderate hemolytic activity.

Figure 1.5 Selection of furanocembranoids with complex polycyclic carbon skeletons.

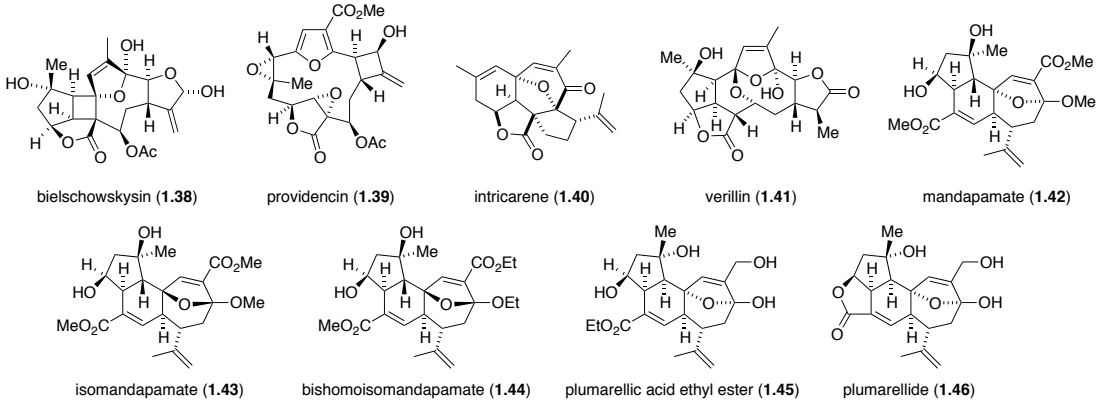

bielschowskysin (**1.38**) providencin (**1.39**) intricarene (**1.40**) verillin (**1.41**) mandapamate (**1.42**)

isomandapamate (**1.43**) bishomoisomandapamate (**1.44**) plumarellic acid ethyl ester (**1.45**) plumarellide (**1.46**)

1.3 Biosynthesis and Biosynthetic Speculations

The furanocembranoids, pseudopteranes, gersolanes and their derivatives display a wide variety of oxidation patterns and carbon skeletons, and between these natural products there are intimate biosynthetic connections that have been proposed and often substantiated through biomimetic total synthesis. These hypothetical connections also derive some credibility from the

fact that these compounds are usually isolated from the same or closely related biological sources.

The furanocembranoids can in principle be derived biosynthetically from the known natural product *neo*-cembrene (**1.49**) (Scheme 1.1). While *neo*-cembrene has not been identified in any extracts of gorgonian corals, it could be easily transformed through a series of chemo- and diastereoselective oxidations, as well as a $\Delta^{7,8}$ double bond isomerization, into rubifolide (**1.1**). Subsequent hydroxylation at C2 would give bipinnatin J (**1.11**). Not much is known about the enzymes involved in these oxidative transformations, but they are presumably cytochrome P450 monooxygenases. The biosynthesis of the natural product *neo*-cembrene (**1.49**) is well-established[19], commencing with a type A cyclization of geranylgeranyl diphosphate (**1.47**) to furnish the fourteen-member macrocycle and yield carbocation **1.48**. Loss of a proton from the isopropyl side chain affords *neo*-cembrene (**1.49**).

Scheme 1.1 Biosynthesis of furanocembranoids from *neo*-cembrene.

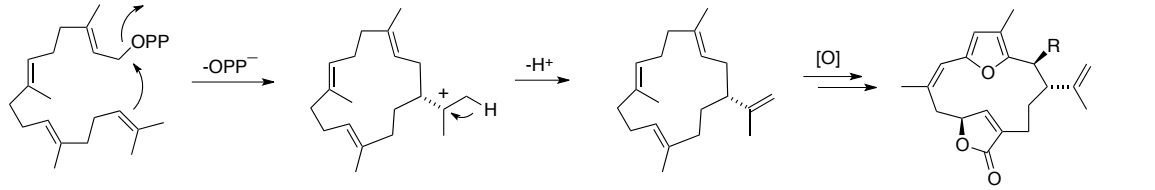

It has been demonstrated by Rodriguez that the pseudopteranes and gersolanes can be formed photochemically from the furanocembranoids. Thus, irradiation of bipinnatin J (**1.11**) in acetonitrile afforded kallolide A (**1.21**), pinnatin A (**1.26**) and pinnatin C (**1.28**) in a 120:1:6 ratio.[20] (Scheme 1.2) The biogenesis of kallolide A appears to involve a photochemically allowed $[_{\sigma}2_s + _{\pi}2_s]$ cycloaddition, whereas pinnatin A could be formed through a $[_{\sigma}2_a + _{\pi}2_a]$ cycloaddition. Note that in this reaction the stereochemistry of the C2-hydroxy group in pinnatin A has been inverted, which reflects the ease with which a carbocation can be formed in this pseudo-benzylic position. Pinnatin C (**1.28**) was presumably formed due to the trace amounts of singlet oxygen formed under these photochemical conditions (see below).

Scheme 1.2 Photochemical formation of pseudopteranes and gersolanes.

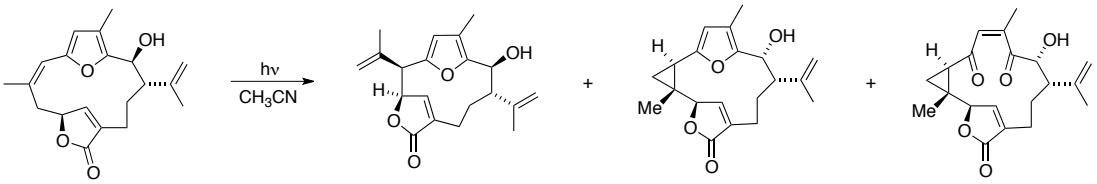

There remains the possibility that these results represent a special case and do not reflect the actual biosynthesis of the pseudopteranes and gersolanes. It is feasible that these rearrangements are, at least in some cases, enzyme-mediated or occur in the presence of a binding-protein.

The furan ring is frequently seen to be oxidatively cleaved in a host of furanocembranoids and their congeners. This transformation could potentially occur either via an enzyme-mediated route or in a photochemical fashion, as exemplified with the simple furanocembranoid rubifolide (**1.1**). In the former case, enzyme-mediated epoxidation of the furan ring could lead to spiroepoxide **1.50**, which would rearrange via **1.51** to afford dienedione **1.52**, a natural product known as isoepilophodione B (**1.52**) (Scheme 1.3). In the latter case, Diels-Alder addition of photochemically generated singlet oxygen could afford *endo*-peroxide **1.53**, whose reduction and/or hydrolysis would also deliver **1.52**.

Scheme 1.3 Oxidative cleavage of the furan moiety.

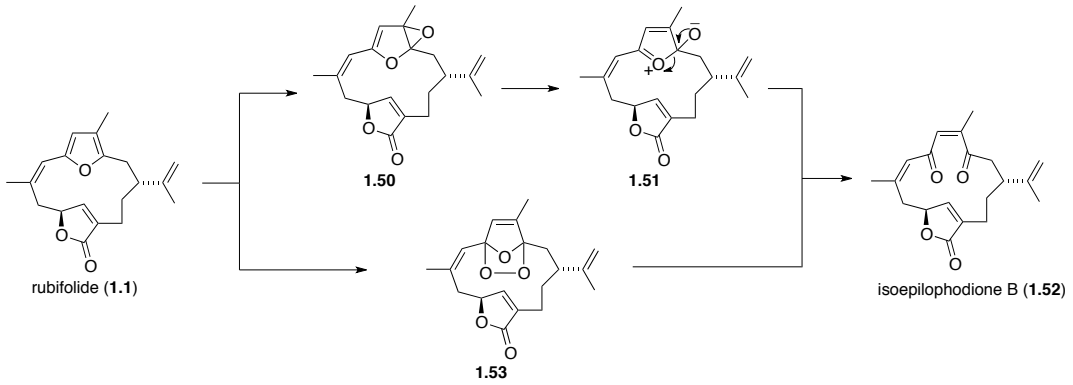

It is intriguing to speculate that the coralloidolide family of natural products (coralloidolides A-F) could be derived naturally from rubifolide (**1.1**). Rubifolide (**1.1**) has been found in other tropical corals, such as *Gersemia rubiformis*, but it was not found in *A. coralloides*. In the biosynthesis, presumably epoxidation of the electrophilic $\Delta^{11,12}$ double bond of rubifolide yields coralloidolide A (**1.32**). Oxidative cleavage of the furan ring of **1.32** then affords coralloidolide E (**1.36**), which features a prominent 2,5-diene-1,4-dione moiety (Scheme 1.4). This functional group lends itself to several alternative reaction pathways resulting in the formation of the other members of the coralloidolide family. In the first of these, hydration of the dienedione functionality and transannular opening of the epoxide in **1.36** would give the tetracyclic coralloidolide B (**1.33**). It is conceivable that this intricate bis-acetal could rearrange to yield coralloidolide D (**1.35**). Alternatively, coralloidolide D could form via hydration and epoxide opening directly from coralloidolide E (**1.36**).

Scheme 1.4 Proposed biosynthetic relations of rubifolide with coralloidolides A, B, D and E.

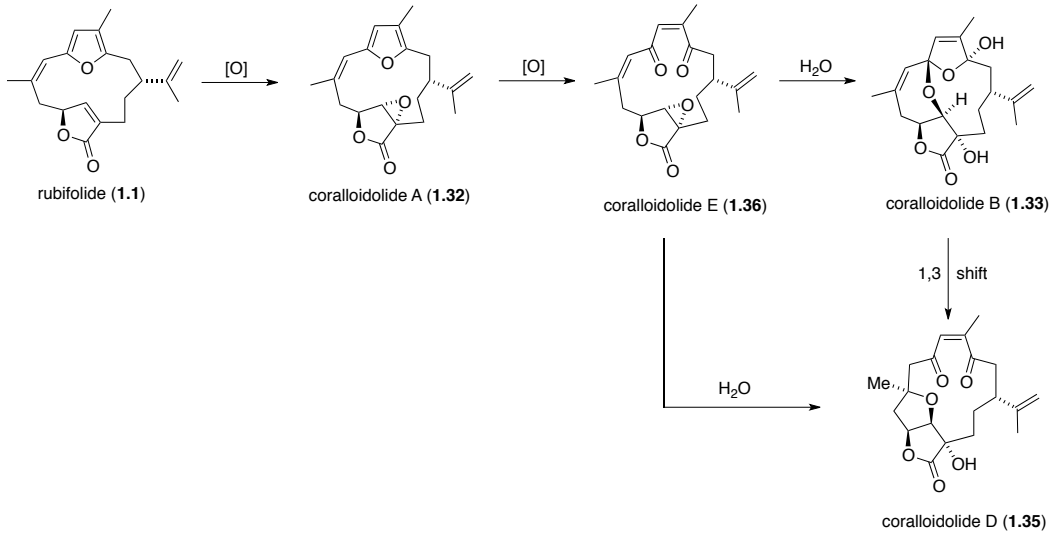

In the second pathway, selective tautomerization of coralloidolide E (**1.36)** and double-bond isomerization could afford dienone enol **1.54**, which could undergo transannular aldol addition to the C6 carbonyl to afford coralloidolide F (**1.37**). Finally, an alternate mode of tautomerization and aldol addition (via **1.55**), followed by shifting of the double bond to the thermodynamically more stable position, would afford coralloidolide C (**1.34**) (Scheme 1.5).[11b,11c]

Scheme 1.5 Proposed biosynthetic relations of coralloidolide E with coralloidolides C and F.

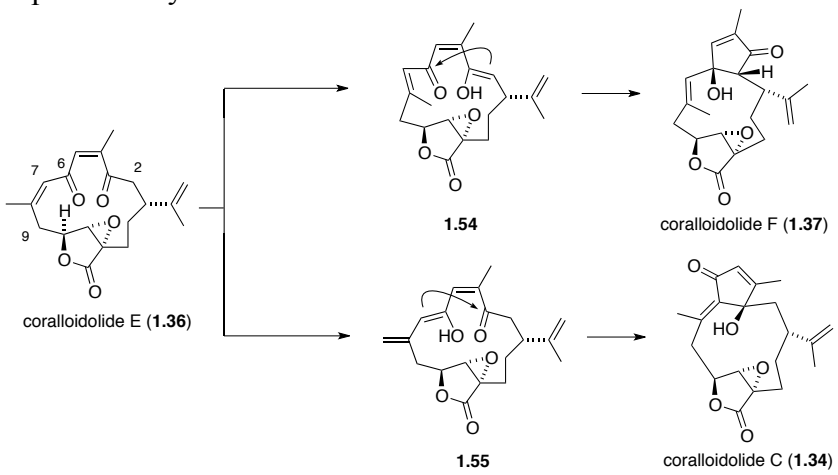

In contrast with coralloidolides C (**1.34**) and F (**1.37**), the extra C-C bond in the four-membered ring of providencin (**1.39**) appears to arise from a photochemical Norrish type II rearrangement of bipinnatin E (**1.6**) (Scheme 1.6). This hypothesis has been bolstered recently by a biogenetically patterned synthetic study.[21]

-

Scheme 1.6 Photochemical formation of providencin from bipinnatin E.

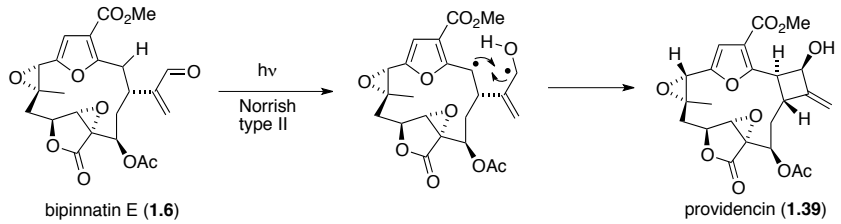

bipinnatin E (**1.6**)

A proposed biosynthesis of intricarene (**1.40**) is illustrated in Scheme 1.7. An Achmatowicz-type oxidation of the furan of bipinnatin J (**1.11**) by an enzyme or via a mechanism involving singlet oxygen would afford hydroxy pyranone **1.56**. Subsequent 1,3-elimination of water could yield an oxidopyrilium zwitterion (**1.57**), which would then be poised to undergo a transannular 1,3-dipolar cycloaddition to give intricarene (**1.40**). This hypothesis has received support from two synthetic studies which describe the synthesis of intricarene from bipinnatin J.[22] However it is noteworthy than in both of these cases, extreme temperatures (150 °C) were required to generate the intermediate oxidopyrilium species from the hydroxy pyranone – conditions that can hardly be deemed biomimetic.

Scheme 1.7 Proposed biosynthesis of intricarene.

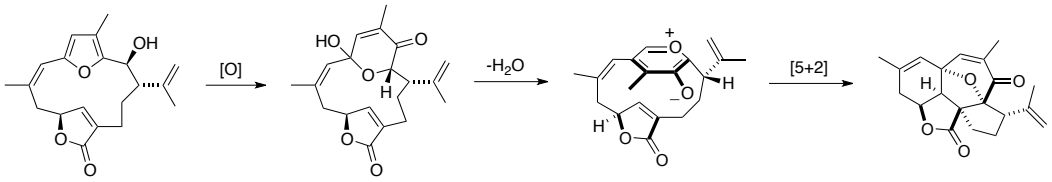

bipinnatin J (**1.11**) **1.56** **1.57** intricarene (**1.40**)

It is conceivable that similar processes involving enzymatic oxidations and transannular (cyclo)additions could account for the formation of bielschowskysin (**1.38**), verrillin (**1.41**), and plumarellide (**1.46**). These natural products may be ultimately derived from simpler furanocembranoids, such as rubifolide or bipinnatin J (Scheme 1.8). The *exo*-alkylidene dihydrofurans **1.58**, **1.59**, and **1.60** are all potential biosynthetic intermediates en route to bielschowskysin, verrillin, and plumarellide, respectively. These intermediates could be generated by epoxidation of the $\Delta^{7,8}$ double bond, followed by addition of water to C3 of the furan. Alternatively, they could arise through hydration of a dienedione stemming from the oxidative cleavage of the furan.

Scheme 1.8 Proposed biosynthesis of bielschowskysin, verrillin and plumarellide.

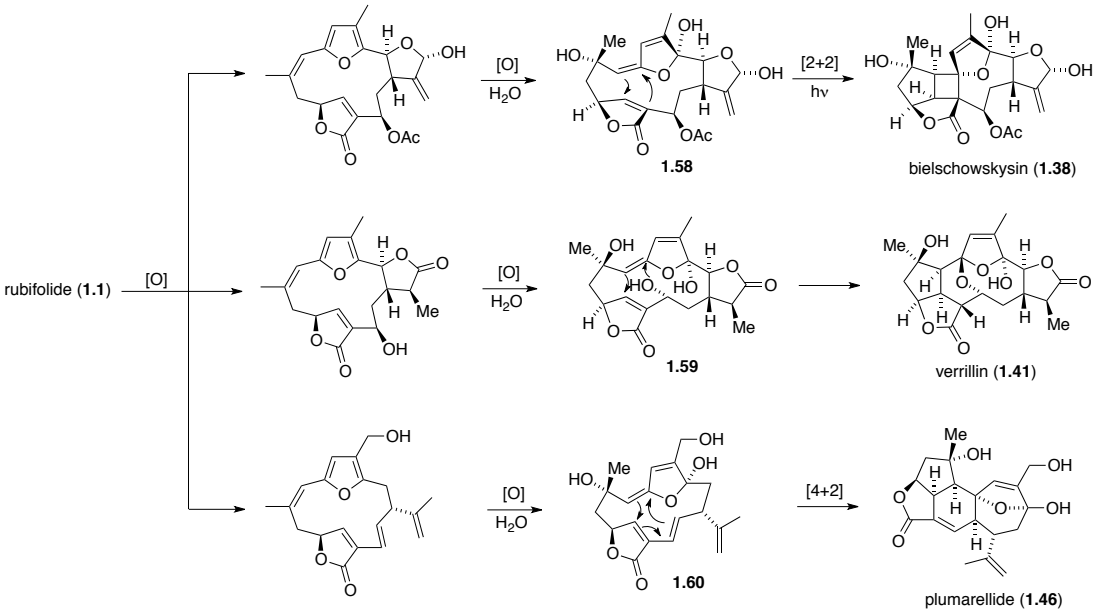

It is important to remember that the biosynthetic pathways discussed in this section are speculative. The precise steps that nature uses to assemble the furanocembranoids remain to date unknown. However, there are many recurring motifs – such as epoxidations and hydroxylations at conserved positions – that suggest that the more complex natural products may be derived biosynthetically from the simpler specimens. This notion is further reinforced by the fact that many of these molecules are derived from the same or closely related organisms. For these reasons the furanocembranoids provide an excellent platform to test out biomimetically-inspired synthetic routes.

1.4 Prior Work in the Total Synthesis of Furanocembranoids

Owing to their elegant structures and range of bioactivities, the furanocembranoids have been subjected to numerous efforts at total synthesis. The majority of these efforts have been summarized recently in the literature.[1] Since much of the work described in this dissertation revolves around the rich oxidation chemistry exhibited by bipinnatin J (**1.11**), it would prove worthwhile to review the synthetic route to this key natural product devised by Trauner *et al.*[23] which was employed so frequently throughout the course of this research. Subsequent transformations with bipinnatin J will also contribute to this background.

Trauner's synthesis of bipinnatin J (Scheme 1.9) proceeds from known vinyl iodide **1.61**.[24] Dess-Martin periodinane oxidation of **1.61** followed by addition of lithiated ethyl propiolate gave propargylic alcohol **1.63** as a racemate. A ruthenium(II)-catalyzed Trost Alder-ene reaction of **1.63** with allyl alcohol was used to install the butenolide moiety of **1.65** while also producing an aldehyde as a functional handle.[25] This reaction presumably proceeds through enol **1.64**, which underwent tautomerization and intramolecular transesterification under these conditions. Subsequent Wittig olefination with stabilized Wittig reagent **1.66** extended the side-chain and was followed by chemoselective reduction of the resulting aldehyde **1.67**, thereby giving primary allylic alcohol **1.68**. In preparation for a Stille coupling, furylstannane **1.72** was

generated in a single step from known 3-methylfurfural (**1.69**).[26] This component was then coupled with vinyl iodide **1.68** utilizing Baldwin's conditions[27] in the Stille reaction, proceeding with excellent yield to give **1.73**, a compound containing all 20 carbons of the target molecule. Conversion of allylic alcohol **1.73** into allylic bromide **1.74** proceeded smoothly using triphenylphosphine and N-bromosuccinimide. The stage was then set for the Nozaki-Hiyama-Kishi macrocyclization[28], which proceeded with excellent diastereoselectivity (d.r. > 9:1) to give bipinnatin J (**1.11**) in 72% yield.

Scheme 1.9 Trauner's synthesis of bipinnatin J.

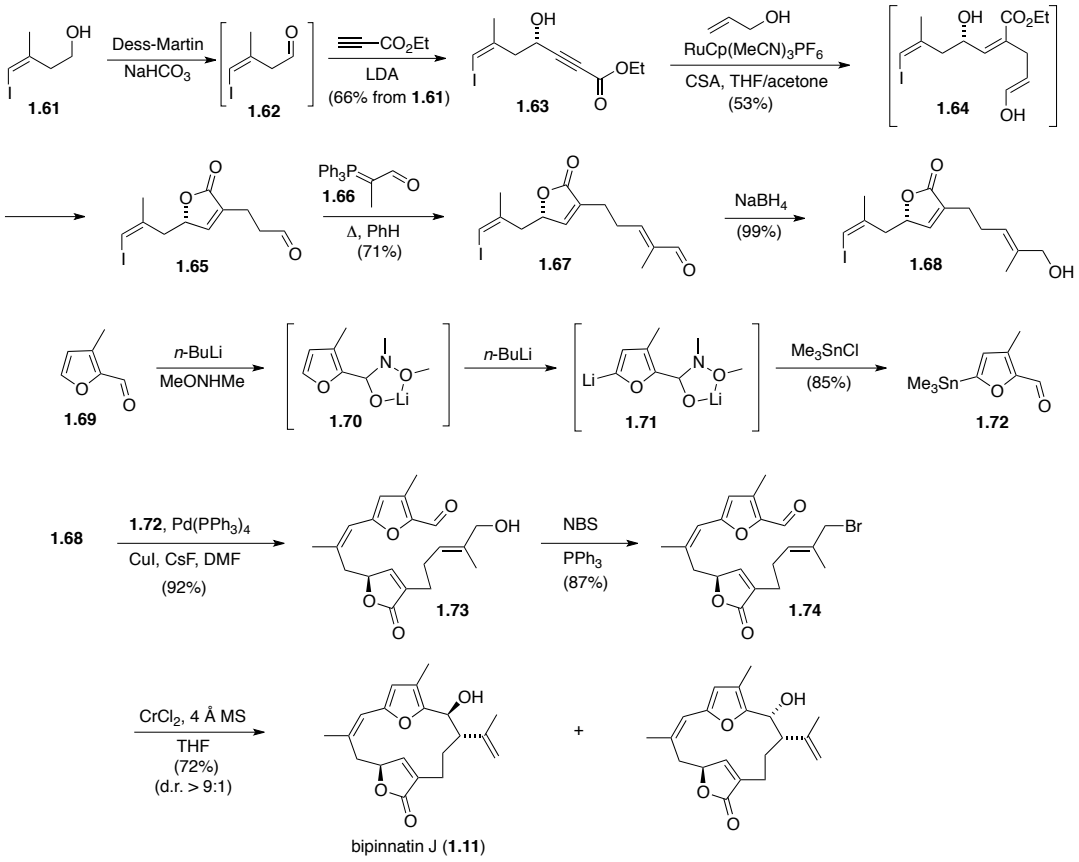

Further explorations of chemical transformations starting from bipinnatin J have been described by Trauner *et al.*[22a,29] With the primary goal of converting bipinnatin J (**1.11**) into intricarene (**1.40**), oxidation of the furan of **1.11** with *m*-chloroperoxybenzoic acid followed by an Achmatowicz rearrangement and subsequent acetylation furnished pyranone **1.75** in high yield. Heating of this intermediate at 150 °C with tetramethylpiperidine in dimethylsulfoxide presumably gave an oxidopyrilium ion that underwent a transannular 1,3-dipolar cycloaddition to afford intricarene (**1.40**) in moderate yield (Scheme 1.10).

Scheme 1.10 Synthesis of intricarene from bipinnatin J.

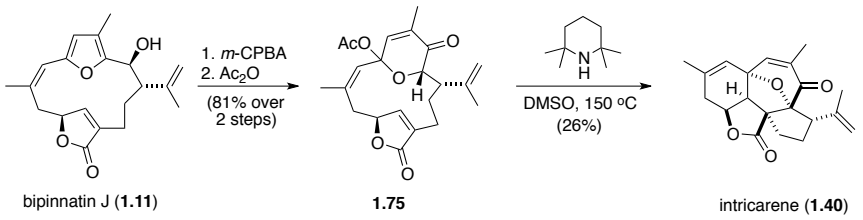

Bipinnatin J (**1.11**) could also be converted to rubifolide (**1.1**) in essentially quantitative yield via deoxygenation with trifluoroacetic acid and triethylsilane. (Scheme 1.11) Rubifolide was then oxidized with *m*-chloroperoxybenzoic acid to yield the natural product isoepilophodione B (**1.52**).

Scheme 1.11 Synthesis of rubifolide and isoepilophodione B from bipinnatin J.

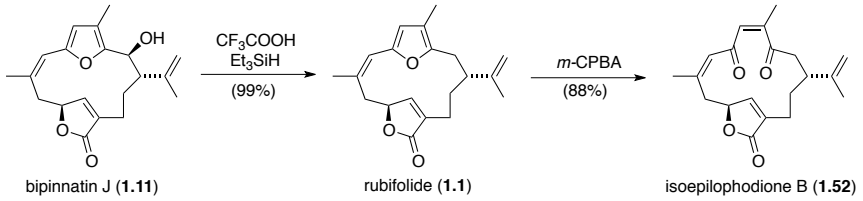

It was also demonstrated by Trauner *et al.* that rubifolide (**1.1**) could be converted to coralloidolide A (**1.32**) via a nucleophilic epoxidation of the butenolide moiety with hydrogen peroxide and sodium hydroxide (Scheme 1.12). This reaction yields a single diastereomer, thus demonstrating the rigid macrocyclic structure of rubifolide with its inherent facial bias. Finally, the furan of coralloidolide A (**1.32**) was shown to be oxidized easily with *m*-chloroperoxybenzoic acid to give coralloidolide E (**1.36**) in good yield.

Scheme 1.12 Synthesis of coralloidolide A and coralloidolide E from rubifolide.

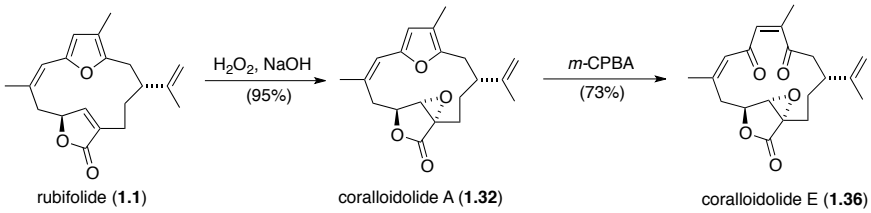

1.5 Conclusion

The harvesting of sea corals by natural product chemists over the past few decades has yielded a plethora of furanocembranoid derivatives – many with potent biological activities. The amazing diversity of structures within this family is underpinned by a network of oxidative transformations and skeletal rearrangements. While the exact sequence of steps that nature uses to assemble these molecules remains speculative at this date, the study of potential biosynthetic connections has already born fruit in the area of total synthesis. It is likely that as investigation into this family of molecules continues, more connections will be recognized and hence more synthetic progress should be made. This progress will no doubt be accompanied by

advancements in synthetic methodology as well as benefit our understanding of the biosynthetic origin of these compounds.

1.6 References and Notes

1. P. Roethle and D. Trauner, *Nat. Prod. Rep.*, 2008, **25**, 298.
2. (a) A. E. Wright, N. S. Burres and G. K. Schulte, *Tetrahedron Lett.*, 1989, **30**, 3491. (b) A. D. Rodríguez, J.-G. Shi and S. D. Huang, *J. Nat. Prod.*, 1999, **62**, 1228.
3. J. Marrero, J. Benítez, A. D. Rodríguez, H. Zhao and R. G. Raptis, *J. Nat. Prod.*, 2008, **71**, 381.
4. (a) D. Williams, R. J. Andersen, G. D. Van Duyne and J. Clardy, *J. Org. Chem.*, 1987, **52**, 332. (b) D. Williams and R. J. Andersen, *Can. J. Chem.*, 1987, **65**, 2244.
5. W. Fenical, R. K. Okuda, M. M. Bandurraga, P. Culver and R. S. Jacobs, *Science*, 1981, **212**, 1512.
6. M. C. Sánchez, M. J. Ortega, E. Zubía and J. L. Carballo, *J. Nat. Prod.*, 2006, **69**, 1749.
7. (a) S. N. Abramson, Y. Li, P. Culver and P. Taylor, *J. Biol. Chem.*, 1989, **264**, 12666. (b) S. N. Abramson, J. A. Trischman, D. M. Tapiolas, E. E. Harold, W. Fenical and P. Taylor, *J. Med. Chem.*, 1991, **34**, 1798. (c) D. Bai, S. N. Abramson and D. B. Sattelle, *Arch. Insect Biochem. Physiol.*, 1993, **23**, 155. (d) D. R. Groebe, J. M. Dumm and S. N. Abramson, *J. Biol. Chem.*, 1994, **269**, 8885. (e) D. R. Groebe and S. N. Abramson, *J. Biol. Chem.*, 1995, **270**, 281. (f) E. G. Hyde, A. Boyer, P. Tang, Y. Xu and S. N. Abramson, *J. Med. Chem.*, 1995, **38**, 2231. (g) C. TornØe, L. Holden-Dye, C. Garland, S. N. Abramson, J. T. Fleming and D. B. Sattelle, *J. Exp. Biol.*, 1996, **199**, 2161 and references therein. See also: (h) P. Culver, M. Burch, C. Potenza, L. Wasserman, W. Fenical and P. Taylor, *Mol. Pharmacol.*, 1985, **28**, 436. (i) R. M. Hann, O. R. Pagán, L. Gregory, T. Jácome, A. D. Rodríguez, P. A. Ferchmin, R. Lu and V. A. Eterovic, *J. Pharmacol. Exp. Ther.*, 1998, **287**, 253.
8. S. A. Look, M. T. Burch, W. Fenical, Z. Qi-tai and J. Clardy, *J. Org. Chem.*, 1985, **50**, 5741.
9. M. M. Bandurraga, W. Fenical, S. F. Donovan and J. Clardy, *J. Am. Chem. Soc.*, 1982, **104**, 6463.
10. (a) J. Marrero, C. A. Ospina, A. D. Rodríguez, P. Baran, H. Zhao, S. G. Franzblau and E. Ortega-Barria, *Tetrahedron*, 2006, **62**, 6998. (b) A. D. Rodríguez, J.-G. Shi and S. D. Huang, *J. Org. Chem.*, 1998, **63**, 4425. (c) J. Marrero, A. D. Rodríguez, P. Baran and R. G. Raptis, *Eur. J. Org. Chem.*, 2004, 3909. (d) J. Marrero, A. D. Rodríguez, P. Baran and R. G. Raptis, *J. Org. Chem.*, 2003, **68**, 4977.
11. (a) M. D'Ambrosio, D. Fabbri, A. Guerriero and F. Pietra, *Helv. Chim. Acta.* 1987, **70**, 63. (b) M. D'Ambrosio, A. Guerriero and F. Pietra, *Helv. Chim. Acta*, 1989, **72**, 1590. (c) M. D'Ambrosio, A. Guerriero and F. Pietra, *Helv. Chim. Acta*, 1990, **73**, 804.
12. J. Marrero, A. D. Rodríguez, P. Baran, R. G. Raptis, J. A. Sánchez, E. Orterga-Barria and T. L. Capson, *Org. Lett.*, 2004, **6**, 1661.
13. (a) J. Marrero, A. D. Rodríguez and C. L. Barnes, *Org. Lett.*, 2005, **7**, 1877. (b) J. Marrero, A. D. Rodríguez, P. Baran and R. G. Raptis, *Org. Lett.*, 2003, **5**, 2551.
14. A. D. Rodríguez and Y.-P. Shi, *J. Org. Chem.*, 2000, **65**, 5839.
15. Y. Venkateswerlu, M. A. Farooq Biabani, M. Venkata Rami Reddy, T. Prabhakar Rao and A. C. Kunwar, *Tetrahedron Lett.*, 1994, **35**, 2249.
16. (a) A. S. R. Anjaneyulu, K. S. Sagar and M. J. R. V. Venugopal, *Tetrahedron*, 1995, **51**, 10997. (b) A. S. R. Anjaneyulu and P. Sarada, *J. Chem. Res.*, 1999, 600.

17. V. A. Stonik, I. I. Kapustina, A. I. Kalinovsky, P. S. Dmitrenok and B. B. Grebnev, *Tetrahedron Lett.*, 2002, **43**, 315.
18. (a) A. S. R. Anjaneyulu, M. J. R. V. Venugopal, P. Sarada, J. Clardy and E. Lobkovsky, *Tetrahedron Lett.*, 1998, **39**, 139. (b) P. Ramesh, N. Srinivasa Reddy, Y. Venkateswarlu, M. Venkata Rami Reddy and D. J. Faulkner, *Tetrahedron Lett.*, 1998, **39**, 8217. (c) A. S. R. Anjaneyulu, M. J. R. V. Venugopal and P. Sarada, *Indian J. Chem.*, 2000, **39B**, 530.
19. J. MacMillan and M. H. Beale, In *Comprehensive Natural Products Chemistry*, Vol. 2, D. H. R. Barton and K. Nakanishi, Eds.; Pergamon, 1999, pp 217.
20. A. D. Rodríguez and J.-G. Shi, *J. Org. Chem.*, 1998, **63**, 420.
21. C. D. Bray and G. Pattenden, *Tetrahedron Lett.*, 2006, **47**, 3937.
22. (a) P. A. Roethle, P. T. Hernandez and D. Trauner, *Org. Lett.*, 2006, **8**, 5901. (b) B. Tang, C. D. Bray, G. Pattenden, *Tetrahedron Lett.*, 2006, **47**, 6401.
23. P. A. Roethle and D. Trauner, *Org. Lett.*, 2006, **8**, 345.
24. S. Ma, E. Negishi, *J. Org. Chem.*, 1997, **62**, 784.
25. B.M. Trost, F.D. Toste, *Tetrahedron Lett*., 1999, **40**, 7739.
26. L. L. Klein, *J. Org. Chem.*, 1985, **50**, 1770.
27. S. Mee, V. Lee, J. Baldwin, *Chem. Eur. J.*, 2005, **11**, 3294.
28. A. Fürstner, *Chem. Rev.*, 1999, **99**, 991.
29. T.J. Kimbrough, P.A. Roethle, P. Mayer, D. Trauner, *Angew. Chem. Int. Ed.*, 2010, **49**, 2619.

Chapter 2

Total Synthesis of Coralloidolide B and Coralloidolide C

2.1 Introduction

In the late 1980's, Pietra and co-workers reported the isolation of six highly oxygenated diterpenes from the alcynoacean coral *Alcyonium coralloides.*[1] Coralloidolides A through F were the first furanocembranoids to be isolated from a Mediterranean organism, in contrast to others of Caribbean or Pacific origin. For natural products that are only available in scarce amounts such as the coralloidolides, total synthesis is often the only method which can produce sufficient quantities for extensive biological screening. Considering their intricate structures, the dearth of material available to scientists, and the potential to explore biosynthetic connections, the coralloidolides are attractive targets for total synthesis.

As discussed in Chapter 1, the coralloidolides can be envisioned to be biosynthetically related to one another and all could be potentially derived from rubifolide (**1.1**). It was with these connections in mind that we developed a biomimetic strategy starting from rubifolide. Having developed a synthesis of coralloidolides A (**1.32**) and E (**1.36**) from rubifolide[2], we turned our attention to the four remaining members of the family.

2.2 Total Synthesis of Coralloidolide B

Coralloidolides B (**1.33**), C (**1.34**), D (**1.35**) and F (**1.37**) could all be produced in theory from coralloidolide E (**1.36**) in a single synthetic step (Scheme 2.1). With a reliable synthesis of coralloidolide E in hand, we set out to explore conditions for the conversion of this natural product into the four remaining coralloidolides. Initially we focused our attention on coralloidolides B and D, while mindful that under acidic conditions we could potentially effect an aldol transformation to give coralloidolide C or F. The structures of coralloidolides B (**1.33**) and D (**1.35**) can both be viewed as hydrated forms of coralloidolide E (**1.36**) with a concomitant transannular opening of the epoxide. Thus we sought to explore various acidic conditions in the presence of water to achieve these transformations.

Scheme 2.1 Proposed routes to coralloidolides B, C, D and F.

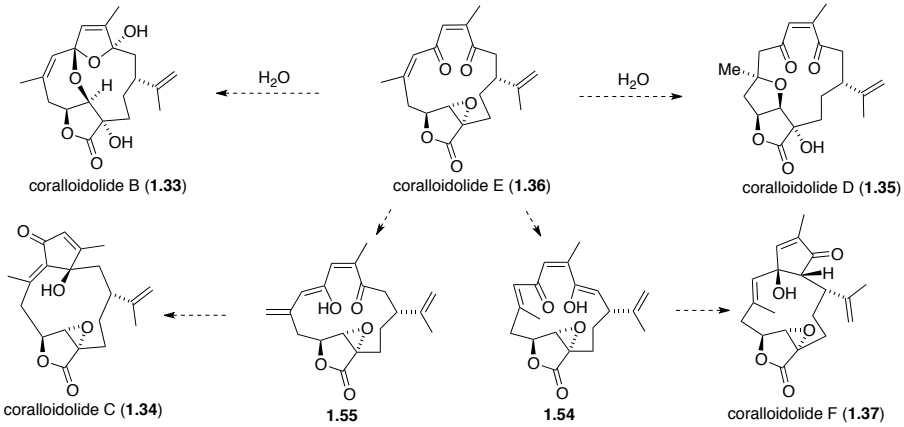

Numerous Brønsted and Lewis acids were examined in a variety of solvents in the presence of coralloidolide E (**1.36**) and water: HCl, LiCl, NaCl, SiO_2, $FeCl_3$, citric acid, and $Yb(OTf)_3$. Typically these conditions resulted in no reaction or an intractable mixture of unstable products. However, treatment of **1.36** with neat acetic acid yielded 18-acetoxycoralloidolide A (**2.3**) as the only identifiable product. Similarly, when **1.36** was subjected to a mixture of aqueous sulfuric acid and acetone, only the corresponding 18-hydroxycoralloidolide A (**2.4**) was isolated (Scheme 2.2).

Scheme 2.2 Formation of 18-acetoxycoralloidolide A and 18-hydroxycoralloidolide A.

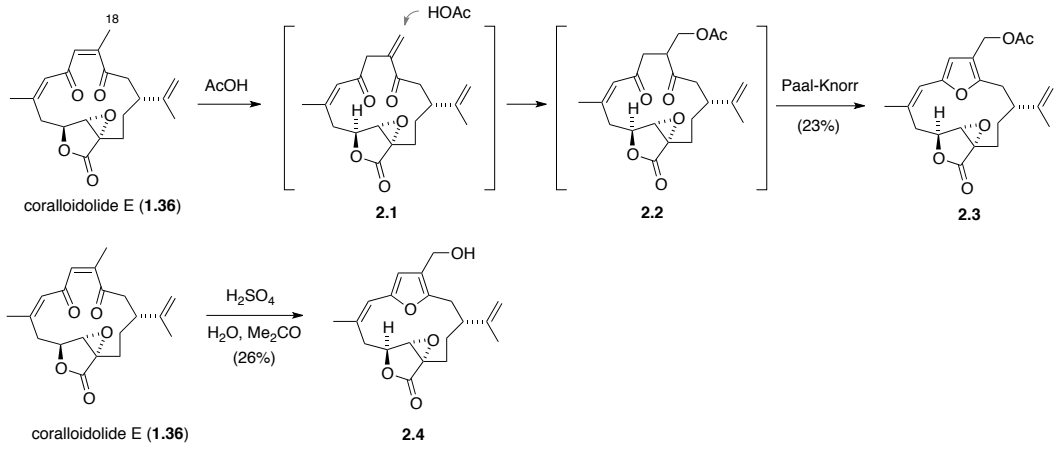

Presumably, these transformations proceed through the intermediacy of double bond isomer **2.1**, which undergoes conjugate addition of either acetate (→**2.2**) or water, followed by Paal-Knorr-type furan formation. *Exo*-methylene isomer **2.1** has been previously observed upon dissolution of coralloidolide E (**1.36**) in pyridine-d_6 by Pietra and co-workers.[1b] It is interesting to speculate whether oxidation of the C18 methyl group in furanocembranoids can proceed through the mechanism depicted in Scheme 2.2 or requires enzymatic hydroxylation. It should be noted, however, that hydroxymethylene derivatives of type **2.4** are rarely observed among furanocembranoids.

After numerous experiments we decided to examine scandium for its potential to engender the hydration and epoxide opening of coralloidolide E (**1.36**). We screened a variety of solvents (DMF, dioxane, 1:1 dioxane/H_2O, DCE, and acetone) and it was discovered that dioxane provided the cleanest reaction. Thus, treatment of coralloidolide E (**1.36**) with scandium triflate in its hydrated form in dioxane led to its clean conversion into coralloidolide B (**1.33**) (Scheme 2.3). The reaction was substantially slower in both DMF and DCE and yielded substantially more products in acetone - the only stable one still being coralloidolide B (**1.33**). Surprisingly, the reaction was exceedingly sluggish in 1:1 dioxane/H_2O, perhaps owing to hydration of the catalyst, thereby rendering it less Lewis acidic.

Scheme 2.3 Synthesis of coralloidolide B from coralloidolide E.

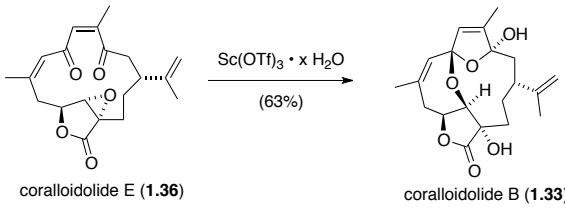

We were able to obtain an X-ray crystal structure of coralloidolide E (**1.36)**, which provided useful insights into the mechanism and diastereoselectivity of this transformation. As can be seen in Scheme 2.4, the molecule adopts a conformation wherein the C4-C8 segment of the dienedione moiety of **1.36** is fully planar. The remaining C2-carbonyl group resides in an almost perpendicular orientation (the C5-C4-C3-O dihedral angle is -106°). Although this places the oxygen of the C6-carbonyl group in close proximity (within 3.2 Å) to the electrophilic C11 of the epoxide, the oxocarbenium ion **2.5** resulting from direct nucleophilic attack would afford an exceedingly strained isomer **2.6** upon hydration. Therefore, it appears more likely that the transannular epoxide opening proceeds in a stepwise fashion *via* the hydrate **2.7**, as originally suggested by Pietra.[1a] It is plausible that scandium triflate plays a twofold role in this process, catalyzing both the initial hydration of the dienedione and the subsequent intramolecular nucleophilic attack of the resulting diol **2.7** to afford coralloidolide B (**1.33**).

Scheme 2.4 Crystal structure of coralloidolide E and diastereoselectivity of transannular cyclizations.

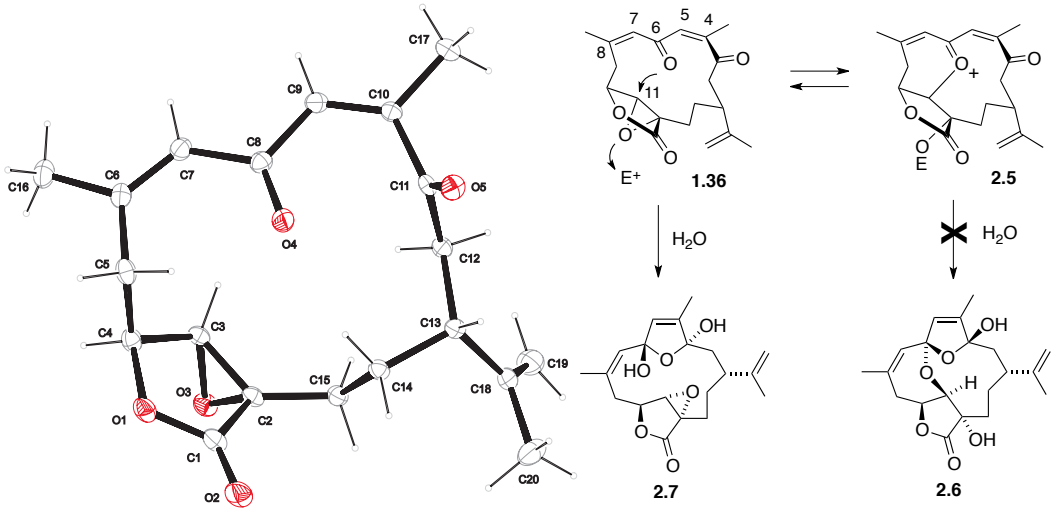

In an additional effort to probe the nature of this reaction, we subjected isoepilophodione B (**1.52**) to the same conditions as in the screening to generate coralloidolide B (**1.33**) with scandium triflate (Scheme 2.5). No reaction was observed in any solvent system at room temperature, in stark contrast to the same conditions using coralloidolide E (**1.36**) as the starting material. It is clear that the epoxide of **1.36** is necessary for any productive reaction manifold when treating **1.36** with scandium triflate – at least at room temperature.

Scheme 2.5 Treatment of isoepilophodione B with scandium triflate.

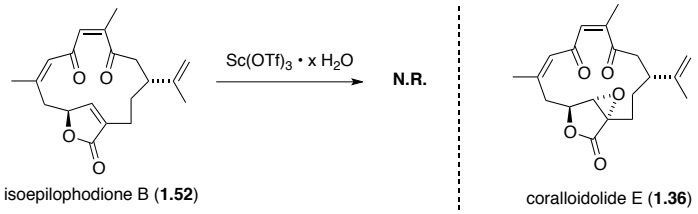

isoepilophodione B (**1.52**) coralloidolide E (**1.36**)

A single attempt was made to convert coralloidolide B (**1.33**) into coralloidolide D (**1.35**) by stirring **1.33** in DCM with 1,8-diazabicyclo[5.4.0]undec-7-ene (DBU). This resulted in no reaction, but it could prove fruitful in the future to screen a variety of bases and solvents at different temperatures in order to effect the 1,3-rearrangement depicted in Scheme 2.6. Alternatively, coralloidolide D (**1.35**) might be formed under similar conditions to coralloidolide B (**1.33**) in a single step from coralloidolide E (**1.36**). It is clear that solvent effects play a critical role in these transformations, and additional screening of acids and solvents may reveal the conditions necessary for the formation of **1.35**.

Scheme 2.6 Proposed formation of coralloidolide D from coralloidolide B

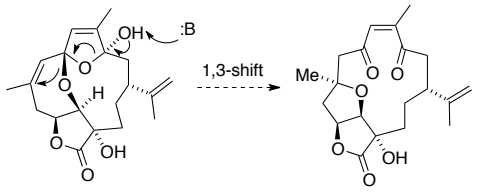

coralloidolide B (**1.33**) coralloidolide D (**1.35**)

2.3 Total Synthesis of Coralloidolide C

Coralloidolide C (**1.34**) and coralloidolide F (**1.37**) each contain an extra C-C bond relative to coralloidolide E (**1.36**). Both molecules in theory could be produced via selective keto-enol tautomerization of **1.36** and subsequent transannular aldol addition. In the case of **1.34**, enol formation at the C6 carbonyl to give intermediate **1.55** is followed by C3-C7 cyclization to give **2.8**. Shifting of the double bond to the thermodynamically more stable position would then afford coralloidolide C (**1.34**). For coralloidolide F (**1.37**), C7-C8 double bond isomerization with concomitant enol formation at the C3 carbonyl would give intermediate enol **1.54**. This is followed by C2-C6 cyclization to give **1.37** (Scheme 2.7).

Scheme 2.7 Proposed formation of coralloidolides C and F via transannular aldol addition.

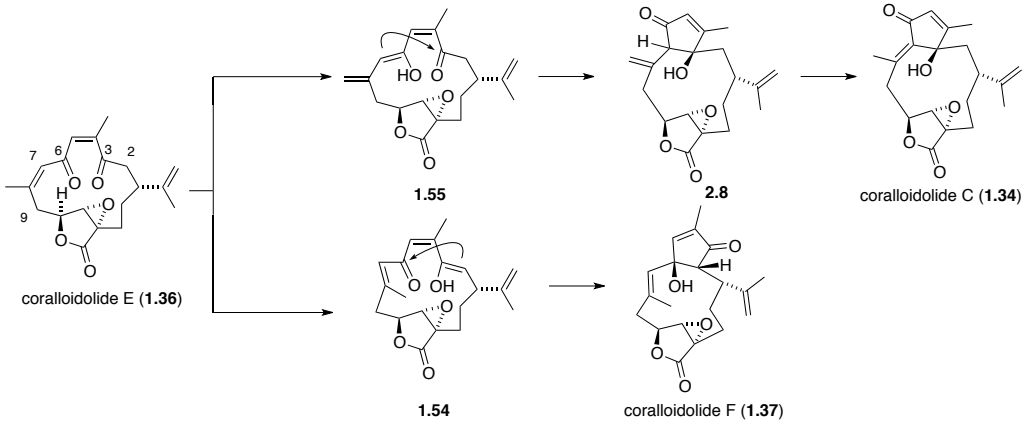

In our efforts to synthesize coralloidolides B (**1.33**) and D (**1.35**), we were always mindful of the fact that a transannular aldol addition might be effected under acidic conditions. However this was never observed with any of the conditions we screened. Additional attempts to effect an aldol reaction with coralloidolide E (**1.36**) made use of a variety of bases: LDA, KHMDS, triethylamine, and DBU. Stirring **1.36** with catalytic amounts of triethylamine in DCM yielded a mixture of the starting material and the *exo*-methylene isomer **2.1** (Scheme 2.8) in a 2:3 ratio. As previously discussed, **2.1** was observed by Pietra *et al.* in their attempt to characterize coralloidolide E (**1.36**) in pyridine-d_6. When isomer **2.1** was isolated and treated again with triethylamine, coralloidolide E was reformed. It stands to reason that this isomer with a less-substituted double bond (**2.1**) exists as the major component at equilibrium due to a relief of macrocyclic ring strain. Given its facile formation under mild basic and acidic conditions, it is possible that **2.1** exists in the coral that produces coralloidolides and thus would qualify as a genuine natural product.

Scheme 2.8 Formation of the *exo*-methylene isomer of coralloidolide E.

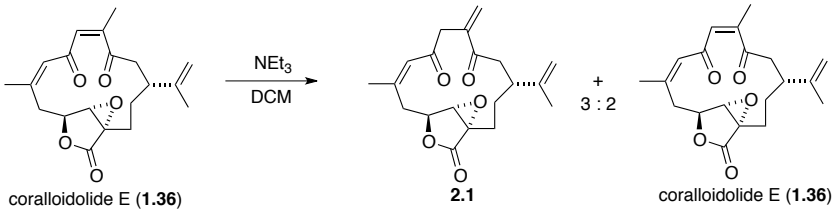

Exo-methylene isomer **2.1** was shown to be a major product in our attempts to effect an aldol reaction with both LDA and KHMDS as well. An additional product was also seen by TLC in both cases – however this product proved difficult to characterize as it decomposed to a complex mixture of products upon work-up and attempted purification.

Additional experimentation with DBU as the base in catalytic amounts produced a similar result to our experiments with triethylamine, yielding a mixture of starting material **1.36** and its *exo*-methylene isomer (**2.1**). However, it was discovered that a large excess of DBU allowed the starting material (**1.36**) and its isomer (**2.1**) to be consumed, promoting an aldol reaction to give coralloidolide C (**1.34**) in modest yield (Scheme 2.9). Another intermediate was observed during the course of this reaction by TLC, but this unidentified product, coralloidolide

E (**1.36**), and its isomer (**2.1**) all converged to coralloidolide C (**1.34**), thus suggesting that **1.34** is the thermodynamic minimum of this series of products. It is interesting to speculate whether the unidentified product may be intermediate **2.8** before double-bond migration occurs to give the more substituted double bond in coralloidolide C (**1.34**). Efforts are ongoing to investigate this possibility, in addition to efforts directed towards the synthesis of coralloidolide F (**1.37**) through similar means. Efforts are also under way to test the bioactivities of coralloidolides A, B, C and E.

Scheme 2.9 Synthesis of coralloidolide C from coralloidolide E.

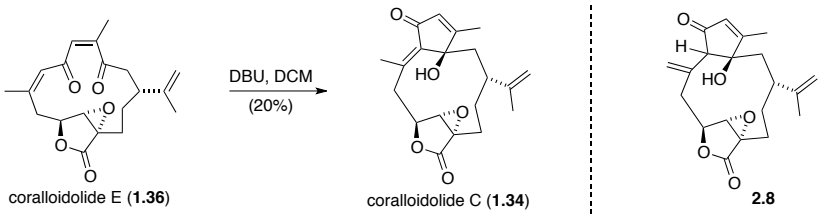

coralloidolide E (**1.36**) coralloidolide C (**1.34**) **2.8**

2.4 Conclusion

In summary, the total synthesis of the furanocembranoids coralloidolides B and C has been achieved, adding to our previous syntheses of coralloidolides A and E. Racemic coralloidolides B and C were synthesized without recourse to protecting-group chemistry, each in thirteen steps. Since the asymmetric synthesis of bipinnatin J has been accomplished previously through a similar route to the racemic route described in Chapter 1, the routes to the coralloidolides that we have developed can in principle be rendered asymmetric.[3] Several highly selective transformations have been discovered which will undoubtedly find utility in synthetic approaches toward other members of the furanocembranoid class of natural products. Our synthetic work provides insight into the biogenetic relationships within this family and adds to the matrix of chemical and biosynthetic relations among furanocembranoids.

2.5 Experimental Methods

General Experimental Details: All reactions were carried out under an inert N_2 atmosphere in oven-dried glassware. Flash column chromatography was carried out with EcoChrom ICN SiliTech 32-63 D 60 Å silica gel. Reactions and chromatography fractions were monitored with Merck silica gel 60 F_{254} plates and visualized with potassium permanganate, ceric ammonium molybdate, and vanillin. Tetrahydrofuran (THF) and methylene chloride (CH_2Cl_2) were dried by passage through activated alumina columns. Benzene (PhH) and diisopropylamine (*i*-Pr_2NH) were distilled from CaH_2 prior to use. DMSO was stored over 3 Å molecular sieves. *n*-Butyllithium was titrated with diphenylacetic acid prior to use. All other reagents and solvents were used without further purification from commercial sources. Organic extracts were dried over $MgSO_4$ unless otherwise noted.

Instrumentation: FT-IR spectra were obtained on NaCl plates with an ATI Mattson Gemini spectrometer. Proton and carbon NMR spectra (^{1}H NMR and ^{13}C NMR) were recorded in deuterated chloroform ($CDCl_3$) unless otherwise noted on a Varian VXR 400 S, Bruker AXR-300 or Bruker AMX 600 spectrometer and calibrated to residual solvent peaks. Multiplicities are abbreviated as follows: s = singlet, d = doublet, t = triplet, q = quartet, br = broad, m = multiplet. High-resolution (HR-MS) and low resolution (MS) mass spectra were recorded on a

Finnigan MAT 95 instrument. Melting points were determined with an electrothermal apparatus and are uncorrected.

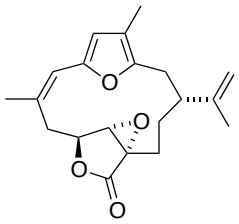

Coralloidolide A (1.32). To a solution of rubifolide (**1.1**) (50 mg, 0.16 mmol) in MeOH (3.2 mL) and CH_2Cl_2 (3.2 mL) at 0 °C was added a solution of hydrogen peroxide (30% aqueous, 100 μL) and a solution of sodium hydroxide (3 M, 15 μL). After 1 hr at 0 °C, the reaction mixture was warmed to rt. After 5 hr, additional hydrogen peroxide solution (200 μL) and sodium hydroxide solution (60 μL) were added. After 8 hr, the reaction mixture was poured onto H_2O (10 mL) and Et_2O (10 mL). The aqueous layer was made acidic with a 1 M HCl solution. The layers were separated, and the aqueous layer was extracted with Et_2O (2 x 10 mL). The combined organic extracts were dried, filtered, and concentrated *in vacuo*. The resulting crude product was purified by flash column chromatography (8% EtOAc/hexanes) to give 50 mg (95%) of coralloidolide A (**1.32**) as a white solid.
R_f 0.69, 20% EtOAc/Hexanes. HRMS $(EI)^+$ calcd for $C_{20}H_{24}O_4$ $(M)^+$ 328.1675, found 328.1676. NMR data were recorded in C_6D_6 solution.

^{1}H NMR isolation	^{1}H NMR synthetic	^{13}C NMR isolation	^{13}C NMR synthetic
5.78 (br q, 1 H, *J* = 1.5 Hz)	5.79 (s, 1 H)	172.3	172.4
5.73 (br s, 1 H)	5.74 (s, 1 H)	150.1	150.2
5.00 (br dq, 1 H, *J* = 1.5, 0.8 Hz)	4.99 (s, 1 H)	148.6	148.6
4.95 (dq, 1 H, *J* = 1.5, 1.5 Hz)	4.95 (s, 1 H)	145.0	145.2
4.30 (dd, 1 H, *J* = 12.6, 4.5 Hz)	4.31 (dd, 1 H, *J* = 12.5, 4.5 Hz)	128.1	128.4
3.60 (br dd, 1 H, *J* = 12.6, 12.6 Hz)	3.60 (m, 1 H)	117.9	118.0
3.58 (s, 1 H)	3.58 (s, 1 H)	117.0	117.1
2.76 (ddd, 1 H, *J* = 15.3, 13.1, 2.5 Hz)	2.75 (td, 1 H, *J* = 15.5, 2 Hz)	113.4	113.6
2.58 (br ddd, 1 H, *J* = 12, 12, 3.5 Hz)	2.56 (br t, 1 H, *J* = 11.5 Hz)	113.3	113.3
2.39 (br d, 1 H, *J* = 15.5, 3.5 Hz)	2.39 (br d, 1 H, *J* = 15 Hz)	76.9	77.0
2.25 (dd, 1 H, *J* = 15.5, 12 Hz)	2.26 (dd, 1 H, *J* = 15.5, 12 Hz)	61.4	61.5
2.20 (br dd, 1 H, *J* = 12.6, 4.5 Hz)	2.20 (br dd, 1 H, *J* = 12.5, 3.5 Hz)	61.0	61.0
1.66 (br d, 3 H, *J* = 1.4 Hz)	1.67 (s, 3 H)	44.1	44.1

1.58 (dd, 3 H, *J* = 1.5, 0.8 Hz)	1.57 (s, 3 H)	36.4	36.5
1.44 (ddd, 1 H, *J* = 15.3, 4.9, 3.0 Hz)	1.44 (br td, 1 H, *J* = 15.5, 4 Hz)	31.0	31.1
1.37 (br d, 3 H, *J* = 1.5 Hz)	1.39 (s, 3 H)	28.2	28.3
1.20 (br dd, 1 H, *J* = 12, 2.5 Hz)	1.20 (br t, 1 H, *J* = 12.5 Hz)	24.5	24.6
0.84 (br dd, 1 H, *J* = 14, 2.5 Hz)	0.83 (br t, 1 H, *J* = 14 Hz)	22.1	22.1
		19.7	19.7
		9.4	9.4

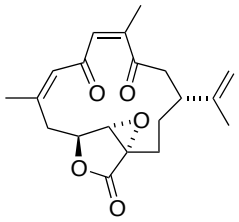

Coralloidolide E (1.36). To a solution a solution of coralloidolide A (**1.32**) (45 mg, 0.14 mmol) in CH_2Cl_2 (2.8 mL) at 0 °C was added m-chloroperoxybenzoic acid (77% purity, 38 mg, 0.17 mmol). After 30 min, additional m-CPBA (30 mg) was added. After an additional 30 min, a saturated solution of Na_2SO_3 (5 mL) was added. The layers were separated, and the aqueous layer was extracted with CH_2Cl_2 (5 mL). The combined organic extracts were dried, filtered, and concentrated in vacuo. The resulting product was purified by flash column chromatography (40% EtOAc/hexanes) to give 34 mg (73%) of coralloidolide E (**1.36**) as a white solid. R_f 0.32, 40% EtOAc/Hexanes. HRMS $(EI)^+$ calcd for $C_{20}H_{24}O_5$ $(M)^+$ 344.1624, found 344.1620. NMR data were recorded in acetone-d_6 solution (the compound is only slightly soluble in acetone).

^{1}H NMR isolation	^{1}H NMR synthetic	^{13}C NMR isolation	^{13}C NMR synthetic
6.60 (dq, 1 H, *J* = 1.5, 0.6 Hz)	6.60 (s, 1 H)	205.4	?
6.38 (q, 1 H, *J* = 1.5 Hz)	6.37 (d, 1 H, *J* = 1 Hz)	188.6	188.6
4.80 (br dq, 1 H, *J* =1.5, 0.6 Hz)	4.80 (s, 1 H)	172.2	172.4
4.72 (br dd, 1 H, *J* = 11.1, 6.2 Hz)	4.71 (dd, 1 H, *J* = 11, 6.5 Hz)	161.1	161.2 (br)
4.58 (br dq, 1 H, *J* = 1.5, 0.6 Hz)	4.58 (s, 1 H)	156.8	156.7
3.87 (s, 1 H)	3.87 (s, 1 H)	147.8	147.8
3.77 (br dd, 1 H, *J* = 11.1, 0.6 Hz)	3.75 (br t, 1 H, *J* = 10 Hz)	126.9	126.9

3.10 (br d, 1 H, *J* = 11.1, 0.6 Hz)	3.09 (br m, 1 H)	126.1	126.1
2.72 (dd, 1 H, *J* = 18, 10.2 Hz)	2.71 (dd, 1 H, *J* = 17.5, 10.5 Hz)	110.6	110.6
2.65 (br dd, 1 H, *J* = 11.1, 6.2 Hz)	2.64 (br m, 1 H)	76.6	76.5
2.38 (ddd, 1 H, *J* = 18, 2.2, 1.5 Hz)	2.38 (m, 1 H)	64.7	64.7
2.36 (m, 1 H)	2.35 (m, 1 H)	60.8	60.8
2.12 (br d, 3 H, *J* = 1.5 Hz)	2.13 (s, 3 H)	41.7	41.7
2.02 (d, 3 H, *J* = 1.5 Hz)	2.02 (d, 3 H, *J* = 1.5 Hz)	37.6	37.6
1.98 (m, 1 H)	1.98 (m, 1 H)	37.5	37.4
1.90 (m, 1 H)	1.91 (m, 1 H)	26.3	26.3
1.82 (br dd, 3 H, *J* = 1.5, 0.6 Hz)	1.83 (s, 3 H)	22.7	22.7
1.07 (ddd, 1 H, *J* = 13.8, 8.7, 1.2 Hz)	1.07 (m, 1 H)	22.6	22.5
		21.1	21.1
		20.9	20.9

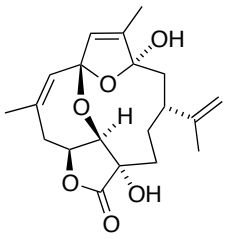

Coralloidolide B (1.33). To a solution of coralloidolide E (**1.36**) (7.7 mg, 0.022 mmol) in dioxane (2 mL) was added $Sc(OTf)_3$ (2.17 mg, 0.004 mmol) at once. After 3 hr, the solution was diluted with Et_2O (8 mL) and brine (8 mL). The layers were separated, and the aqueous layer was extracted with EtOAc (2 X 8 mL). The combined organic extracts were dried, filtered and concentrated *in vacuo*. The crude material was purified by flash chromatography (10% EtOAc/dichloromethane) to give 5.1 mg (63%) of coralloidolide B (**1.33**) as a white solid.

R_f 0.49. 50% EtOAc/Hexanes. HRMS $(EI)^+$ calcd for $C_{20}H_{26}O_6$ $(M)^+$ 362.1729, found 362.1723.

NMR data were recorded in $CDCl_3$.

^{1}H NMR isolation	^{1}H NMR synthetic	^{13}C NMR isolation	^{13}C NMR synthetic
5.63 (q, 1 H, *J* = 1.3 Hz)	5.62 (q, 1 H, *J* = 1.5 Hz)	176.5	176.4
5.26 (m, 1 H, *J* = 2.2, 1.7, 1.0 Hz)	5.24 (tt, 1 H, *J* = 3.1, 1.6 Hz)	148.6	148.6

4.86 (ddd, 1 H, *J* = 11.2, 6.0, 4.2 Hz)	4.84 (ddd, 1 H, *J* = 11.3, 6.1, 4.2 Hz)	143.5	143.5
4.66 (m, 1 H)	4.64 (m, 1 H)	134.8	134.8
4.59 (m, 1 H)	4.58 (m, 1 H)	126.8	126.7
4.46 (d, 1 H, *J* = 4.2 Hz)	4.45 (d, 1 H, *J* = 4.2 Hz)	126.6	126.6
2.91 (br. dd, 1 H, *J* = 12.5, 11.2, 2.2 Hz)	2.95-2.86 (m, 1 H)	113.1	113.1
-	2.38 (s, 1 H)	110.5	110.5
2.33 (ddd, 1 H, *J* = 12.5, 6.0, 1.0 Hz)	2.33 (dd, 1 H, *J* = 12.3, 5.8 Hz)	110.1	110.0
2.00 (br. dd, 1 H, *J* = 9.0, "small" Hz)	1.99 (t, 1 H, *J* = 8.3 Hz)	80.4	80.4
"submerged"	1.95-1.86 (m, 2 H)	80.1	80.0
1.86 (dd, 3 H, *J* = 1.5, 0.9 Hz)	1.85 (dd, 3 H, *J* = 1.4, 0.5 Hz)	75.5	75.5
"submerged"	1.82-1.74 (m, 3 H)	46.8	46.8
1.73 (d, 3 H, *J* = 1.3 Hz)	1.72 (d, 3 H, *J* = 1.6 Hz)	40.1	40.1
"submerged"	1.71-1.66 (m, 1 H)	32.7	32.7
1.66 (dd, 3 H, *J* = 1.7, 0.8 Hz)	1.66 (d, 3 H, *J* = 0.5 Hz)	32.4	32.4
"submerged"	1.58 (t, 1 H, *J* = 3.6 Hz)	26.5	26.5
1.55 (ddd, 1 H, *J* = 15.0, 3.5, 3.5 Hz)	1.54 (t, 1 H, *J* = 3.7 Hz)	26.4	26.4
		18.8	18.8
		11.2	11.2

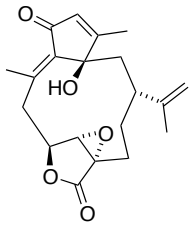

Coralloidolide C (1.34). To a solution of coralloidolide E (**1.36**) (6.1 mg, 0.018 mmol) in CH_2Cl_2 (0.8 mL) was added DBU (27.4 mg, 0.18 mmol) at room temperature. After 12 hr, the solution was diluted with 5 mLs DCM and a 0.01 M solution of AcOH was added (5 mLs). The layers were separated, and the organic layer was washed with 0.01 M AcOH (3 mLs). The organic fraction was dried, filtered, and concentrated in vacuo. The resulting product was purified by flash column chromatography (50% EtOAc/hexanes) to give 1.2 mg (20%) of coralloidolide C (**1.34**) as a white solid.

R_f 0.11. 50% EtOAc/Hexanes. HRMS (ESI) calcd for $C_{20}H_{25}O_5$ $(M+H^+)^+$ 345.1702, found 345.1697.

NMR data were recorded in pyridine-D_5.

^{1}H NMR isolation	^{1}H NMR synthetic	^{13}C NMR isolation	^{13}C NMR synthetic
6.20 (q, 1 H, *J* = 1.6 Hz)	6.20 (d, 1 H, *J* = 1.3 Hz)	193.76	193.80
5.12 (dd, 1 H, *J* = 14.0, 2.8 Hz)	5.12 (dd, 1 H, *J* = 13.9, 2.8 Hz)	172.92	172.95
5.08 (br. dq, 1 H, *J* = 2.6, 0.6 Hz)	5.08 (d, 1 H, *J* = 2.4 Hz)	172.22	172.27
4.98 (ddd, 1 H, *J* = 4.2, 2.8, 0.6 Hz)	4.98 (m, 1H)	146.21	146.15
4.78 (dq, 1 H, *J* = 2.6, 1.4 Hz)	4.79 (dd, 1 H, *J* = 2.4, 1.4 Hz)	140.79	140.82
4.61 (s, 1 H)	4.58 (s, 1 H)	138.96	138.92
2.54 (br. dd, 1 H, *J* = 14.5, 13.0, 2.0, 0.6 Hz)	2.55 (m, 1 H)	133.67	133.63
2.50 (s, 3 H)	2.49 (s, 3 H)	113.52	113.52
2.32 (dd, 1 H, *J* = 14.5, 4.0 Hz)	2.32 (m, 1 H)	81.03	80.98
2.18 (dd, 1 H, *J* = 14.5, 3.5 Hz)	2.18 (dd, 1 H, *J* = 14.6, 3.5 Hz)	79.18	79.18
2.11 (dd, 1 H, *J* = 14.0, 4.2 Hz)	2.11 (dd, 1 H, *J* = 13.9, 4.2 Hz)	62.20	62.20
1.96 (d, 3 H, *J* = 1.6 Hz)	1.96 (d, 3 H, *J* = 1.3 Hz)	60.34	60.31
1.92 (dddd, 1 H, *J* = 14.0, 11.0, 5.5, 2.0 Hz)	1.93 (m, 1H)	41.39	41.36
1.80 (br. ddd, 1 H, *J* = 11.0, 4.0, 3.5, “small“ Hz)	1.81 (m, 1 H)	39.73	39.65
1.65 (dd, 3 H, *J* = 1.4, 0.6 Hz)	1.66 (s, 3 H)	35.20	35.16
1.43 (ddd, 1 H, *J* = 14.0, 13.0, 2.0 Hz)	1.45 (m, 1 H)	34.96	34.90
1.40 (ddd, 1 H, *J* = 14.5, 5.5, 2.0 Hz)	1.40 (ddd, 1 H, *J* = 14.4, 5.7, 2.1 Hz)	24.53	24.51
		22.85	22.81
		17.32	17.26
		12.65	12.65

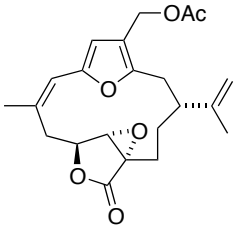

18-Acetoxy coralloidolide A (2.3). A solution of coralloidolide E (**1.36**) (8.0 mg, 0.023 mmol) in AcOH (0.4 mL) was stirred for 12 hr at room temperature. The solution was diluted with Et_2O (5 mL) and H_2O (5 mL). The layers were separated, and the aqueous layer was extracted with Et_2O (3 X 5 mL). The combined organic extracts were washed 1 X saturated $NaHCO_3$ (5 mL), 1 X brine (5 mL), dried, filtered and concentrated *in vacuo*. The crude material was purified by flash chromatography (20% EtOAc/hexanes) to give 2.1 mg (23%) of **2.3** as a clear residue.

R_f 0.91. 50% EtOAc/Hexanes. ^{1}H NMR (600 MHz): δ 6.38 (s, 1 H), 6.18 (s, 1 H), 4.97 (s, 1 H), 4.87 (s, 1 H), 4.65 (m, 3 H), 3.75 (s, 1 H), 3.60 (t, 1 H, *J* = 12.9 Hz), 2.69-2.46 (m, 5 H), 2.11 (s, 3 H), 1.92 (s, 3 H), 1.75 (s, 3 H), 1.58 (m, 1 H), 1.01 (t, 1 H, *J* = 13.7 Hz), 0.84 (m, 1 H). ^{13}C (150 MHz): δ 172.2, 170.1, 150.0, 148.4, 144.6, 123.8, 121.2, 117.6, 116.7, 113.3, 77.4, 69.2, 61.2, 60.7, 43.9, 32.9, 30.9, 27.8, 21.6, 21.0, 19.3, 9.4. IR: 2924, 2361, 1782, 1621, 1447, 1376, 1225, 1035. HRMS (EI)$^+$ calcd for $C_{22}H_{26}O_6$ (M)$^+$ 386.1729, found 386.1726.

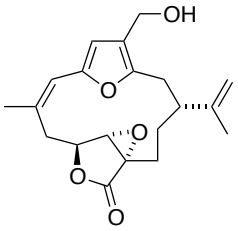

18-Hydroxy coralloidolide A (2.4). A solution of coralloidolide E (**1.36**) (8.0 mg, 0.023 mmol) in 3:1 acetone/0.5% H_2SO_4 (3.2 mL) was stirred for 12 hr at room temperature. The solution was diluted with EtOAc (8 mL) and brine (8 mL). The layers were separated, and the aqueous layer was extracted with EtOAc (2 X 8 mL). The combined organic extracts were dried, filtered and concentrated *in vacuo*. The crude material was purified by flash chromatography (5% EtOAc/dichloromethane) to give 2.1 mg (26%) of **2.4** as an off-white solid.

R_f 0.75. 33% Hexanes/EtOAc. ^{1}H NMR (600 MHz): δ 6.39 (s, 1 H), 6.13 (s, 1 H), 4.96 (s, 1 H), 4.87 (s, 1 H), 4.65 (dd, 1 H, *J* = 12.6, 4.4 Hz), 4.25 (d, 2 H, *J* = 4.6 Hz), 3.76 (s, 1 H), 3.58 (t, 1 H, *J* = 12.8 Hz), 2.60 (m, 6 H), 1.92 (s, 3 H), 1.75 (s, 3 H), 1.58 (m, 2 H), 1.02 (t, 1 H, *J* = 13.7 Hz). ^{13}C (150 MHz): δ 172.3, 149.5, 149.0, 144.7, 128.9, 118.0, 117.5, 115.6, 113.3, 77.8, 67.7, 61.3, 60.8, 44.0, 32.5, 30.8, 27.7, 21.6, 19.3, 9.4. IR: 3433, 2936, 2361, 1778, 1693, 1439, 1076, 908, 737. HRMS (EI)$^+$ calcd for $C_{20}H_{24}O_5$ (M)$^+$ 342.1467, found 342.1460.

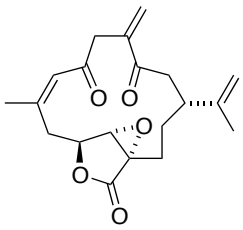

***Exo*-methylene isomer of coralloidolide E (2.1).** To a solution of coralloidolide E (**1.36**) (21.6 mg, 0.063 mmol) in CH_2Cl_2 (0.6 mL) was added DBU (1.9 mg, 0.013 mmol). After 12 hr, the solution was diluted with CH_2Cl_2 (5 mL) and H_2O (5 mL). The layers were separated, and the aqueous layer was extracted with CH_2Cl_2 (5 mL). The combined organic extracts were dried, filtered and concentrated *in vacuo*. The crude material was purified by flash chromatography (20% EtOAc/hexanes) to give 11.0 mg (51%) of **2.1** as an off-white solid and 8.0 mg (37%) of coralloidolide E (**1.36**) as a white solid.

R_f 0.75, 50% EtOAc/Hexanes. HRMS $(EI)^+$ calcd for $C_{20}H_{24}O_5$ $(M)^+$ 344.1624, found 344.1620. NMR data were recorded in acetone-d_6 solution (the compound is only slightly soluble in acetone).

^{1}H NMR reported	^{1}H NMR synthetic	^{13}C NMR reported	^{13}C NMR synthetic
6.54 (br q, 1 H, *J* = 1.3, "small" Hz)	6.54 (d, 1 H, *J* = 1.8 Hz)	none reported	202.5
6.30 (br d, 1 H, *J* = 0.9, "small" Hz)	6.30 (s, 1 H)	none reported	198.8
6.04 (br dd, 1 H, *J* =1.5, 0.6, "small" Hz)	6.03 (d, 1 H, *J* = 1.5 Hz)	none reported	171.9
4.86 (dq, 1 H, *J* = 1.8, 1.5 Hz)	4.86 (p, 1 H, *J* = 1.3 Hz)	151.9	151.9
4.84 (ddq, 1 H, *J* = 1.8, 0.9, 0.9 Hz)	4.84 (dd, 1 H, *J* = 1.6, 0.8 Hz)	146.6	146.6
4.73 (dd, 1 H, *J* = 10.0, 5.0 Hz)	4.73 (dd, 1 H, *J* = 10.1, 4.9 Hz)	144.3	144.3
3.79 (s, 1 H)	3.80 (s, 1 H)	128.4	128.4
3.72 (br d, 1 H, *J* = 15.0, 1.5, 0.9 Hz)	3.72 (d, 1 H, *J* = 15.3 Hz)	127.7	127.7
3.55 (dd, 1 H, *J* = 12.0, 10.0 Hz)	3.55 (t, 1 H, *J* = 11.2 Hz)	111.0	111.0
3.28 (br d, 1 H, *J* = 15.0, 0.6 Hz)	3.28 (d, 1 H, *J* = 15.2 Hz)	76.3	76.3
3.12 (dd, 1 H, *J* = 12.0, 3.8 Hz)	3.12 (dd, 1 H, *J* = 12.5, 3.6 Hz)	61.3	61.3
2.93 (br dd, 1 H, *J* = 12.0, 5.0, "small" Hz)	2.94 (m, 1 H)	60.3	60.3
2.66 (m, 1 H, *J* =	2.67 (ddt, 1 H, *J* =	46.9	46.9

11.5, 3.8, 0.9 Hz)	11.3, 7.5, 4.0 Hz)		
2.36 (dd, 1 H, *J* = 12.0, 11.5 Hz)	2.37 (t, 1 H, *J* = 12.0 Hz)	43.3	43.3
2.05 ("submerged", 3 H)	presumably submerged beneath acetone signal	40.7	40.7
"ca.1.98" ("superimposed", 2 H)	none observed	34.9	35.0
"ca.1.8" ("superimposed", 2 H)	1.85 (m, 1 H)	25.2	25.2
1.77 (dd, 3 H, *J* = 1.5, 0.9 Hz)	1.78 (s, 3 H)	23.9	23.9
	1.76 (m, 1 H)	20.3	20.3
		19.9	19.9

2.6 - Appendix

Characterization Data for 1.32, 1.33, 1.34, 1.36, 2.1, 2.3 and 2.4.

1.32

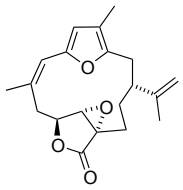

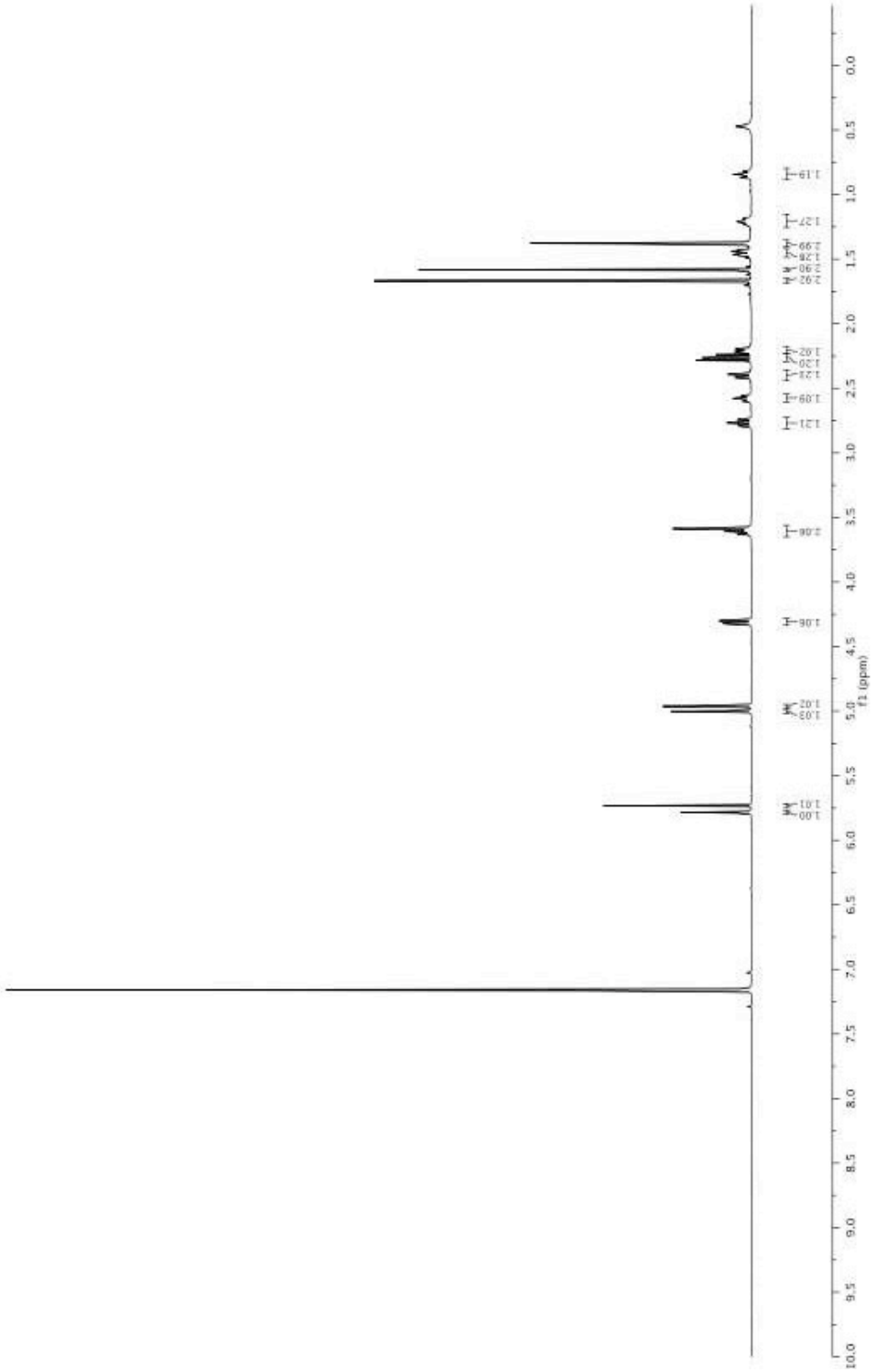
1.19
1.27
2.99
2.98
2.90
2.92
1.02
1.20
1.24
1.09
1.21
2.06
1.06
1.03
1.02
1.00
1.01
f1 (ppm)

1.32

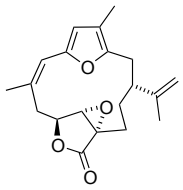

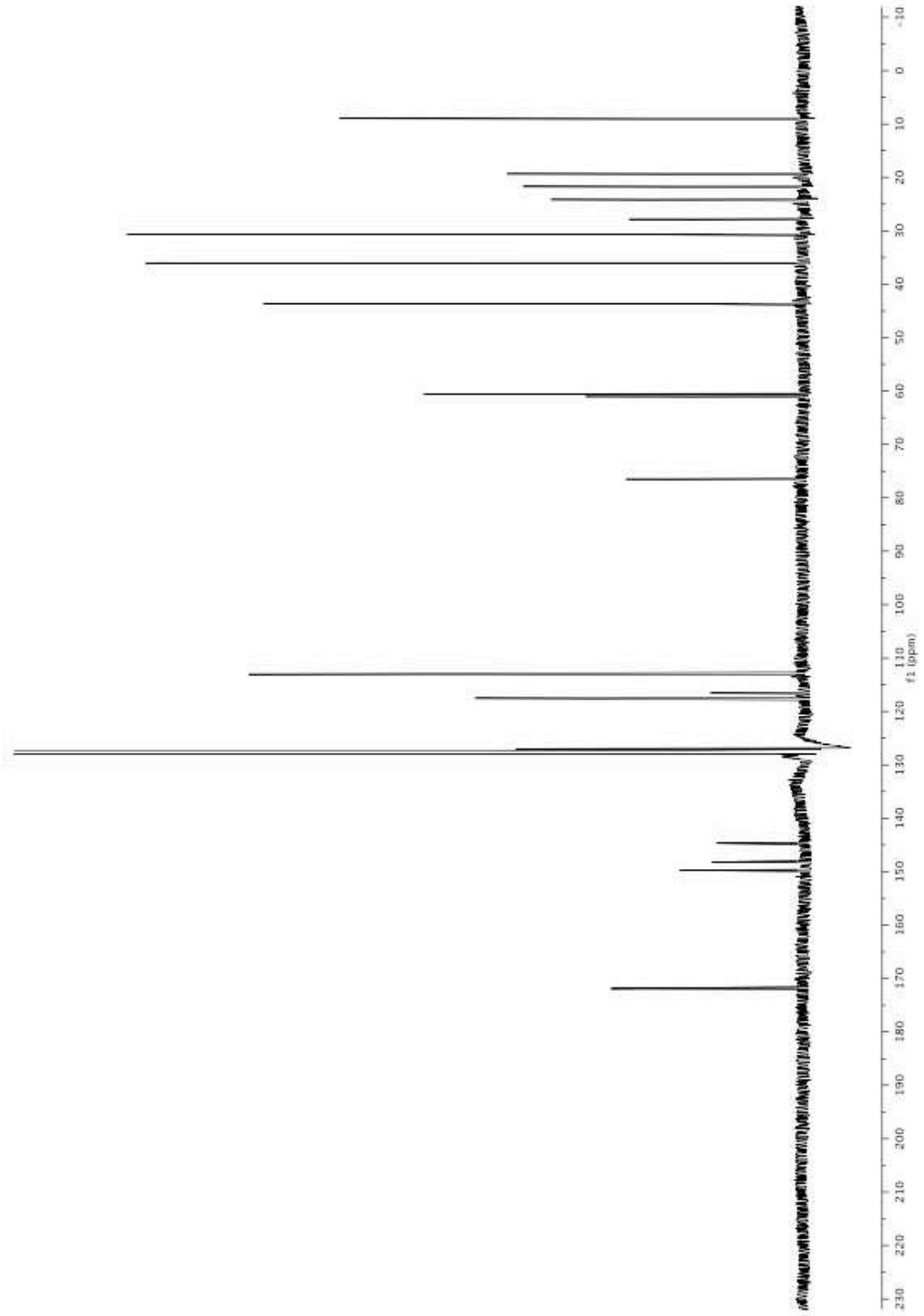

1.36

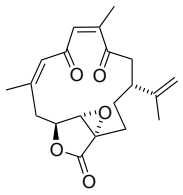

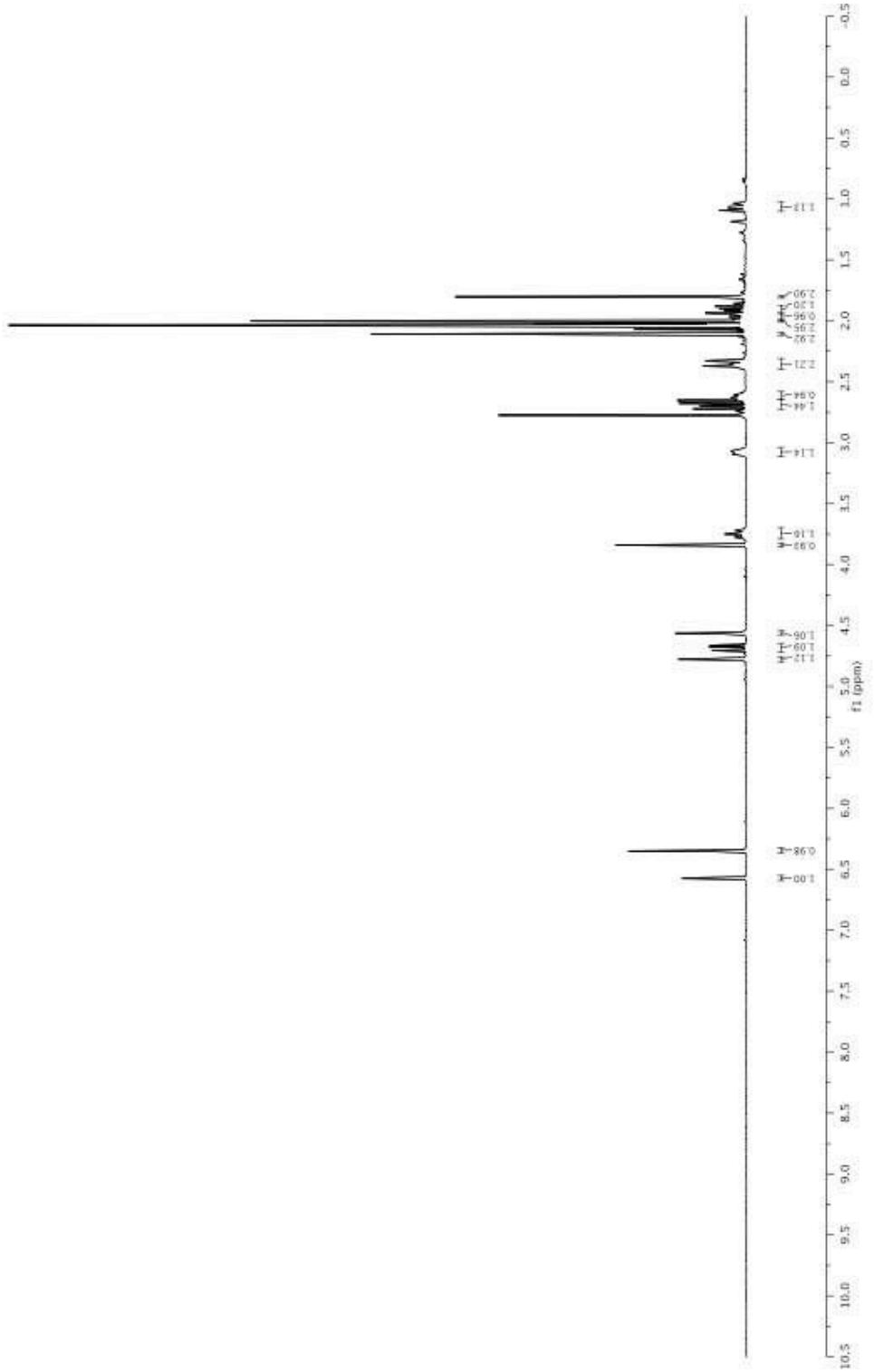

1.36

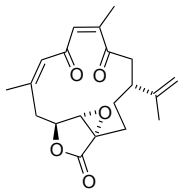

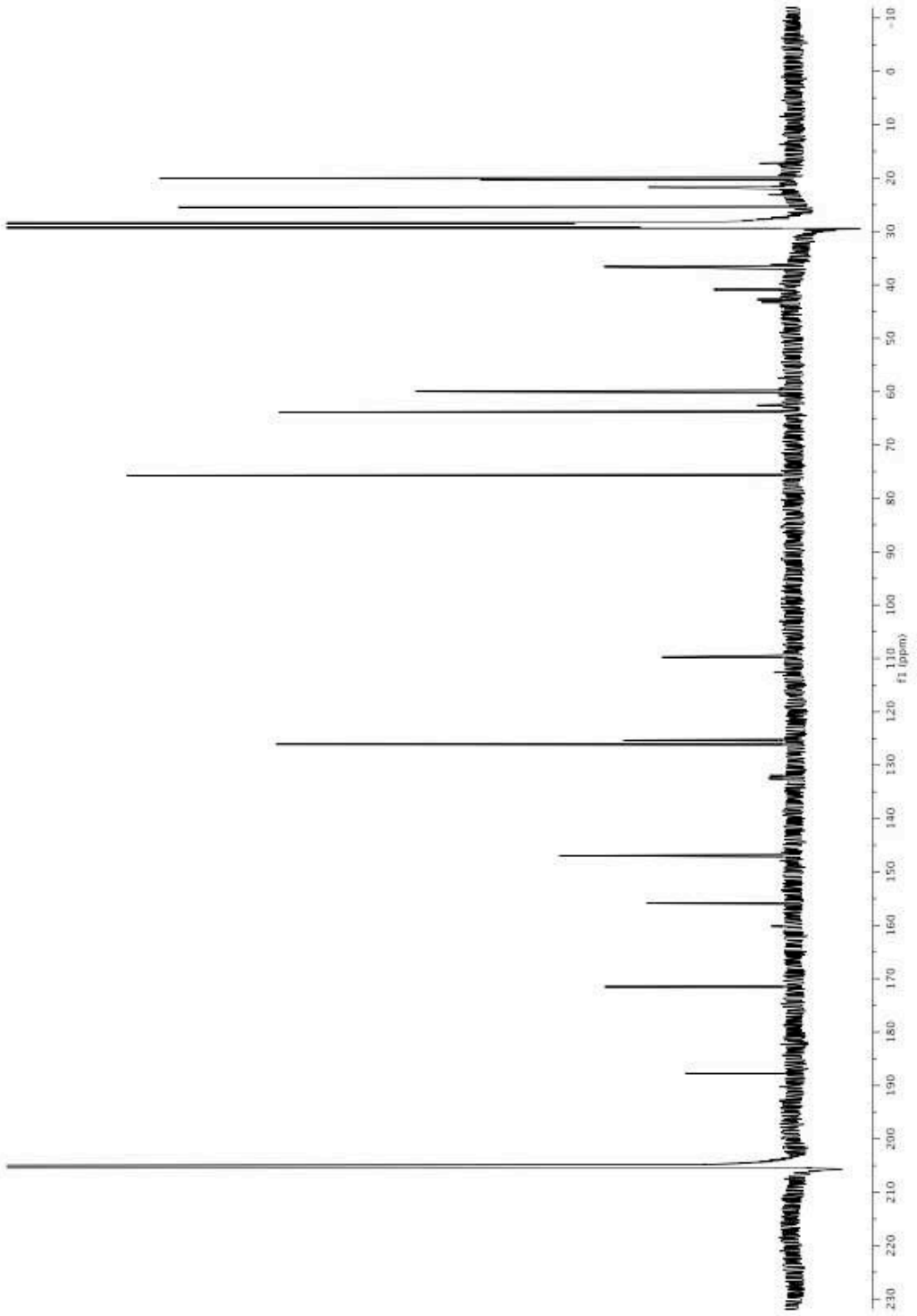

1.33

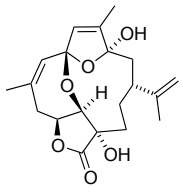

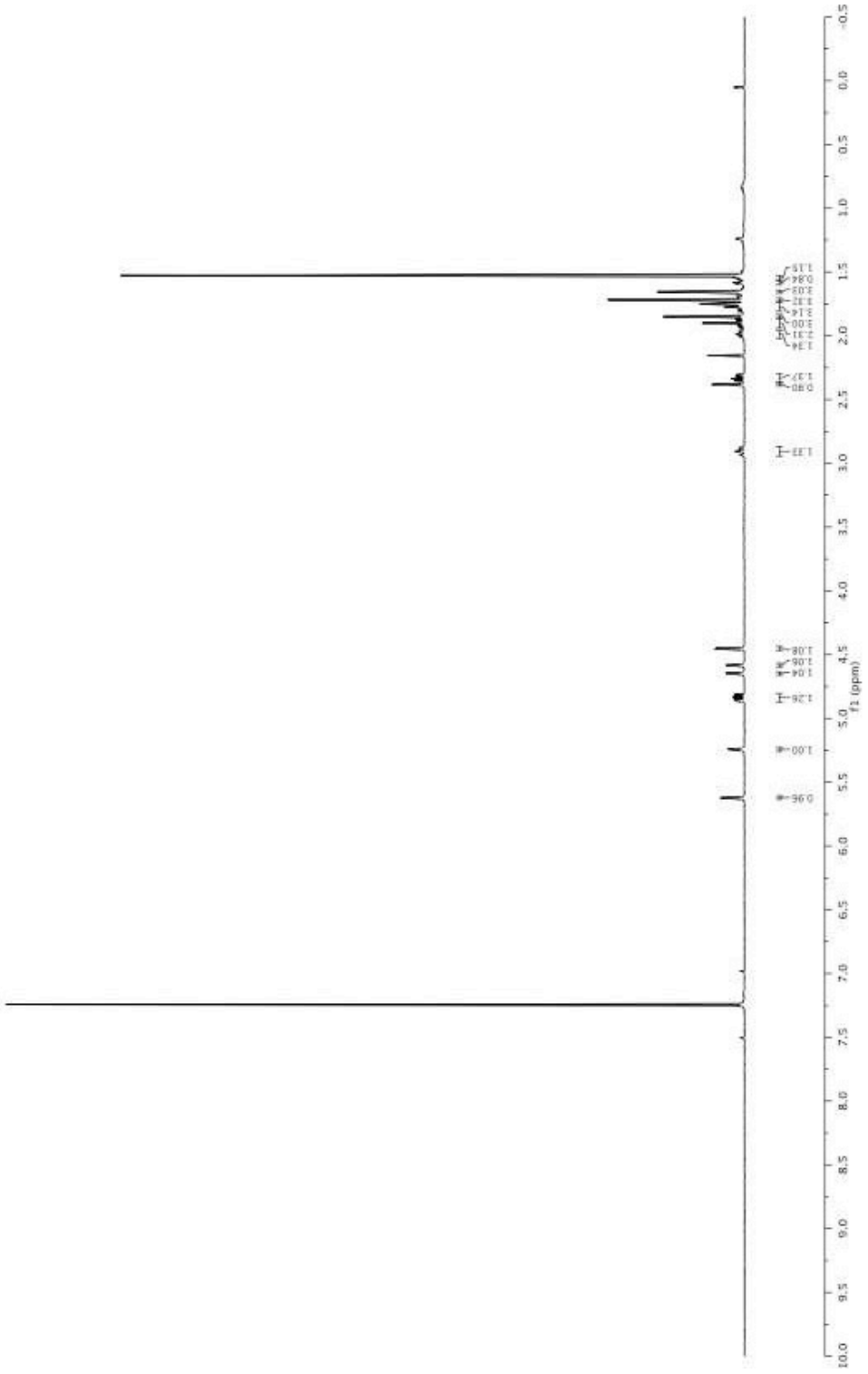

1.33

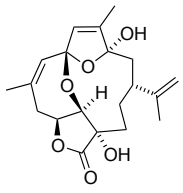

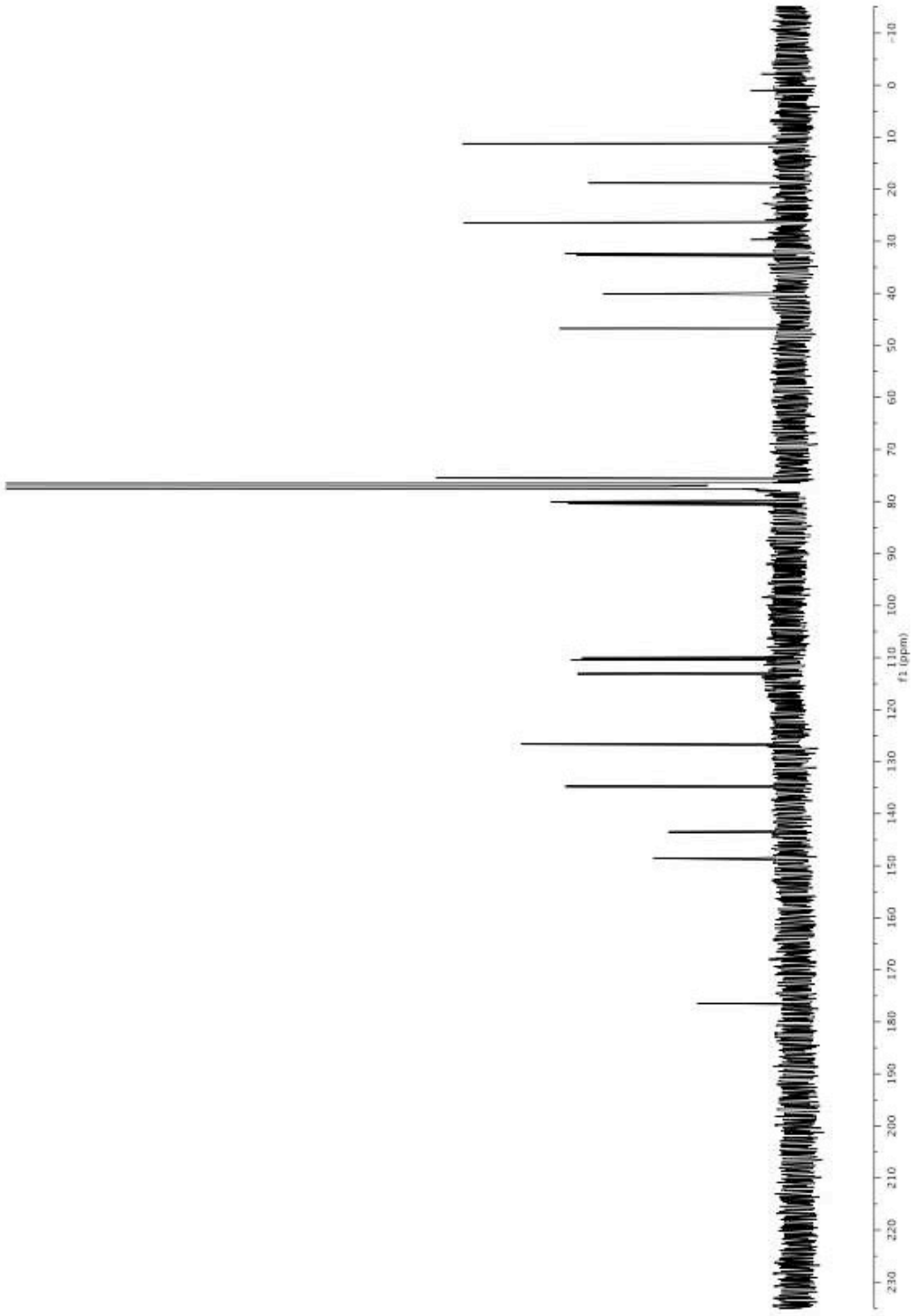

1.34

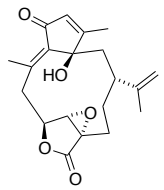

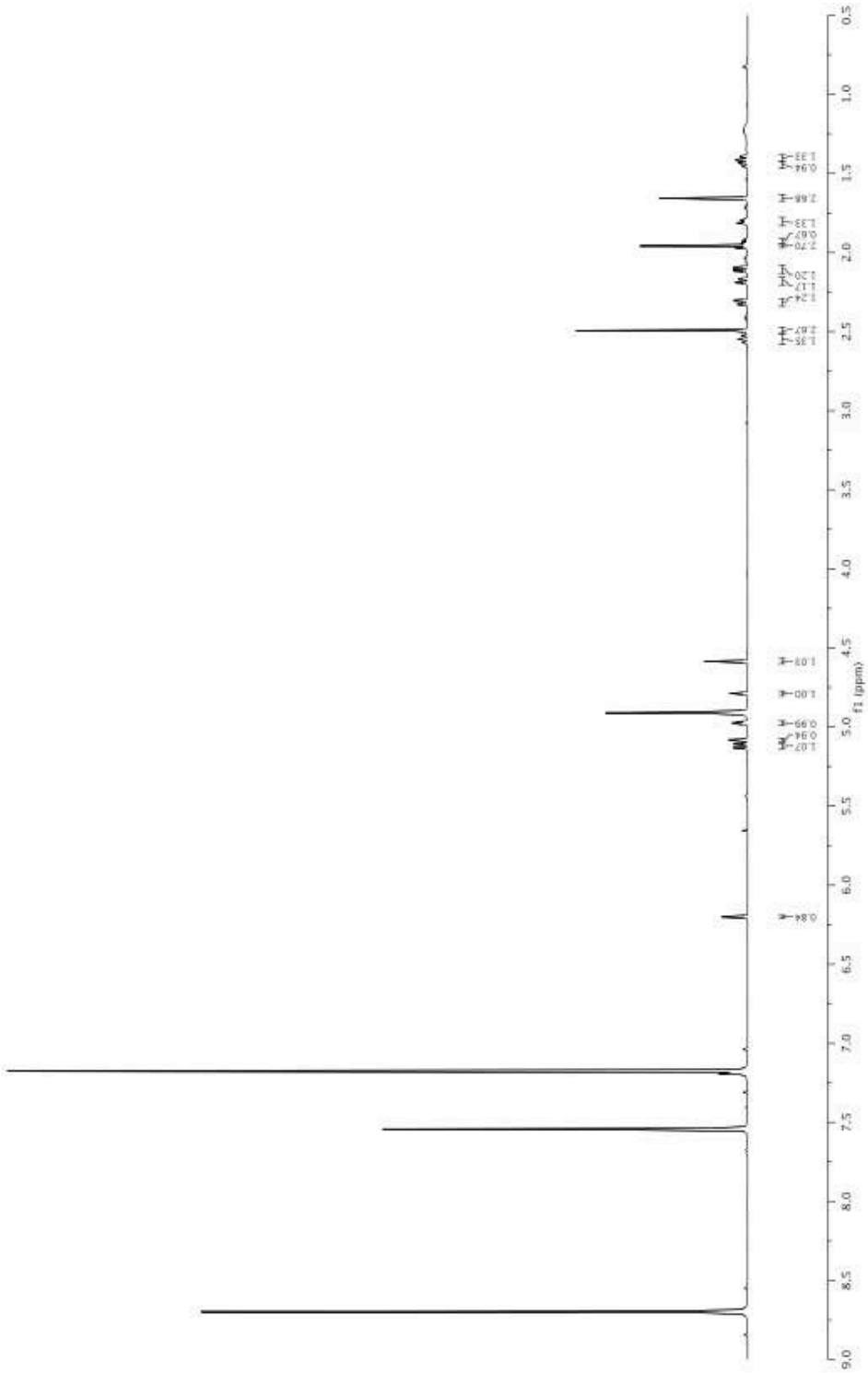

1.34

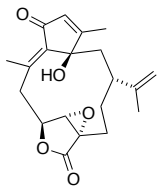

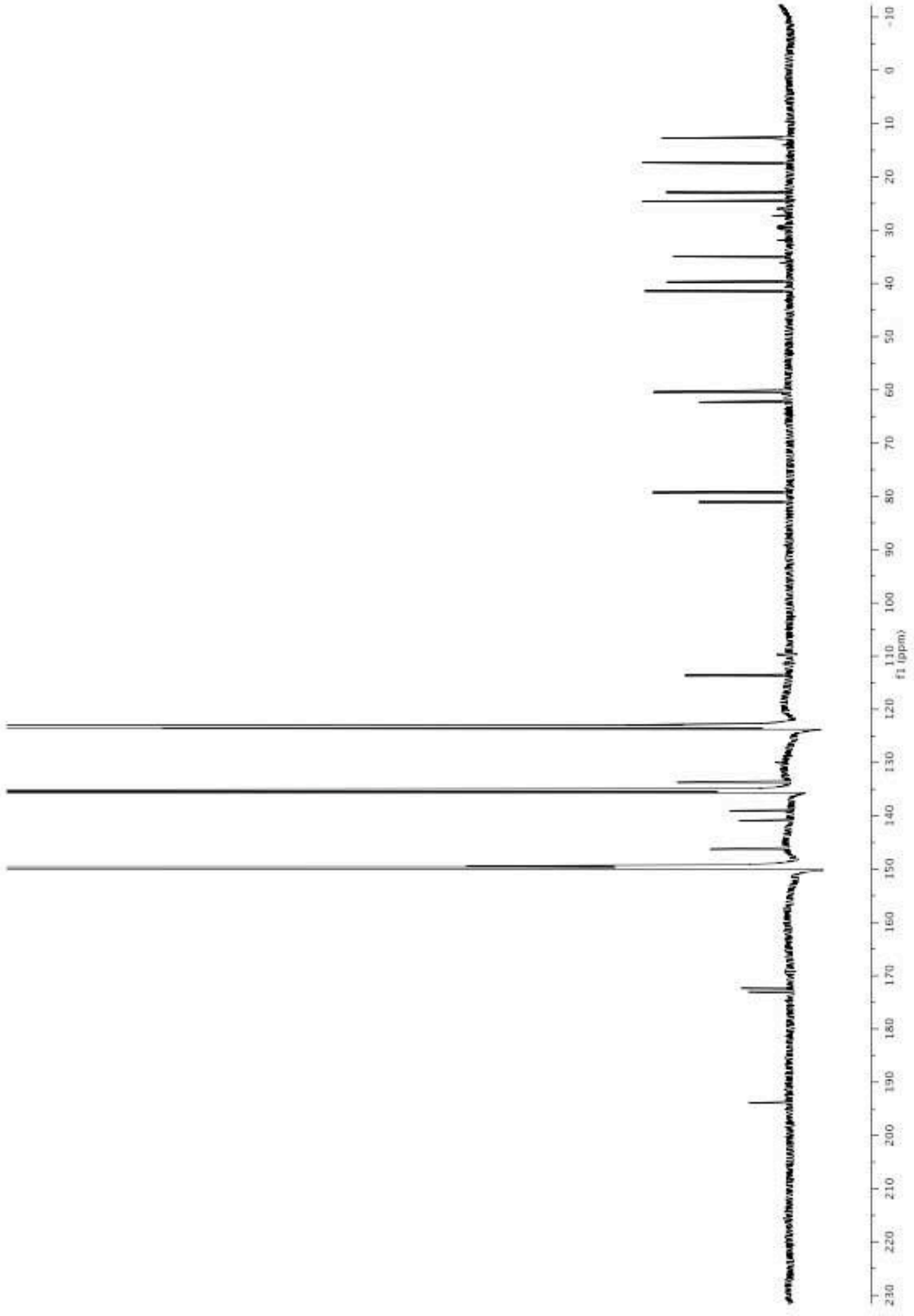

2.3

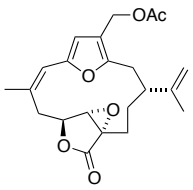
OAc
O
O
O
O

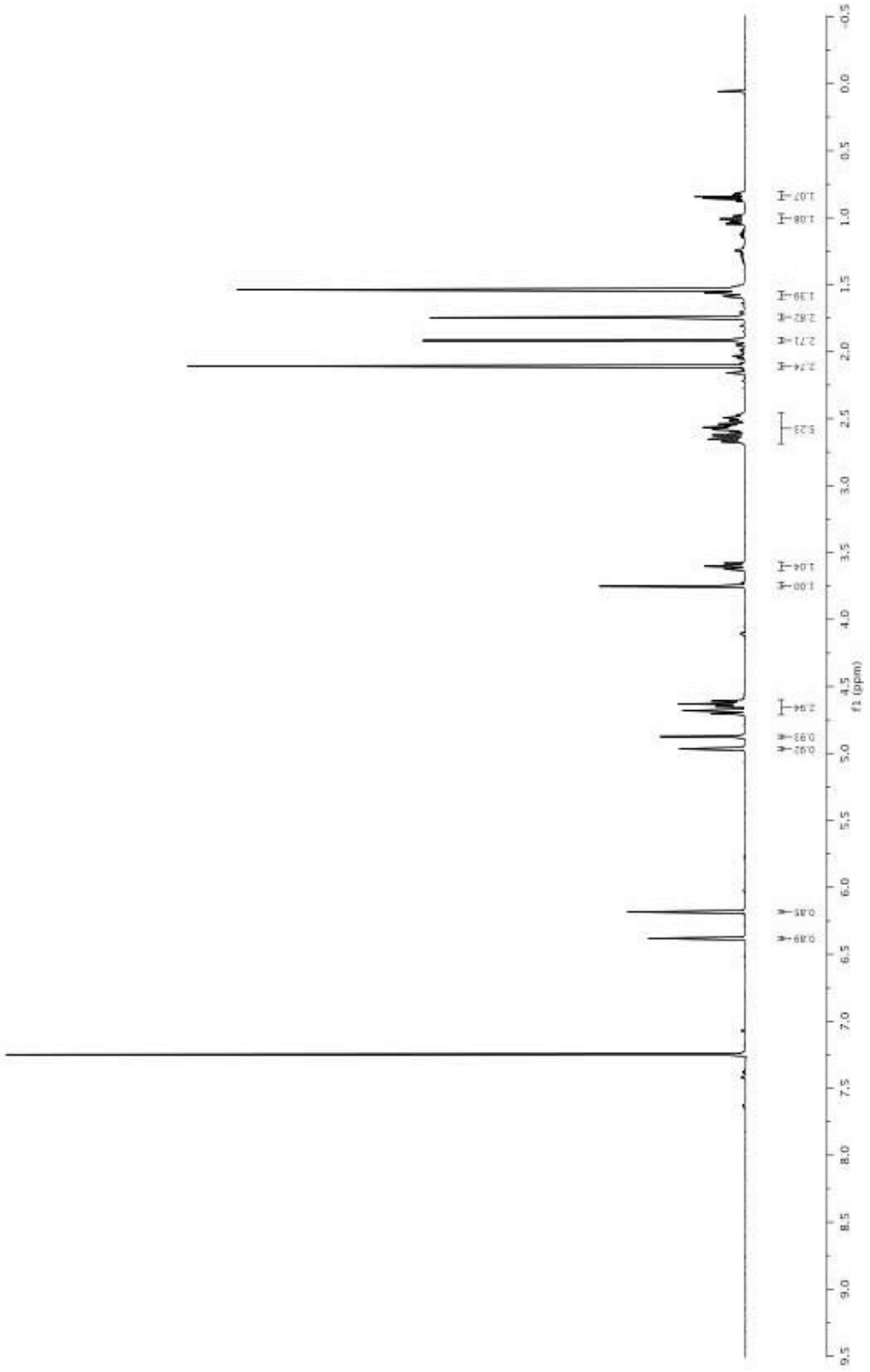
1.07
1.08
1.39
2.82
2.71
2.74
5.23
1.04
1.00
2.94
0.93
0.92
0.85
0.89
f1 (ppm)

2.4

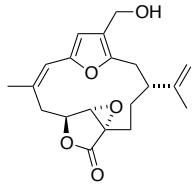

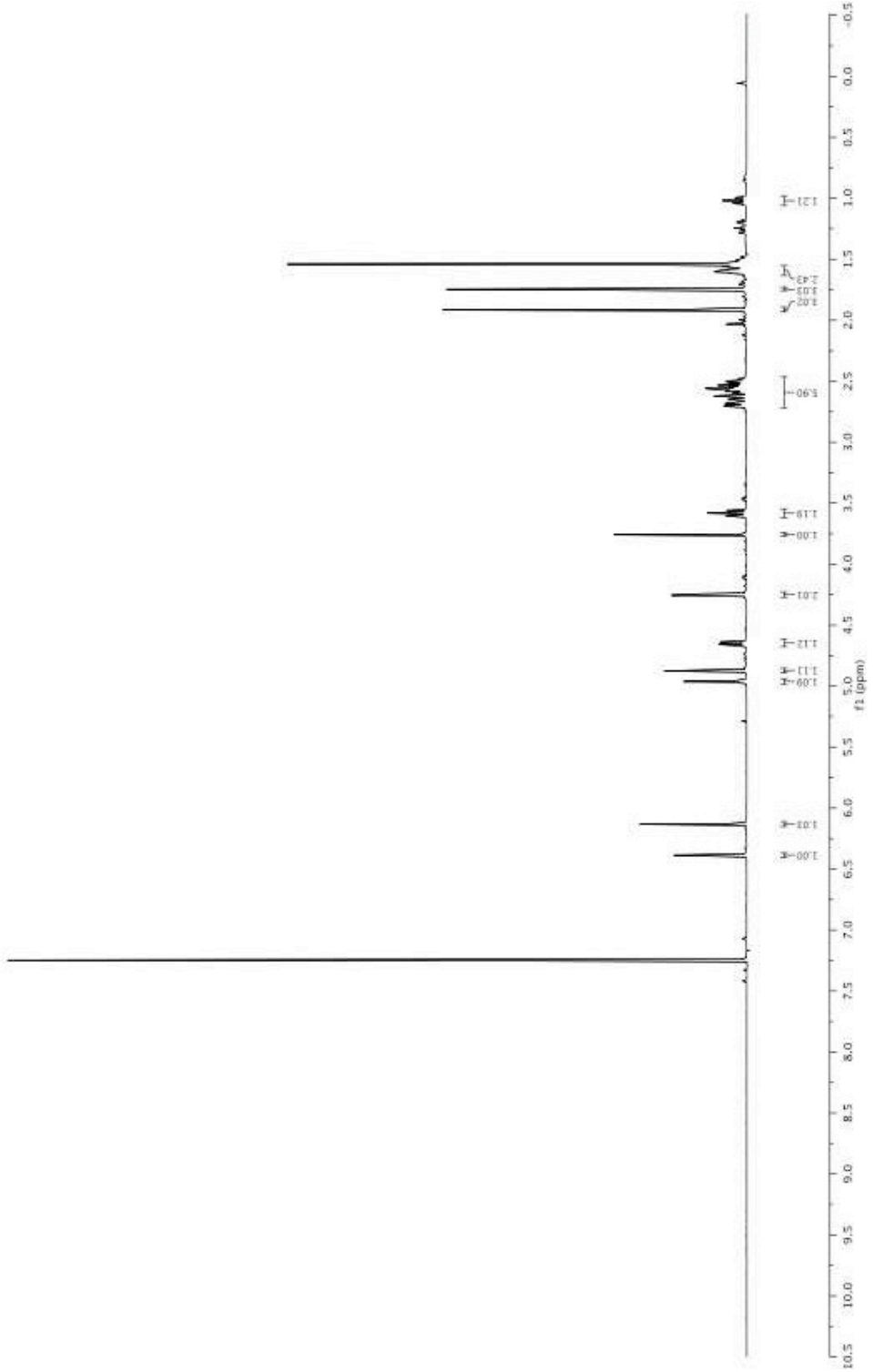

2.1

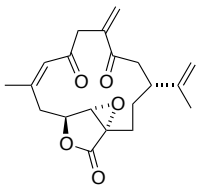

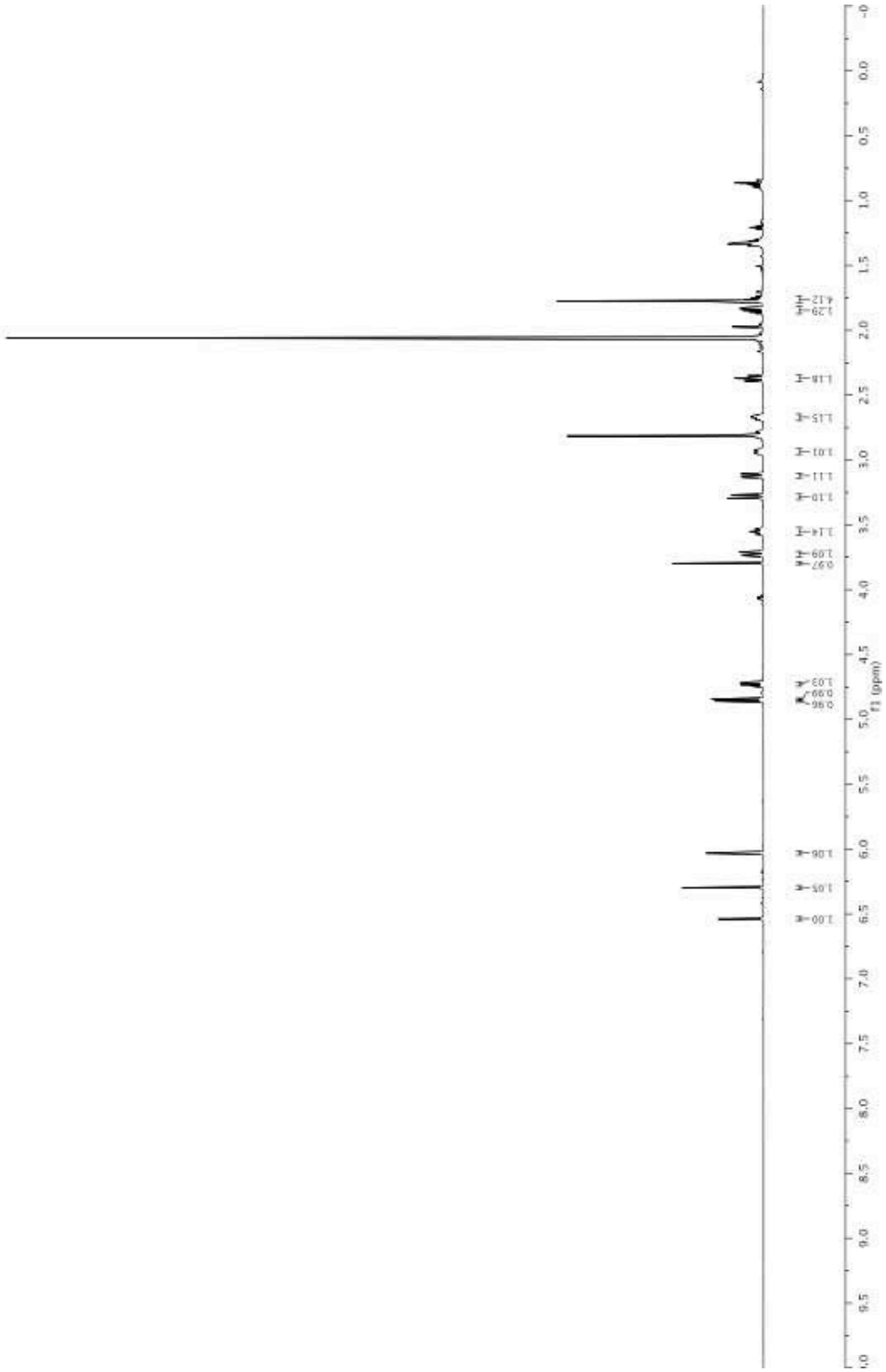

2.1

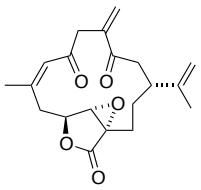

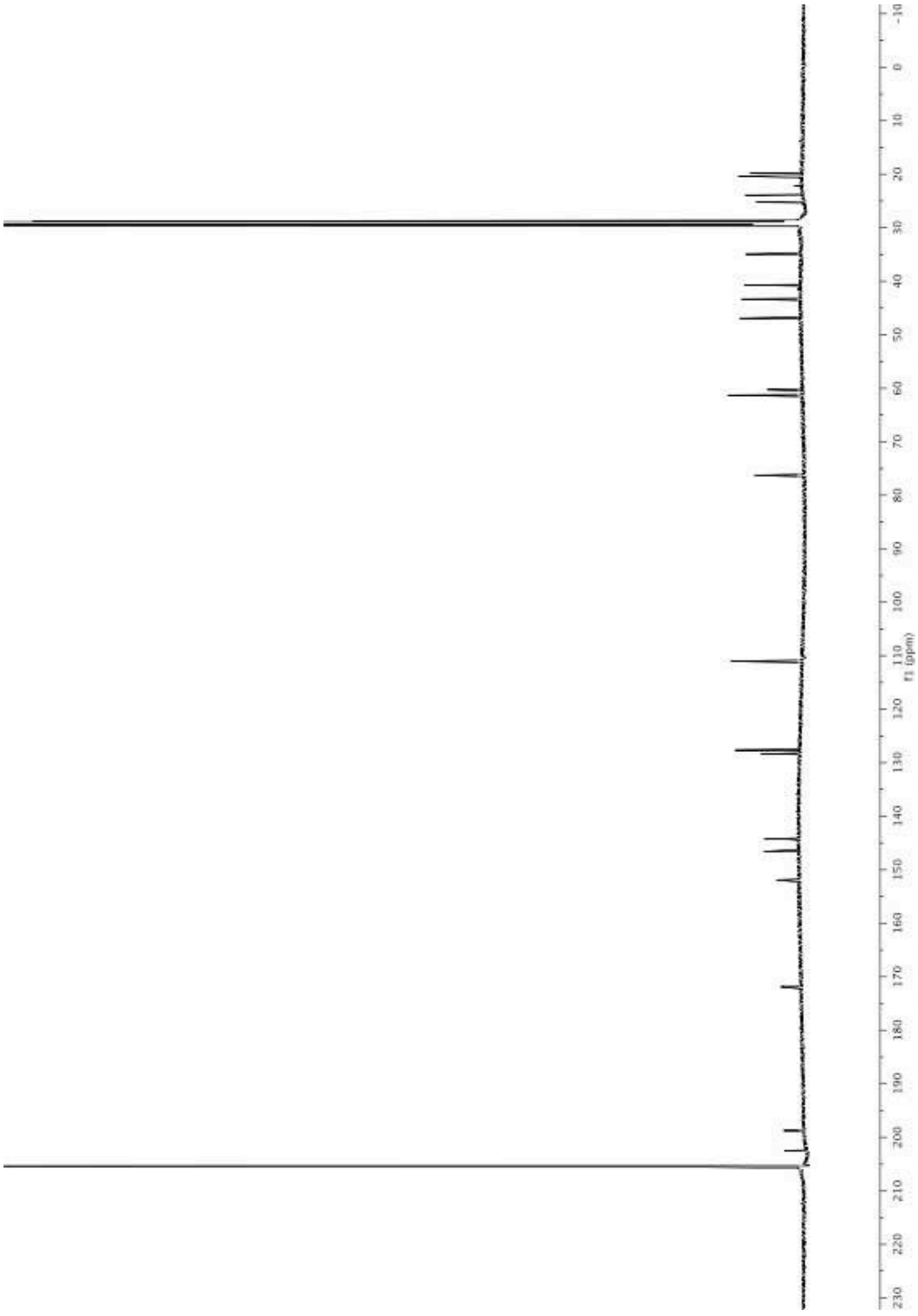

2.7 - Appendix

X-ray Crystallographic Data for Compound 1.36

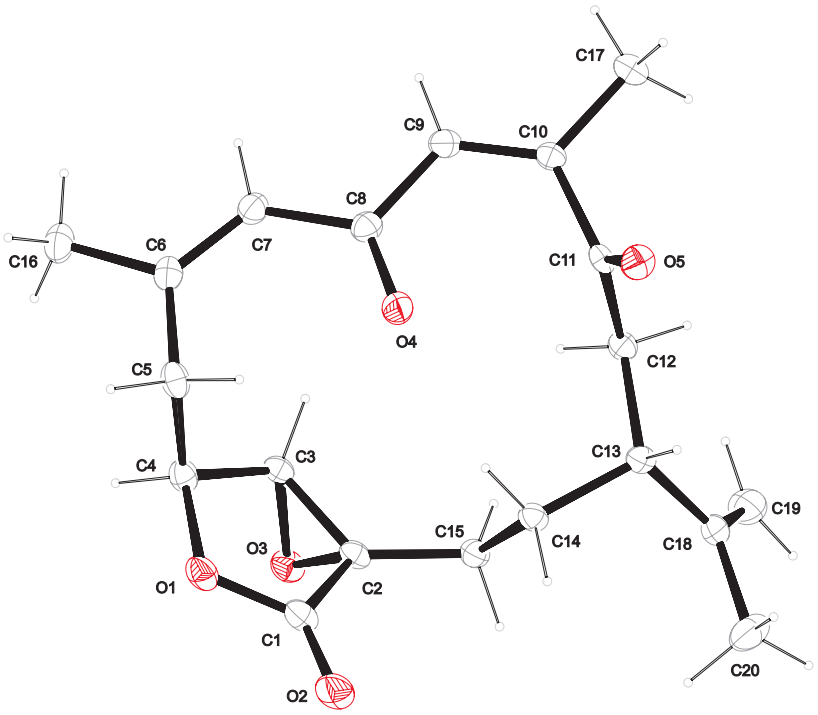

Crystallographic data for coralloidolide E (**1.36**).

	1
net formula	$C_{20}H_{24}O_5$
M_r/g mol^{-1}	344.402
crystal size/mm	0.49 × 0.10 × 0.06
T/K	200(2)
radiation	MoKα
diffractometer	'Oxford XCalibur'
crystal system	triclinic
space group	*P*1bar
a/Å	6.2781(5)
b/Å	11.6000(7)
c/Å	12.4238(10)
α/°	91.699(6)
β/°	98.947(7)
γ/°	95.379(6)
V/Å^3	888.93(11)
Z	2
calc. density/g cm^{-3}	1.28672(16)
μ/mm^{-1}	0.092
absorption correction	'multi-scan'
transmission factor range	0.99166–1.00000
refls. measured	6224
R_{int}	0.0270
mean σ(I)/I	0.0920
θ range	4.30–26.35
observed refls.	1967
x, y (weighting scheme)	0.0315, 0
hydrogen refinement	constr
refls in refinement	3598
parameters	229
restraints	0
$R(F_{obs})$	0.0389
$R_w(F^2)$	0.0773
S	0.792
shift/error$_{max}$	0.001
max electron density/e Å^{-3}	0.175
min electron density/e Å^{-3}	−0.188

2.8 References and Notes

1. (a) M. D'Ambrosio, D. Fabbri, A. Guerriero and F. Pietra, *Helv. Chim. Acta.* 1987, **70**, 63. (b) M. D'Ambrosio, A. Guerriero and F. Pietra, *Helv. Chim. Acta*, 1989, **72**, 1590. (c) M. D'Ambrosio, A. Guerriero and F. Pietra, *Helv. Chim. Acta*, 1990, **73**, 804.
2. T.J. Kimbrough, P.A. Roethle, P. Mayer, D. Trauner, *Angew. Chem. Int. Ed.*, 2010, **49**, 2619.
3. P. A. Roethle, P. T. Hernandez and D. Trauner, *Org. Lett.*, 2006, **8**, 5901.

Chapter 3

Progress Towards the Pentacyclic Core of Bielschowskysin – a Model System Based on Bipinnatin J

3.1 Introduction

The majority of the world's corals lie at shallow depths in tropical waters. Near the surface they absorb sunlight, which is important for the animals' survival. This is due to the fact that many of these organisms exist in a symbiotic relationship with photosynthetic algae. The algae – typically dinoflagellates of the genus *Symbiodinium* - provide the host corals with oxygen, energy-rich carbon compounds such as glucose, and amino acids.[1] In return the corals provide the algae with shelter and carbon dioxide. They also provide nitrogenous compounds and phosphates as waste products, which are used in photosynthesis.

Gorgonian octocorals (the sea whips, sea feathers, sea plumes, and sea fans) are found primarily in the shallow waters of the Atlantic near Florida, Bermuda, and the West Indies. With over 190 documented species, the gorgonians have proven to be an excellent source of bioactive natural products.[2] It was near Old Providence Island in the Southwestern Caribbean Sea that in 2003, a specimen of the reef-dwelling sea plume *Pseudopterogorgia kallos* was harvested and extracted by Rodriguez *et al.* to yield bielschowskysin (**1.38**)[3]. Bielschowskysin derives its name from the marine biologist who classified *P. kallos*, Eva Bielschowsky.

Figure 3.1 Bielschowskysin.

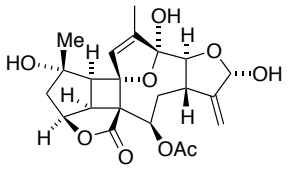

bielschowskysin (**1.38**)

The framework of bielschowskysin (**1.38**) (Figure 3.1) contains a highly substituted cyclobutane ring at its core, in addition to two cyclic hemiacetals, two isolated alkenes, one acetate, one tertiary alcohol and one lactone as functional groups. The absolute configuration is unknown, but the relative configuration has been confirmed via X-ray crystallography. Bielschowskysin exhibits antimalarial activity against *Plasmodium falciparum* (IC_{50} = 10 μg/ml) and potent, specific *in vitro* cytotoxic activity against EKVX nonsmall cell lung cancer (GI_{50} < 0.01 μM) and CAKI-1 renal cancer (GI_{50} = 0.51 μM).[3] The beguiling architecture of this densely functionalized molecule, its bioactivity, and its scarcity render it an ideal target for total synthesis.

Although the biosynthetic pathway to bielschowskysin has not been confirmed, it has been proposed that the cyclobutane ring is the result of a transannular [2+2] cycloaddition of *exo*-alkylidene dihydrofuran **1.58** (Scheme 3.1).[4] Intermediate **1.58** may result from epoxidation of hypothetical starting material **3.1** to give **3.2**, followed by vinylogous hydrolysis to give **1.58**. Alternatively, oxidation of the furan of **3.1** would furnish dienedione **3.3**, to which water could add in a conjugate addition to yield **1.58**. Although compound **3.1** is unknown as a natural

product, there remains the possibility that it is synthesized by the coral before being funneled into the various oxidative manifolds.

Scheme 3.1 Proposed alternate biosynthetic pathways to bielschowskysin**.**

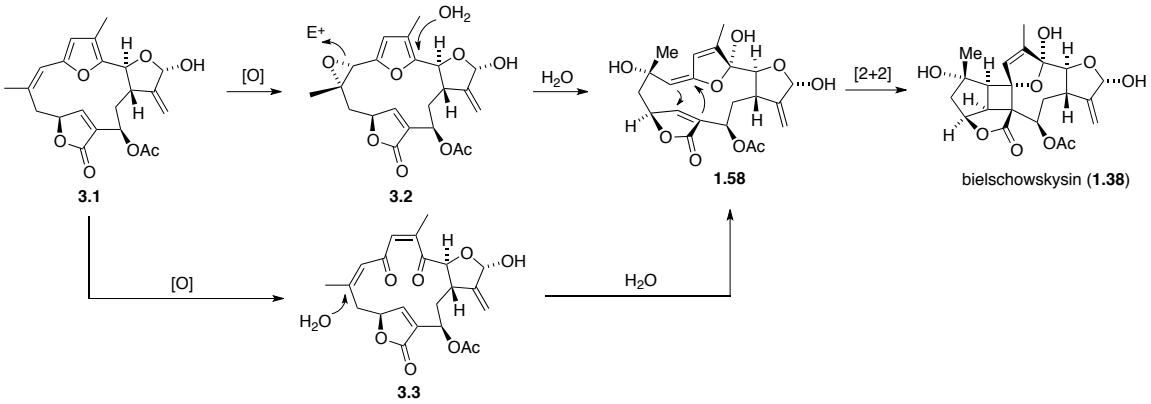

3.2 Published Work Towards the Total Synthesis of Bielschowskysin

To date there have been no total syntheses of bielschowskysin reported. However, two successful efforts to synthesize the cyclobutane core of the natural product have appeared. In the first, Sulikowski *et al.* subjected alcohol **3.4** to irradiation in acetone with a sun lamp, effecting an intramolecular [2+2] cycloaddition to provide cyclobutane **3.5** in 50% yield with a 3.6:1 diastereomeric ratio (Scheme 3.2).[5] This reaction is believed to proceed through diradical intermediate **3.7**. Intermediate **3.7** could interconvert with diradical **3.9** by simple bond rotation. Also, under the photochemical conditions, starting material **3.4** was observed to isomerize and equilibrate with geometric isomer **3.8**. These two processes could account for the presence of the undesired diastereomeric product (**3.6**).

Scheme 3.2 Sulikowski's approach to the tetracyclic core of bielschowskysin.

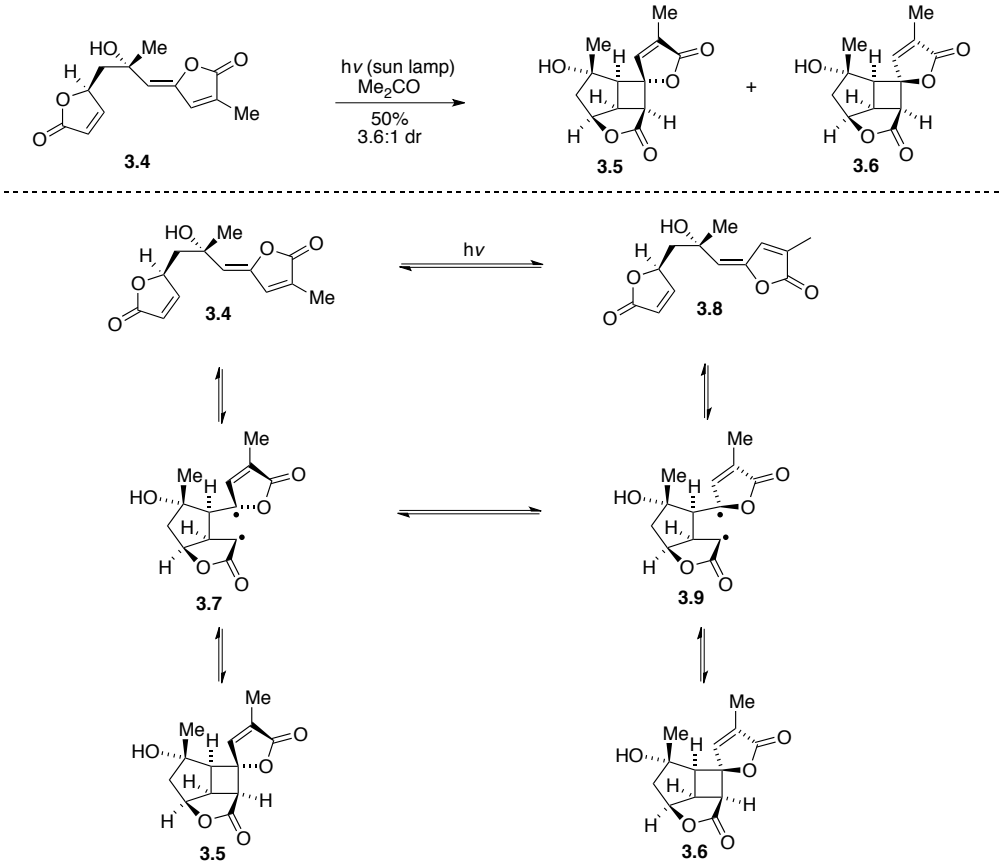

In the second approach, Lear *et al.* first prepared allene **3.11** in twelve steps from L-malic acid (**3.10**). Irradiation of **3.11** with three conventional UV lamps (λ=254 nm) in hexane/DCM effected an intramolecular [2+2] cycloaddition to give the single diastereomeric photoadduct **3.12** in 70% yield (Scheme 3.3).[6] The combination of geminal-substituted and 1,3-allenylic conformational effects are believed to play a role in enforcing the stereochemical outcome.

Scheme 3.3 Lear's approach to the tricyclic core of bielschowskysin.

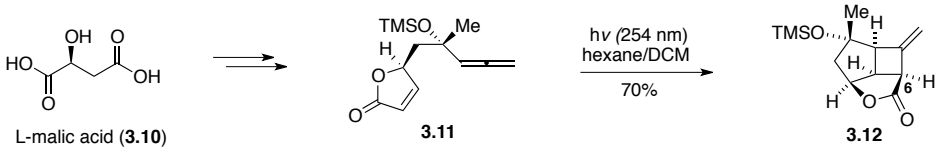

While these studies lend credence to the potential of using photochemical methods to produce the strained cyclobutane core of bielschowskysin, neither address the formation of a quarternary stereocenter at C6. This challenge would have to be met in order for these routes to ultimately be successful. Though the exact sequence of steps that nature uses to construct the natural product is unknown, biosynthetic considerations seem to point to a late-stage cycloaddition after the precursor macrocycle has been assembled. It is plausible that a well-organized transition state must be enforced by either an enzyme or the natural conformation of

the macrocycle in order to generate the cyclobutane core of bielschowskysin with all of the requisite substituents.

3.3 [2+2] Photocycloadditions of α,β-Unsaturated Lactones with Alkenes

The use of [2+2] photocycloadditions between enones and alkenes in the context of natural product synthesis is well established.[7] Frequently these reactions are carried out in an intramolecular fashion with the olefin being tethered to the enone or enoate. The earliest known observation of this reaction came in 1908 when Ciamician discovered that carvone (**3.13**) which had been exposed to "Italian sunlight" for one year had spontaneously undergone a [2+2] cycloaddition.[8] (Scheme 3.4). Later in the 1960s when this process was heavily investigated, the reaction was used by Eaton[9] to construct cubane (**3.17**), by Wiesner[10] to prepare 12-epilycopodine (**3.20**), and by Corey[11] who employed an intermolecular variant in his synthesis of caryophyllene (**3.23**). The methodology has continued to be refined over the past few decades to enable chemists to rapidly construct molecules of great complexity – often via a strategy of cyclobutane formation and subsequent fragmentation. In addition to enones, numerous examples have appeared which feature enoates or α,β-unsaturated lactones.[12]

Scheme 3.4 Classic examples of [2+2] photocycloadditions of enones.

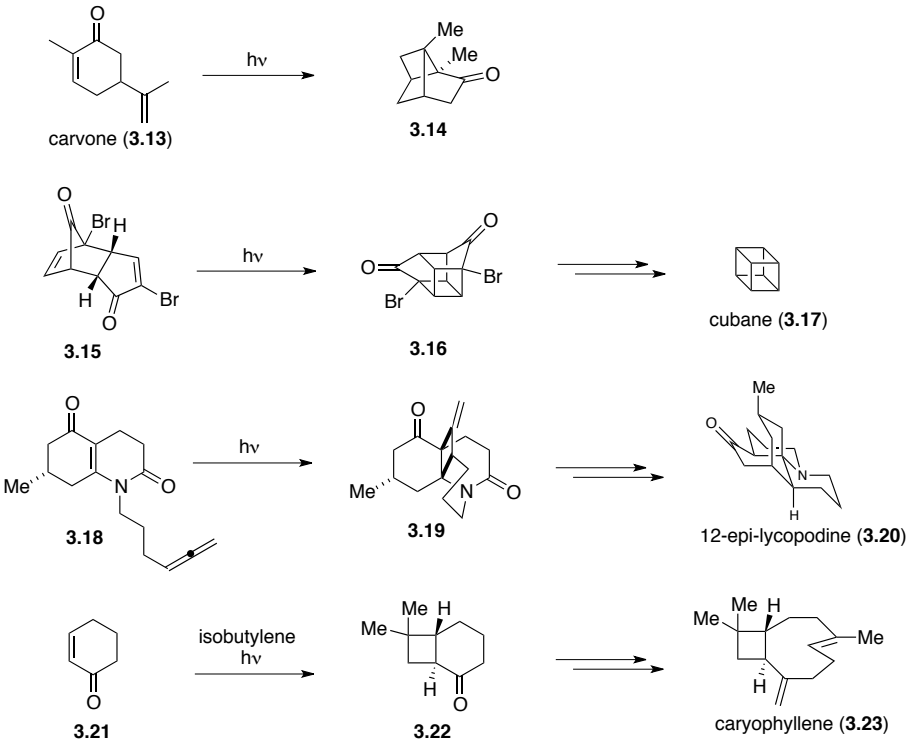

The mechanism of the reaction is thought to begin with photoexcitation of the enone to a singlet excited state. This state is typically very short lived and decays via intersystem crossing to the triplet state. Next, the enone forms an exciplex with the ground state alkene, and eventually single bond formation leads to the triplet diradical. This diradical must undergo spin inversion to the singlet diradical in order to allow closure to the cyclobutane (Scheme 3.5).[13]

Scheme 3.5 Mechanism of [2+2] photocycloaddition of enones.

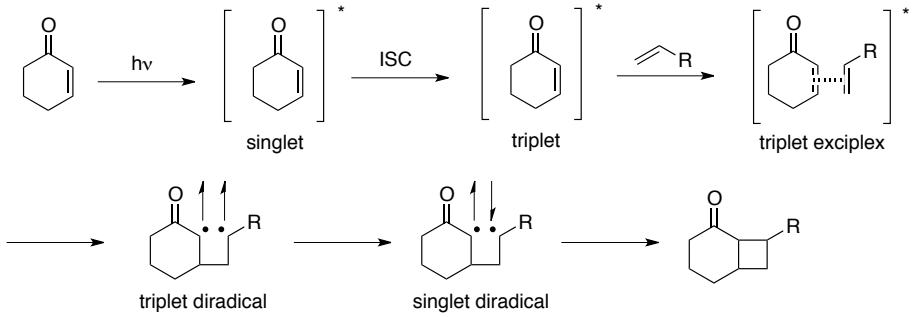

In the case of intermolecular reactions between enones and alkenes, the regioselectivity is controlled primarily by steric interactions and electrostatic interactions between the excited enone and alkene. The typical polarity of an enone is reversed in the excited state such that the ß carbon possesses a partial negative charge. This frequently results in a "head-to-tail" alignment of the reacting partners in which the alkene tends to align itself such that the electron-rich carbon bonds with the α carbon of the enone. In the case of intramolecular reactions, the regioselectivity is governed by the length of the tether. When the tether is two atoms long, "bent" products tend to predominate, while longer tethers tend to yield straight products (Scheme 3.6).[14] In cases where the precursor is more rigidified, such as when a transannular cycloaddition is to occur, the selectivity is controlled mainly by the orientations of reacting functional groups dictated by the framework of the precursor.

Scheme 3.6 Regioselectivity of [2+2] photocycloaddition of enones.

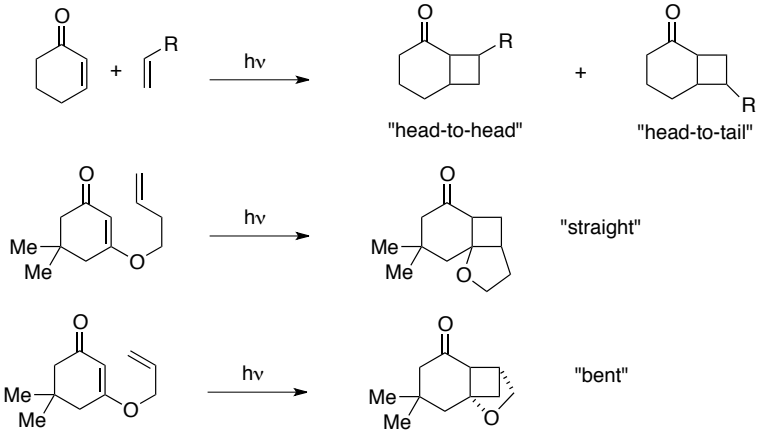

In addition to the model systems for bielschowskysin previously discussed, several natural product syntheses have appeared in the literature which employ butenolides (α,β-unsaturated γ-lactones) in [2+2] photocycloadditions. With butenolides, a stereogenic center in the γ-position can serve as a control element to achieve facial diastereoselectivity. For example, in two cases involving the chemically similar butenolides **3.24** and **3.27**, an intermolecular [2+2] photocycloaddition with 1,2-dichloroethylene was utilized to produce intermediates which were reductively converted to the cyclobutenes **3.25** and **3.28** (Scheme 3.7). In the first case, direct excitation (Hg lamp, quartz) in acetonitrile provided a superior yield (89%) to sensitized irradiation (Hg lamp, Pyrex) in acetone (45%). This reaction proceeded with an 88/12

diastereomeric ratio, reflecting the influence of the chiral center at the γ-position. Cyclobutene **3.25** was further elaborated to the monoterpenoid pheromone (+)-lineatin (**3.26**).[12a] In the second case, direct excitation provided the cyclobutene product with equivalent diastereoselectivity (d.r. = 91/9), yielding after reduction the major diastereomer **3.28**. This product was then elaborated to the sesquiterpene (-)-merrilactone A (**3.29**).[12b]

Scheme 3.7 Synthesis of (+)-lineatin and (-)-merrilactone A from butenolides.

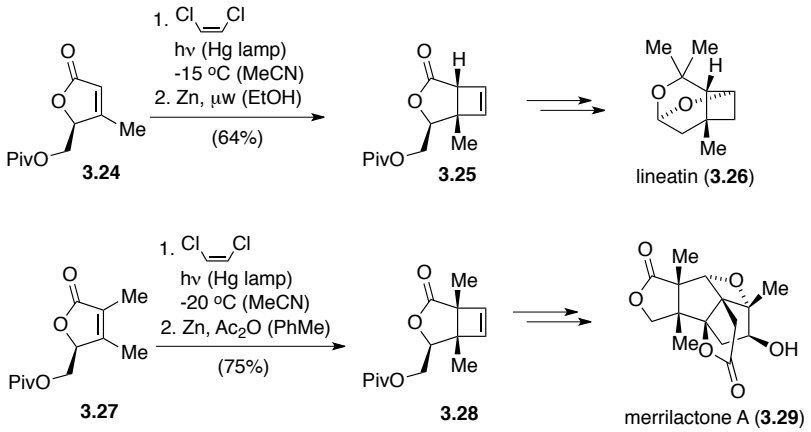

Tanaka *et al.* have employed an intramolecular variant of a [2+2] photocycloaddition with a butenolide in the synthesis of the diterpene stoechospermol (**3.32**) (Scheme 3.8).[12c] Direct irradiation of the ester **3.30** in acetonitrile using a low pressure mercury lamp at 15 °C afforded a single product **3.31** in 61% yield. The regio- and diastereoselectivity are believed to be governed by the chiral center at the γ-position of the butenolide and the length of the tether. This compound was elaborated further to stoechospermol (**3.32**).

Scheme 3.8 Synthesis of stoechospermol from a butenolide.

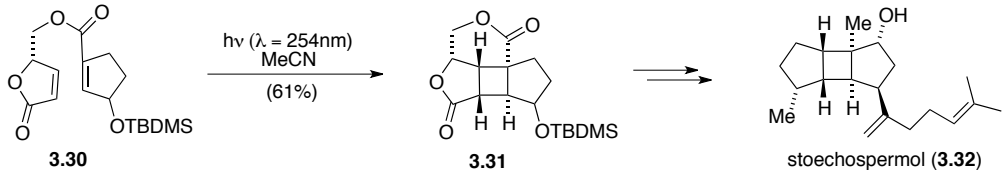

The crossed intramolecular [2+2] photocycloaddition of an allene to a butenolide was utilized in the synthesis of the compact tricyclic substructure of solanoeclepin A (**3.35**) by Hiemstra *et al.* (Scheme 3.9).[12d] The sensitized irradiation of butenolide **3.33** in 9:1 benzene/acetone led selectively to the strained photocycloadduct **3.34**. The facial diastereoselectivity is determined by the stereogenic center, to which the allene is attached. The exocyclic methylene is later converted to a carbonyl via oxidative cleavage to match the natural product.

Scheme 3.9 Synthesis of the core of solanoeclepin A from a butenolide.

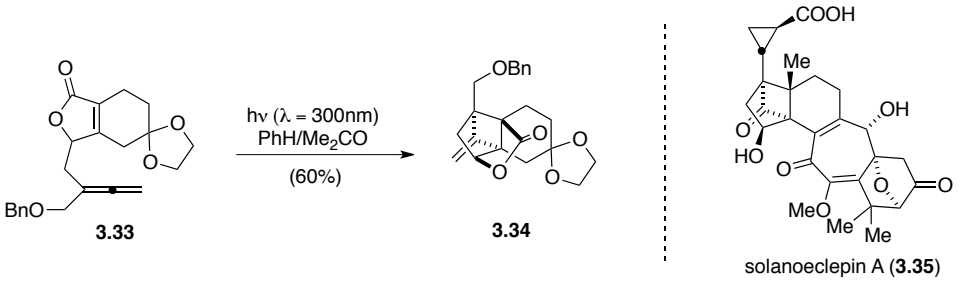

3.33 **3.34** solanoeclepin A (**3.35**)

3.4 Bipinnatin J as Model System for the [2+2] Cycloaddition – the Epoxide Approach

It has been proposed by Trauner that bielschowskysin arises in nature via a transannular [2+2] cycloaddition.[4] One of our initial goals was to test the feasibility of using this transformation in the course of a total synthesis. Accordingly, we developed a model system to test this biomimetic [2+2] cycloaddition. The model system we decided upon is based on another furanocembranoid previously synthesized by Trauner *et al.* - bipinnatin J (**1.11**).[15] The substrate **3.36** for the model cycloaddition could be prepared from bipinnatin J via epoxidation of the $\Delta^{7,8}$ double bond (Scheme 3.10). Addition of water to C3 would generate the key intermediate **3.37**, from which the cycloaddition may then proceed via a light-induced process or perhaps through a stepwise cationic process.[16] This model substrate **3.36** is analogous to the natural precursor from which bielschowskysin has been proposed to arise, lacking only the C-13 acetoxy moiety and the lactol ring.

Scheme 3.10 Epoxide of bipinnatin J as a model system for the [2+2] cycloaddition.

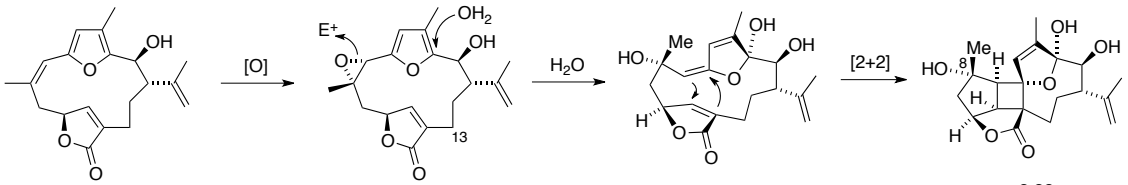

bipinnatin J (**1.11**) **3.36** **3.37** **3.38**

One of our concerns with this plan was the stereoselectivity of the epoxidation. In order to produce the natural configuration of methyl and hydroxyl groups at C8 that bielschowskysin possesses, the epoxidation of bipinnatin J (**1.11**) must occur from the α-face. We evaluated the conformational bias of the macrocycle towards approach of an epoxidizing agent to the $\Delta^{7,8}$ alkene using computational methods. MacroModel calculations revealed that the lowest energy conformation of bipinnatin J gives a clear bias towards the undesired β-face. We then performed the same calculations on the $\Delta^{7,8}$ geometric isomer of bipinnatin J (**3.39)** (Figure 3.2). In this case epoxidation must occur from the β-face to give the desired configuration at C8, and our calculations revealed a clear bias towards this face. Thus we undertook the synthesis of **3.39** via an analogous route to that which was used for bipinnatin J.

Figure 3.2 Bipinnatin J and its $\Delta^{7,8}$ geometric isomer.

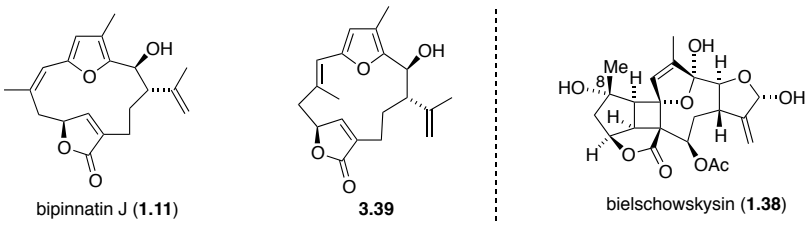

The geometric configuration of the $\Delta^{7,8}$ double bond of bipinnatin J is decided in the first step of the synthesis. The known vinyl iodide **3.41** is prepared via a zirconium-mediated carboalumination of commercially available 3-butyn-1-ol (**3.40**) followed by iodination. In the synthesis of bipinnatin J, refluxing for three days before addition of iodine allows for the isomerization of the double bond to the desired (*Z*)-isomer. To obtain the (*E*)-isomer (**3.41**) the reaction is simply quenched after stirring overnight at room temperature.[17] The remaining steps of the synthesis up to the macrocyclization are identical to that for bipinnatin J and the yields are comparable (Scheme 3.11). However, when we carried out the Nozaki-Hiyama-Kishi macrocyclization to make the (*E*)-isomer of bipinnatin J (**3.39**), the yield was substantially lower. We obtained two diastereomers in 21% and 8% yield (d.r. 2.7:1). These results contrast with those from the cyclization to form bipinnatin J which gives a 72% yield with d.r. > 9:1. The lower yield in this case might be due to a greater inherent strain in the macrocycle with an *E* double bond and hence its formation may be less facile than in the case for bipinnatin J. Due to this low yield and the efforts required to bring up starting material, it was decided that we would carry out further experiments with bipinnatin J itself and adjust our efforts accordingly should the (*E*)-isomer prove indispensable in obtaining the proper configuration of methyl group and alcohol at C8. It should also be noted that the relative stereochemistry of the alcohol, butenolide, and isopropenyl groups at C-2, C-10 and C-1 respectively was not established for **3.39** or **3.49** due to a lack of sufficient material.

Scheme 3.11 Synthesis of the $\Delta^{7,8}$ isomer of bipinnatin J.

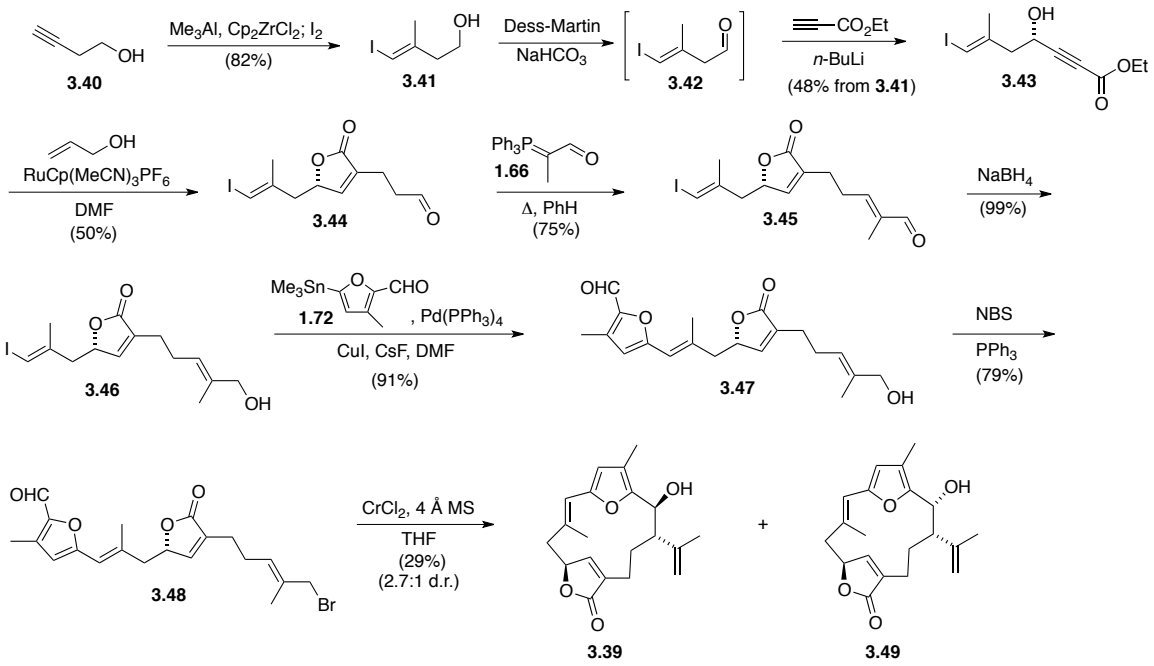

With a robust route to bipinnatin J at our disposal, we set about to explore conditions for the epoxidation of the $\Delta^{7,8}$ alkene. It was known from the previous synthesis of intricarene that treatment of bipinnatin J with *m*-chloroperoxybenzoic acid (*m*-CPBA) selectively oxidized the furan ring to give the hydroxypyranone. We therefore attempted oxidation with dimethyldioxirane (DMDO) in the hope that at least a portion of the starting material could be epoxidized at the $\Delta^{7,8}$ double bond. However this reaction resulted in an intractable mixture of products. We then began to consider various methods to inductively withdraw electrons from the furan ring with the goal of rendering the $\Delta^{7,8}$ alkene more nucleophilic than the ring.

Our first attempt to deactivate the furan ring hinged upon an oxidation of the hydroxyl group at C2 to a ketone (Scheme 3.12). This alcohol proved particularly resistant to oxidation, and range of oxidative conditions including manganese dioxide, Dess-Martin periodinane, tetrapropylammonium perruthenate (TPAP), and a Swern oxidation all failed to yield any product. However a successful reaction was eventually realized in 50% yield through treatment of bipinnatin J (**1.11**) with 2-iodoxybenzoic acid (IBX) in DMSO at 50 °C. The ketone (**3.50**) was subsequently treated with DMDO and, gratifyingly, the $\Delta^{7,8}$ epoxide (**3.51**) was produced as the major product in 37% yield. We were unable to grow a crystal of this compound, however, in order to confirm the relative stereochemistry.

Scheme 3.12 Oxidation of C2 alcohol of bipinnatin J and epoxidation.

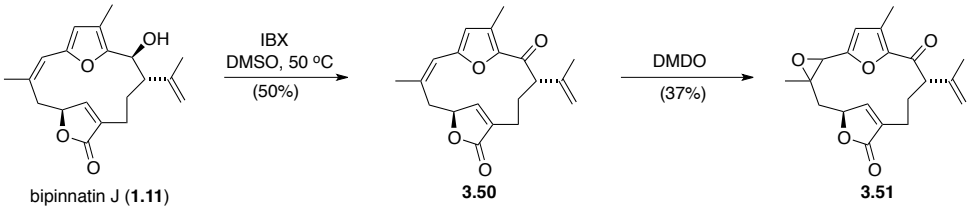

With epoxide **3.51** in hand, we set about to effect the key [2+2] cycloaddition as depicted in Scheme 3.13. We desired to open the epoxide with a Lewis acid while simultaneously trapping the *exo*-alkylidene dihydrofuran with methanol (Scheme 3.13). Irradiation of intermediate **3.52** would ideally result in a [2+2] cycloaddition to give **3.53**. After the cycloaddition we could reduce the ketone back to an alcohol, utilizing the natural facial bias of the molecule to enforce the proper stereochemistry.

Scheme 3.13 Proposed formation of *exo*-alkylidene dihydrofuran and [2+2] cycloaddition.

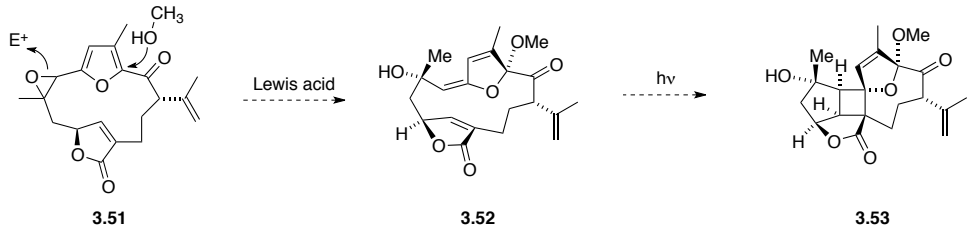

3.51 **3.52** **3.53**

Initial treatment of the epoxide with a catalytic amount of zinc(II) chloride in methanol was not noted to produce any reaction at room temperature. However, with concomitant irradiation by a 275 W sun lamp, the reaction proceeded to completion to give an unexpected product (**3.54**) in low yield (13%) (Scheme 3.14). The structure of this product was confirmed by X-ray crystallography. The remaining mass balance from the reaction was composed of a complex mixture of products – none of which we were able to obtain in sufficient mass or purity to characterize.

Scheme 3.14 Formation of an unexpected lactone.

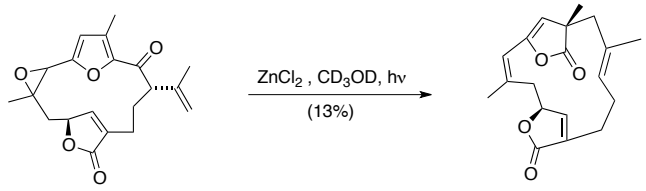

3.51 **3.54**

The proposed mechanism is outlined in Scheme 3.15. Zinc ion catalyzes the opening of the epoxide. Adventitious water from the methanol adds into the 2-position of the furan, and formation of a ketone is accompanied by a 1,2-shift to give β-ketoester **3.55**. Photoinduced Norrish type I extrusion of carbon monoxide then leads to the product **3.54**. Given this mechanistic hypothesis, it remains unclear why treatment of the epoxide with zinc alone does not lead to the *exo*-alkylidene dihydrofuran with methanol attached to the C2 carbon, or why **3.55** would not be formed and isolated prior to irradiation. It may be that the photoelimination occurs prior to the opening of the epoxide by zinc. A control experiment in which the starting material **3.51** is photolysed without the presence of a Lewis acid could prove illuminating in this regard.

Scheme 3.15 Mechanism of formation of lactone **3.54**.

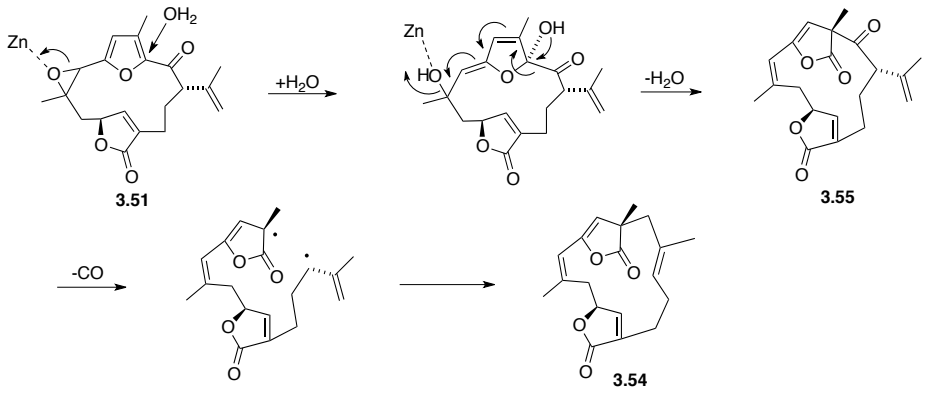

The deactivation of the furan ring relative to the $\Delta^{7,8}$ double bond could also be achieved by other methods. For instance, it was discovered that exposure of bipinnatin J to excess 2,3-dichloro-5,6-dicyano-1,4-benzoquinone (DDQ) provided aldehyde **3.56** in 46% yield (Scheme 3.16). This method represents another example of a highly selective oxidation of the furanocembranoid framework. Numerous furanocembranoids, such as lophotoxin, exist in nature with an aldehyde or ester at this position. However, as discussed in Chapter 1, when the C-18 methyl is oxidized to any extent in nature, the C-2 carbon does not possess an alcohol group. In this regard aldehyde **3.56** represents an "unnatural" example of a furanocembranoid in which both the C-2 and C-18 carbons have been oxidized.

Scheme 3.16 Oxidation of C-18 of bipinnatin J.

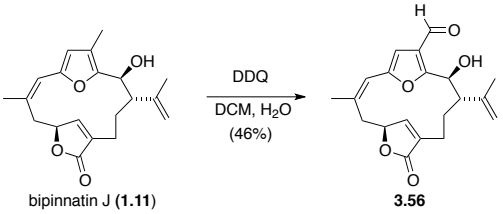

We sought to epoxidize aldehyde **3.56** selectively at the $\Delta^{7,8}$ double bond, reasoning that the aldehyde might be reduced back to a methyl at a later stage. However, to our dismay, when aldehyde **3.56** was treated with DMDO, selective epoxidation of the isopropylidene moiety had occurred to furnish epoxide **3.57** (Scheme 3.17). Apparently the C-18 aldehyde group deactivated the $\Delta^{7,8}$ double bond through resonance with the furan to such an extent that the isopropylidene became the next most electron-rich group in the molecule. The stereochemistry of the epoxide was not determined, but the crude NMR revealed that a single compound had been made, reflecting a clear facial bias in the molecule. Further treatment of **3.57** with DMDO resulted in an intractable mixture of products.

Scheme 3.17 Epoxidation of the isopropylidene moiety of 18-oxobipinnatin J.

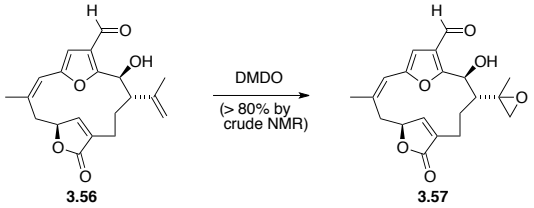

During our consideration of various methods to deactivate the furan, we realized an interesting trend upon close inspection of the naturally occurring furanocembranoids. Namely, that the vast majority of the natural products possessing both an oxygen at C-2 and a $\Delta^{7,8}$ epoxide also possess an acetyl group on the C-2 hydroxy. The only furanocembranoids with a 14-membered macrocycle besides bipinnatin J to possess a naked hydroxy group at C-2 are from the bipinnatolide series (Figure 3.3), and amongst these the furan has been oxidized. Therefore we reasoned that an acetoxy group at C-2 might be able to inductively withdraw electrons from the furan sufficiently to render the $\Delta^{7,8}$ double bond amenable to epoxidation.

Figure 3.3 Selection of bipinnatolide furanocembranoids.

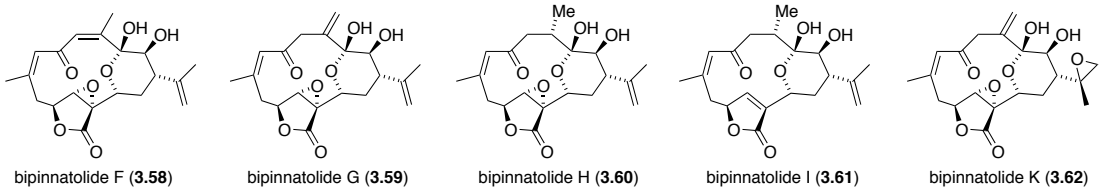

Acetylation of bipinnatin J (**1.11**) was readily achieved in high yield with acetic anhydride under standard conditions (Scheme 3.18). Interestingly, the product **3.63** was found to be unstable on silica and hydrolysis would occur to give back starting material. This most likely proceeds via an S_N1 mechanism through the intermediacy of a carbocation at the C-2 carbon which is attack by atmospheric moisture. The carbocation would be stabilized by the adjacent vinylfuran moiety. It was found that pre-treatment of silica with triethylamine, however, allowed for reaction monitoring by TLC and purification by column chromatography.

Scheme 3.18 Acetylation of bipinnatin J.

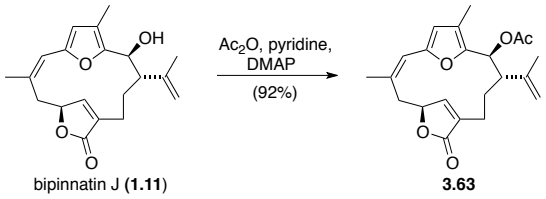

O-acetyl-bipinnatin J (**3.63**) was then treated with DMDO at reduced temperature. The reaction proceeded to deliver a low-yielding mixture of both the desired $\Delta^{7,8}$ epoxide (**3.64**) and the dienedione product from the oxidized furan (**3.65**) (Scheme 3.19). The ratio favored the epoxide **3.64** and was found to be dependent on temperature, giving a 5:4 ratio of epoxide to dienedione at 0 °C and a 2.5:1 ratio at -50 °C. The stereochemistry of the epoxide was determined via x-ray crystallography and found to lie on the undesired β-face of the macrocycle,

as predicted by MacroModel for unacetylated bipinnatin J (**1.11**). This stereochemistry would give the wrong configuration of methyl group and alcohol at C-8 for bielschowskysin and therefore is unlikely to represent the true biosynthetic precursor. Nevertheless, investigation is underway in our lab to probe the reactivity of this epoxide **3.64** in the hope that we can glean some insight into the conditions for the [2+2] cycloaddition.

Scheme 3.19 Epoxidation of O-acetyl-bipinnatin J.

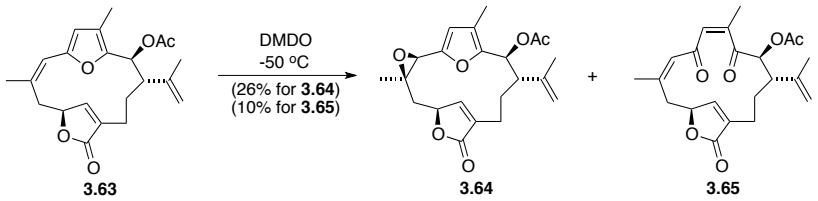

One possible way in which this epoxide **3.64** could be used to accomplish a [2+2] cycloaddition and still obtain the proper stereochemistry at C-8 would be through the elimination of the alcohol at C-8 to give a triene, such as **3.66** depicted in Scheme 3.20. In this manner an important *exo*-alkylidene dihydrofuran intermediate could be trapped with methanol and possibly isolated. This would benefit experimentation greatly by allowing for a range of photochemical conditions to be tried out on a species which is closely related to the suspected biosynthetic precursor for the cycloaddition.

Scheme 3.20 Proposed formation of an *exo*-alkylidene dihydrofuran species.

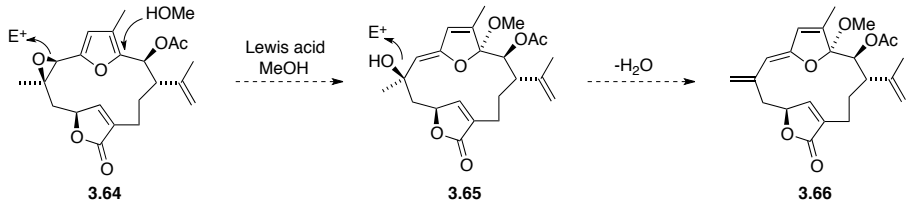

A critical issue with this or any strategy involving formation of an *exo*-alkylidene dihydrofuran is the geometry of the newly formed *exo*-alkene (Scheme 3.21). Based on studies with a molecular model, in order for the [2+2] cycloaddition to proceed at all the reaction must proceed from the *exo*-(*E*)-alkene, as a cycloaddition from the *exo*-(*Z*)-alkene would lead to an impossibly strained cyclobutane. If the elimination of the C8 alcohol proceeds to give a (*Z*)-alkene as in triene **3.66**, the *exo*-alkene must then be isomerized before cycloaddition may occur. This could potentially happen under photochemical conditions, and upon formation of **3.67**, the cycloaddition would be geometrically allowed to proceed. After formation of **3.68** the exocyclic alkene would have to be rehydrated from the opposite face in order to generate the proper stereochemistry at C-8. From studying a model of compound **3.68**, it appears the desired face of the alkene would be clearly biased towards addition of water.

Scheme 3.21 Proposed elaboration of triene **3.66** to give the framework of bielschowskysin.

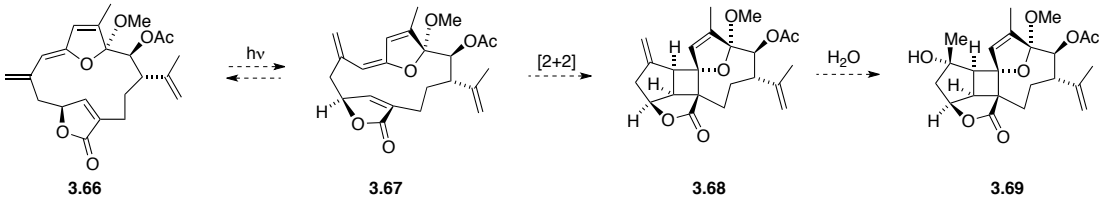

Alternatively, the epoxide could be formed from the $\Delta^{7,8}$ isomer of O-acetylbipinnatin J as discussed previously. If the MacroModel predictions are accurate, epoxidation should occur from the desired face of the alkene to give the correct stereochemistry at C-8. However the low yield of the macrocyclization must be taken into account with this strategy.

3.5 Bipinnatin J as Model System for the [2+2] Cycloaddition – the Dienedione Approach

In addition to the epoxide approach previously outlined, we considered another model system for the key [2+2] cycloaddition. Our second approach centers around the oxidation of a protected bipinnatin J derivative to the dienedione followed by Michael addition of water to give the *exo*-alkylidene dihydrofuran. The selective oxidation of the furan by *m*-CPBA had been previously demonstrated in the synthesis of intricarene and coralloidolide E. However, rather than effecting an Achmatowicz rearrangement to give the hydroxy pyranone, we sought to preserve the integrity of the dienedione by masking the hydroxy group and preventing its addition into the C6 ketone. A robust protecting group was sought for this purpose – one that would be stable under acidic and basic conditions – and so we decided to employ a methyl ether for the purposes of studying the cycloaddition (Scheme 3.22).

Scheme 3.22 Utilization of a dienedione to model the [2+2] cycloaddition.

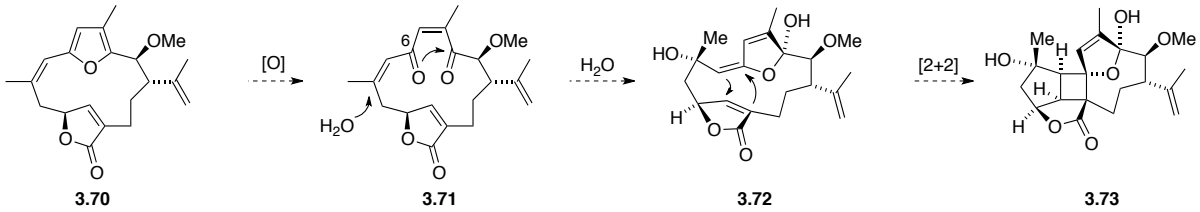

O-methyl bipinnatin J (**3.70**) was known from the literature as an unnatural derivative of bipinnatin J (**1.11**).[18] Its synthesis was carried out in high yield through exposure of bipinnatin J (**1.11**) to trifluoroacetic acid in the presence of a large excess of methanol. The mechanism proceeds through the intermediacy of a carbocation at C-2 which is stabilized by the adjacent furan (Scheme 3.23). Interestingly, only a single diastereomer is obtained in this reaction, presumably reflecting the natural facial bias of the macrocycle. The product **3.70** was also found to be unstable on silica in the same manner as O-acetyl-bipinnatin J (**3.63**).

Scheme 3.23 Synthesis of O-methylbipinnatin J.

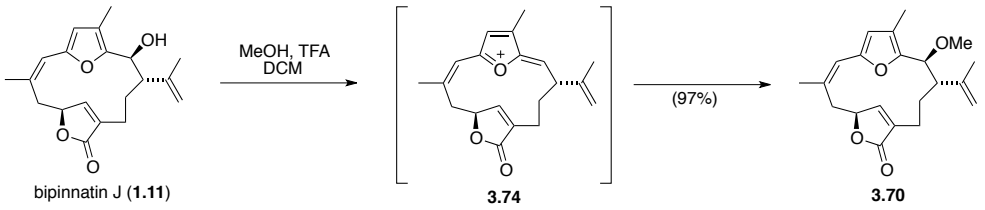

Oxidation of the furan was initially attempted with *m*-CPBA, but the water and trace acid present in the reagent caused much of the O-methylated starting material (**3.70**) to revert back to bipinnatin J (**1.11**) via the same mechanism. Next we attempted oxidation with singlet oxygen, and through this method a successful reaction was realized in good yield. (Scheme 3.24). The proton NMR of the dienedione product (**3.75**) displays some broad resonances that can be attributed to the conformational flexibility of the macrocycle. This phenomenon has been previously observed in the case of isoepilophodione B (**1.52**)[19], a naturally occurring relative of the product (**3.75**) which also possesses a dienedione moiety but lacks the methoxy group. The geometries of the two new double bonds in **3.75** were both confirmed to be (*Z*) through a NOESY experiment, showing correlations between the C18 methyl and the C5 proton, and between the C19 methyl and the C7 proton.

Scheme 3.24 Oxidation of the furan of O-methylbipinnatin J.

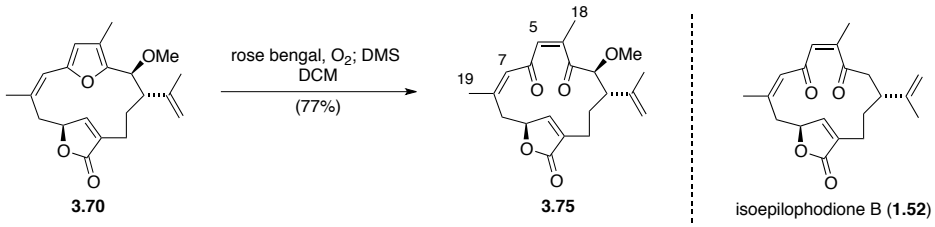

With the O-methylated dienedione in hand, we set about to explore conditions for the Michael addition of water and subsequent [2+2] cycloaddition. The macrocycle was irradiated with a 275 W sun lamp in a mixture of acetone and water at room temperature while simultaneously being treated with a Lewis acid. Amongst those tested were lanthanum triflate, scandium triflate, and Zn(II) chloride. In each case, and in the case of irradiation without a Lewis acid, the same reaction took place. Namely, a mixture of four products was generated. While the two minor products decomposed and eluded characterization, the two major products were identified as a novel ketone (**3.76**) with an interesting structure, and, much to our surprise and delight, the natural product intricarene (**1.40**) (Scheme 3.25). The structure of **3.76** was confirmed by X-ray crystallography. We also managed to obtain a crystal structure of intricarene.

Scheme 3.25 Photolysis of the O-methylated dienedione.

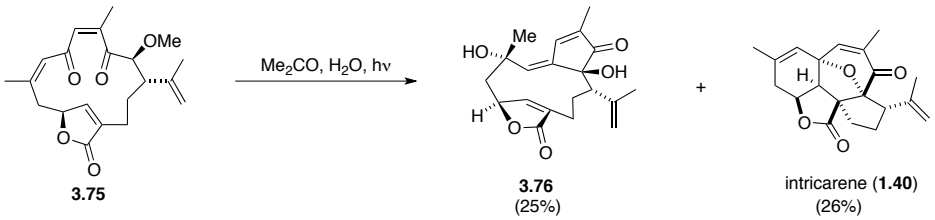

We have crafted a mechanistic hypothesis that accounts for the formation of both of these products (Scheme 3.26). The dienedione **3.75** is brought to an excited state through irradiation and subsequently loses methanol to form oxidopyrilium **1.57**. This reactive species undergoes either a photoinduced 4π disrotatory electrocyclization to give epoxide **3.77** or a [3+2] cycloaddition to give intricarene (**1.40**). Water then adds to the presumably reactive epoxide **3.77** in an S_N' fashion to give ketone product **3.76**.

Scheme 3.26 Mechanism for the formation of **3.76** and intricarene.

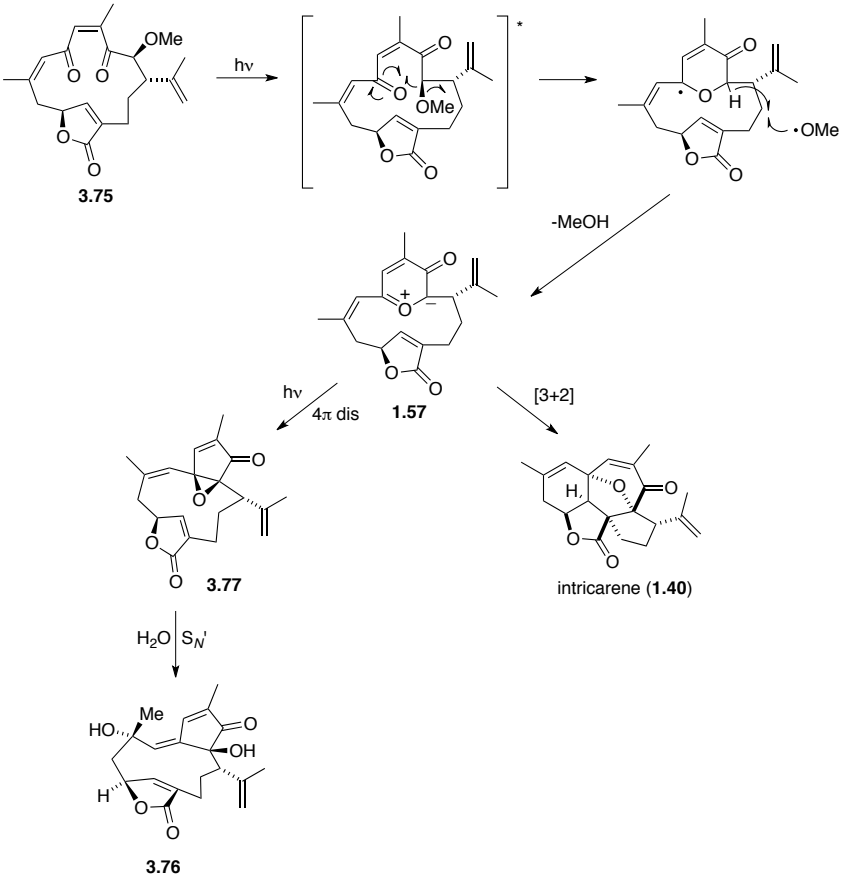

This hypothesis neatly explains the formation of both products. In addition, this discovery raises interesting questions about the formation of intricarene in nature. The fact that this reaction occurs at room temperature is notable. When the exposure of corals to sunlight is considered, one must question whether the natural formation of intricarene occurs through a photocatalyzed process rather than an enzymatic process as has been previously suggested.

Indeed, Wang and Tantillo performed theoretical studies on oxidopyrilium-alkene 1,3-dipolar cycloadditions with a focus on the formation of intricarene.[20] Quantum mechanical calculations (B3LYP) were used to determine the energy barrier between oxidopyrilium **1.57** and intricarene (**1.40**). They concluded that their "calculations on various combinations of model oxidopyrilium zwitterions and alkenes show that preorganization of the cycloaddition partners into a ring benefits the naturally occurring system both in terms of enthalpy and entropy, leading to an activation barrier for the (+)-intricarene forming cycloaddition that is calculated to be approximately 20 kcal/mol (both in terms of $\Delta E^{\ddagger}$ and $\Delta G^{\ddagger}$, and in both nonpolar and polar environments). Thus, although enzymatic intervention may be needed to generate the oxidopyrilium zwitterions, its subsequent cycloaddition would not require much, if any, additional intervention."

It does seem unlikely that the O-methyldienedione **3.75** is the actual biosynthetic precursor, however, since no furanocembranoids are known to possess an O-methoxy at C-2. It might be that a close relative of this molecule - perhaps the O-acetate - could be the natural precursor. We also attempted to illuminate the oxidized form of bipinnatin J itself (**1.56**), as this molecule would be more likely to exist in the coral. This molecule, which was an intermediate in the previous synthesis of intricarene, was known to be unstable, and could be expected to exist in an equilibrium that would favor the closed hydroxypyranone (Scheme 3.27). Irradiation of this species failed to produce any intricarene however, yielding an extremely complex mixture of products. We also attempted oxidation of bipinnatin J (**1.11**) with singlet oxygen while using the same 275 W sun lamp, but this too failed to yield any intricarene. It may be that the hydroxy group needs to be masked in some fashion in order to stabilize the molecule and prevent formation of the hydroxypyranone before the oxidopyrilium can be allowed to form through our proposed mechanism.

Scheme 3.27 Irradiation of hydroxypyranone **1.56**.

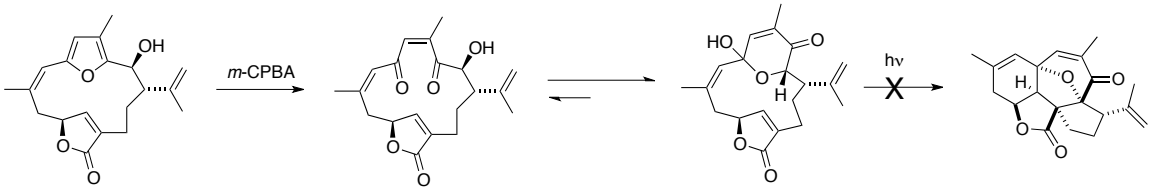

3.6 Additional Selective Oxidations of Bipinnatin J

In the course of our research we have discovered several methods for oxidizing selectively various positions around the carbon framework of bipinnatin J. We have demonstrated that the C-18 methyl can be selectively oxidized with DDQ, that the furan can be oxidized with *m*-CPBA, and that the butenolide, $\Delta^{7,8}$ and $\Delta^{15,16}$ double bonds can be selectively epoxidized. In addition to these reactions, we have discovered two other oxidative methods.

Our impetus to explore the first method stems from the fact that bielschowskysin (**1.38**) possesses an oxidized carbon at the C-17 methyl of the isopropylidene moiety. We anticipated that this carbon could be subject to allylic oxidation. Indeed, standard treatment of acetylated bipinnatin J with selenium dioxide in dioxane led selectively to the formation of aldehyde **3.78** in 48% yield (Scheme 3.28). Similar treatment of bipinnatin J itself, however, led to a complex

mixture of products. This method could be used at a late stage in the synthesis of bielschowskysin.

Scheme 3.28 Allylic oxidation of O-acetylbipinnatin J.

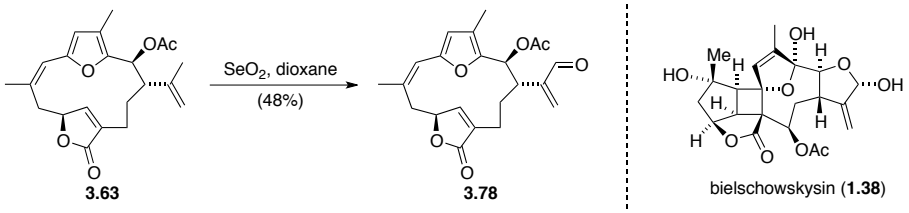

We also discovered that the C7-C8 alkene of bipinnatin J can be dihydroxylated under standard conditions. Treatment with catalytic osmium tetroxide and stoichiometric N-methylmorpholine-N-oxide (NMO) directly led to the triol **3.79** in 45% yield (Scheme 3.29). The stereochemistry of the resultant alcohols was not determined. This represents yet another selective oxidation in the toolbox of methods we have devised.

Scheme 3.29 Dihydroxylation of bipinnatin J.

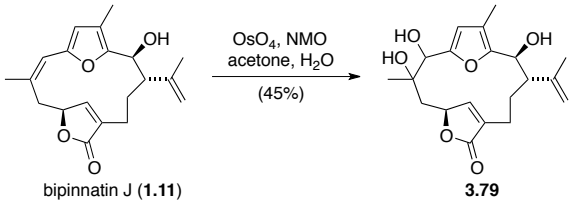

3.7 Conclusion

While the synthesis of the cyclobutane core of bielschowskysin from bipinnatin J was not achieved, a number of highly selective oxidations of the furanocembranoid framework were discovered. These oxidations will very likely find utility in the synthesis of bielschowskysin and other members of the furanocembranoid family. It would no doubt greatly aid experimentation involving the [2+2] cycloaddition to find a method of trapping the key *exo*-alkylidene dihydrofuran intermediate. Once its formation has been established, then one may go about systematically testing out photochemical conditions to achieve the cycloaddition.

In addition to the selective oxidations, a number of fascinating transformations were effected, including the photochemical synthesis of intricarene and a novel ketone. The synthesis of intricarene in this manner raises interesting questions about its formation in nature, and will also stimulate more investigation into the formation of oxidopyriliums from dienediones through photochemical means.

3.8 Experimental Methods

General Experimental Details: All reactions were carried out under an inert N_2 atmosphere in oven-dried glassware. Flash column chromatography was carried out with EcoChrom ICN SiliTech 32-63 D 60 Å silica gel. Reactions and chromatography fractions were monitored with Merck silica gel 60 F_{254} plates and visualized with potassium permanganate, ceric ammonium molybdate, and vanillin. Tetrahydrofuran (THF) and methylene chloride (CH_2Cl_2) were dried by

passage through activated alumina columns. Benzene (PhH) and diisopropylamine (*i*-Pr_2NH) were distilled from CaH_2 prior to use. DMSO was stored over 3 Å molecular sieves. *n*-Butyllithium was titrated with diphenylacetic acid prior to use. All other reagents and solvents were used without further purification from commercial sources. Organic extracts were dried over $MgSO_4$ unless otherwise noted.

Instrumentation: FT-IR spectra were obtained on NaCl plates with an ATI Mattson Gemini spectrometer. Proton and carbon NMR spectra (^1H NMR and ^{13}C NMR) were recorded in deuterated chloroform ($CDCl_3$) unless otherwise noted on a Bruker DRX-500, Bruker AVQ-400, Varian VXR 400 S, Bruker AXR-300 or Bruker AMX 600 spectrometer and calibrated to residual solvent peaks. Multiplicities are abbreviated as follows: s = singlet, d = doublet, t = triplet, q = quartet, br = broad, m = multiplet. High-resolution (HR-MS) and low resolution (MS) mass spectra were recorded on a Finnigan MAT 95 instrument. Melting points were determined with an electrothermal apparatus and are uncorrected. Photochemical reactions were carried out with a T-Rex 275 W UVB/heat lamp for reptiles (www.t-rexproducts.com).

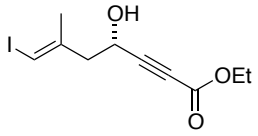

Propargylic alcohol (3.43). To a solution of (E)-4-iodo-3-methyl-but-3-en-1-ol (**3.41**) (2.00g, 9.42 mmol) in CH_2Cl_2 (50mL) was added $NaHCO_3$ (3.96, 47.1 mmol) followed by Dess-Martin periodinane (6.40g, 15.1 mmol). After 20 min at rt, a 1:1:1 solution of saturated $Na_2S_2O_3$, saturated $NaHCO_3$, H_2O was added. The resulting biphasic solution was stirred vigorously for 20 min. The layers were separated, and the aqueous was extracted 2 x CH_2Cl_2 (30 mL). The organics were dried, filtered and concentrated *in vacuo*. To the resulting oil was added a 1:1 solution of hexane/Et_2O. The mixture was filtered and concentrated *in vacuo*. If additional solids precipitated, the mixture was filtered and concentrated again from 1:1 hexane/Et_2O. The crude aldehyde was taken up in THF (15 mL) and used without further purification. Meanwhile, to a solution of ethyl propiolate (1.44 mL, 14.2 mmol) in THF at -78 °C (50 mL) was added *n*-butyllithium (2.5 M in hexanes, 5.68 mL, 14.2 mmol) dropwise over 5 min. After 30 min, the aldehyde solution at -78 °C was added via cannula to the acetylide solution at -78 °C. After 30 min, a saturated soluion of NH_4Cl (20 mL) was added. The reaction mixture was allowed to warm to rt. The layers were separated, and the aqueous layer was extracted 2 x Et_2O (30 mL). The organics were dried, filtered, and concentrated *in vacuo*. The crude oil was purified by flash column chromatography (15% EtOAc/hexanes) to give 1.44 g (50% for 2 steps) of **3.43** as a yellow oil.

R_f 0.71, 33% EtOAc/Hexanes. ^1H NMR (400 MHz): δ 6.16 (s, 1 H), 4.62 (dt, 1 H, J = 9, 6 Hz), 4.24 (q, 2 H, J = 7 Hz), 2.68 (m, 2 H), 2.02 (bs, 1 H), 1.92 (s, 3H), 1.32 (t, 3 H, J = 7 Hz). ^{13}C (100 MHz): δ 153.3, 142.2, 86.6, 79.6, 76.9, 62.4, 60.0, 46.1, 24.2, 14.0. HRMS (FAB) calcd for $C_{10}H_{14}IO_3$ ($M+H^+$): 308.99877, found: 308.99914.

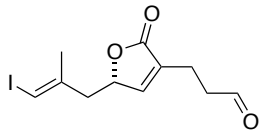

Butenolide (3.44). To a solution of **3.43** (1.77g, 5.74 mmol) in DMF (30 mL) was added allyl alcohol (585 μL, 8.61 mmol) and $RuCp(MeCN)_3PF_6$ (200mg, 0.460 mmol). After 4 h at rt, the reaction mixture was concentrated *in vacuo*. The crude oil was purified by flash column chromatography (40% EtOAc/hexanes) to 920 mg (50%) of **3.44** as a red oil in addition to 139 mg of the regioisomeric product.

R_f 0.36, 40% EtOAc/Hexanes. ^{1}H NMR (400 MHz): δ 9.76 (s, 1 H), 7.05 (s, 1H), 6.07 (s, 1 H), 4.98 (m, 1 H), 2.76 (m, 2 H), 2.56 (m, 4 H), 1.88 (s, 3 H). ^{13}C (100 MHz): δ 200.6, 172.9, 148.7, 142.0, 132.7, 79.4, 79.1, 42.4, 41.0, 24.6, 17.9. HRMS (FAB) calcd for $C_{11}H_{14}IO_3$ ($M+H^+$): 320.99877, found: 320.99796.

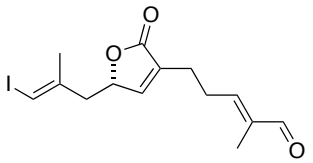

Enal (3.45). To a solution of **3.44** (1.24 g, 3.87 mmol) in $CHCl_3$ was added **1.66** (2.46 g, 7.74 mmol). After heating at reflux for 14 h, the dark solution was cooled to rt. A saturated solution of NH_4Cl (20 mL) and Et_2O (20 mL) were added. The layers were separated, and the aqueous was extracted 2 x Et_2O (20 mL). The organics were dried, filtered and concentrated *in vacuo*. The crude oil was purified by flash column chromatography (25-30% EtOAc/hexanes) to give 1.05 g (75%) of **3.45** as a light red oil.

R_f 0.50, 50% EtOAc/Hexanes. ^{1}H NMR (400 MHz): δ 9.35 (s, 1 H), 7.04 (s, 1H), 6.40 (t, 1 H, *J* = 7 Hz), 6.05 (s, 1 H), 5.00 (m, 1 H), 2.52 (m, 6 H), 1.86 (s, 3 H), 1.69 (s, 3 H). ^{13}C (100 MHz): δ 194.9, 172.8, 151.7, 148.1, 141.9, 140.3, 133.4, 79.4, 79.1, 42.7, 26.7, 24.5, 24.1, 9.4. HRMS (FAB) calcd for $C_{14}H_{18}IO_3$ ($M+H^+$): 361.03007, found: 361.02904.

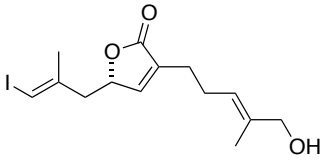

Allylic alcohol (3.46). To a solution of **3.45** (1.04 g, 2.78 mmol) in MeOH (30 mL) was added sodium borohydride (116 mg, 3.06 mmol). After 30 min, a saturated NH_4Cl solution (10 mL) was carefully added. The solution was concentrated *in vacuo*, and Et_2O (30 mL) was added followed by a saturated NH_4Cl solution (30 mL). The layers were separated, and the aqueous was extracted 2 x Et_2O (30 mL). The organics were dried, filtered, and concentrated *in vacuo*. The crude oil was purified by flash column chromatography (50% EtOAc/hexanes) to give 1.01 g (97%) of **3.46** as a colorless oil.

R_f 0.26, 50% EtOAc/Hexanes. ^{1}H NMR (400 MHz): δ 6.99 (s, 1 H), 6.11 (s, 1 H), 5.38 (m, 1 H), 4.99 (m, 1 H), 4.00 (s, 2 H), 2.57 (d, 2 H, *J* = 14 Hz), 2.32 (m, 4 H), 1.92 (s, 3H), 1.66 (s, 3 H), 1.42 (br s, 1H). ^{13}C (100 MHz): δ 173.5, 147.9, 142.1, 136.3, 134.1, 123.5, 79.3, 79.1, 68.1, 44.8, 25.4, 25.0, 24.5, 13.8. HRMS (FAB) calcd for $C_{14}H_{19}ILiO_3$ (M+Li$^+$): 369.05390, found: 369.05327.

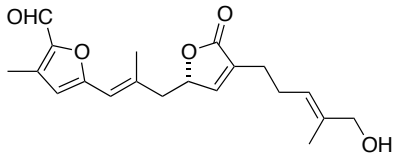

Vinyl furan (3.47). To a solution of **3.46** (430 mg, 1.18 mmol) in DMF (8 mL) was added **1.72** (418 mg, 1.53 mmol) followed by $Pd(PPh_3)_4$ (54.0 mg, 0.0467 mmol), CuI (18.0 mg, 0.0944 mmol), CsF (358 mg, 2.36 mmol). After 20 min at rt, the solution was poured onto saturated NH_4Cl (20 mL) and Et_2O (20 mL). The layers were separated, and the aqueous extracted 2 x Et_2O (20 mL). The organics were then washed 1 x brine (20 mL). The organics were dried, filtered, and concentrated *in vacuo*. The crude oil was purified by flash column chromatography (60% EtOAc/hexanes) to give 382 mg (94%) of **3.47** as a yellow oil.

R_f 0.32, 60% EtOAc/Hexanes. ^{1}H NMR (400 MHz): δ 9.59 (s, 1 H), 7.03 (s, 1 H), 6.23 (s, 1 H), 6.11 (s, 1 H), 5.31 (m, 1 H), 5.02 (m, 1 H), 3.91 (s, 2 H), 2.48 (m, 3 H), 2.30 (s, 3 H), 2.25 (m, 4 H), 2.07 (s, 3 H), 1.56 (s, 3 H). ^{13}C (100 MHz): δ 173.6, 173.4, 156.9, 147.9, 147.0, 139.3, 136.6, 136.3, 134.1, 123.4, 116.9, 114.4, 79.4, 68.3, 44.7, 25.3, 25.0, 19.7, 13.7, 10.3. HRMS (FAB) calcd for $C_{20}H_{24}LiO_5$ (M+Li$^+$): 351.17838, found: 351.17816.

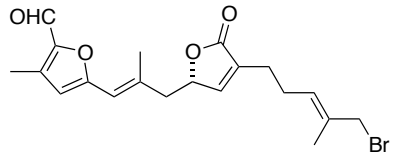

Allylic bromide (3.48). To a solution of **3.47** (380 mg, 1.10 mmol) in CH_2Cl_2 (22 mL) at -5 °C was added PPh_3 (346 mg, 1.32 mmol) and *N*-bromosuccinimide (235 mg, 1.32 mmol). After 20 min, the solution was poured onto H_2O. The layers were separated, and the aqueous was extracted 2 x CH_2Cl_2. The organics were dried, filtered, and concentrated *in vacuo*. The crude oil was purified by flash column chromatography (30% EtOAc/hexanes) to give 354 mg (79%) of **3.48** as light green oil.

R_f 0.65, 50% EtOAc/Hexanes. ^{1}H NMR (400 MHz): δ 9.65 (s, 1 H), 7.03 (s, 1 H), 6.25 (s, 1 H), 6.15 (s, 1 H), 5.51 (t, 1 H, *J* = 7 Hz), 5.05 (m, 1 H), 3.91 (s, 2 H), 2.52 (m, 2 H), 2.34 (s, 3 H), 2.28 (m, 4 H), 2.11 (s, 3 H), 1.70 (s, 3 H). ^{13}C (100 MHz): δ 175.2, 172.1, 155.6, 149.1, 147.2, 141.8, 134.2, 133.3, 132.9, 129.0, 116.9, 113.5, 81.1, 41.4, 38.5, 26.4, 26.0, 24.8, 14.2, 10.1. HRMS (FAB) calcd for $C_{20}H_{24}BrO_4$ (M+H$^+$): 407.08580, found: 407.08614.

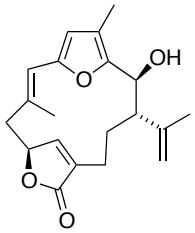

$\Delta^{7,8}$ isomer of bipinnatin J (3.39). To a suspension of $CrCl_2$ (1.06 g, 8.60 mmol) and 4 Å molecular sieves (4.5 g) in THF (900 mL) was added **3.48** (350 mg, 0.860 mmol) in THF (8 mL). After 12 h at rt, H_2O (100 mL) was added. The biphasic solution was filtered and concentrated to about 400 mL. The solution was diluted with Et_2O (200 mL), the layers were separated, and the aqueous was extracted 2 x Et_2O (100 mL). The organics were dried, filtered, and concentrated *in vacuo*. The crude oil was purified by flash column chromatography (25% EtOAc/hexanes) to give 60.1 mg (21%) of **3.39** as an off-white residue and 22.0 mg (7.8%) of a diastereomer as an off-white residue.

R_f 0.65, 50% EtOAc/Hexanes. ^{1}H NMR (400 MHz) (only peaks >4 ppm will be listed due to lack of clarity for additional peaks below 4 ppm): δ 6.84 (s, 1 H), 5.94 (s, 1 H), 5.86 (s, 1 H), 5.34 (s, 1 H), 5.20 (s, 1 H), 4.37 (d, 1 H, J = 11 Hz). HRMS (FAB) calcd for $C_{20}H_{24}O_4$ (M^+): 328.16746, found: 328.16419.

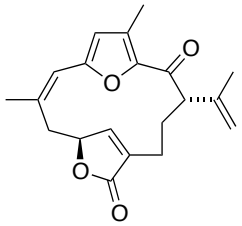

Bipinnatin J ketone (3.50). To a solution of bipinnatin J (**1.11**) (50.0 mg, 0.152 mmol) in DMSO (1.5 mL) was added IBX (68.0 mg, 0.243 mmol) at once. The solution was stirred at 50 °C for 4 hr. During this time the solution turned orange. The solution was diluted with 40 mL EtOAc and 40 mL 1:1 brine/H_2O. The layers were separated, and the organic layer was washed one additional time with 1:1 brine/H_2O (40 mL). The organic layer was dried, filtered and concentrated *in vacuo*. The crude material was purified by flash chromatography (33% EtOAc/hexanes) to give 25.1 mg (51%) of **3.50** as a white solid.

R_f 0.70, 50% EtOAc/Hexanes. ^{1}H NMR (500 MHz): δ 7.07 (br s, 1 H), 6.22 (br s, 1 H), 6.21 (s, 1 H), 5.11 (m, 1 H), 5.07 (br s, 1 H), 4.89 (br s, 1 H), 3.61 (m, 1 H), 3.01 (t, 1 H, J = 11.5 Hz), 2.86 (dd, 1 H, J = 12, 4.5 Hz), 2.55 (m, 1 H), 2.35 (s, 3 H), 2.29 (m, 1 H), 2.24 (m, 1 H), 2.07 (br s, 3 H), 1.90 (m, 1 H), 1.80 (br s, 3 H). ^{13}C (125 MHz): δ 191.2, 173.5, 152.8, 152.7, 147.2, 140.8, 135.2, 133.4, 132.0, 117.2, 116.4, 114.2, 77.9, 51.7, 41.0, 30.6, 25.9, 22.2, 21.5, 11.7. HRMS (EI)$^+$ calcd for $C_{20}H_{22}O_4$ $(M)^+$ 326.1518, found 326.1516.

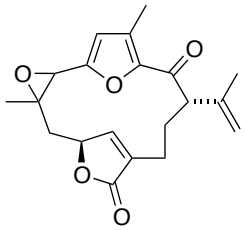

$\Delta^{7,8}$ epoxide of bipinnatin J ketone (3.51). To a solution of ketone **3.50** (20.0 mg, 0.061 mmol) in acetone (1.0 mL) at -40 °C was added dropwise 0.77 mL (0.067 mmol) of a 0.087M dimethyldioxirane solution in acetone. After stirring for 1 hr the solution was warmed to 0 °C. After 1 hr the solution was concentrated *in vacuo* and the crude material purified by flash chromatography (33% EtOAc/hexanes) to give 7.8 mg (37%) of **3.51** as clear residue.

R_f 0.50, 50% EtOAc/Hexanes. ^{1}H NMR (500 MHz): δ 7.10 (br s, 1 H), 6.04 (br s, 1 H), 5.14 (br s, 1 H), 5.02 (m, 1 H), 4.98 (br s, 1 H), 4.71 (s, 1 H), 2.94 (dd, 1 H, *J* = 8.9, 5.0 Hz), 2.85 (m, 2 H), 2.41 (td, 1 H, *J* = 12.8, 11.2, 3.3 Hz), 2.25 (m, 1 H), 2.16 (m, 1 H), 2.03 (d, 3 H, *J* = 1.7 Hz), 1.79 (ddd, 1 H, *J* = 14.6, 9.6, 4.7 Hz), 1.72 (s, 3 H), 1.49 (s, 3 H). ^{13}C (125 MHz): δ 199.3, 175.9, 172.6, 152.5, 150.6, 143.4, 139.3, 132.1, 116.4, 108.0, 78.6, 62.6, 55.0, 39.8, 28.1, 24.8, 21.0, 20.0, 18.1. HRMS (ES)$^+$ calcd for $C_{20}H_{22}O_5Na$ $(M+Na^+)^+$ 365.1365, found 365.1365.

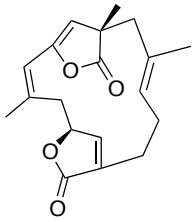

Lactone (3.54). To a solution of epoxide **3.51** (8.0 mg, 0.025 mmol) in CD_3OD (0.8 mL) in a Pyrex NMR tube was added $ZnCl_2$ (0.34 mg, 0.0025 mmol) at once. The solution was irradiated with a 275 W sun lamp. After 12 hr the solution was diluted with 10 mL EtOAc and 10 mL H_2O. The layers were separated, and the aqueous layer was extracted with EtOAc (2 X 10 mL). The combined organic extracts were dried, filtered, and concentrated *in vacuo*. The crude material was purified by flash chromatography (25% EtOAc/hexanes) to give 1.0 mg (13%) of **3.54** as a clear residue.

R_f 0.65, 50% EtOAc/Hexanes. ^{1}H NMR (500 MHz): δ 6.70 (br s, 1 H), 5.87 (br s, 1 H), 5.28 (s, 1 H), 5.07 (m, 1 H), 4.80 (m, 1 H), 3.29 (t, 1 H, *J* = 12.5 Hz), 2.65 (d, 1 H, *J* = 10 Hz), 2.56 (dd, 1 H, *J* = 15, 5.0 Hz), 2.34 (m, 4 H), 2.11 (d, 1 H, *J* = 10 Hz), 1.98 (br s, 3 H), 1.70 (br s, 3 H), 1.29 (s, 3 H). ^{13}C (125 MHz): δ 180.4, 173.7, 149.7, 146.2, 136.6, 133.4, 131.2, 129.0, 116.5, 112.5, 79.5, 49.9, 47.9, 37.3, 26.1, 24.5, 24.4, 23.2, 19.9. HRMS (EI)$^+$ calcd for $C_{19}H_{22}O_4$ $(M)^+$ 314.1518, found 314.1514.

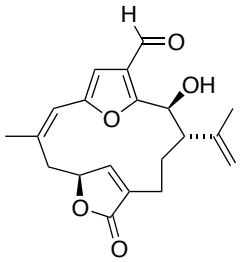

18-Oxobipinnatin J (3.56). To a biphasic solution of bipinnatin J (**1.11**) (31.5 mg, 0.096 mmol) in CH_2Cl_2 (2.3 mL) and pH 7 aqueous phosphate buffer (0.23 mL) at 0°C was added DDQ (49.0 mg, 0.216 mmol) at once. The solution immediately turned dark green. After 1.5 hr, a saturated solution of $NaHCO_3$ was added in addition to 8 mL EtOAc. The layers were separated, and the aqueous layer was extracted with EtOAc (2 X 8 mL). The combined organic extracts were dried, filtered, and concentrated *in vacuo*. The crude material was purified by flash chromatography (33% EtOAc/hexanes) to give 15.2 mg (46%) of **3.56** as a white solid.

R_f 0.30, 50% EtOAc/Hexanes. ^{1}H NMR (400 MHz): δ 9.53 (d, 1 H, *J* = 1.08 Hz), 7.03 (s, 1 H), 6.71 (s, 1 H), 6.71 (s, 1 H), 5.22 (br s, 1 H), 5.11 (br s, 1 H), 4.97 (m, 1 H), 4.56 (dd, 1 H, *J* = 11, 2.8 Hz), 3.53 (dd, 1 H, *J* = 11.7, 5.0 Hz), 2.81 (t, 1 H, *J* = 11.5 Hz), 2.44 (d, 1 H, *J* = 11.1 Hz), 2.39 (m, 1 H), 2.14 (s, 3 H), 2.10 (m, 1H), 1.98 (d, 1 H, *J* = 2.9 Hz), 1.81 (d, 3 H, *J* = 0.6 Hz), 1.72 (m, 1 H), 0.84 (m, 1 H). ^{13}C (100 MHz): δ 193.4, 173.9, 154.9, 151.1, 148.8, 141.3, 136.6, 133.3, 130.8, 123.7, 123.0, 119.7, 78.5, 64.8, 51.0, 31.3, 30.3, 19.7, 17.5, 9.4. IR: 3434, 2932, 2362, 1748, 1628, 1375, 1132, 997. HRMS $(EI)^+$ calcd for $C_{20}H_{22}O_5$ $(M)^+$ 342.1467, found 342.1460.

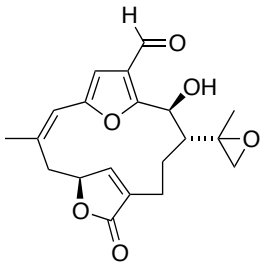

$\Delta^{15,16}$ epoxide of 18-oxobipinnatin J (3.57). To a solution of 18-oxobipinnatin J **3.56** (15.2 mg, 0.044 mmol) in acetone (1.0 mL) at -10 °C was added dropwise 1.0 mL (0.055 mmol) of a 0.055M dimethyldioxirane (DMDO) solution in acetone. After stirring for 4 hr an additional 0.2 mL of the DMDO solution was added. After 30 min the solution was concentrated *in vacuo* to give 16.0 mg of crude product (**3.57**). The crude material was analyzed by NMR which showed a single compound determined to be >80% pure.

R_f 0.20, 33% EtOAc/Hexanes. ^{1}H NMR (500 MHz) (only peaks >3.5 ppm will be listed due to lack of clarity for additional peaks below 3.5 ppm): δ 9.50 (s, 1 H), 7.03 (s, 1 H), 6.72 (s, 1 H), 6.71 (s, 1 H), 4.95 (m, 1 H), 4.84 (d, 1 H, *J* = 10.5 Hz), 3.54 (m, 1 H), 3.52 (s, 1 H), 3.51 (s, 1 H), . HRMS $(EI)^+$ calcd for $C_{20}H_{22}O_6$ (M^+): 358.1416, found: 358.1413.

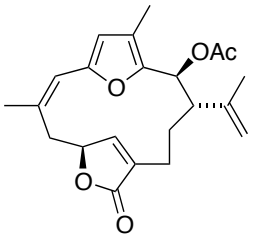

O-acetyl-bipinnatin J (3.63). To a solution of bipinnatin J (**1.11**) (60.0 mg, 0.183 mmol) in CH_2Cl_2 (2 mL) was added pyridine (43.4 mg, 0.549 mmol), DMAP (1.1 mg, 0.009 mmol), acetic anhydride (22.5 mg, 0.220 mmol). NOTE: the acetyl group hydrolyzes on silica. Silica TLC plates must be pre-treated with triethylamine in order to monitor the reaction. After 1 hr the solution was diluted with CH_2Cl_2 (8 mL) and 1:1 H_2O/saturated bicarbonate (8 mL). The layers were separated, and the aqueous layer was extracted with CH_2Cl_2 (8 mL). The combined organic extracts were washed with brine (8 mL), dried, filtered and concentrated *in vacuo* to give 62.0 mg (92%) of **3.63** as a white solid. If necessary, this material could be further purified by flash chromatography (25% EtOAc/hexanes, 2% NEt_3).

R_f 0.45, 33% EtOAc/Hexanes. ^{1}H NMR (600 MHz): δ 6.85 (br s, 1 H), 6.11 (br s, 1 H), 6.02 (s, 1 H), 5.79 (d, 1 H, J = 11.6 Hz), 5.00 (br s, 1 H), 4.99 (m, 1 H), 4.95 (br s, 1 H), 3.22 (t, 1 H, J = 11.8 Hz), 2.76 (dd, 1 H, J = 11.8, 4.5 Hz), 2.51 (t, 1 H, J = 11.3 Hz), 2.43 (m, 1 H), 2.10 (m, 1 H), 2.08 (s, 3 H), 2.01 (br s, 3 H), 1.93 (s, 3 H), 1.71 (s, 3 H), 1.65 (m, 1 H), 0.89 (m, 1 H). ^{13}C (150 MHz): δ 174.2, 170.0, 152.2, 151.4, 146.9, 141.8, 132.8, 129.5, 122.4, 117.2, 116.5, 114.0, 78.6, 67.0, 47.9, 39.7, 30.3, 25.9, 20.8, 19.6, 18.6, 9.5. HRMS $(EI)^+$ calcd for $C_{22}H_{26}O_5$ $(M)^+$ 370.1780, found 370.1774.

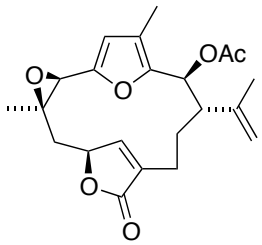

$\Delta^{7,8}$ epoxide of O-acetyl-bipinnatin J (3.64). To a solution of O-acetyl-bipinnatin J (**3.63**) (25.6 mg, 0.069 mmol) in acetone (1.0 mL) at –50 °C was added dropwise 1.02 mL (0.083 mmol) of a 0.081M dimethyldioxirane solution in acetone. After 12 hr an additional 0.20 mL (0.016 mmol) of the DMDO solution was added dropwise. After 6 hr the solution was concentrated *in vacuo* and the crude material purified by flash chromatography (33% EtOAc/hexanes) to give 12 mg of a mixture of epoxide **3.64** and dienedione **3.65** as a clear residue. NOTE: the epoxide and dienedione are co-polar in EtOAc/hexanes. The mixture was separated by flash chromatography (100% DCM) to give 6.9 mg (26%) of epoxide **3.64** and 2.8 mg (10%) of dienedione **3.65** as a white solid and a clear residue, respectively.

Epoxide **3.64**: R_f 0.45, 50% EtOAc/Hexanes. ^{1}H NMR (500 MHz): δ 6.55 (br s, 1 H), 6.48 (s, 1 H), 5.65 (d, 1 H, J = 12.0 Hz), 5.04 (m, 1 H), 4.97 (br s, 1 H), 4.85 (br s, 1 H), 3.67 (s, 1 H), 2.90 (m, 1 H), 2.40 (m, 2 H), 2.23 (t, 1 H, J = 12.5 Hz), 2.11 (s, 3 H), 2.08 (m, 1 H), 1.96 (s, 3 H),

1.67 (s, 3 H), 1.60 (m, 1 H), 1.57 (s, 3 H), 0.91 (m, 1 H). HRMS $(EI)^+$ calcd for $C_{22}H_{26}O_6$ $(M)^+$ 386.1729, found 386.1735.

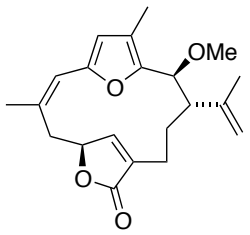

O-methyl-bipinnatin J (3.70). To a solution of bipinnatin J (**1.11**) (41.0 mg, 0.125 mmol) in CH_2Cl_2 (2.5 mL) was added MeOH (160.2 mg, 5.00 mmol) and TFA (15.7 mg, 0.138 mmol). NOTE: silica TLC plates must be pre-treated with triethylamine in order to monitor the reaction. After 2 hr the solution was diluted with Et_2O (12 mL) and 1:1 H_2O/saturated bicarbonate (12 mL). The layers were separated, and the organic extract was washed with brine (12 mL). The organic extract was dried, filtered, and concentrated *in vacuo* to give 41.7 mg (97%) of O-methyl-bipinnatin J (**3.70**) as a white solid. If necessary, this material could be further purified by flash chromatography (25% EtOAc/hexanes, 2% NEt_3).

R_f 0.60, 33% EtOAc/Hexanes. ^1H NMR (500 MHz): δ 6.78 (br s, 1 H), 6.12 (s, 1 H), 6.05 (s, 1 H), 5.01 (br s, 1 H), 4.96 (m, 1H), 4.94 (br s, 1 H), 4.10 (dd, 1 H, J = 11.1, 1.3 Hz), 3.22 (t, 1 H, J = 11.8 Hz), 3.13 (s, 3 H), 2.70 (dd, 1 H, J = 11.8, 4.1 Hz), 2.44 (m, 2 H), 2.07 (s, 3 H), 2.03 (m, 1 H), 2.00 (s, 3 H), 1.76 (s, 3 H), 1.53 (m, 1 H), 0.86 (td, 1 H, J = 13.7, 3.5 Hz). ^{13}C (125 MHz): δ 174.2, 152.0, 151.3, 147.2, 142.9, 132.7, 129.4, 122.4, 117.2, 155.5, 113.5, 78.6, 74.4, 55.8, 48.5, 39.6, 30.2, 25.9, 19.5, 18.0, 9.8. HRMS $(EI)^+$ calcd for $C_{21}H_{26}O_4$ $(M)^+$ 342.1831, found 342.1828.

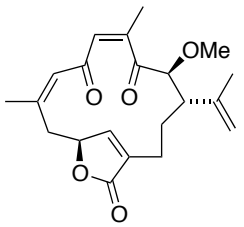

Oxidation of O-methyl-bipinnatin J (**3.71**). To a solution of O-methyl-bipinnatin J (**3.70**) (20.0 mg, 0.058 mmol) in CH_2Cl_2 (8 mL) at -78 °C was added Rose Bengal (1.8 mg, 0.002 mmol). While oxygen was bubbled through the pink solution, it was irradiated with a 275W sun lamp. After 10 min dimethyl sulfide (18.0 mg, 0.290 mmol) was added and the solution stirred for 5 min before being allowed to warm to room temperature. The solution was concentrated *in vacuo* and the pink residue dissolved in 1:1 Et_2O/H_2O (15 mL). The layers were separated and the organic extract washed with H_2O (8 mL). The organic extract was dried, filtered and concentrated *in vacuo*. The crude material was purified by flash chromatography (33% EtOAc/hexanes) to give 16 mg (77%) of **3.71** as cream-colored solid.

R_f 0.50, 50% EtOAc/Hexanes. Note: the ^1H NMR displays unusually broad signals which reflects conformational flexibility of the macrocycle. The ^{13}C NMR displays so many broad and short peaks as to render the spectrum almost useless. Only the sharp peaks will be listed. ^1H

NMR (400 MHz): δ 7.00 (br m, 1 H), 6.28 (br s, 1 H), 6.04 (br m, 1 H), 5.02 (br m, 1 H), 4.84 (br m, 1 H), 4.71 (br s, 1 H), 3.98 (br m, 1 H), 3.55 (br s, 3 H), 2.78 (br t, 1 H, J = 10.8 Hz), 2.44 (br m, 1 H), 2.27 (ddd, 1 H, J = 15.0, 11.1, 4.3 Hz), 2.04 (m, 1 H), 2.03 (m, 1 H), 2.00 (s, 3 H), 1.88 (m, 1 H), 1.88 (s, 3 H), 1.75 (m, 1 H), 1.61 (s, 3 H). ^{13}C (100 MHz): δ 206.0, 150.5, 145.0, 114.9, 46.0, 23.1, 21.7. HRMS (EI)$^+$ calcd for $C_{21}H_{26}O_5$ $(M)^+$ 358.1780, found 358.1786.

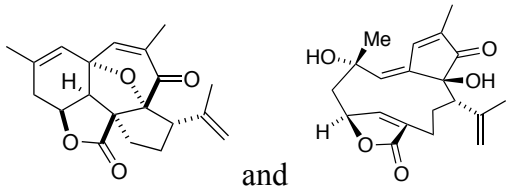

and

Intricarene (1.40) and ketone (3.76). A solution of dienedione **3.71** (30.0 mg, 0.084 mmol) in H_2O (0.8 mL) and acetone (1.1 mL) was irradiated with a 275 W sun lamp for 12 hr. The solution was concentrated *in vacuo* to approximately 0.8 mL and the aqueous phase diluted with EtOAc (8 mL) and H_2O (7 mL). The layers were separated and the aqueous phase was extracted with EtOAc (2 X 8 mL). The combined organic extracts were dried, filtered and concentrated *in vacuo*. The crude material was purified by flash chromatography (25% EtOAc/hexanes) to give 7.0 mg (26%) of intricarene (**1.40**) as a clear residue and 7.1 mg (25%) of ketone **3.76** as a clear residue.

Intricarene (**1.40**): R_f 0.85, 50% EtOAc/Hexanes.

^{1}H NMR isolation	^{1}H NMR synthetic	^{13}C NMR isolation	^{13}C NMR synthetic
6.41 (q, 1 H, J = 1.6 Hz)	6.41 (br s, 1 H)	193.0	193.0
6.27 (q, 1 H, J = 1.6 Hz)	6.27 (q, 1 H, J = 1.4 Hz)	177.9	178.0
4.92 (q, 1 H, J = 1.3 Hz)	4.92 (br s, 1 H)	147.3	147.3
4.86 (br s, 1 H)	4.86 (br s, 1 H)	141.8	141.7
4.77 (ddd, 1 H, J = 8.6, 5.3, 2.6 Hz)	4.78 (ddd, 1 H, J = 8.3, 5.3, 2.6 Hz)	137.2	137.1
3.38 (dd, 1 H, J = 11.9, 5.7 Hz)	3.38 (dd, 1 H, J = 12.1, 5.8 Hz)	135.2	135.2
2.82 (dd, 1 H, J = 18.6, 8.6 Hz)	2.83 (dd, 1 H, J = 18.6, 8.6 Hz)	128.1	128.0
2.54 (d, 1 H, J = 5.3 Hz)	2.54 (d, 1 H, J = 5.3 Hz)	113.3	113.3
2.41 (br d, 1 H, J = 18.6 Hz)	2.41 (br d, 1 H, J = 18.0 Hz)	102.8	102.7
2.11 (m, 1 H)	2.10 (m, 1 H)	84.6	84.6
2.01 (m, 1 H)	2.01 (m, 1 H)	70.7	70.7
1.92 (m, 1 H)	1.91 (m, 1 H)	64.2	64.1
1.84 (t, 3 H, J = 1.2 Hz)	1.84 (t, 3 H, J = 1.5 Hz)	58.0	57.9
1.76 (d, 3 H, J = 1.6	1.76 (br s, 6 H)	46.4	46.3

Hz)			
1.75 (br s, 3 H)		35.7	35.6
		29.3	29.3
		28.5	28.5
		23.13	23.14
		23.06	23.07
		14.4	14.4

Ketone (**3.76**): R_f 0.20, 50% EtOAc/Hexanes. ^{1}H NMR (400 MHz): δ 8.39 (t, 1 H, *J* = 1.4 Hz), 7.42 (t, 1 H, *J* = 1.6 Hz), 5.40 (s, 1 H), 5.25 (t, 1 H, *J* = 1.7 Hz), 5.22 (m, 1 H), 5.08 (d, 1 H, *J* = 2.0 Hz), 3.02 (s, 1 H), 2.55 (m, 1 H), 2.46 (m, 1 H), 2.26 (m, 1 H), 2.18 (m, 1 H), 2.06 (m, 1 H), 1.90 (s, 3 H), 1.85 (s, 3 H), 1.78 (m, 1 H), 1.72 (s, 1 H), 1.50 (s, 3 H), 1.08 (m, 1 H). ^{13}C (100 MHz): δ 206.1, 174.8, 152.8, 152.4, 142.1, 139.7, 132.5, 129.8, 120.8, 76.7, 75.9, 58.0, 53.8, 49.0, 32.3, 26.9, 21.7, 21.3, 18.3, 11.0. HRMS (EI)$^+$ calcd for $C_{20}H_{24}O_5$ (M)$^+$ 344.1624, found 344.1628.

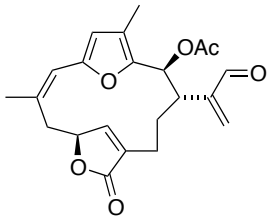

2-O-Acetyl-17-oxobipinnatin J (3.78). To a solution of O-acetyl-bipinnatin J (**3.63**) (20.0 mg, 0.054 mmol) in dioxane (8 mL) was added SeO_2 (30.0 mg, 0.270 mmol). The solution was stirred at 80 °C for 2 hr. The solution was diluted with brine (20 mL) and Et_2O (20 mL). The layers were separated, and the aqueous phase extracted with Et_2O (2 X 20 mL). The combined organic extracts were dried, filtered and concentrated *in vacuo*. The crude material was purified by flash chromatography (20% EtOAc/hexanes) to give 10.1 mg (48%) of **3.78** as a white solid.

R_f 0.75, 50% EtOAc/Hexanes. ^{1}H NMR (400 MHz): δ 9.54 (d, 1 H, *J* = 1.7 Hz), 6.89 (br s, 1 H), 6.53 (s, 1 H), 6.26 (d, 1 H, *J* = 11.4 Hz), 6.23 (br s, 1 H), 6.12 (m, 1 H), 6.03 (s, 1 H), 5.04 (m, 1 H), 3.24 (t, 1 H, *J* = 11.8 Hz), 2.78 (dd, 1 H, *J* = 11.8, 4.6 Hz), 2.73 (m, 1 H), 2.26 (m, 1 H), 2.11 (m, 1 H), 2.10 (s, 3 H), 2.01 (br s, 3 H), 1.97 (m, 1 H), 1.86 (s, 3 H), 1.00 (m, 1 H). ^{13}C (100 MHz): δ 193.9, 174.4, 169.5, 152.5, 151.4, 146.7, 146.3, 140.6, 132.5, 129.4, 123.2, 117.3, 114.1, 78.7, 66.5, 43.5, 39.8, 30.2, 25.8, 20.7, 19.6, 9.6. HRMS (EI)$^+$ calcd for $C_{22}H_{24}O_6$ (M)$^+$ 384.1573, found 384.1568.

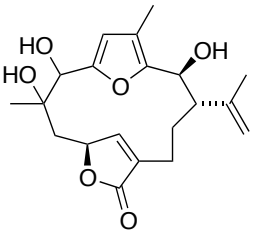

Dihydroxylation of bipinnatin J (3.79). To a solution of bipinnatin J (**1.11**) (50.0 mg, 0.152 mmol) in acetone (7 mL) and H_2O (7 mL) was added OsO_4 (3.0 mg, 0.012 mmol) and NMO (26.7 mg, 0.228 mmol). The solution was stirred at 50 °C for 12 hr. To the dark solution was added $NaHSO_3$ (125 mg, 1.201 mmol) and celite (50 mg). The mixture was stirred for 10 min, filtered, and diluted with EtOAc (30 mL) and H_2O (20 mL). The layers were separated, and the aqueous phase extracted with EtOAc (2 X 15 mL). The combined organic extracts were dried, filtered, and concentrated *in vacuo*. The crude material was purified by flash chromatography (100% EtOAc) to give 24.5 mg (45%) of **3.79** as a clear residue.

R_f 0.20, 100% EtOAc. ^{1}H NMR (500 MHz): δ 6.13 (br s, 1 H), 5.53 (s, 1 H), 5.00 (s, 1 H), 4.91 (m, 1 H), 4.87 (s, 1 H), 4.43 (s, 1 H), 4.42 (d, 1 H, J = 10.7 Hz), 4.05 (br s (OH), 1 H), 3.59 (br s (OH), 1 H), 3.02 (br s (OH), 1 H), 2.32 (m, 2 H), 2.22 (m, 2 H), 2.07 (s, 3 H), 2.02 (m, 1 H), 1.79 (s, 3 H), 1.65 (m, 1 H), 1.31 (s, 3 H), 1.24 (m, 1 H). ^{13}C (125 MHz): δ 174.1, 149.8, 149.3, 143.8, 133.3, 199.9, 117.4, 112.6, 79.8, 76.2, 73.6, 66.2, 53.9, 52.1, 39.7, 26.2, 23.4, 21.5, 17.8, 10.2. HRMS $(ESI)^+$ calcd for $C_{20}H_{26}O_6Li$ $(M+Li^+)^+$ 369.1889, found 369.1887.

3.9 - Appendix

Characterization Data for 3.43, 3.44, 3.45, 3.46, 3.47, 3.48, 3.39, 3.50, 3.51, 3.54, 3.56, 3.57, 3.63, 3.64, 3.70, 3.71, 1.40, 3.76, 3.78 and 3.79.

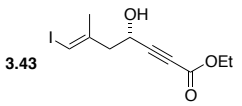

3.43

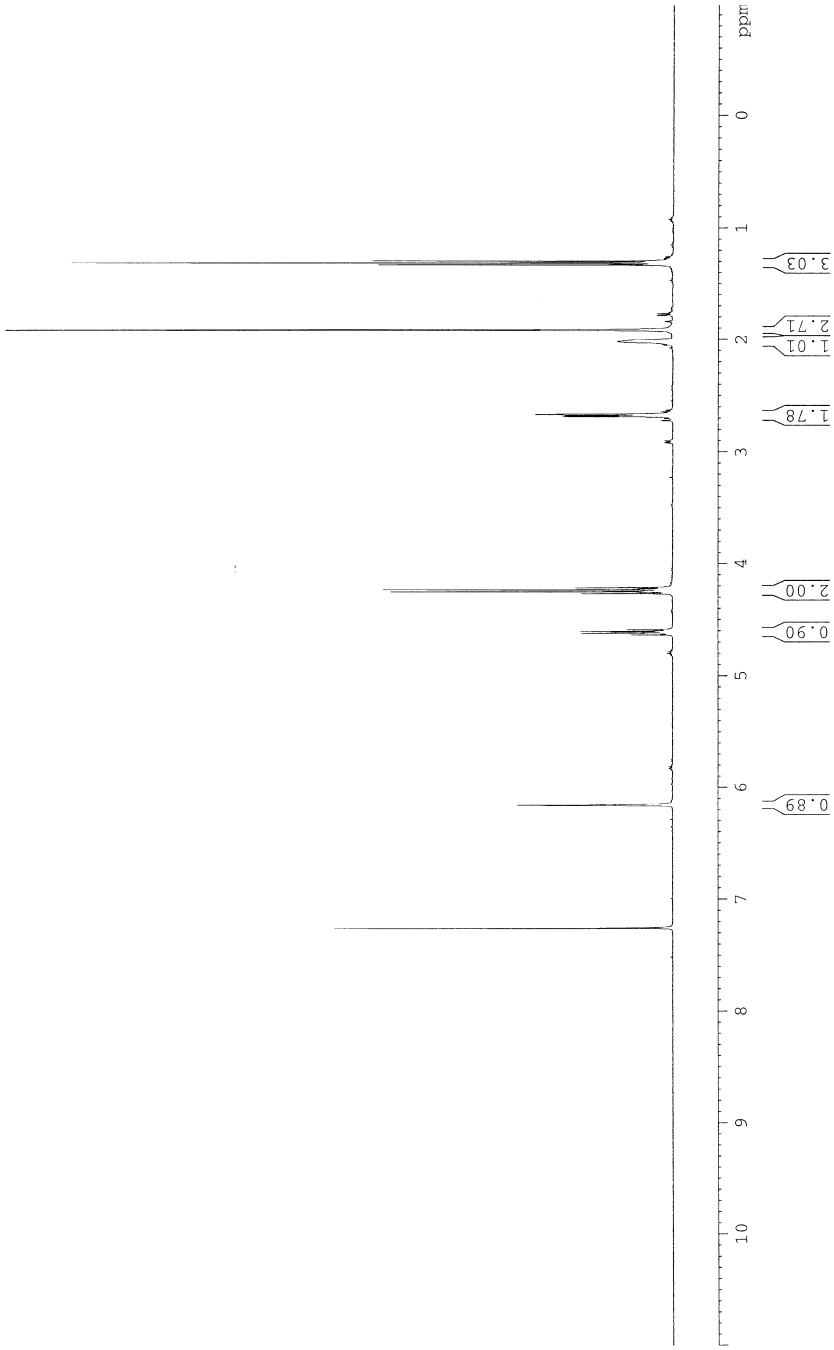

3.44

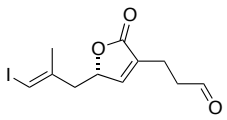

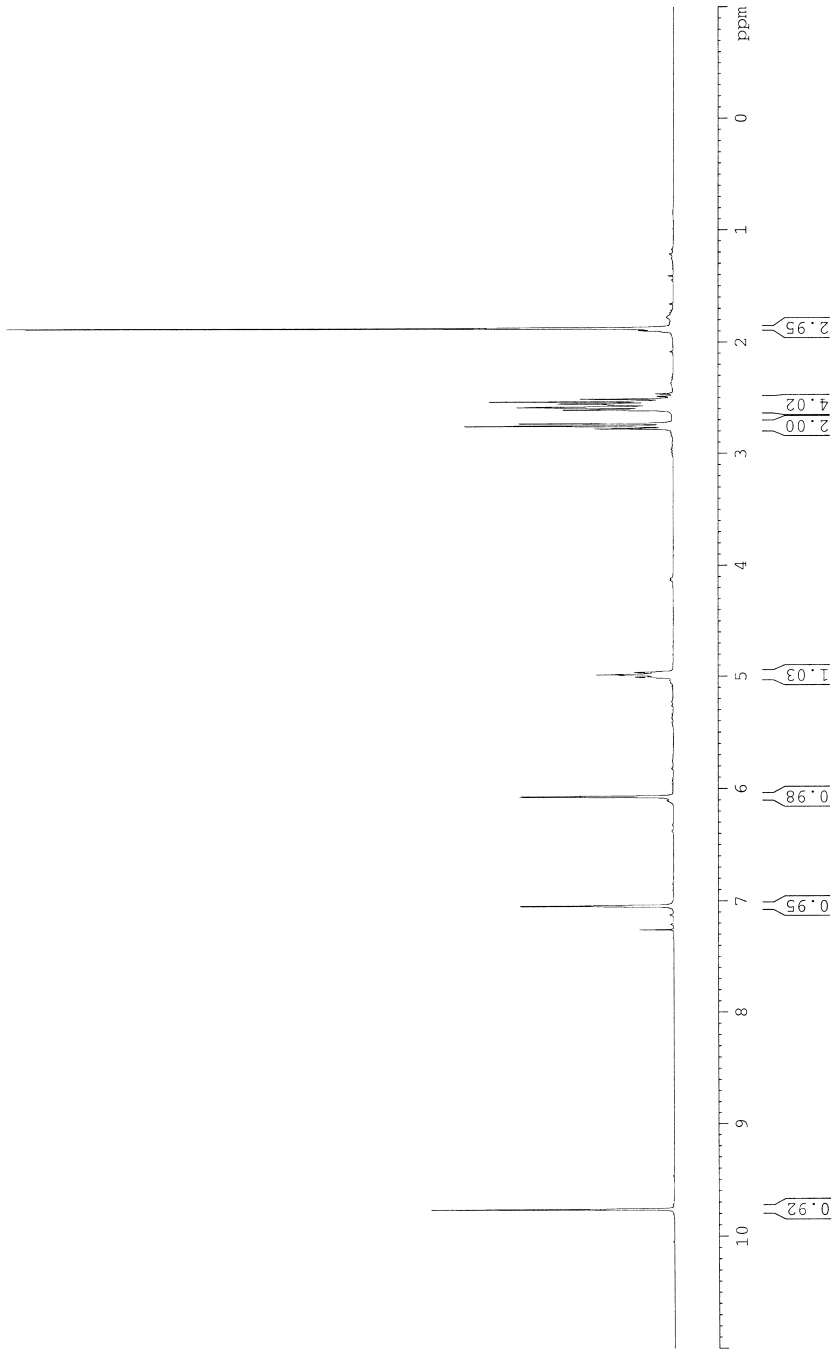

3.45

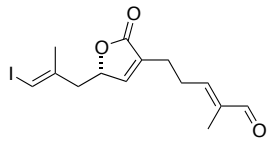

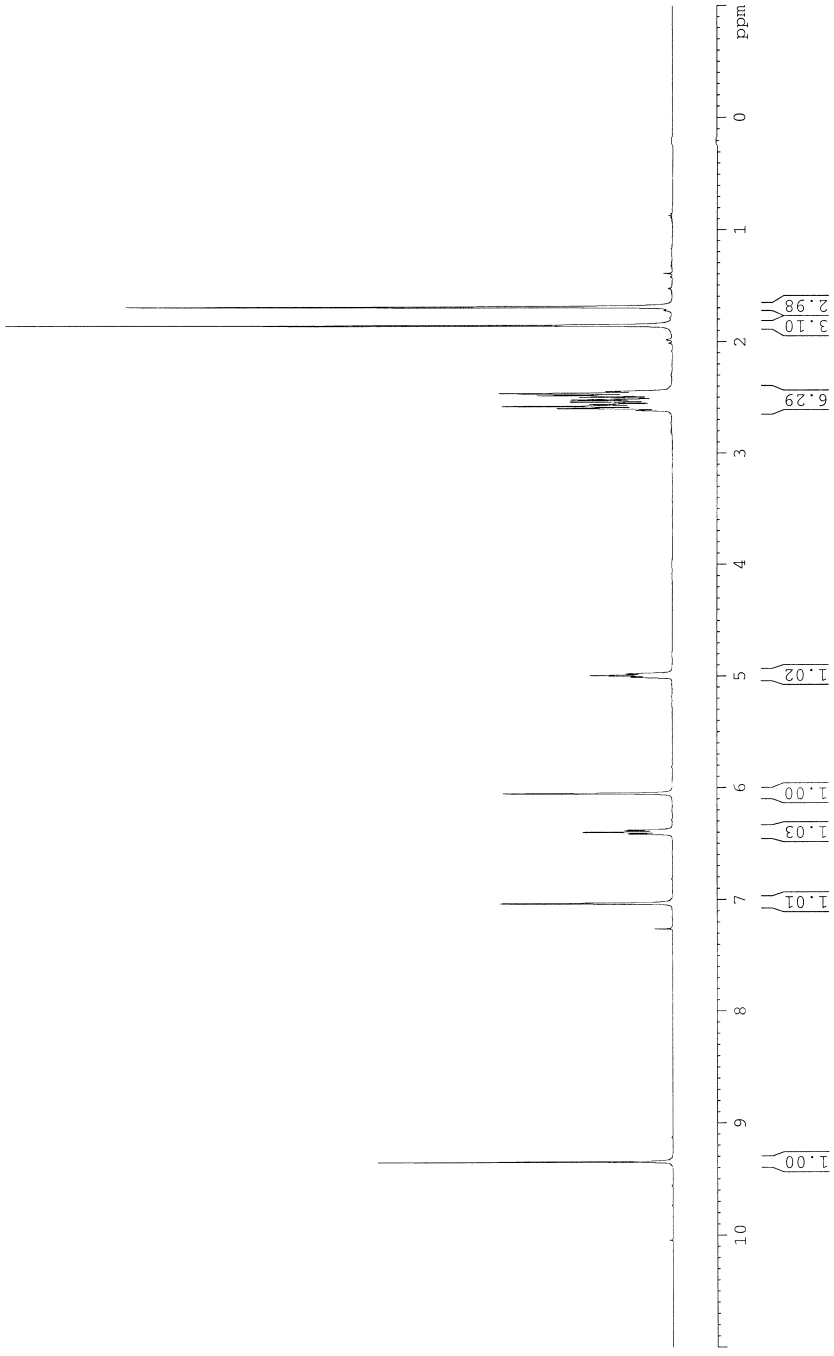

3.46

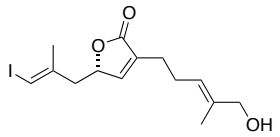
O
O
I
OH

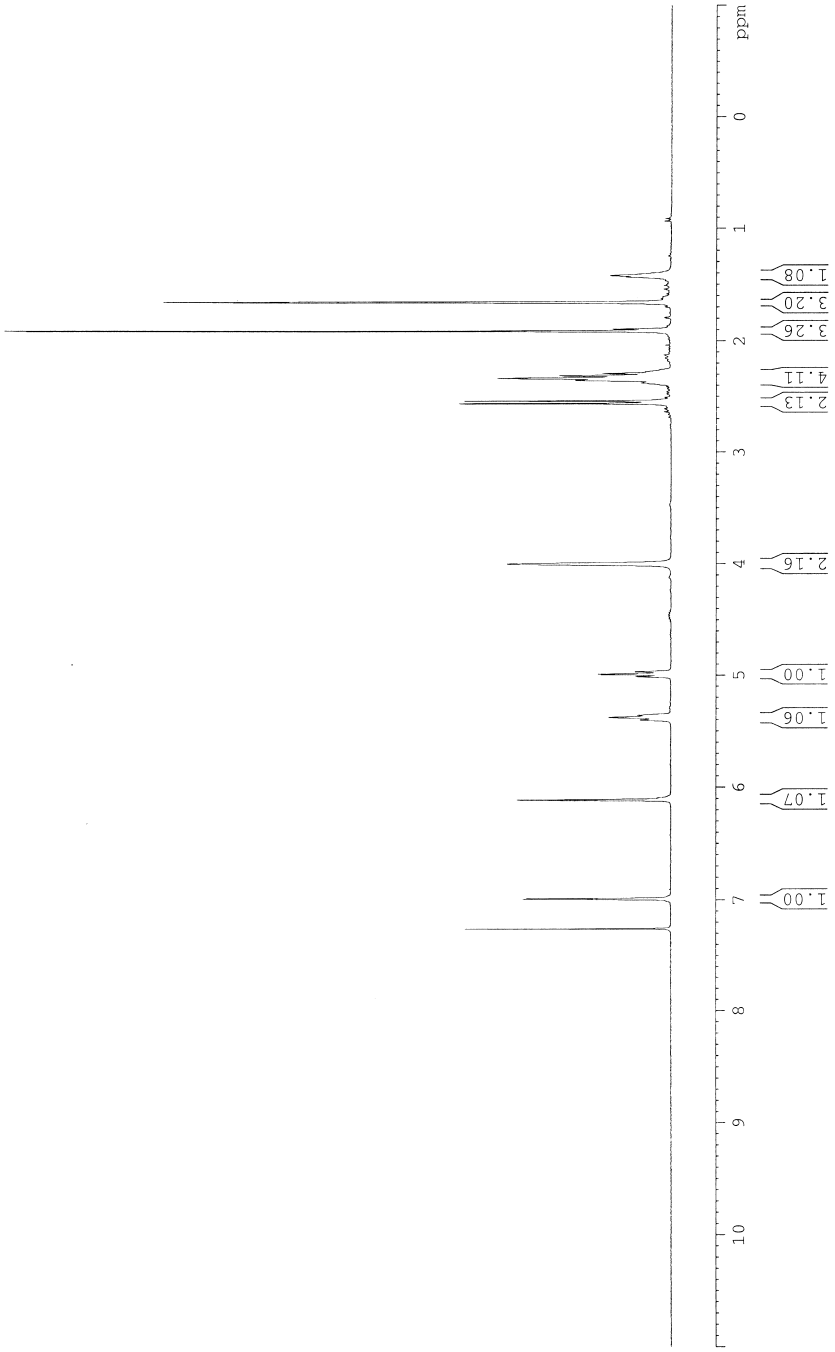
ppm
0
1
2
3
4
5
6
7
8
9
10
1.08
3.20
3.26
4.11
2.13
2.16
1.00
1.06
1.07
1.00

3.47

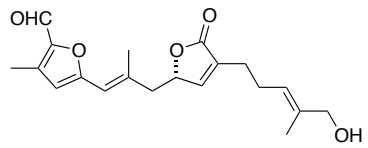
OHC
O
O
O
OH

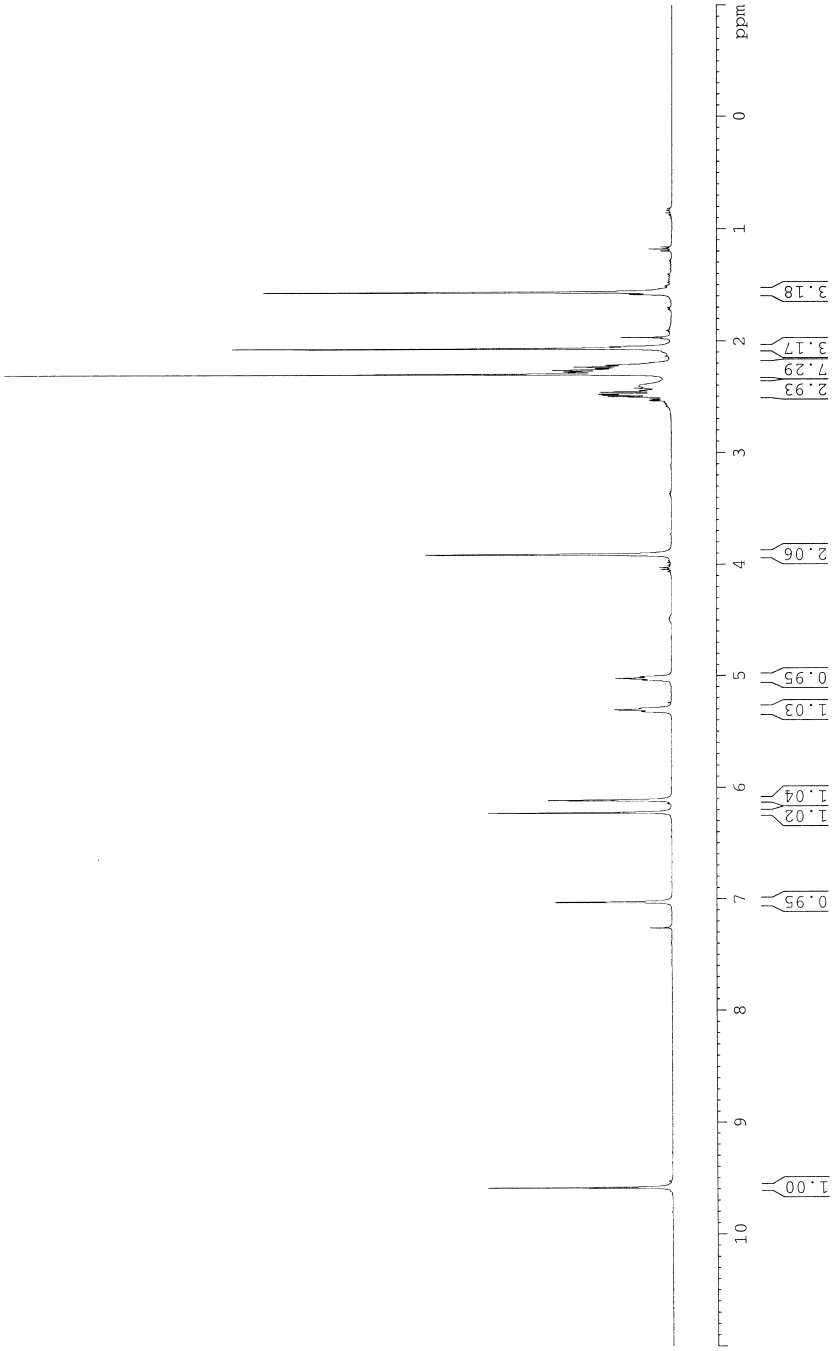
ppm
0
1
2
3
4
5
6
7
8
9
10
3.18
3.17
7.29
2.93
2.06
0.95
1.03
1.02
1.04
0.95
1.00

3.48

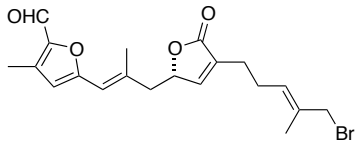
OHC
O
O
O
Br

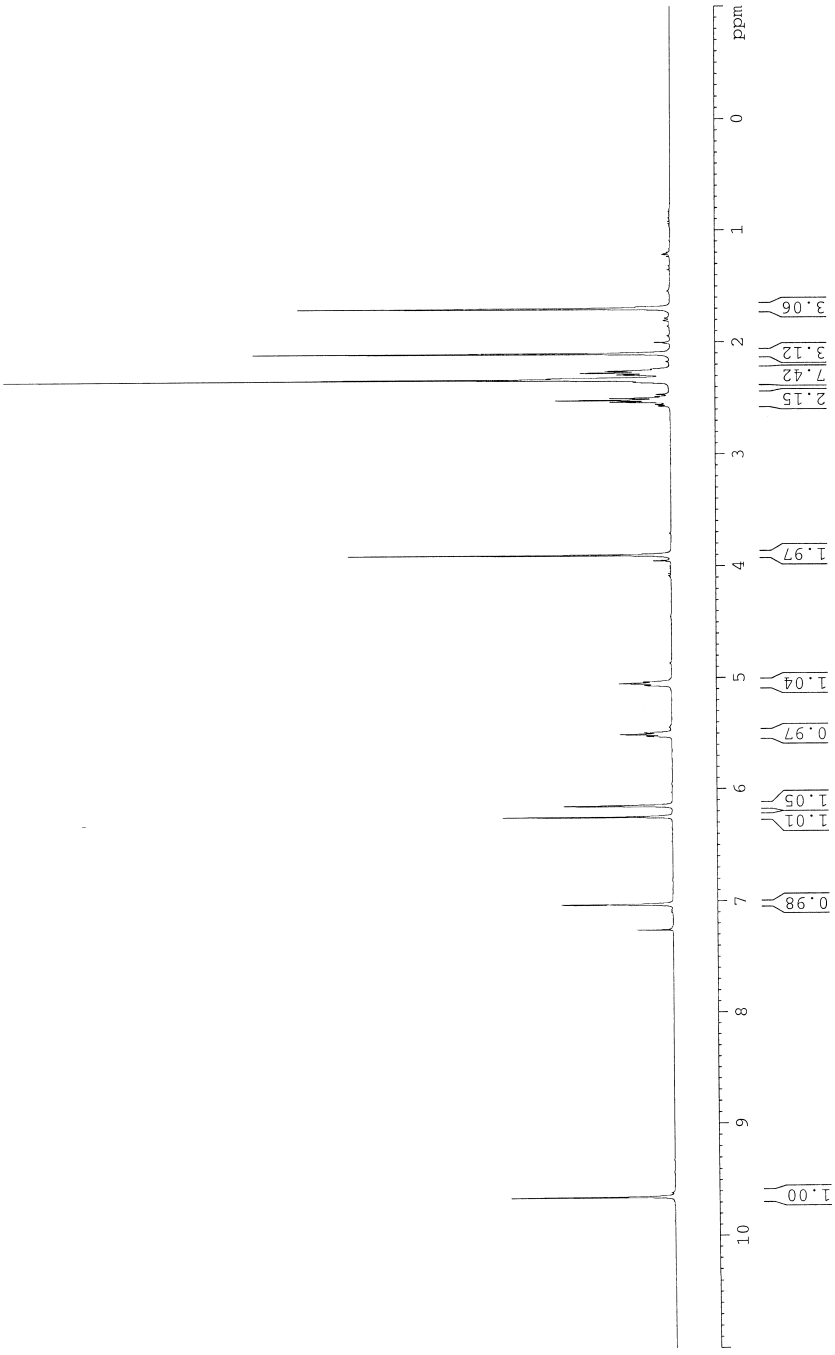
ppm
0
1
2
3
4
5
6
7
8
9
10
3.06
3.12
7.42
2.15
1.97
1.04
0.97
1.01
1.05
0.98
1.00

3.39

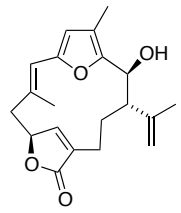

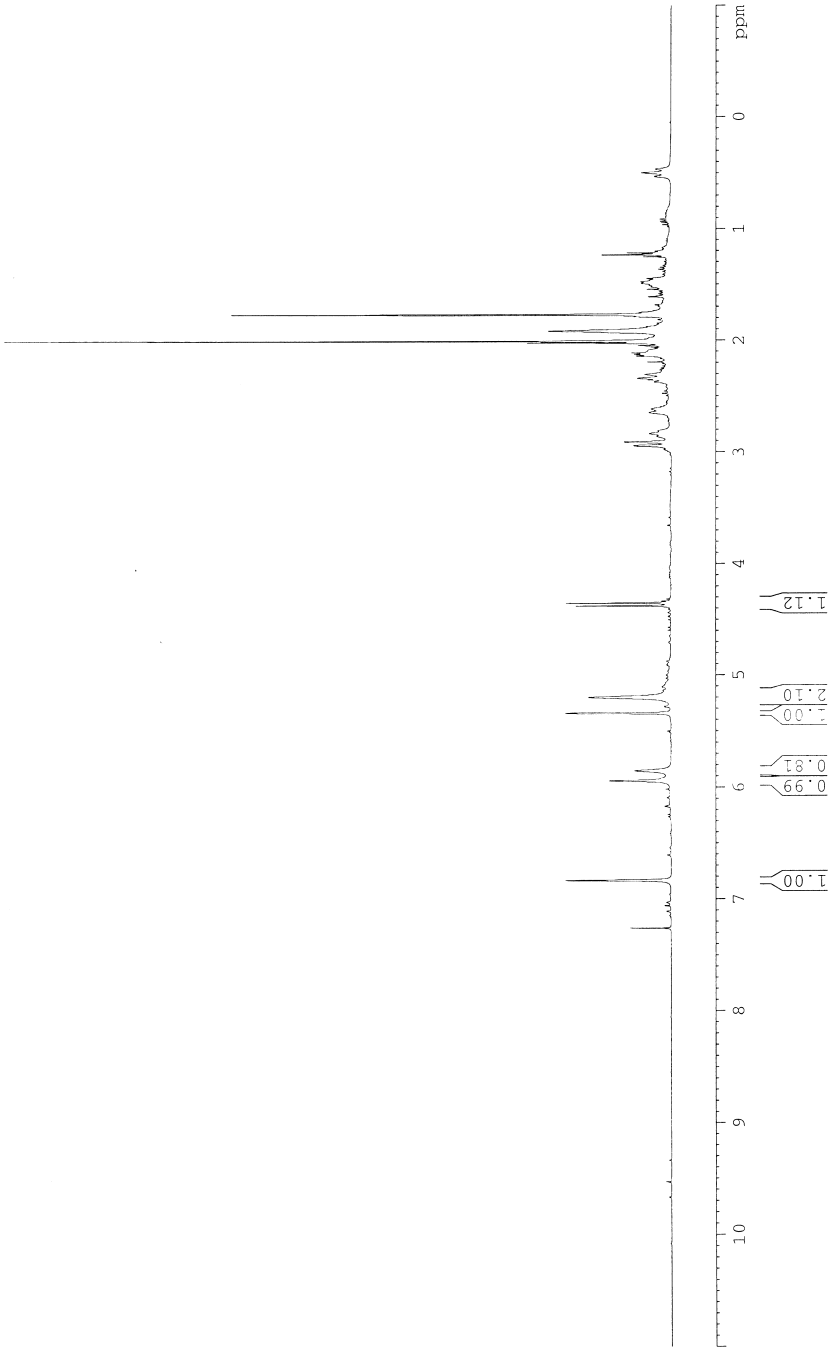

3.50

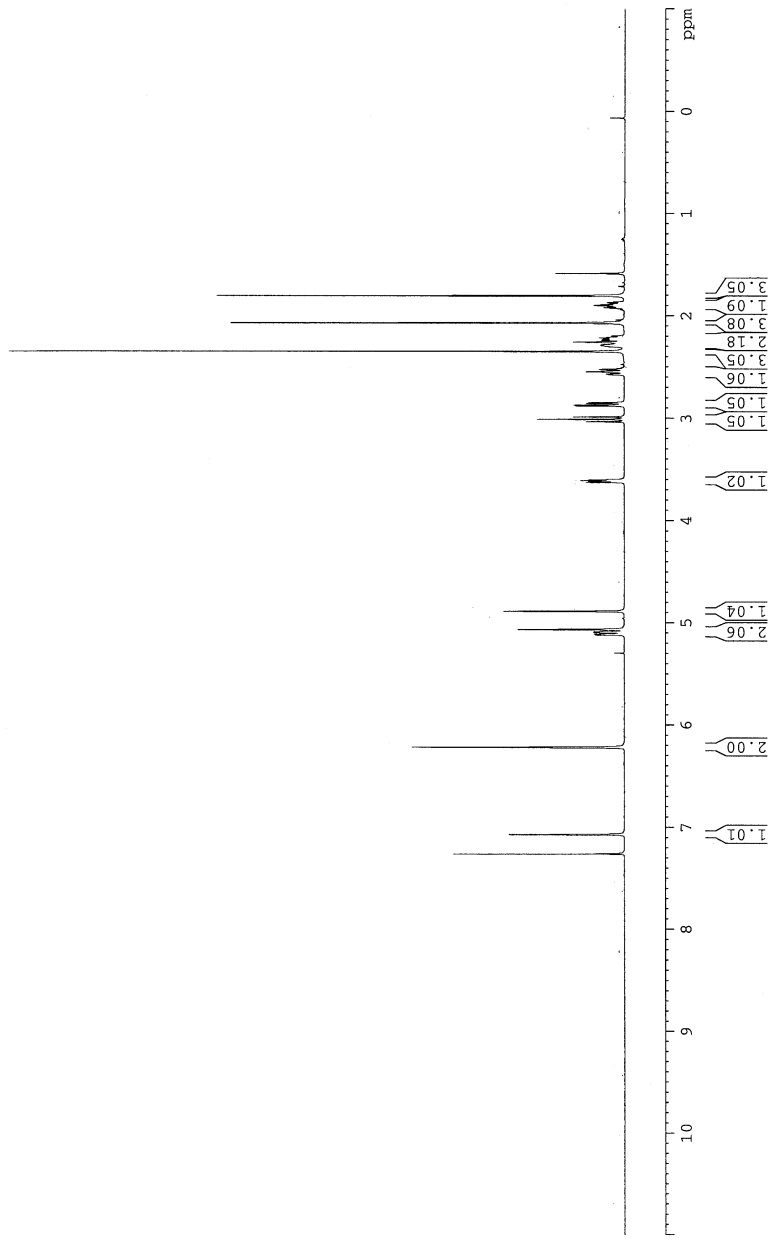
ppm
0
1
2
3
4
5
6
7
8
9
10
3.05
1.09
3.08
2.18
3.05
1.06
1.05
1.05
1.02
1.04
2.06
2.00
1.01

3.51

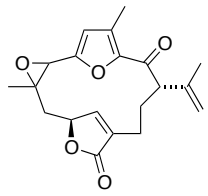

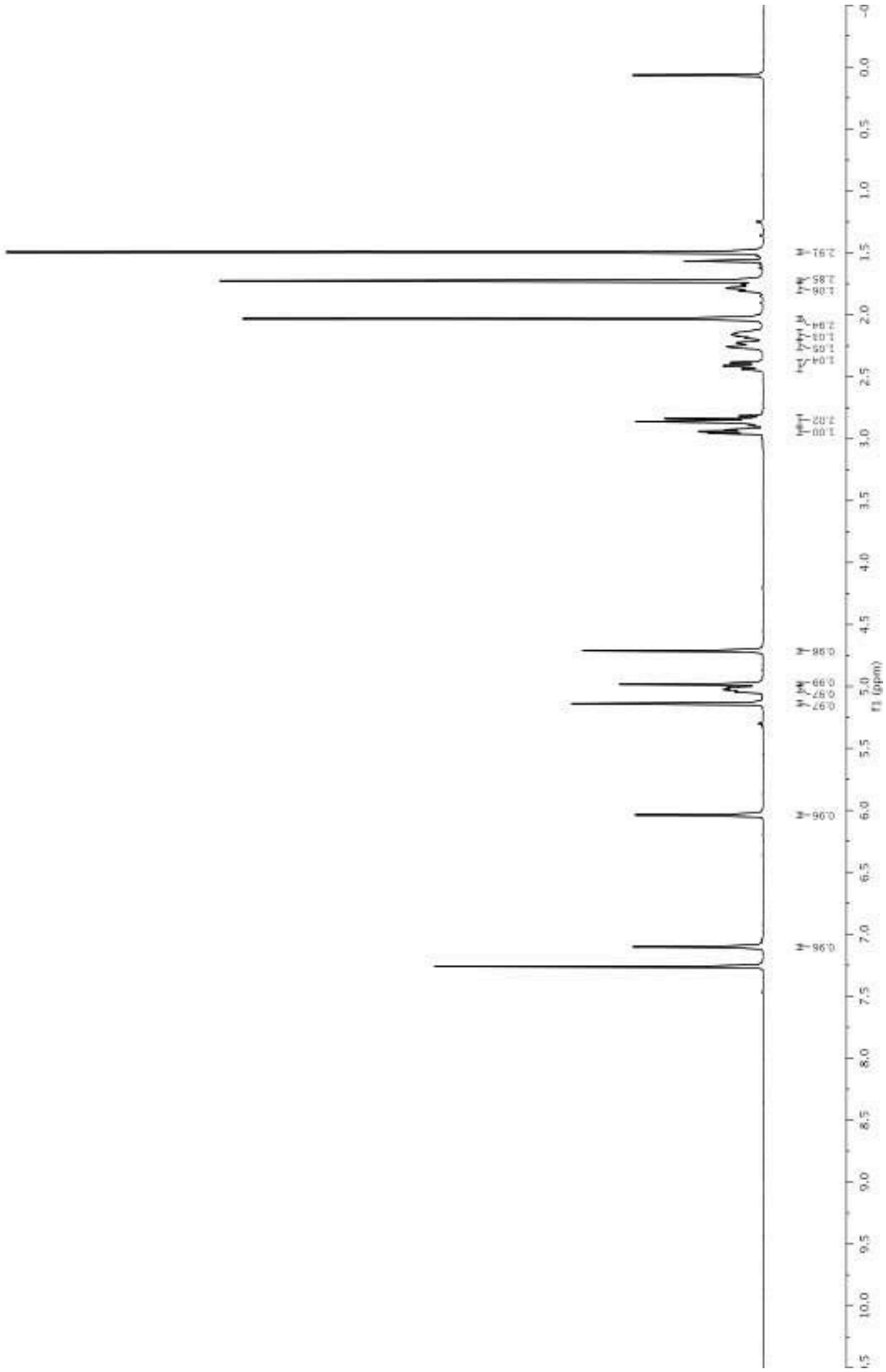

3.54

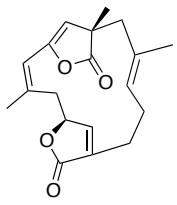

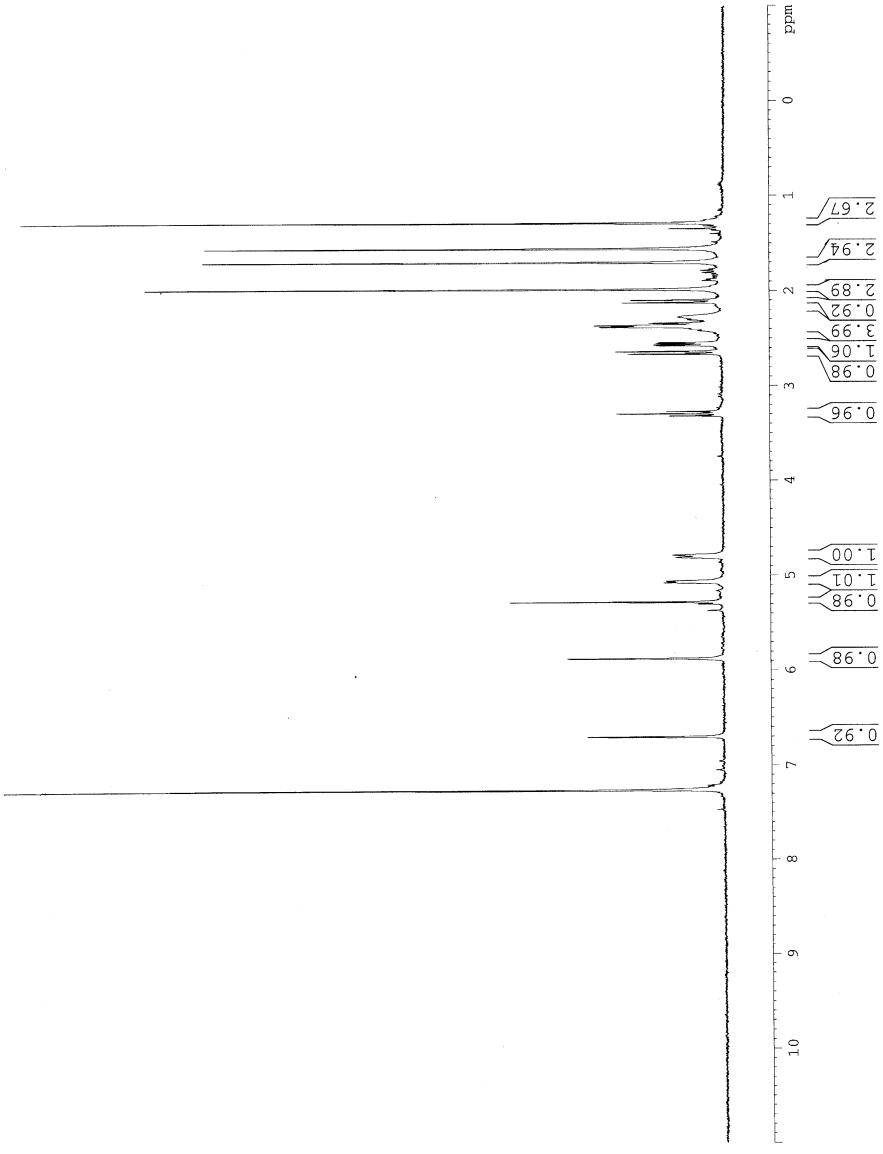
ppm
0
1
2
3
4
5
6
7
8
9
10
2.67
2.94
2.89
0.92
3.99
1.06
0.98
0.96
1.00
1.01
0.98
0.98
0.92

3.56

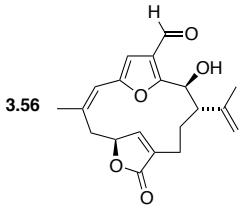

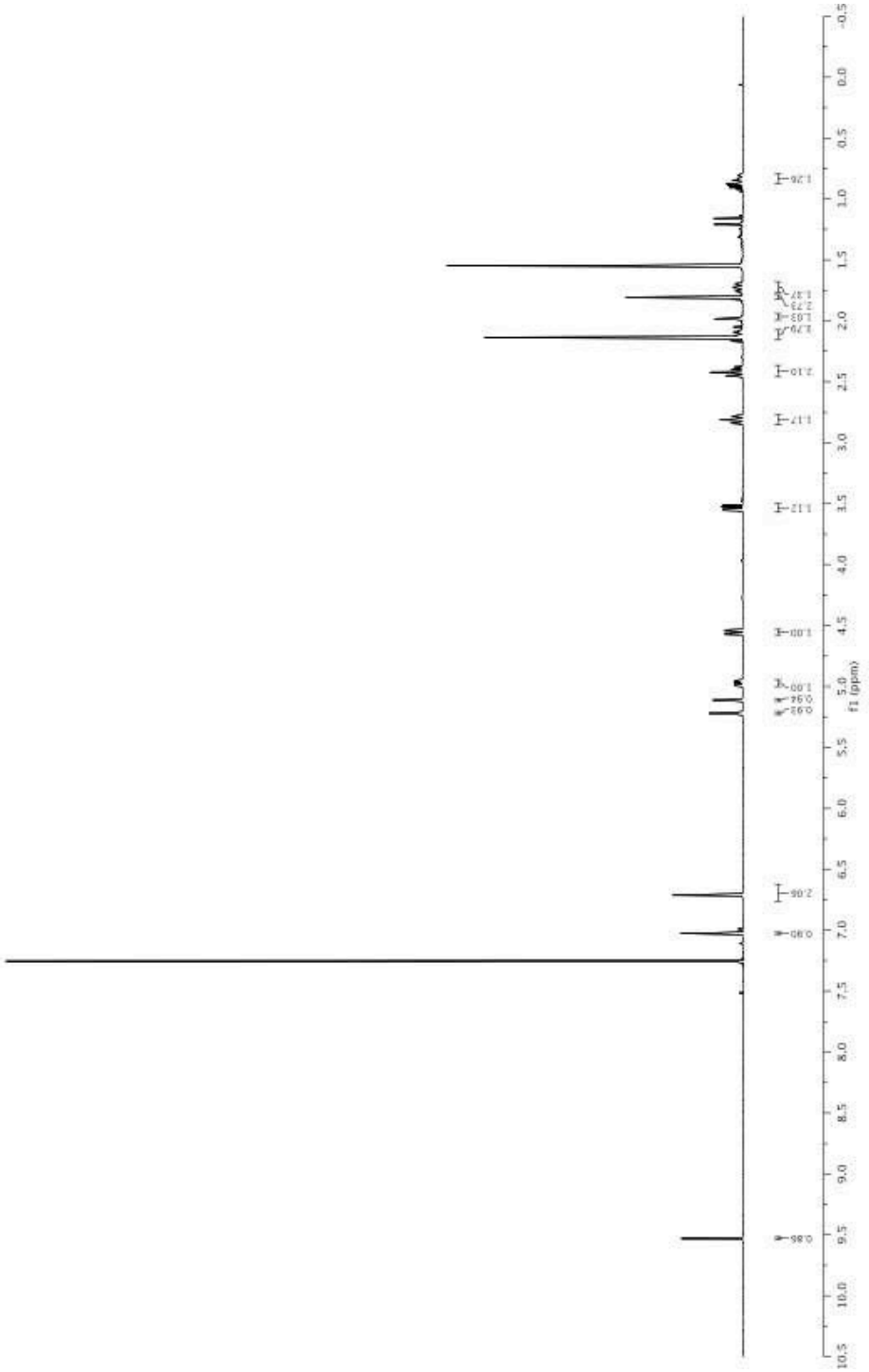

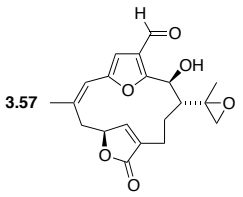
H
O
OH
O
O
O
O
3.57

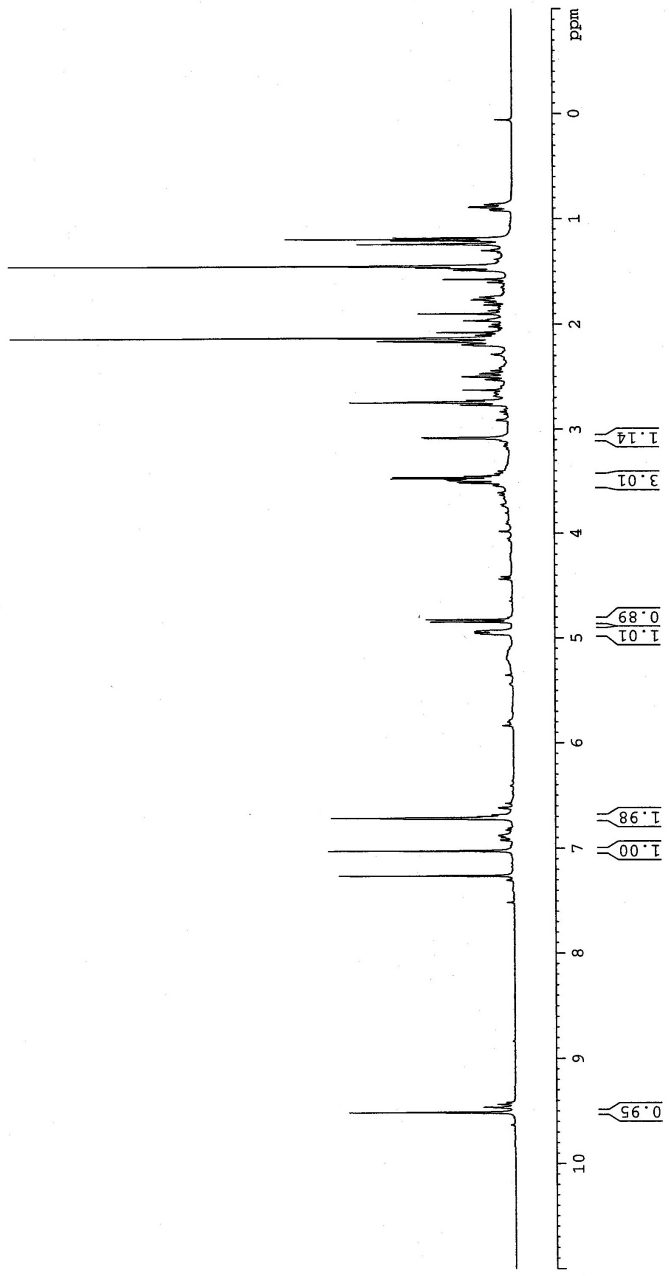
ppm
0
1
2
3
4
5
6
7
8
9
10
1.14
3.01
0.89
1.01
1.98
1.00
0.95

3.63

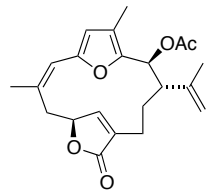

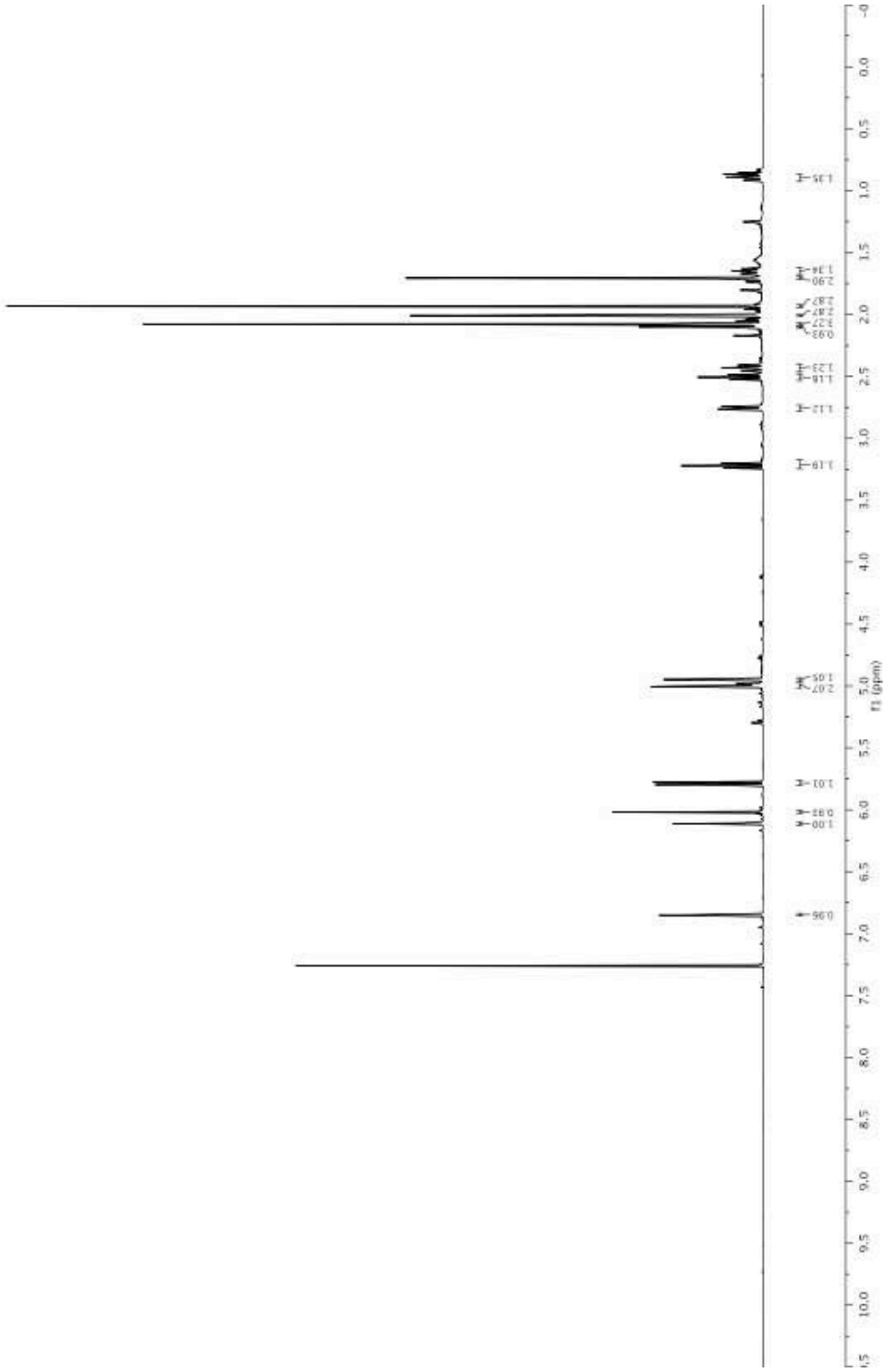

3.64

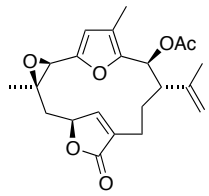
OAc
O
O
O
O
O

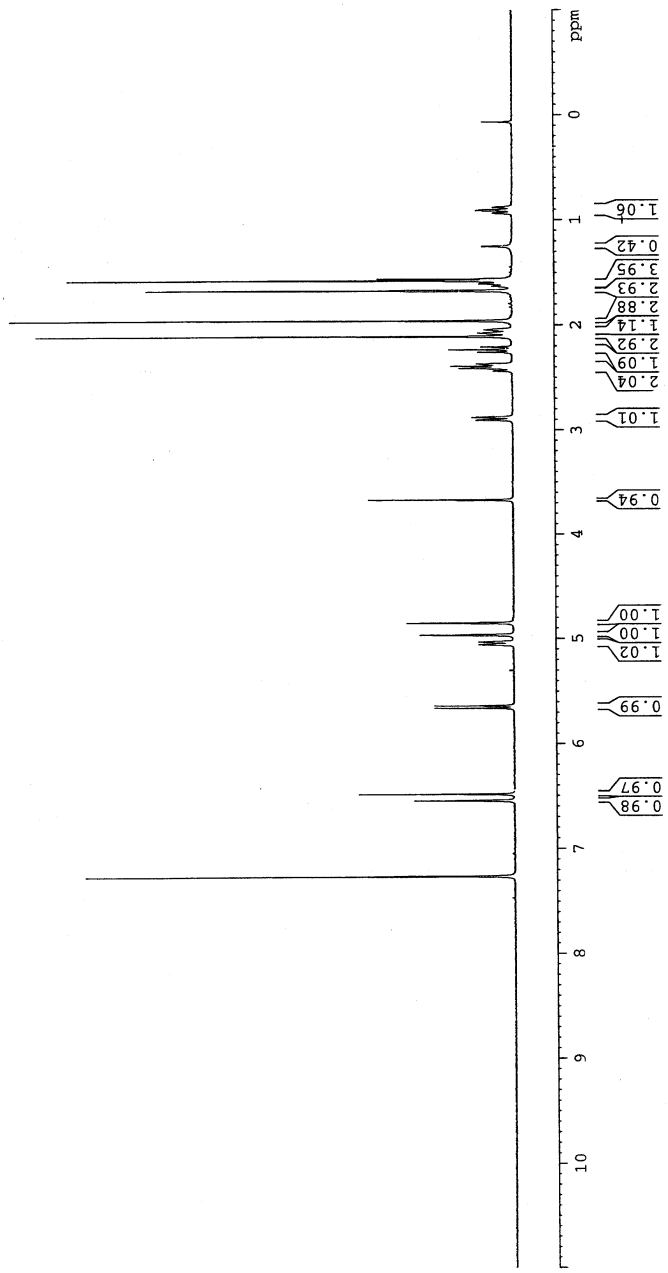
ppm
0
1
2
3
4
5
6
7
8
9
10
1.06
0.42
3.95
2.93
2.88
1.14
2.92
1.09
2.04
1.01
0.94
1.00
1.00
1.02
0.99
0.97
0.98

3.70

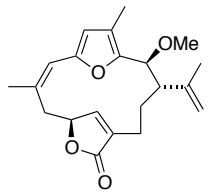

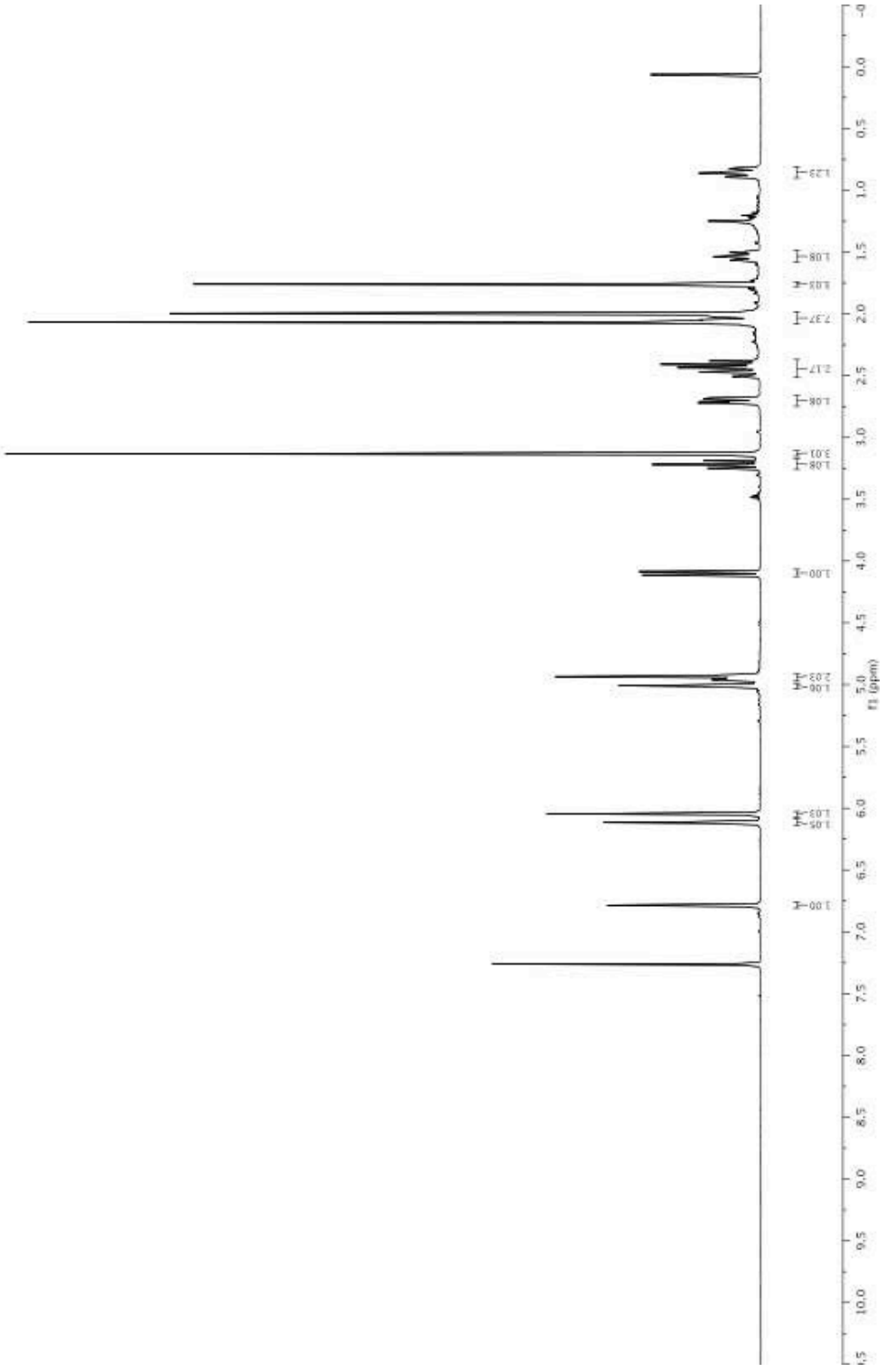

3.71

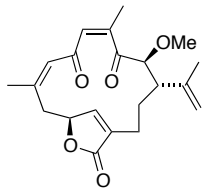

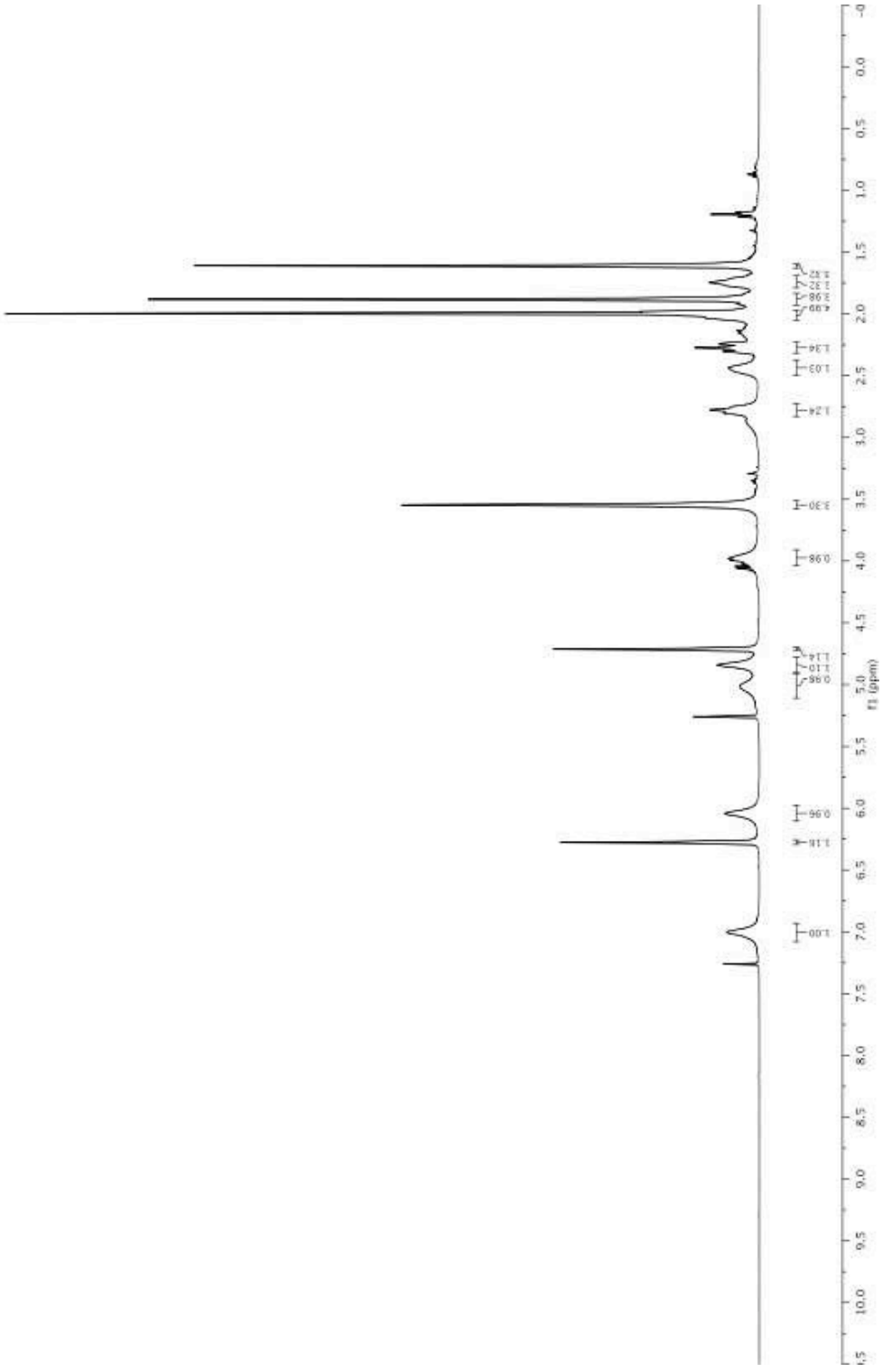

1.40

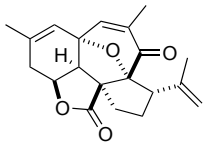

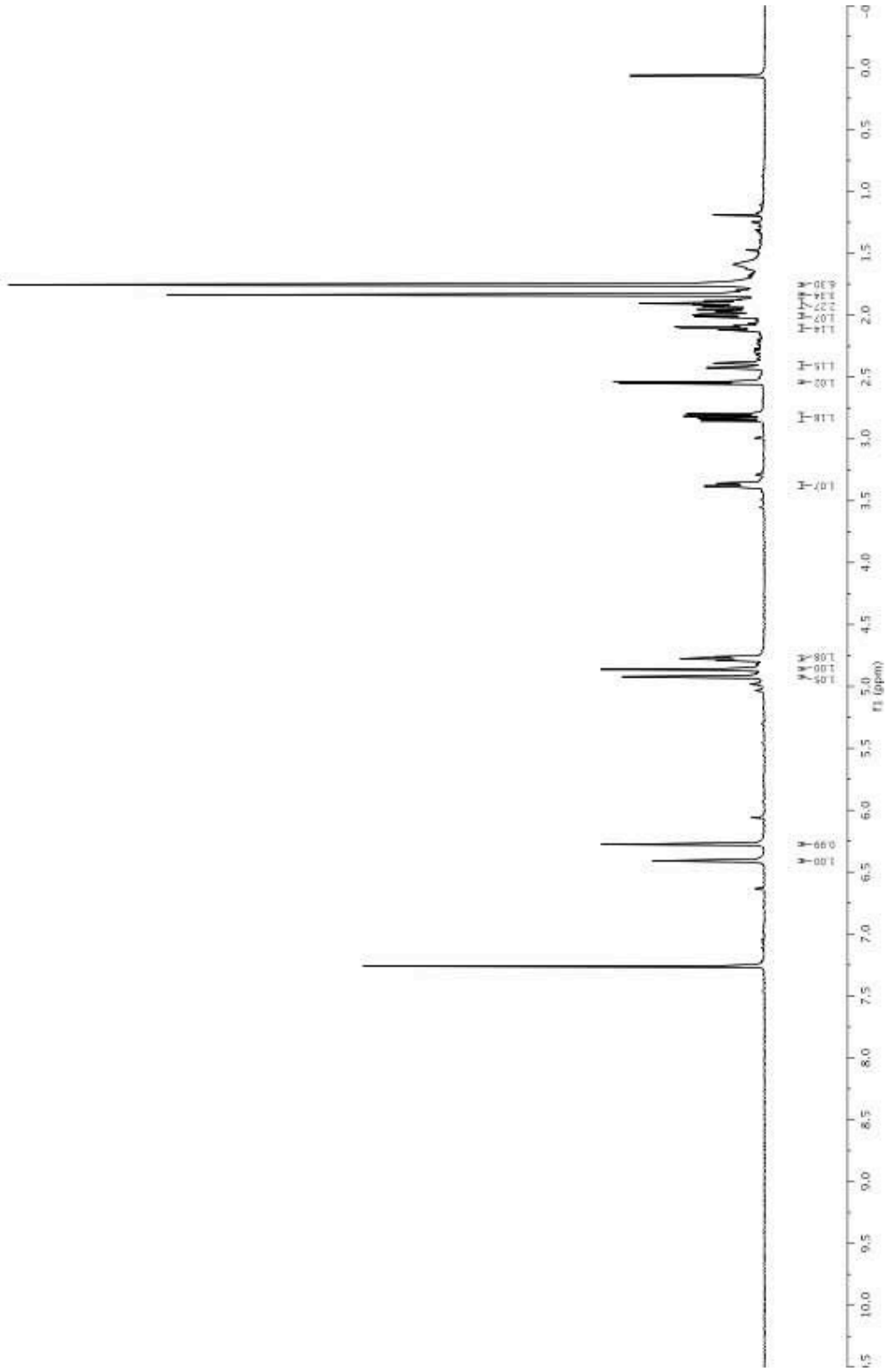

1.40

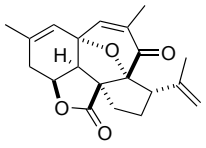

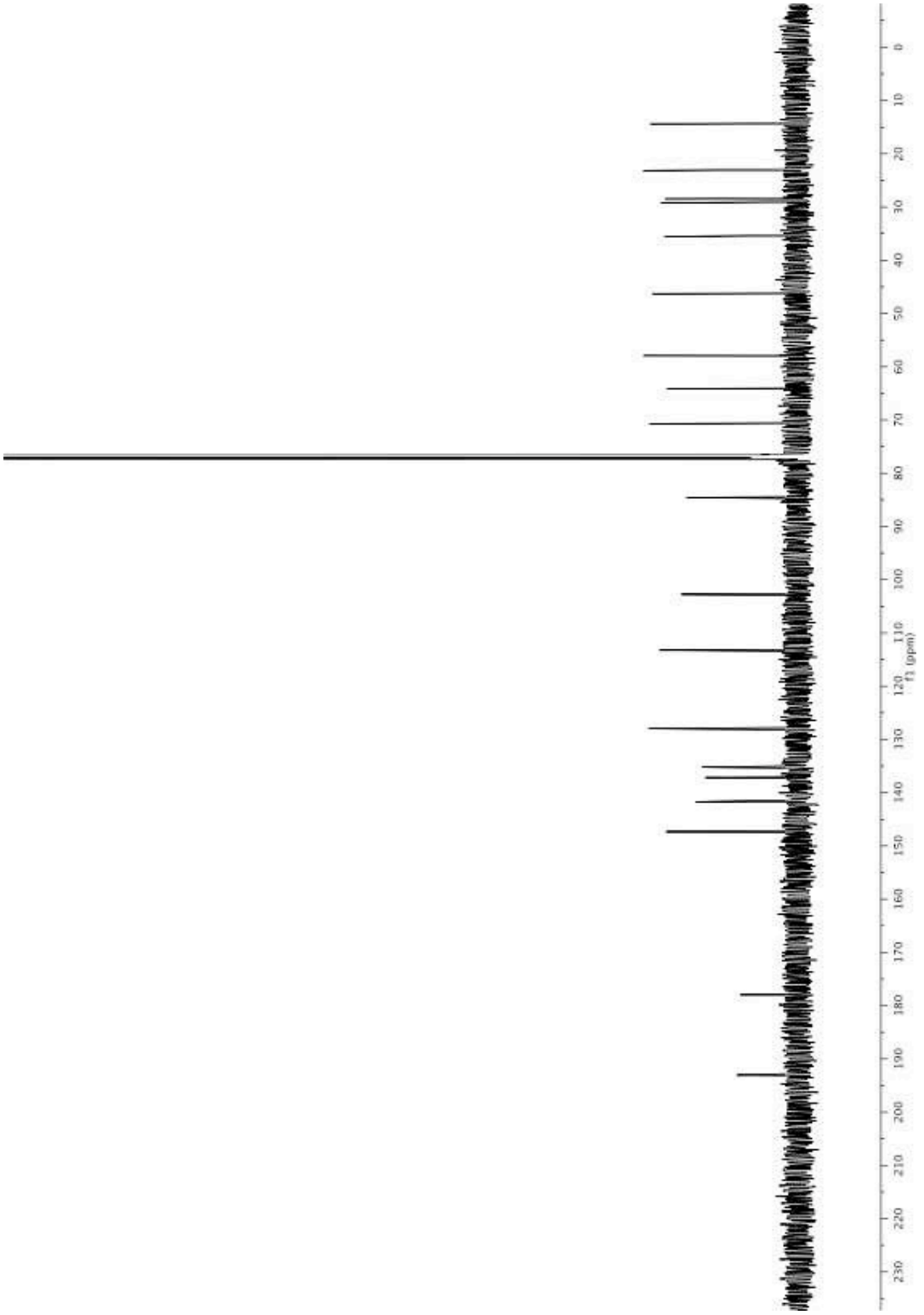

3.76

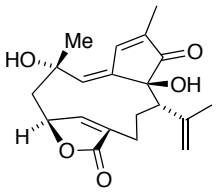

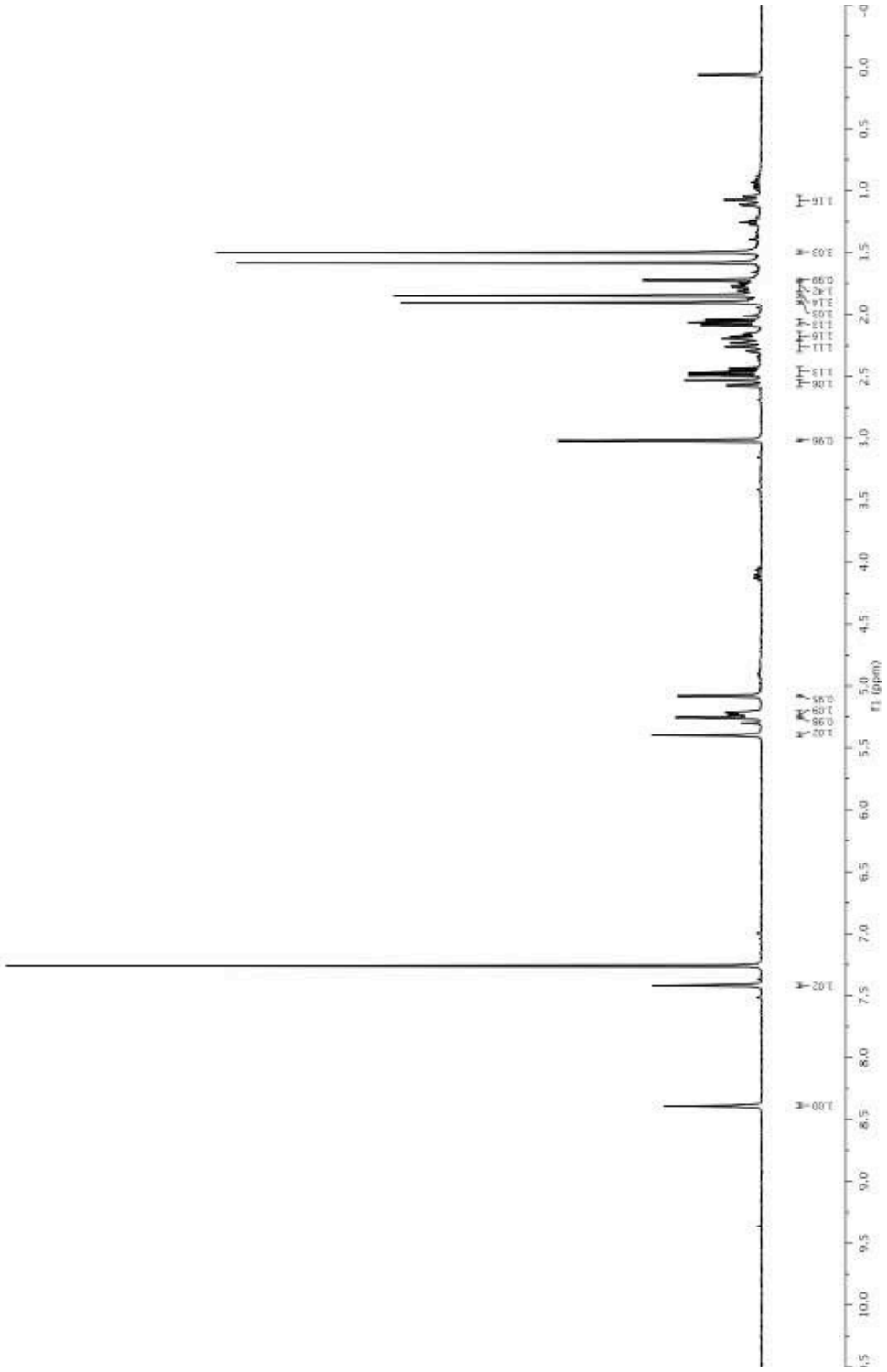

3.78

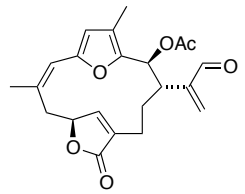

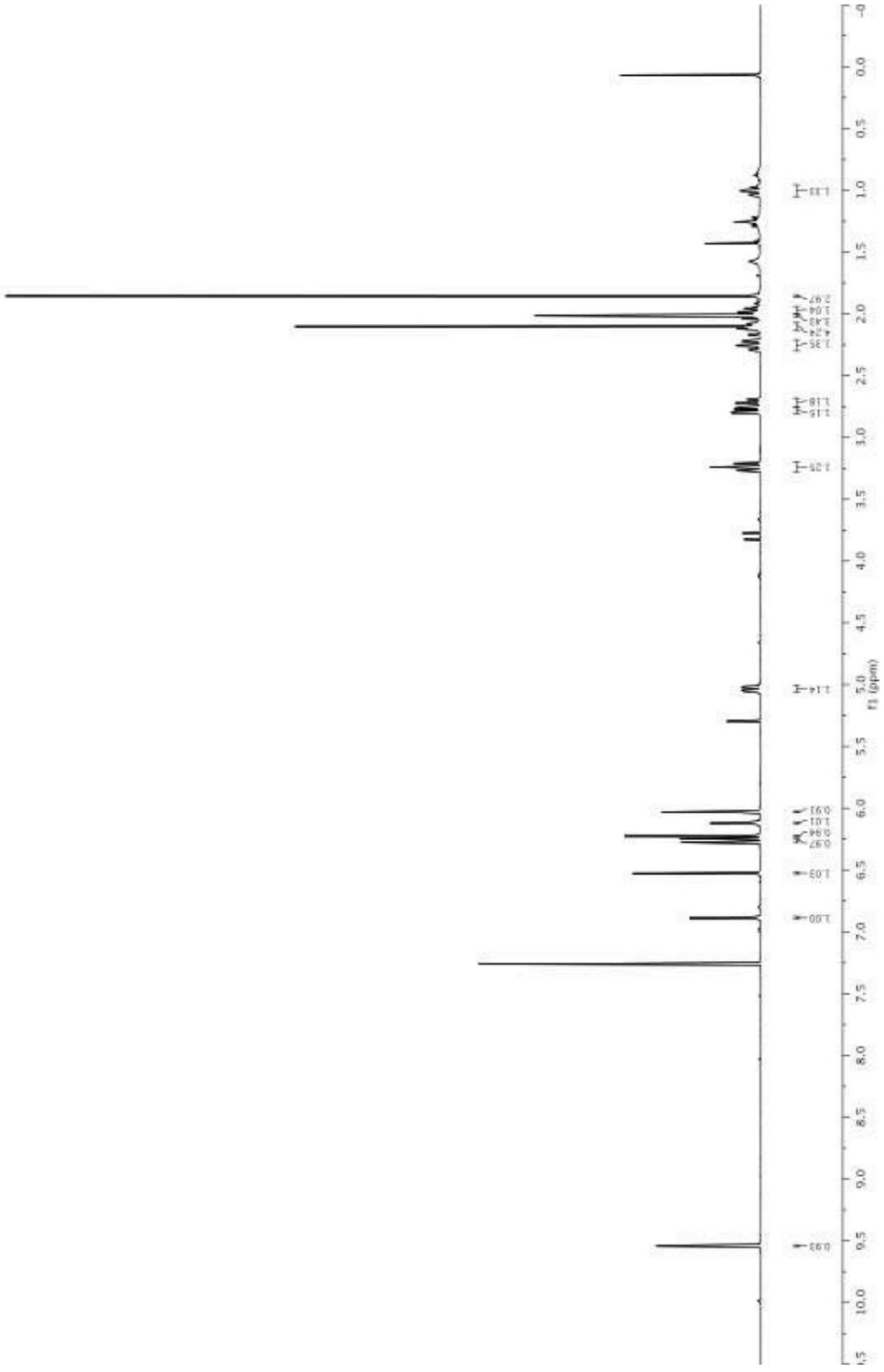

3.79

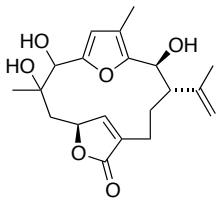

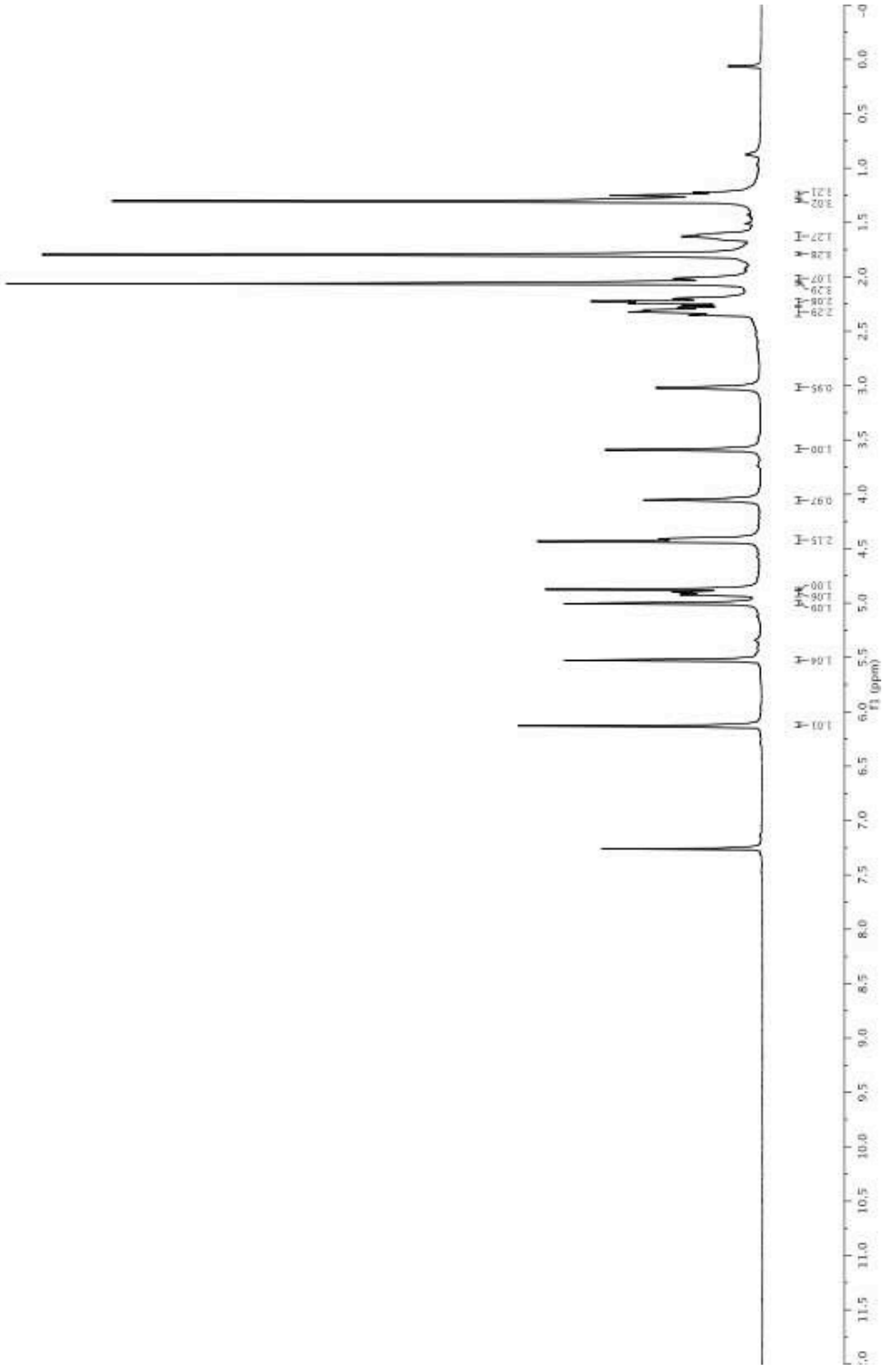

3.10 - Appendix

X-ray Crystallographic Data for Compound 3.54

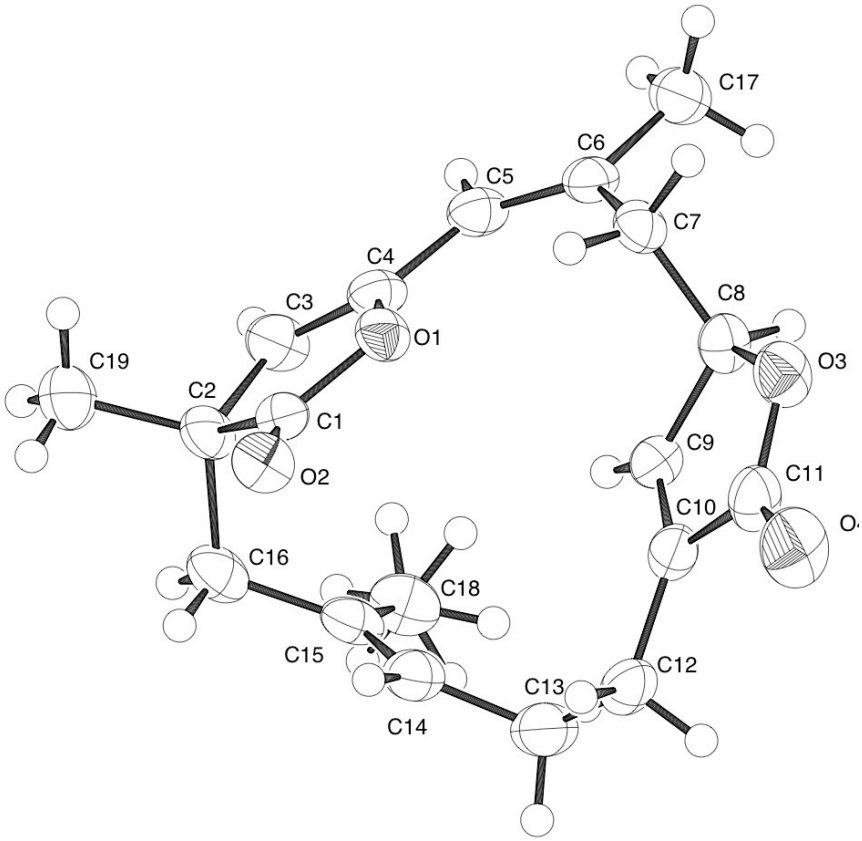

EXPERIMENTAL DETAILS

A. Crystal Data

Empirical Formula	$C_{19}O_4H_{22}$
Formula Weight	314.38
Crystal Color, Habit	colorless, polyhedral
Crystal Dimensions	0.15 X 0.22 X 0.34 mm
Crystal System	monoclinic
Lattice Type	Primitive
Lattice Parameters	a = 10.257(3)Å
	b = 12.135(4) Å
	c = 14.006(2) Å
	$\beta = 106.230(4)^o$
	V = 1673.7(8) $Å^3$
Space Group	$P2_1/n$ (#14)
Z value	4
D_{calc}	1.248 g/cm^3
F_{000}	672.00
μ(MoKα)	0.86 cm^{-1}

B. Intensity Measurements

Diffractometer	Bruker SMART CCD
Radiation	MoKα (λ = 0.71069 Å)
	graphite monochromated
Detector Position	60.00 mm
Exposure Time	10.0 seconds per frame.
Scan Type	ω (0.3 degrees per frame)
$2\theta_{max}$	50.7^o
No. of Reflections Measured	Total: 7676
	Unique: 3242 (R_{int} = 0.023)
Corrections	Lorentz-polarization
	Absorption (Tmax = 1.00 Tmin = 0.86)

C. Structure Solution and Refinement

Structure Solution	Direct Methods (SIR97)
Refinement	Full-matrix least-squares
Function Minimized	$\Sigma w (\|Fo\| - \|Fc\|)^2$
Least Squares Weights	$1/\sigma^2(Fo) = 4Fo^2/\sigma^2(Fo^2)$
p-factor	0.0400
Anomalous Dispersion	All non-hydrogen atoms
No. Observations (I>3.00σ(I))	1976
No. Variables	208
Reflection/Parameter Ratio	9.50
Residuals: R; Rw; Rall	0.041 ; 0.050; 0.070
Goodness of Fit Indicator	1.77
Max Shift/Error in Final Cycle	0.00
Maximum peak in Final Diff. Map	0.21 $e^-/Å^3$
Minimum peak in Final Diff. Map	-0.16 $e^-/Å^3$

Table 1. Atomic coordinates and B_{iso}/B_{eq} and occupancy

atom	x	y	z	B_{eq}	occ
O1	0.4320(1)	0.2937(1)	0.76552(9)	2.72(3)	
O2	0.3546(1)	0.3638(1)	0.6120(1)	3.28(4)	
O3	0.0983(1)	0.1377(1)	0.8515(1)	3.45(4)	
O4	-0.0745(2)	0.1246(1)	0.7121(1)	4.79(5)	
C1	0.4439(2)	0.3180(2)	0.6725(2)	2.74(5)	
C2	0.5806(2)	0.2800(2)	0.6640(1)	2.98(5)	
C3	0.6429(2)	0.2379(2)	0.7671(2)	3.28(5)	
C4	0.5547(2)	0.2435(2)	0.8201(2)	2.74(5)	
C5	0.5648(2)	0.2038(2)	0.9194(2)	2.84(5)	
C6	0.4699(2)	0.1905(2)	0.9678(1)	2.62(5)	
C7	0.3213(2)	0.2152(2)	0.9247(1)	2.69(5)	
C8	0.2420(2)	0.1130(2)	0.8798(2)	2.69(5)	
C9	0.2676(2)	0.0739(2)	0.7861(1)	2.56(5)	
C10	0.1539(2)	0.0735(2)	0.7124(1)	2.72(5)	
C11	0.0444(2)	0.1129(2)	0.7529(2)	3.32(5)	
C12	0.1250(2)	0.0393(2)	0.6063(2)	3.13(5)	
C13	0.2480(3)	0.0005(2)	0.5743(2)	3.79(5)	
C14	0.3443(2)	0.0888(2)	0.5660(2)	3.24(5)	
C15	0.4790(2)	0.0897(2)	0.6030(1)	3.03(5)	
C16	0.5574(2)	0.1885(2)	0.5837(2)	3.30(5)	
C17	0.5078(2)	0.1431(2)	1.0705(2)	3.42(5)	
C18	0.5616(2)	-0.0019(2)	0.6619(2)	4.10(6)	

C19	0.6552(2)	0.3782(2)	0.6340(2)	4.27(6)	
H1	0.7331	0.2109	0.7911	3.9332	
H2	0.6540	0.1838	0.9568	3.4132	
H3	0.2859	0.2425	0.9760	3.2288	
H4	0.3111	0.2696	0.8744	3.2288	
H5	0.2605	0.0552	0.9274	3.2238	
H6	0.3538	0.0520	0.7799	3.0703	
H7	0.0611	-0.0193	0.5951	3.7594	
H8	0.0864	0.1005	0.5659	3.7594	
H9	0.2960	-0.0517	0.6218	4.5427	
H10	0.2160	-0.0341	0.5112	4.5427	
H11	0.3052	0.1525	0.5298	3.8881	
H12	0.5088	0.2198	0.5218	3.9589	
H13	0.6436	0.1638	0.5798	3.9589	
H14	0.4857	0.1943	1.1149	4.1071	
H15	0.6026	0.1286	1.0912	4.1071	
H16	0.4593	0.0765	1.0707	4.1071	
H17	0.5567	0.0013	0.7286	4.9140	1/2
H18	0.5269	-0.0707	0.6334	4.9140	1/2
H19	0.6534	0.0055	0.6611	4.9140	1/2
H20	0.6612	0.4365	0.6803	5.1215	
H21	0.7440	0.3562	0.6337	5.1215	
H22	0.6066	0.4027	0.5695	5.1215	
H23	0.6113	-0.0376	0.6229	4.9140	1/2
H24	0.6228	0.0273	0.7203	4.9140	1/2
H25	0.5029	-0.0536	0.6799	4.9140	1/2

$B_{eq} = 8/3\ \pi^2(U_{11}(aa^*)^2 + U_{22}(bb^*)^2 + U_{33}(cc^*)^2 + 2U_{12}(aa^*bb^*)\cos\gamma + 2U_{13}(aa^*cc^*)\cos\beta + 2U_{23}(bb^*cc^*)\cos\alpha)$

Table 2. Anisotropic Displacement Parameters

atom	U_{11}	U_{22}	U_{33}	U_{12}	U_{13}	U_{23}
O1	0.0302(8)	0.0422(8)	0.0337(8)	0.0011(6)	0.0133(6)	0.0040(7)
O2	0.0387(9)	0.0451(9)	0.0402(9)	0.0054(7)	0.0101(7)	0.0008(7)
O3	0.0303(8)	0.058(1)	0.0453(9)	0.0014(7)	0.0142(7)	0.0022(8)
O4	0.0264(9)	0.091(1)	0.062(1)	0.0009(8)	0.0072(8)	0.0107(10)
C1	0.036(1)	0.036(1)	0.033(1)	-0.0074(10)	0.0106(10)	-0.007(1)
C2	0.030(1)	0.054(1)	0.034(1)	-0.0026(10)	0.0147(9)	-0.007(1)
C3	0.024(1)	0.062(2)	0.037(1)	0.002(1)	0.0074(9)	-0.006(1)
C4	0.026(1)	0.042(1)	0.033(1)	-0.0018(10)	0.0051(9)	-0.0098(10)
C5	0.029(1)	0.042(1)	0.034(1)	-0.0011(9)	0.0044(9)	-0.009(1)
C6	0.035(1)	0.032(1)	0.032(1)	-0.0022(9)	0.0087(9)	-0.0082(9)
C7	0.038(1)	0.034(1)	0.034(1)	0.0023(9)	0.0171(9)	-0.0032(10)

C8	0.026(1)	0.038(1)	0.037(1)	0.0027(9)	0.0084(9)	0.0055(10)
C9	0.031(1)	0.030(1)	0.035(1)	-0.0011(9)	0.0087(9)	-0.0022(9)
C10	0.032(1)	0.034(1)	0.036(1)	-0.0050(9)	0.0069(10)	0.0042(10)
C11	0.028(1)	0.053(1)	0.043(1)	-0.006(1)	0.006(1)	0.009(1)
C12	0.034(1)	0.042(1)	0.038(1)	-0.008(1)	0.0001(10)	0.002(1)
C13	0.059(2)	0.043(1)	0.038(1)	-0.006(1)	0.007(1)	-0.006(1)
C14	0.049(1)	0.040(1)	0.034(1)	-0.001(1)	0.012(1)	-0.006(1)
C15	0.041(1)	0.048(1)	0.027(1)	0.003(1)	0.0108(10)	-0.0089(10)
C16	0.037(1)	0.056(1)	0.035(1)	0.005(1)	0.0151(10)	-0.004(1)
C17	0.041(1)	0.052(1)	0.038(1)	-0.001(1)	0.0111(10)	-0.004(1)
C18	0.055(2)	0.055(2)	0.045(1)	0.005(1)	0.014(1)	-0.005(1)
C19	0.045(1)	0.073(2)	0.051(1)	-0.015(1)	0.025(1)	-0.009(1)

The general temperature factor expression:
$\exp(-2\pi^2(a^{*2}U_{11}h^2 + b^{*2}U_{22}k^2 + c^{*2}U_{33}l^2 + 2a^*b^*U_{12}hk + 2a^*c^*U_{13}hl + 2b^*c^*U_{23}kl))$

Table 3. Bond Lengths(Å)

atom	atom	distance	atom	atom	distance
O1	C1	1.374(2)	O1	C4	1.415(2)
O2	C1	1.196(2)	O3	C8	1.447(2)
O3	C11	1.369(3)	O4	C11	1.202(2)
C1	C2	1.513(3)	C2	C3	1.497(3)
C2	C16	1.550(3)	C2	C19	1.537(3)
C3	C4	1.323(3)	C4	C5	1.448(3)
C5	C6	1.342(3)	C6	C7	1.505(3)
C6	C17	1.497(3)	C7	C8	1.520(3)
C8	C9	1.486(3)	C9	C10	1.324(3)
C10	C11	1.472(3)	C10	C12	1.491(3)
C12	C13	1.527(3)	C13	C14	1.484(3)
C14	C15	1.333(3)	C15	C16	1.510(3)
C15	C18	1.498(3)			

Table 4. Bond Lengths(Å)

atom	atom	distance	atom	atom	distance
C3	H1	0.95	C5	H2	0.95
C7	H3	0.95	C7	H4	0.95
C8	H5	0.95	C9	H6	0.95

C12	H7	0.95	C12	H8	0.95
C13	H9	0.95	C13	H10	0.95
C14	H11	0.95	C16	H12	0.95
C16	H13	0.95	C17	H14	0.95
C17	H15	0.95	C17	H16	0.95
C18	H17	0.95	C18	H18	0.95
C18	H19	0.95	C18	H23	0.95
C18	H24	0.95	C18	H25	0.95
C19	H20	0.95	C19	H21	0.95
C19	H22	0.95			

Table 5. Bond Angles(^{o})

atom	atom	atom	angle	atom	atom	atom	angle
C1	O1	C4	107.6(2)	C8	O3	C11	108.9(2)
O1	C1	O2	121.2(2)	O1	C1	C2	109.8(2)
O2	C1	C2	129.0(2)	C1	C2	C3	100.6(2)
C1	C2	C16	108.5(2)	C1	C2	C19	109.2(2)
C3	C2	C16	113.1(2)	C3	C2	C19	114.7(2)
C16	C2	C19	110.2(2)	C2	C3	C4	110.4(2)
O1	C4	C3	111.4(2)	O1	C4	C5	118.4(2)
C3	C4	C5	130.2(2)	C4	C5	C6	131.1(2)
C5	C6	C7	124.7(2)	C5	C6	C17	120.1(2)
C7	C6	C17	115.1(2)	C6	C7	C8	111.6(2)
O3	C8	C7	109.3(2)	O3	C8	C9	104.0(2)
C7	C8	C9	114.9(2)	C8	C9	C10	110.8(2)
C9	C10	C11	107.4(2)	C9	C10	C12	131.6(2)
C11	C10	C12	121.0(2)	O3	C11	O4	121.6(2)
O3	C11	C10	108.9(2)	O4	C11	C10	129.5(2)
C10	C12	C13	115.4(2)	C12	C13	C14	115.0(2)
C13	C14	C15	128.0(2)	C14	C15	C16	118.9(2)
C14	C15	C18	125.0(2)	C16	C15	C18	116.1(2)
C2	C16	C15	114.8(2)				

Table 6. Bond Angles(°)

atom	atom	atom	angle	atom	atom	atom	angle
C2	C3	H1	124.8	C4	C3	H1	124.8
C4	C5	H2	114.4	C6	C5	H2	114.4
C6	C7	H3	108.9	C6	C7	H4	108.9
C8	C7	H3	108.9	C8	C7	H4	108.9
H3	C7	H4	109.5	O3	C8	H5	109.5
C7	C8	H5	109.5	C9	C8	H5	109.5
C8	C9	H6	124.6	C10	C9	H6	124.6
C10	C12	H7	108.0	C10	C12	H8	108.0
C13	C12	H7	108.0	C13	C12	H8	108.0
H7	C12	H8	109.5	C12	C13	H9	108.1
C12	C13	H10	108.1	C14	C13	H9	108.1
C14	C13	H10	108.1	H9	C13	H10	109.5
C13	C14	H11	116.0	C15	C14	H11	116.0
C2	C16	H12	108.1	C2	C16	H13	108.1
C15	C16	H12	108.1	C15	C16	H13	108.1
H12	C16	H13	109.5	C6	C17	H14	109.5
C6	C17	H15	109.5	C6	C17	H16	109.5
H14	C17	H15	109.5	H14	C17	H16	109.5
H15	C17	H16	109.5	C15	C18	H17	109.5
C15	C18	H18	109.5	C15	C18	H19	109.5
C15	C18	H23	109.5	C15	C18	H24	109.5
C15	C18	H25	109.5	H17	C18	H18	109.5
H17	C18	H19	109.5	H17	C18	H23	140.3
H17	C18	H24	48.8	H17	C18	H25	63.6
H18	C18	H19	109.5	H18	C18	H23	63.6
H18	C18	H24	140.3	H18	C18	H25	48.8
H19	C18	H23	48.8	H19	C18	H24	63.6
H19	C18	H25	140.3	H23	C18	H24	109.5
H23	C18	H25	109.5	H24	C18	H25	109.5
C2	C19	H20	109.5	C2	C19	H21	109.5
C2	C19	H22	109.5	H20	C19	H21	109.5
H20	C19	H22	109.5	H21	C19	H22	109.5

Table 7. Torsion Angles(°)

atom	atom	atom	atom	angle	atom	atom	atom	atom	angle
O1	C1	C2	C3	-3.1(2)	O1	C1	C2	C16	115.9(2)
O1	C1	C2	C19	-124.0(2)	O1	C4	C3	C2	-3.7(3)
O1	C4	C5	C6	11.3(3)	O2	C1	O1	C4	-178.1(2)

O2	C1	C2	C3	176.1(2)	O2	C1	C2	C16	-64.9(3)
O2	C1	C2	C19	55.2(3)	O3	C8	C7	C6	172.5(2)
O3	C8	C9	C10	-0.9(2)	O3	C11	C10	C9	1.0(2)
O3	C11	C10	C12	179.5(2)	O4	C11	O3	C8	178.7(2)
O4	C11	C10	C9	-179.4(2)	O4	C11	C10	C12	-0.9(4)
C1	O1	C4	C3	1.6(2)	C1	O1	C4	C5	-176.4(2)
C1	C2	C3	C4	4.1(2)	C1	C2	C16	C15	-57.9(2)
C2	C1	O1	C4	1.2(2)	C2	C3	C4	C5	174.0(2)
C2	C16	C15	C14	91.3(2)	C2	C16	C15	C18	-89.9(2)
C3	C2	C16	C15	52.8(2)	C3	C4	C5	C6	-166.3(2)
C4	C3	C2	C16	-111.5(2)	C4	C3	C2	C19	121.0(2)
C4	C5	C6	C7	0.5(3)	C4	C5	C6	C17	177.7(2)
C5	C6	C7	C8	94.5(2)	C6	C7	C8	C9	-71.1(2)
C7	C8	O3	C11	124.7(2)	C7	C8	C9	C10	-120.4(2)
C8	O3	C11	C10	-1.6(2)	C8	C7	C6	C17	-82.8(2)
C8	C9	C10	C11	-0.0(2)	C8	C9	C10	C12	-178.2(2)
C9	C8	O3	C11	1.5(2)	C9	C10	C12	C13	-2.1(3)
C10	C12	C13	C14	-71.9(2)	C11	C10	C12	C13	179.9(2)
C12	C13	C14	C15	131.6(2)	C13	C14	C15	C16	179.0(2)
C13	C14	C15	C18	0.3(4)	C15	C16	C2	C19	-177.3(2)

Table 8. Non-bonded Contacts out to 3.75 Å

atom	atom	distance	ADC	atom	atom	distance	ADC
O1	C10	3.543(2)	55602	O1	C12	3.611(2)	55602
O2	C8	3.194(2)	55602	O2	C9	3.332(3)	55602
O2	O3	3.377(2)	55602	O2	C17	3.441(3)	45404
O2	C5	3.508(3)	45404	O2	C10	3.557(2)	55602
O2	C11	3.562(3)	55602	O4	C3	3.484(3)	45501
O4	C17	3.677(3)	45404	C1	C11	3.720(3)	55602
C7	C13	3.534(3)	55602	C9	C17	3.700(3)	65703
C12	C12	3.476(4)	55603	C14	C18	3.736(3)	65603
C15	C15	3.736(4)	65603				

3.11 - Appendix

X-ray Crystallographic Data for Compound 3.64

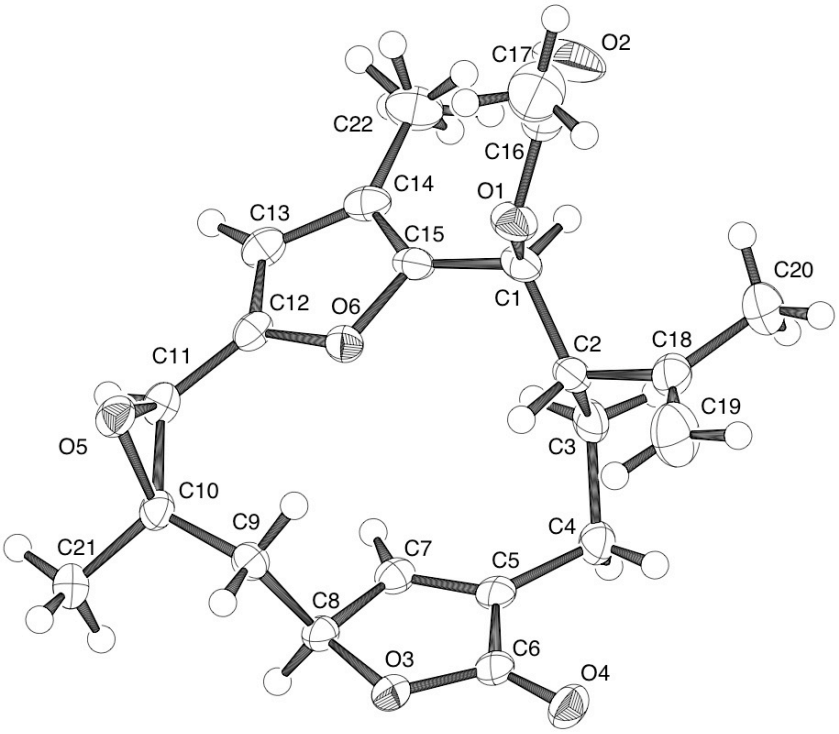

EXPERIMENTAL DETAILS

A. Crystal Data

Empirical Formula	$C_{22}O_6H_{26}$
Formula Weight	386.44
Crystal Color, Habit	colorless, bladelike
Crystal Dimensions	0.05 X 0.11 X 0.16 mm
Crystal System	triclinic
Lattice Type	Primitive
Lattice Parameters	a = 6.3422(9)Å
	b = 9.665(1) Å
	c = 17.495(3) Å
	α = 80.359(2)°
	β = 88.180(2)°
	γ = 72.416(2)°
	V = 1007.6(3) Å^3
Space Group	P -1 (#2)
Z value	2
D_{calc}	1.274 g/cm^3
F_{000}	412.00
μ(MoKα)	0.92 cm^{-1}

B. Intensity Measurements

Diffractometer	Bruker APEX CCD
Radiation	MoKα (λ = 0.71069 Å)
	graphite monochromated
Detector Position	60.00 mm
Exposure Time	10.0 seconds per frame.
Scan Type	ω (0.3 degrees per frame)
$2\theta_{max}$	52.8°
No. of Reflections Measured	Total: 9312
	Unique: 4221 (R_{int} = 0.042)
Corrections	Lorentz-polarization
	Absorption (Tmax = 1.00 Tmin = 0.80)

C. Structure Solution and Refinement

Structure Solution	Direct Methods (SIR97)
Refinement	Full-matrix least-squares
Function Minimized	Σ w (|Fo| - |Fc|)^2
Least Squares Weights	$1/\sigma^2(Fo) = 4Fo^2/\sigma^2(Fo^2)$
p-factor	0.0300
Anomalous Dispersion	All non-hydrogen atoms
No. Observations (I>3.00σ(I))	2419
No. Variables	253
Reflection/Parameter Ratio	9.56
Residuals: R; Rw; Rall	0.047 ; 0.057; 0.093
Goodness of Fit Indicator	1.45
Max Shift/Error in Final Cycle	0.00
Maximum peak in Final Diff. Map	0.26 $e^-/Å^3$
Minimum peak in Final Diff. Map	-0.16 $e^-/Å^3$

Table 1. Atomic coordinates and B_{iso}/B_{eq} and occupancy

atom	x	y	z	B_{eq}	occ
O1	0.8875(3)	0.2347(2)	0.39952(10)	2.56(4)	
O2	0.6334(4)	0.2115(3)	0.4886(1)	5.34(7)	
O3	1.2195(3)	0.3550(2)	0.06905(10)	2.18(4)	
O4	1.1005(3)	0.5839(2)	0.09756(10)	2.58(4)	
O5	1.2896(3)	-0.1489(2)	0.19323(10)	2.21(4)	
O6	0.9164(3)	0.0964(2)	0.25333(9)	1.97(4)	
C1	0.7219(4)	0.2708(3)	0.3370(1)	2.05(6)	
C2	0.7615(4)	0.3982(3)	0.2795(1)	2.01(6)	
C3	0.5822(4)	0.4512(3)	0.2149(1)	2.23(6)	
C4	0.6555(4)	0.5297(3)	0.1402(1)	2.29(6)	
C5	0.8554(4)	0.4312(3)	0.1075(1)	1.85(6)	
C6	1.0626(4)	0.4706(3)	0.0925(1)	2.02(6)	
C7	0.8934(4)	0.2960(3)	0.0922(1)	1.89(6)	
C8	1.1263(4)	0.2344(3)	0.0696(1)	1.90(6)	
C9	1.2624(4)	0.1032(3)	0.1267(1)	1.89(6)	
C10	1.2197(4)	-0.0417(3)	0.1234(1)	1.94(5)	
C11	1.0557(4)	-0.0966(3)	0.1715(1)	2.07(6)	
C12	0.8943(4)	-0.0236(3)	0.2260(1)	1.95(6)	
C13	0.7140(4)	-0.0567(3)	0.2559(1)	2.18(6)	
C14	0.6125(4)	0.0470(3)	0.3054(1)	2.17(6)	
C15	0.7392(4)	0.1377(3)	0.3022(1)	1.97(5)	

C16	0.8197(6)	0.2106(3)	0.4725(2)	3.24(8)	
C17	1.0043(6)	0.1839(4)	0.5290(2)	4.79(9)	
C18	0.7831(5)	0.5212(3)	0.3191(2)	2.52(6)	
C19	0.9693(5)	0.5576(3)	0.3134(2)	4.14(8)	
C20	0.5905(6)	0.5985(3)	0.3625(2)	3.89(8)	
C21	1.2910(4)	-0.1043(3)	0.0500(2)	2.50(6)	
C22	0.4098(5)	0.0522(3)	0.3526(2)	3.25(7)	
H1	0.5788	0.3033	0.3579	2.4595	
H2	0.8988	0.3600	0.2556	2.4094	
H3	0.5460	0.3683	0.2035	2.6764	
H4	0.4548	0.5174	0.2331	2.6764	
H5	0.5378	0.5601	0.1030	2.7437	
H6	0.6898	0.6136	0.1511	2.7437	
H7	0.7856	0.2452	0.0952	2.2674	
H8	1.1311	0.2094	0.0192	2.2772	
H9	1.4144	0.0912	0.1166	2.2727	
H10	1.2311	0.1249	0.1776	2.2727	
H11	1.0090	-0.1662	0.1495	2.4871	
H12	0.6634	-0.1351	0.2458	2.6154	
H13	0.9535	0.1652	0.5803	5.7422	
H14	1.1225	0.1012	0.5196	5.7422	
H15	1.0544	0.2682	0.5233	5.7422	
H16	0.9828	0.6357	0.3375	4.9669	
H17	1.0892	0.5057	0.2852	4.9669	
H18	0.4669	0.6431	0.3281	4.6709	
H19	0.6259	0.6722	0.3847	4.6709	
H20	0.5556	0.5298	0.4025	4.6709	
H21	1.2198	-0.0346	0.0066	3.0035	
H22	1.4468	-0.1258	0.0454	3.0035	
H23	1.2513	-0.1920	0.0519	3.0035	
H24	0.3082	0.0230	0.3250	3.9005	3/4
H25	0.3428	0.1496	0.3623	3.9005	3/4
H26	0.4499	-0.0128	0.4005	3.9005	3/4
H27	0.4189	0.0931	0.3977	3.9005	1/4
H28	0.3996	-0.0447	0.3675	3.9005	1/4
H29	0.2824	0.1114	0.3226	3.9005	1/4

$B_{eq} = 8/3\ \pi^2(U_{11}(aa^*)^2 + U_{22}(bb^*)^2 + U_{33}(cc^*)^2 + 2U_{12}(aa^*bb^*)\cos\gamma + 2U_{13}(aa^*cc^*)\cos\beta + 2U_{23}(bb^*cc^*)\cos\alpha)$

Table 2. Anisotropic Displacement Parameters

atom	U_{11}	U_{22}	U_{33}	U_{12}	U_{13}	U_{23}
O1	0.036(1)	0.038(1)	0.020(1)	-0.0068(9)	-0.0006(9)	-0.0028(8)

O2	0.073(2)	0.094(2)	0.032(1)	-0.025(2)	0.018(1)	-0.002(1)
O3	0.031(1)	0.0221(10)	0.030(1)	-0.0101(8)	0.0056(8)	-0.0016(8)
O4	0.043(1)	0.022(1)	0.036(1)	-0.0142(9)	-0.0003(9)	-0.0039(8)
O5	0.025(1)	0.0228(10)	0.032(1)	-0.0038(8)	-0.0013(8)	0.0007(8)
O6	0.0245(10)	0.0246(10)	0.0270(10)	-0.0090(8)	0.0053(8)	-0.0052(8)
C1	0.022(1)	0.031(2)	0.022(1)	-0.004(1)	0.003(1)	-0.003(1)
C2	0.026(1)	0.028(1)	0.021(1)	-0.005(1)	0.005(1)	-0.005(1)
C3	0.022(1)	0.026(1)	0.032(2)	0.000(1)	0.003(1)	-0.007(1)
C4	0.031(2)	0.023(1)	0.029(2)	-0.001(1)	-0.001(1)	-0.004(1)
C5	0.029(1)	0.024(1)	0.015(1)	-0.007(1)	-0.004(1)	0.002(1)
C6	0.034(2)	0.022(1)	0.017(1)	-0.006(1)	-0.002(1)	0.002(1)
C7	0.027(1)	0.024(1)	0.020(1)	-0.009(1)	-0.003(1)	-0.001(1)
C8	0.032(1)	0.022(1)	0.020(1)	-0.010(1)	0.000(1)	-0.003(1)
C9	0.020(1)	0.025(1)	0.026(1)	-0.006(1)	0.002(1)	-0.004(1)
C10	0.025(1)	0.019(1)	0.026(1)	-0.002(1)	-0.002(1)	-0.002(1)
C11	0.025(1)	0.022(1)	0.031(2)	-0.006(1)	-0.004(1)	-0.003(1)
C12	0.028(1)	0.021(1)	0.025(1)	-0.009(1)	-0.006(1)	-0.000(1)
C13	0.026(1)	0.027(1)	0.031(2)	-0.011(1)	-0.004(1)	0.001(1)
C14	0.024(1)	0.032(2)	0.023(1)	-0.009(1)	-0.002(1)	0.005(1)
C15	0.021(1)	0.029(1)	0.020(1)	-0.004(1)	0.003(1)	0.002(1)
C16	0.066(2)	0.028(2)	0.025(2)	-0.008(2)	0.004(2)	-0.004(1)
C17	0.093(3)	0.053(2)	0.033(2)	-0.017(2)	-0.015(2)	-0.007(2)
C18	0.041(2)	0.026(2)	0.025(1)	-0.006(1)	-0.002(1)	-0.003(1)
C19	0.055(2)	0.049(2)	0.064(2)	-0.021(2)	0.001(2)	-0.028(2)
C20	0.066(2)	0.037(2)	0.042(2)	-0.008(2)	0.011(2)	-0.015(2)
C21	0.034(2)	0.023(1)	0.036(2)	-0.004(1)	0.004(1)	-0.007(1)
C22	0.034(2)	0.055(2)	0.037(2)	-0.020(2)	0.004(1)	-0.005(1)

The general temperature factor expression:
$\exp(-2\pi^2(a^{*2}U_{11}h^2 + b^{*2}U_{22}k^2 + c^{*2}U_{33}l^2 + 2a^*b^*U_{12}hk + 2a^*c^*U_{13}hl + 2b^*c^*U_{23}kl))$

Table 3. Bond Lengths(Å)

atom	atom	distance	atom	atom	distance
O1	C1	1.465(3)	O1	C16	1.340(3)
O2	C16	1.203(4)	O3	C6	1.365(3)
O3	C8	1.456(3)	O4	C6	1.208(3)
O5	C10	1.448(3)	O5	C11	1.456(3)
O6	C12	1.372(3)	O6	C15	1.392(3)
C1	C2	1.532(3)	C1	C15	1.487(4)
C2	C3	1.539(4)	C2	C18	1.514(3)
C3	C4	1.530(3)	C4	C5	1.500(4)

C5	C6	1.479(3)	C5	C7	1.327(3)
C7	C8	1.484(3)	C8	C9	1.524(3)
C9	C10	1.515(3)	C10	C11	1.483(3)
C10	C21	1.508(3)	C11	C12	1.477(3)
C12	C13	1.346(3)	C13	C14	1.427(4)
C14	C15	1.350(3)	C14	C22	1.498(3)
C16	C17	1.490(4)	C18	C19	1.327(4)
C18	C20	1.485(4)			

Table 4. Bond Lengths(Å)

atom	atom	distance	atom	atom	distance
C1	H1	0.95	C2	H2	0.95
C3	H3	0.95	C3	H4	0.95
C4	H5	0.95	C4	H6	0.95
C7	H7	0.95	C8	H8	0.95
C9	H9	0.95	C9	H10	0.95
C11	H11	0.95	C13	H12	0.95
C17	H13	0.95	C17	H14	0.95
C17	H15	0.95	C19	H16	0.95
C19	H17	0.95	C20	H18	0.95
C20	H19	0.95	C20	H20	0.95
C21	H21	0.95	C21	H22	0.95
C21	H23	0.95	C22	H24	0.95
C22	H25	0.95	C22	H26	0.95
C22	H27	0.95	C22	H28	0.95
C22	H29	0.95			

Table 5. Bond Angles(^{o})

atom	atom	atom	angle	atom	atom	atom	angle
C1	O1	C16	117.6(2)	C6	O3	C8	109.0(2)
C10	O5	C11	61.4(2)	C12	O6	C15	105.9(2)
O1	C1	C2	106.6(2)	O1	C1	C15	109.8(2)
C2	C1	C15	113.8(2)	C1	C2	C3	110.0(2)
C1	C2	C18	112.4(2)	C3	C2	C18	113.1(2)
C2	C3	C4	113.1(2)	C3	C4	C5	111.6(2)
C4	C5	C6	122.5(2)	C4	C5	C7	130.3(2)
C6	C5	C7	107.0(2)	O3	C6	O4	121.7(2)
O3	C6	C5	109.0(2)	O4	C6	C5	129.3(2)

C5	C7	C8	111.1(2)	O3	C8	C7	103.8(2)
O3	C8	C9	107.9(2)	C7	C8	C9	114.4(2)
C8	C9	C10	115.4(2)	O5	C10	C9	113.3(2)
O5	C10	C11	59.6(1)	O5	C10	C21	113.4(2)
C9	C10	C11	124.1(2)	C9	C10	C21	115.3(2)
C11	C10	C21	117.4(2)	O5	C11	C10	59.0(1)
O5	C11	C12	119.0(2)	C10	C11	C12	129.4(2)
O6	C12	C11	120.7(2)	O6	C12	C13	110.1(2)
C11	C12	C13	129.3(2)	C12	C13	C14	107.7(2)
C13	C14	C15	105.9(2)	C13	C14	C22	127.1(2)
C15	C14	C22	127.1(2)	O6	C15	C1	116.0(2)
O6	C15	C14	110.4(2)	C1	C15	C14	133.5(2)
O1	C16	O2	123.4(3)	O1	C16	C17	110.8(3)
O2	C16	C17	125.8(3)	C2	C18	C19	119.7(3)
C2	C18	C20	118.0(2)	C19	C18	C20	122.3(3)

Table 6. Bond Angles(^{o})

atom	atom	atom	angle	atom	atom	atom	angle
O1	C1	H1	108.8	C2	C1	H1	108.8
C15	C1	H1	108.8	C1	C2	H2	107.0
C3	C2	H2	107.0	C18	C2	H2	107.0
C2	C3	H3	108.6	C2	C3	H4	108.6
C4	C3	H3	108.6	C4	C3	H4	108.6
H3	C3	H4	109.5	C3	C4	H5	108.9
C3	C4	H6	108.9	C5	C4	H5	108.9
C5	C4	H6	108.9	H5	C4	H6	109.5
C5	C7	H7	124.4	C8	C7	H7	124.4
O3	C8	H8	110.2	C7	C8	H8	110.2
C9	C8	H8	110.2	C8	C9	H9	108.0
C8	C9	H10	108.0	C10	C9	H9	108.0
C10	C9	H10	108.0	H9	C9	H10	109.5
O5	C11	H11	112.7	C10	C11	H11	112.7
C12	C11	H11	112.7	C12	C13	H12	126.1
C14	C13	H12	126.1	C16	C17	H13	109.5
C16	C17	H14	109.5	C16	C17	H15	109.5
H13	C17	H14	109.5	H13	C17	H15	109.5
H14	C17	H15	109.5	C18	C19	H16	120.0
C18	C19	H17	120.0	H16	C19	H17	120.0
C18	C20	H18	109.5	C18	C20	H19	109.5
C18	C20	H20	109.5	H18	C20	H19	109.5
H18	C20	H20	109.5	H19	C20	H20	109.5
C10	C21	H21	109.5	C10	C21	H22	109.5

C10	C21	H23	109.5	H21	C21	H22	109.5
H21	C21	H23	109.5	H22	C21	H23	109.5
C14	C22	H24	109.5	C14	C22	H25	109.5
C14	C22	H26	109.5	C14	C22	H27	109.5
C14	C22	H28	109.5	C14	C22	H29	109.5
H24	C22	H25	109.5	H24	C22	H26	109.5
H24	C22	H27	140.6	H24	C22	H28	61.8
H24	C22	H29	50.7	H25	C22	H26	109.5
H25	C22	H27	50.7	H25	C22	H28	140.6
H25	C22	H29	61.8	H26	C22	H27	61.8
H26	C22	H28	50.7	H26	C22	H29	140.6
H27	C22	H28	109.5	H27	C22	H29	109.5
H28	C22	H29	109.5				

Table 7. Torsion Angles(^{o})

atom	atom	atom	atom	angle	atom	atom	atom	atom	angle
O1	C1	C2	C3	-175.6(2)	O1	C1	C2	C18	-48.6(3)
O1	C1	C15	O6	-75.6(2)	O1	C1	C15	C14	107.2(3)
O2	C16	O1	C1	3.0(4)	O3	C6	C5	C4	175.0(2)
O3	C6	C5	C7	-0.5(3)	O3	C8	C7	C5	-3.2(3)
O3	C8	C9	C10	-168.2(2)	O4	C6	O3	C8	179.4(2)
O4	C6	C5	C4	-6.1(4)	O4	C6	C5	C7	178.4(3)
O5	C10	C9	C8	-159.9(2)	O5	C10	C11	C12	103.8(3)
O5	C11	C10	C9	-98.9(3)	O5	C11	C10	C21	102.3(2)
O5	C11	C12	O6	55.4(3)	O5	C11	C12	C13	-124.8(3)
O6	C12	C11	C10	-16.8(4)	O6	C12	C13	C14	0.0(3)
O6	C15	C1	C2	43.8(3)	O6	C15	C14	C13	-0.2(3)
O6	C15	C14	C22	178.6(2)	C1	O1	C16	C17	-176.8(2)
C1	C2	C3	C4	-156.6(2)	C1	C2	C18	C19	119.1(3)
C1	C2	C18	C20	-61.8(3)	C1	C15	O6	C12	-177.6(2)
C1	C15	C14	C13	177.1(3)	C1	C15	C14	C22	-4.0(5)
C2	C1	O1	C16	136.2(2)	C2	C1	C15	C14	-133.4(3)
C2	C3	C4	C5	60.0(3)	C3	C2	C1	C15	63.2(3)
C3	C2	C18	C19	-115.6(3)	C3	C2	C18	C20	63.5(3)
C3	C4	C5	C6	-123.2(2)	C3	C4	C5	C7	51.1(4)
C4	C3	C2	C18	76.9(3)	C4	C5	C7	C8	-172.7(2)
C5	C6	O3	C8	-1.6(3)	C5	C7	C8	C9	114.1(2)
C6	O3	C8	C7	2.8(2)	C6	O3	C8	C9	-118.9(2)
C6	C5	C7	C8	2.3(3)	C7	C8	C9	C10	76.9(3)
C8	C9	C10	C11	-91.9(3)	C8	C9	C10	C21	67.2(3)
C9	C10	O5	C11	117.1(2)	C9	C10	C11	C12	4.8(4)
C10	O5	C11	C12	-120.9(2)	C10	C11	C12	C13	163.0(3)

C11	O5	C10	C21	-109.1(2)	C11	C12	O6	C15	179.7(2)
C11	C12	C13	C14	-179.8(3)	C12	O6	C15	C14	0.2(3)
C12	C11	C10	C21	-153.9(3)	C12	C13	C14	C15	0.1(3)
C12	C13	C14	C22	-178.7(3)	C13	C12	O6	C15	-0.1(3)
C15	C1	O1	C16	-100.1(2)	C15	C1	C2	C18	-169.9(2)

Table 8. Non-bonded Contacts out to 3.75 Å

atom	atom	distance	ADC	atom	atom	distance	ADC
O1	C22	3.397(4)	65501	O2	C20	3.458(4)	66602
O2	C22	3.505(4)	65602	O3	C6	3.307(3)	76502
O3	C5	3.376(3)	76502	O3	O4	3.470(2)	76502
O4	C8	3.274(3)	76502	O4	C7	3.331(3)	76502
O4	C11	3.474(3)	56501	O4	C4	3.485(3)	65501
O4	C3	3.513(3)	65501	O4	C21	3.539(3)	56501
O4	C5	3.613(3)	76502	O4	C6	3.680(3)	76502
O5	C13	3.347(3)	65501	O5	C4	3.516(3)	64501
O5	C20	3.674(4)	64501	O5	C3	3.708(3)	64501
O6	C22	3.504(3)	65501	C4	C21	3.710(4)	46501
C5	C6	3.534(3)	76502	C6	C6	3.273(5)	76502
C6	C8	3.613(3)	76502	C6	C7	3.673(3)	76502
C7	C21	3.745(3)	75502	C9	C13	3.502(4)	65501
C13	C19	3.568(4)	54501	C16	C17	3.639(4)	75602

3.12 - Appendix

X-ray Crystallographic Data for Compound 1.40

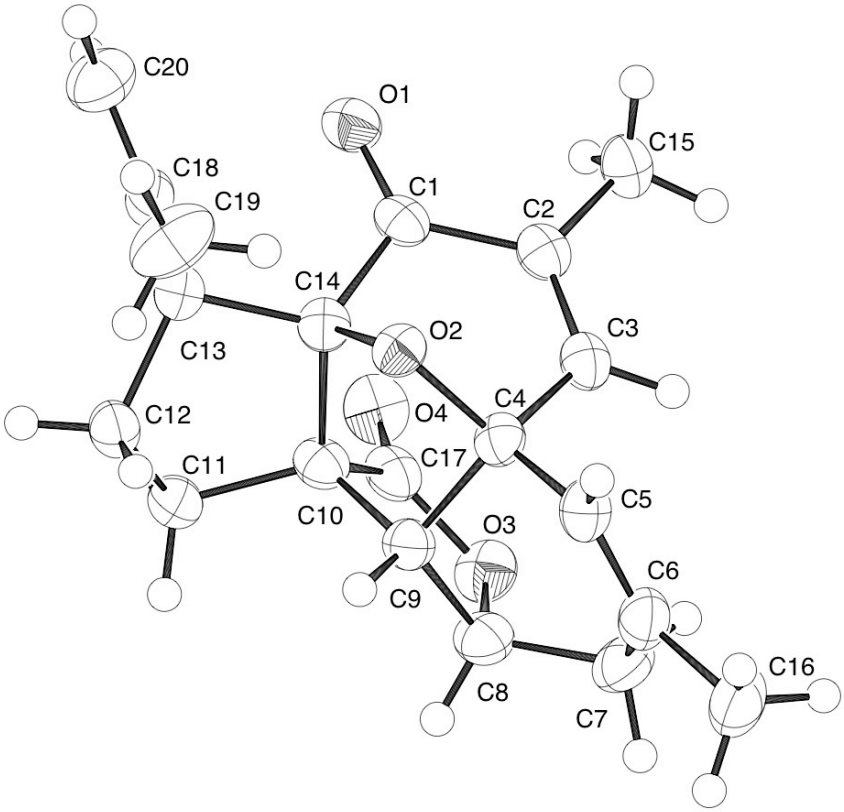

EXPERIMENTAL DETAILS

A. Crystal Data

Empirical Formula	$C_{20}O_4H_{22}$
Formula Weight	326.39
Crystal Color, Habit	colorless, blocky
Crystal Dimensions	0.10 X 0.12 X 0.18 mm
Crystal System	monoclinic
Lattice Type	Primitive
Lattice Parameters	a = 7.1044(7)Å
	b = 12.620(1) Å
	c = 9.4568(9) Å
	$\beta = 105.523(2)^o$
	V = 816.9(1) $Å^3$
Space Group	$P2_1$ (#4)
Z value	2
D_{calc}	1.327 g/cm^3
F_{000}	348.00
μ(MoKα)	0.91 cm^{-1}

B. Intensity Measurements

Diffractometer	Bruker APEX CCD
Radiation	MoKα (λ = 0.71069 Å)
	graphite monochromated
Detector Position	60.00 mm
Exposure Time	10.0 seconds per frame.
Scan Type	ω (0.3 degrees per frame)
$2\theta_{max}$	52.8^o
No. of Reflections Measured	Total: 4656
	Unique: 1920 (R_{int} = 0.024)
Corrections	Lorentz-polarization
	Absorption (Tmax = 1.00 Tmin = 0.84)

C. Structure Solution and Refinement

Structure Solution	Direct Methods (SIR97)
Refinement	Full-matrix least-squares
Function Minimized	Σ w (|Fo| - |Fc|)^2
Least Squares Weights	$1/\sigma^2(Fo) = 4Fo^2/\sigma^2(Fo^2)$
p-factor	0.0300
Anomalous Dispersion	All non-hydrogen atoms
No. Observations (I>2.50σ(I))	1479
No. Variables	216
Reflection/Parameter Ratio	6.85
Residuals: R; Rw; Rall	0.039 ; 0.044; 0.047
Goodness of Fit Indicator	1.58
Max Shift/Error in Final Cycle	0.00
Maximum peak in Final Diff. Map	0.22 $e^-/Å^3$
Minimum peak in Final Diff. Map	-0.16 $e^-/Å^3$

Table 1. Atomic coordinates and B_{iso}/B_{eq}

atom	x	y	z	B_{eq}
O1	0.2856(3)	0.4412	0.0814(2)	2.99(5)
O2	0.2782(3)	0.1726(2)	0.0349(2)	2.33(4)
O3	-0.1768(3)	0.2596(2)	-0.3057(2)	3.09(4)
O4	-0.1539(3)	0.4085(3)	-0.1727(2)	3.33(5)
C1	0.2562(4)	0.3591(3)	0.0112(3)	2.31(6)
C2	0.2981(4)	0.3459(3)	-0.1324(3)	2.47(6)
C3	0.2572(4)	0.2513(3)	-0.1979(3)	2.48(6)
C4	0.2029(4)	0.1541(3)	-0.1209(3)	2.32(5)
C5	0.2582(4)	0.0560(3)	-0.1877(3)	2.81(7)
C6	0.1379(5)	0.0284(3)	-0.3173(3)	3.05(7)
C7	-0.0413(5)	0.0950(3)	-0.3888(3)	3.39(7)
C8	-0.1420(4)	0.1455(3)	-0.2798(3)	2.95(6)
C9	-0.0142(4)	0.1414(3)	-0.1257(3)	2.43(6)
C10	-0.0519(4)	0.2392(3)	-0.0477(3)	2.48(6)
C11	-0.1858(4)	0.2281(3)	0.0552(3)	2.67(6)
C12	-0.0457(4)	0.1935(3)	0.2005(3)	2.74(6)
C13	0.1314(4)	0.2663(3)	0.2123(3)	2.48(6)
C14	0.1608(4)	0.2623(3)	0.0580(3)	2.32(6)
C15	0.3667(4)	0.4408(3)	-0.1991(3)	2.99(7)
C16	0.1722(6)	-0.0658(3)	-0.4048(4)	4.17(9)
C17	-0.1302(4)	0.3144(3)	-0.1757(3)	2.64(7)

C18	0.3085(4)	0.2458(3)	0.3395(3)	2.69(6)
C19	0.3922(6)	0.1358(4)	0.3617(4)	4.71(9)
C20	0.3837(5)	0.3228(3)	0.4317(4)	3.77(8)
H1	0.2622	0.2443	-0.2969	2.9720
H2	0.3709	0.0158	-0.1416	3.3773
H3	-0.0021	0.1503	-0.4429	4.0704
H4	-0.1335	0.0509	-0.4538	4.0704
H5	-0.2620	0.1104	-0.2855	3.5344
H6	-0.0364	0.0789	-0.0765	2.9218
H7	-0.2458	0.2939	0.0658	3.2077
H8	-0.2838	0.1761	0.0198	3.2077
H9	-0.1014	0.2045	0.2801	3.2839
H10	-0.0106	0.1210	0.1974	3.2839
H11	0.0889	0.3361	0.2252	2.9702
H12	0.4958	0.4583	-0.1446	3.5846
H13	0.3655	0.4256	-0.2977	3.5846
H14	0.2824	0.4990	-0.1974	3.5846
H15	0.0593	-0.1096	-0.4277	5.0074
H16	0.1981	-0.0422	-0.4931	5.0074
H17	0.2808	-0.1051	-0.3490	5.0074
H18	0.4895	0.1324	0.4527	5.6556
H19	0.2912	0.0866	0.3622	5.6556
H20	0.4489	0.1189	0.2842	5.6556
H21	0.4921	0.3091	0.5134	4.5275
H22	0.3293	0.3920	0.4163	4.5275

$B_{eq} = 8/3\ \pi^2(U_{11}(aa^*)^2 + U_{22}(bb^*)^2 + U_{33}(cc^*)^2 + 2U_{12}(aa^*bb^*)\cos\gamma + 2U_{13}(aa^*cc^*)\cos\beta + 2U_{23}(bb^*cc^*)\cos\alpha)$

Table 2. Anisotropic Displacement Parameters

atom	U_{11}	U_{22}	U_{33}	U_{12}	U_{13}	U_{23}
O1	0.038(1)	0.034(1)	0.043(1)	-0.0063(9)	0.0130(9)	-0.0026(10)
O2	0.0276(9)	0.032(1)	0.0269(9)	0.0040(8)	0.0031(8)	0.0011(8)
O3	0.039(1)	0.045(1)	0.029(1)	0.005(1)	0.0004(8)	0.007(1)
O4	0.041(1)	0.038(1)	0.047(1)	0.012(1)	0.0108(10)	0.009(1)
C1	0.020(1)	0.033(2)	0.032(1)	0.001(1)	0.003(1)	0.006(1)
C2	0.025(1)	0.034(2)	0.034(1)	0.004(1)	0.007(1)	0.004(1)
C3	0.026(1)	0.039(2)	0.029(1)	0.004(1)	0.008(1)	0.005(1)
C4	0.028(1)	0.035(2)	0.023(1)	0.002(1)	0.004(1)	0.003(1)
C5	0.041(2)	0.037(2)	0.032(2)	0.003(1)	0.014(1)	0.004(1)
C6	0.051(2)	0.036(2)	0.033(2)	-0.003(1)	0.018(1)	-0.000(1)
C7	0.051(2)	0.047(2)	0.027(1)	-0.008(2)	0.004(1)	-0.003(1)
C8	0.033(2)	0.044(2)	0.031(1)	-0.005(1)	0.002(1)	0.002(1)

C9	0.032(1)	0.033(2)	0.026(1)	-0.004(1)	0.006(1)	0.004(1)
C10	0.024(1)	0.036(2)	0.032(1)	-0.000(1)	0.003(1)	0.004(1)
C11	0.028(1)	0.039(2)	0.035(2)	-0.002(1)	0.008(1)	-0.001(1)
C12	0.034(2)	0.040(2)	0.032(1)	-0.002(1)	0.012(1)	0.002(1)
C13	0.033(1)	0.033(2)	0.028(1)	0.001(1)	0.010(1)	0.000(1)
C14	0.026(1)	0.033(2)	0.028(1)	0.004(1)	0.005(1)	0.003(1)
C15	0.041(2)	0.038(2)	0.038(2)	0.000(1)	0.018(1)	0.005(1)
C16	0.072(2)	0.050(2)	0.043(2)	-0.004(2)	0.027(2)	-0.011(2)
C17	0.022(1)	0.043(2)	0.034(2)	0.001(1)	0.004(1)	0.006(1)
C18	0.033(1)	0.045(2)	0.025(1)	-0.001(1)	0.009(1)	-0.001(1)
C19	0.071(2)	0.054(3)	0.041(2)	0.014(2)	-0.009(2)	0.000(2)
C20	0.042(2)	0.054(2)	0.041(2)	0.005(2)	0.002(1)	-0.007(2)

The general temperature factor expression:
$\exp(-2\pi^2(a^{*2}U_{11}h^2 + b^{*2}U_{22}k^2 + c^{*2}U_{33}l^2 + 2a^*b^*U_{12}hk + 2a^*c^*U_{13}hl + 2b^*c^*U_{23}kl))$

Table 3. Bond Lengths(Å)

atom	atom	distance	atom	atom	distance
O1	C1	1.218(4)	O2	C4	1.446(3)
O2	C14	1.457(3)	O3	C8	1.469(4)
O3	C17	1.371(4)	O4	C17	1.201(4)
C1	C2	1.476(4)	C1	C14	1.519(4)
C2	C3	1.342(4)	C2	C15	1.495(4)
C3	C4	1.527(4)	C4	C5	1.490(4)
C4	C9	1.539(4)	C5	C6	1.339(4)
C6	C7	1.525(5)	C6	C16	1.506(5)
C7	C8	1.541(5)	C8	C9	1.498(4)
C9	C10	1.497(4)	C10	C11	1.539(4)
C10	C14	1.600(4)	C10	C17	1.521(4)
C11	C12	1.529(4)	C12	C13	1.538(4)
C13	C14	1.529(4)	C13	C18	1.512(4)
C18	C19	1.503(5)	C18	C20	1.320(4)

Table 4. Bond Lengths(Å)

atom	atom	distance	atom	atom	distance
C3	H1	0.95	C5	H2	0.95
C7	H3	0.95	C7	H4	0.95

C8	H5	0.95	C9	H6	0.95
C11	H7	0.95	C11	H8	0.95
C12	H9	0.95	C12	H10	0.95
C13	H11	0.95	C15	H12	0.95
C15	H13	0.95	C15	H14	0.95
C16	H15	0.95	C16	H16	0.95
C16	H17	0.95	C19	H18	0.95
C19	H19	0.95	C19	H20	0.95
C20	H21	0.95	C20	H22	0.95

Table 5. Bond Angles(^{o})

atom	atom	atom	angle	atom	atom	atom	angle
C4	O2	C14	102.0(2)	C8	O3	C17	110.8(2)
O1	C1	C2	123.4(3)	O1	C1	C14	123.4(3)
C2	C1	C14	113.1(3)	C1	C2	C3	117.0(3)
C1	C2	C15	117.8(3)	C3	C2	C15	125.0(3)
C2	C3	C4	123.1(2)	O2	C4	C3	106.6(2)
O2	C4	C5	119.9(2)	O2	C4	C9	98.1(2)
C3	C4	C5	109.6(2)	C3	C4	C9	116.7(2)
C5	C4	C9	106.1(2)	C4	C5	C6	115.3(3)
C5	C6	C7	121.0(3)	C5	C6	C16	123.4(3)
C7	C6	C16	115.5(3)	C6	C7	C8	114.4(2)
O3	C8	C7	112.4(2)	O3	C8	C9	103.1(2)
C7	C8	C9	111.6(2)	C4	C9	C8	111.5(2)
C4	C9	C10	102.1(2)	C8	C9	C10	108.0(2)
C9	C10	C11	117.3(3)	C9	C10	C14	101.2(2)
C9	C10	C17	101.4(2)	C11	C10	C14	105.1(2)
C11	C10	C17	113.8(2)	C14	C10	C17	117.8(2)
C10	C11	C12	103.3(2)	C11	C12	C13	102.6(2)
C12	C13	C14	103.2(2)	C12	C13	C18	116.5(2)
C14	C13	C18	117.1(2)	O2	C14	C1	105.3(2)
O2	C14	C10	104.3(2)	O2	C14	C13	113.5(2)
C1	C14	C10	112.7(2)	C1	C14	C13	115.9(2)
C10	C14	C13	104.8(2)	O3	C17	O4	121.2(3)
O3	C17	C10	110.3(3)	O4	C17	C10	128.4(3)
C13	C18	C19	118.9(3)	C13	C18	C20	120.2(3)
C19	C18	C20	120.9(3)				

Table 6. Bond Angles(°)

atom	atom	atom	angle	atom	atom	atom	angle
C2	C3	H1	118.5	C4	C3	H1	118.5
C4	C5	H2	122.3	C6	C5	H2	122.3
C6	C7	H3	108.2	C6	C7	H4	108.2
C8	C7	H3	108.2	C8	C7	H4	108.2
H3	C7	H4	109.5	O3	C8	H5	109.9
C7	C8	H5	109.9	C9	C8	H5	109.9
C4	C9	H6	111.6	C8	C9	H6	111.6
C10	C9	H6	111.6	C10	C11	H7	111.0
C10	C11	H8	111.0	C12	C11	H7	111.0
C12	C11	H8	111.0	H7	C11	H8	109.5
C11	C12	H9	111.2	C11	C12	H10	111.2
C13	C12	H9	111.2	C13	C12	H10	111.2
H9	C12	H10	109.5	C12	C13	H11	106.4
C14	C13	H11	106.4	C18	C13	H11	106.4
C2	C15	H12	109.5	C2	C15	H13	109.5
C2	C15	H14	109.5	H12	C15	H13	109.5
H12	C15	H14	109.5	H13	C15	H14	109.5
C6	C16	H15	109.5	C6	C16	H16	109.5
C6	C16	H17	109.5	H15	C16	H16	109.5
H15	C16	H17	109.5	H16	C16	H17	109.5
C18	C19	H18	109.5	C18	C19	H19	109.5
C18	C19	H20	109.5	H18	C19	H19	109.5
H18	C19	H20	109.5	H19	C19	H20	109.5
C18	C20	H21	120.0	C18	C20	H22	120.0
H21	C20	H22	120.0				

Table 7. Torsion Angles(°)

atom	atom	atom	atom	angle	atom	atom	atom	atom	angle
O1	C1	C2	C3	-179.5(3)	O1	C1	C2	C15	-4.5(4)
O1	C1	C14	O2	-135.7(3)	O1	C1	C14	C10	111.3(3)
O1	C1	C14	C13	-9.4(4)	O2	C4	C3	C2	-21.9(3)
O2	C4	C5	C6	159.3(3)	O2	C4	C9	C8	166.9(2)
O2	C4	C9	C10	51.9(2)	O2	C14	C1	C2	48.0(3)
O2	C14	C10	C9	-4.8(3)	O2	C14	C10	C11	117.7(2)
O2	C14	C10	C17	-114.3(3)	O2	C14	C13	C12	-85.1(3)
O2	C14	C13	C18	44.4(3)	O3	C8	C7	C6	129.8(3)
O3	C8	C9	C4	-86.3(3)	O3	C8	C9	C10	25.1(3)

O3	C17	C10	C9	13.7(3)	O3	C17	C10	C11	-113.3(3)
O3	C17	C10	C14	123.0(3)	O4	C17	O3	C8	-177.7(3)
O4	C17	C10	C9	-167.0(3)	O4	C17	C10	C11	66.1(4)
O4	C17	C10	C14	-57.7(4)	C1	C2	C3	C4	-10.3(4)
C1	C14	O2	C4	-80.9(2)	C1	C14	C10	C9	108.8(3)
C1	C14	C10	C11	-128.6(3)	C1	C14	C10	C17	-0.6(3)
C1	C14	C13	C12	152.9(2)	C1	C14	C13	C18	-77.6(3)
C2	C1	C14	C10	-65.1(3)	C2	C1	C14	C13	174.3(2)
C2	C3	C4	C5	-153.1(3)	C2	C3	C4	C9	86.4(3)
C3	C2	C1	C14	-3.2(3)	C3	C4	O2	C14	65.9(2)
C3	C4	C5	C6	-77.0(3)	C3	C4	C9	C8	53.8(3)
C3	C4	C9	C10	-61.3(3)	C4	O2	C14	C10	37.9(2)
C4	O2	C14	C13	151.4(2)	C4	C3	C2	C15	175.0(2)
C4	C5	C6	C7	0.3(4)	C4	C5	C6	C16	177.8(3)
C4	C9	C8	C7	34.5(3)	C4	C9	C10	C11	-141.4(2)
C4	C9	C10	C14	-27.7(2)	C4	C9	C10	C17	94.0(2)
C5	C4	O2	C14	-169.0(2)	C5	C4	C9	C8	-68.7(3)
C5	C4	C9	C10	176.3(2)	C5	C6	C7	C8	-35.4(4)
C6	C5	C4	C9	49.7(3)	C6	C7	C8	C9	14.6(4)
C7	C8	O3	C17	-136.7(2)	C7	C8	C9	C10	145.9(3)
C8	O3	C17	C10	1.7(3)	C8	C7	C6	C16	146.9(3)
C8	C9	C10	C11	101.0(3)	C8	C9	C10	C14	-145.3(2)
C8	C9	C10	C17	-23.6(3)	C9	C4	O2	C14	-55.1(2)
C9	C8	O3	C17	-16.4(3)	C9	C10	C11	C12	86.1(3)
C9	C10	C14	C13	-124.3(2)	C10	C11	C12	C13	43.4(3)
C10	C14	C13	C12	28.1(3)	C10	C14	C13	C18	157.5(3)
C11	C10	C14	C13	-1.7(3)	C11	C12	C13	C14	-44.7(3)
C11	C12	C13	C18	-174.5(2)	C12	C11	C10	C14	-25.4(3)
C12	C11	C10	C17	-155.8(2)	C12	C13	C18	C19	52.9(4)
C12	C13	C18	C20	-124.9(3)	C13	C14	C10	C17	126.3(3)
C14	C1	C2	C15	171.8(2)	C14	C13	C18	C19	-70.0(4)
C14	C13	C18	C20	112.2(3)					

Table 8. Non-bonded Contacts out to 3.75 Å

atom	atom	distance	ADC	atom	atom	distance	ADC
O1	C9	3.273(4)	2	O1	C5	3.445(4)	65502
O1	C8	3.498(4)	2	O3	C16	3.521(4)	55402
O3	C20	3.522(4)	45401	O4	C15	3.373(4)	45501
O4	C19	3.560(4)	2	C15	C19	3.572(5)	65502
C16	C20	3.525(5)	64502				

3.13 - Appendix

X-ray Crystallographic Data for Compound 3.76

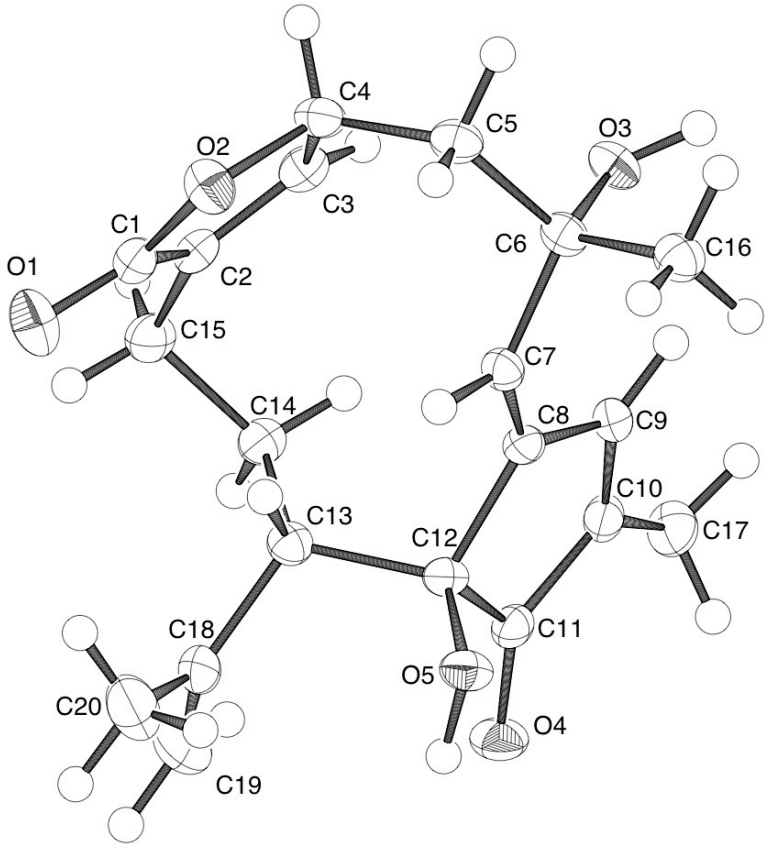

EXPERIMENTAL DETAILS

A. Crystal Data

Empirical Formula	$C_{20}H_{24}O_5$
Formula Weight	344.41
Crystal Color, Habit	colorless, bladelike
Crystal Dimensions	0.18 X 0.15 X 0.03 mm
Crystal System	monoclinic
Lattice Type	Primitive
Lattice Parameters	a = 6.1326(7)Å
	b = 8.7197(9) Å
	c = 32.283(3) Å
	β = 94.632(2)^o
	V = 1720.7(3) Å^3
Space Group	$P2_1/c$ (#14)
Z value	4
D_{calc}	1.329 g/cm^3
F_{000}	736.00
μ(MoKα)	0.95 cm^{-1}

B. Intensity Measurements

Diffractometer	Bruker APEX CCD
Radiation	MoKα (λ = 0.71069 Å)
	graphite monochromated
Detector Position	60.00 mm
Exposure Time	30.0 seconds per frame.
Scan Type	ω (0.3 degrees per frame)
$2\theta_{max}$	52.7^o
No. of Reflections Measured	Total: 9875
	Unique: 2364 (R_{int} = 0.022)
Corrections	Lorentz-polarization
	Absorption (Tmax = 1.00 Tmin = 0.83)

C. Structure Solution and Refinement

Structure Solution	Direct Methods (SIR97)
Refinement	Full-matrix least-squares
Function Minimized	$\Sigma w (\|Fo\| - \|Fc\|)^2$
Least Squares Weights	$1/\sigma^2(Fo) = 4Fo^2/\sigma^2(Fo^2)$
p-factor	0.0300
Anomalous Dispersion	All non-hydrogen atoms
No. Observations (I>3.00σ(I))	2466
No. Variables	226
Reflection/Parameter Ratio	10.91
Residuals: R; Rw; Rall	0.041 ; 0.046; 0.063
Goodness of Fit Indicator	1.82
Max Shift/Error in Final Cycle	0.00
Maximum peak in Final Diff. Map	0.22 $e^-/Å^3$
Minimum peak in Final Diff. Map	-0.23 $e^-/Å^3$

Table 1. Atomic coordinates and B_{iso}/B_{eq}

atom	x	y	z	B_{eq}
O1	-0.1894(2)	-0.2792(1)	0.29901(5)	2.80(3)
O2	-0.2806(2)	-0.0506(1)	0.27187(4)	2.09(3)
O3	-0.0738(2)	0.4051(1)	0.31483(4)	1.89(3)
O4	0.2178(2)	0.1056(1)	0.48521(4)	2.23(3)
O5	-0.2213(2)	0.0653(1)	0.44093(4)	1.81(3)
C1	-0.1392(3)	-0.1466(2)	0.29308(6)	1.85(4)
C2	0.0643(3)	-0.0643(2)	0.30610(6)	1.68(4)
C3	0.0412(3)	0.0776(2)	0.29118(6)	1.74(4)
C4	-0.1763(3)	0.0982(2)	0.26741(6)	1.77(4)
C5	-0.3280(3)	0.2271(2)	0.28028(6)	1.81(4)
C6	-0.2660(3)	0.3152(2)	0.32080(6)	1.57(4)
C7	-0.2156(3)	0.2067(2)	0.35681(6)	1.52(4)
C8	-0.0604(3)	0.2141(2)	0.38832(6)	1.46(4)
C9	0.1093(3)	0.3289(2)	0.39782(6)	1.65(4)
C10	0.2407(3)	0.2944(2)	0.43191(6)	1.69(4)
C11	0.1581(3)	0.1545(2)	0.45071(6)	1.61(4)
C12	-0.0257(3)	0.0873(2)	0.42096(6)	1.50(4)
C13	0.0426(3)	-0.0642(2)	0.39941(6)	1.60(4)
C14	0.2537(3)	-0.0463(2)	0.37703(6)	1.74(4)
C15	0.2417(3)	-0.1322(2)	0.33535(6)	2.03(4)
C16	-0.4553(3)	0.4189(2)	0.32971(6)	1.99(4)
C17	0.4356(3)	0.3772(2)	0.45104(6)	2.25(4)

C18	0.0424(4)	-0.2042(2)	0.42754(6)	2.19(5)
C19	0.2135(4)	-0.2375(2)	0.45629(7)	2.88(5)
C20	-0.1501(4)	-0.3008(2)	0.42287(7)	3.09(5)
H1	-0.1035	0.5061	0.3107	3.1397
H2	-0.1661	0.0155	0.4664	3.1397
H3	0.1489	0.1557	0.2951	2.0820
H4	-0.1525	0.1120	0.2389	2.1222
H5	-0.3380	0.3002	0.2584	2.1710
H6	-0.4677	0.1825	0.2828	2.1710
H7	-0.3088	0.1198	0.3571	1.8185
H8	0.1253	0.4185	0.3816	1.9804
H9	-0.0697	-0.0827	0.3780	1.9163
H10	0.2770	0.0596	0.3720	2.0880
H11	0.3730	-0.0857	0.3944	2.0880
H12	0.2105	-0.2373	0.3399	2.4325
H13	0.3780	-0.1235	0.3235	2.4325
H14	-0.5828	0.3587	0.3321	2.3928
H15	-0.4814	0.4903	0.3076	2.3928
H16	-0.4203	0.4726	0.3550	2.3928
H17	0.4457	0.4748	0.4383	2.6946
H18	0.5637	0.3195	0.4471	2.6946
H19	0.4219	0.3901	0.4799	2.6946
H20	0.3383	-0.1727	0.4589	3.4540
H21	0.2068	-0.3253	0.4736	3.4540
H22	-0.1297	-0.3874	0.4406	3.7128
H23	-0.1729	-0.3342	0.3948	3.7128
H24	-0.2739	-0.2443	0.4301	3.7128

$B_{eq} = 8/3\ \pi^2(U_{11}(aa^*)^2 + U_{22}(bb^*)^2 + U_{33}(cc^*)^2 + 2U_{12}(aa^*bb^*)\cos\gamma + 2U_{13}(aa^*cc^*)\cos\beta + 2U_{23}(bb^*cc^*)\cos\alpha)$

Table 2. Anisotropic Displacement Parameters

atom	U_{11}	U_{22}	U_{33}	U_{12}	U_{13}	U_{23}
O1	0.0364(9)	0.0213(7)	0.0486(10)	-0.0021(7)	0.0026(7)	0.0010(7)
O2	0.0246(8)	0.0237(7)	0.0302(8)	-0.0026(6)	-0.0039(6)	0.0012(6)
O3	0.0224(7)	0.0216(7)	0.0277(8)	-0.0037(6)	0.0005(6)	0.0066(6)
O4	0.0333(8)	0.0332(8)	0.0173(7)	0.0007(7)	-0.0031(6)	0.0051(6)
O5	0.0209(7)	0.0277(7)	0.0206(7)	0.0031(6)	0.0046(6)	0.0061(6)
C1	0.028(1)	0.022(1)	0.020(1)	0.0035(9)	0.0037(9)	-0.0018(8)
C2	0.022(1)	0.0242(10)	0.0176(10)	0.0015(8)	0.0046(8)	-0.0043(8)
C3	0.018(1)	0.027(1)	0.021(1)	-0.0024(9)	0.0032(8)	-0.0032(8)
C4	0.025(1)	0.024(1)	0.018(1)	-0.0043(9)	0.0022(8)	0.0031(8)
C5	0.021(1)	0.0268(10)	0.020(1)	-0.0007(9)	-0.0017(8)	0.0040(8)

C6	0.018(1)	0.0200(9)	0.022(1)	-0.0030(8)	0.0007(8)	0.0026(8)
C7	0.019(1)	0.0172(9)	0.021(1)	-0.0018(8)	0.0041(8)	0.0012(8)
C8	0.020(1)	0.0191(9)	0.0165(10)	0.0024(8)	0.0045(8)	0.0007(8)
C9	0.026(1)	0.0165(9)	0.020(1)	0.0029(8)	0.0023(9)	0.0004(8)
C10	0.024(1)	0.0189(9)	0.021(1)	0.0029(8)	0.0010(9)	-0.0032(8)
C11	0.022(1)	0.0213(9)	0.018(1)	0.0052(8)	0.0024(8)	-0.0015(8)
C12	0.019(1)	0.0213(9)	0.0164(10)	0.0005(8)	0.0023(8)	0.0024(8)
C13	0.020(1)	0.0214(9)	0.0193(10)	0.0014(8)	-0.0005(8)	0.0013(8)
C14	0.020(1)	0.0254(10)	0.0203(10)	0.0039(8)	-0.0001(8)	-0.0001(8)
C15	0.025(1)	0.028(1)	0.025(1)	0.0052(9)	0.0041(9)	0.0004(9)
C16	0.026(1)	0.026(1)	0.024(1)	0.0013(9)	-0.0013(9)	0.0026(9)
C17	0.031(1)	0.027(1)	0.026(1)	-0.0003(9)	-0.0054(9)	-0.0033(9)
C18	0.037(1)	0.0196(10)	0.028(1)	0.0062(9)	0.0120(10)	0.0005(9)
C19	0.043(1)	0.031(1)	0.035(1)	0.009(1)	-0.004(1)	0.0096(10)
C20	0.042(1)	0.026(1)	0.051(2)	0.002(1)	0.008(1)	0.005(1)

The general temperature factor expression:
$\exp(-2\pi^2(a^{*2}U_{11}h^2 + b^{*2}U_{22}k^2 + c^{*2}U_{33}l^2 + 2a^*b^*U_{12}hk + 2a^*c^*U_{13}hl + 2b^*c^*U_{23}kl))$

Table 3. Bond Lengths(Å)

atom	atom	distance	atom	atom	distance
O1	C1	1.216(2)	O2	C1	1.351(2)
O2	C4	1.458(2)	O3	C6	1.442(2)
O4	C11	1.221(2)	O5	C12	1.420(2)
C1	C2	1.471(3)	C2	C3	1.331(3)
C2	C15	1.503(3)	C3	C4	1.495(3)
C4	C5	1.538(3)	C5	C6	1.538(3)
C6	C7	1.511(2)	C6	C16	1.518(3)
C7	C8	1.337(3)	C8	C9	1.459(3)
C8	C12	1.530(2)	C9	C10	1.345(3)
C10	C11	1.470(3)	C10	C17	1.488(3)
C11	C12	1.536(3)	C12	C13	1.566(3)
C13	C14	1.541(3)	C13	C18	1.522(3)
C14	C15	1.536(3)	C18	C19	1.375(3)
C18	C20	1.448(3)			

Table 4. Bond Lengths(Å)

atom	atom	distance	atom	atom	distance
O3	H1	0.91	O5	H2	0.97
C3	H3	0.95	C4	H4	0.95
C5	H5	0.95	C5	H6	0.95
C7	H7	0.95	C9	H8	0.95
C13	H9	0.95	C14	H10	0.95
C14	H11	0.95	C15	H12	0.95
C15	H13	0.95	C16	H14	0.95
C16	H15	0.95	C16	H16	0.95
C17	H17	0.95	C17	H18	0.95
C17	H19	0.95	C19	H20	0.95
C19	H21	0.95	C20	H22	0.95
C20	H23	0.95	C20	H24	0.95

Table 5. Bond Angles(^{o})

atom	atom	atom	angle	atom	atom	atom	angle
C1	O2	C4	109.4(1)	O1	C1	O2	120.6(2)
O1	C1	C2	129.7(2)	O2	C1	C2	109.7(2)
C1	C2	C3	106.7(2)	C1	C2	C15	122.8(2)
C3	C2	C15	130.1(2)	C2	C3	C4	111.2(2)
O2	C4	C3	102.9(1)	O2	C4	C5	110.1(1)
C3	C4	C5	118.9(2)	C4	C5	C6	118.8(2)
O3	C6	C5	107.9(1)	O3	C6	C7	109.0(1)
O3	C6	C16	110.3(1)	C5	C6	C7	111.3(1)
C5	C6	C16	108.6(2)	C7	C6	C16	109.8(1)
C6	C7	C8	130.1(2)	C7	C8	C9	130.1(2)
C7	C8	C12	122.7(2)	C9	C8	C12	107.1(2)
C8	C9	C10	112.9(2)	C9	C10	C11	108.7(2)
C9	C10	C17	129.8(2)	C11	C10	C17	121.6(2)
O4	C11	C10	125.3(2)	O4	C11	C12	126.0(2)
C10	C11	C12	108.5(2)	O5	C12	C8	109.5(1)
O5	C12	C11	111.8(1)	O5	C12	C13	110.7(1)
C8	C12	C11	102.1(1)	C8	C12	C13	109.3(1)
C11	C12	C13	113.0(2)	C12	C13	C14	112.8(1)
C12	C13	C18	113.5(1)	C14	C13	C18	113.7(2)
C13	C14	C15	112.2(2)	C2	C15	C14	109.8(2)
C13	C18	C19	122.3(2)	C13	C18	C20	116.4(2)
C19	C18	C20	121.2(2)				

Table 6. Bond Angles(°)

atom	atom	atom	angle	atom	atom	atom	angle
C6	O3	H1	113.0	C12	O5	H2	101.3
C2	C3	H3	124.4	C4	C3	H3	124.4
O2	C4	H4	108.2	C3	C4	H4	108.2
C5	C4	H4	108.2	C4	C5	H5	107.1
C4	C5	H6	107.1	C6	C5	H5	107.1
C6	C5	H6	107.1	H5	C5	H6	109.5
C6	C7	H7	115.0	C8	C7	H7	115.0
C8	C9	H8	123.6	C10	C9	H8	123.6
C12	C13	H9	105.2	C14	C13	H9	105.2
C18	C13	H9	105.2	C13	C14	H10	108.8
C13	C14	H11	108.8	C15	C14	H10	108.8
C15	C14	H11	108.8	H10	C14	H11	109.5
C2	C15	H12	109.4	C2	C15	H13	109.4
C14	C15	H12	109.4	C14	C15	H13	109.4
H12	C15	H13	109.5	C6	C16	H14	109.5
C6	C16	H15	109.5	C6	C16	H16	109.5
H14	C16	H15	109.5	H14	C16	H16	109.5
H15	C16	H16	109.5	C10	C17	H17	109.5
C10	C17	H18	109.5	C10	C17	H19	109.5
H17	C17	H18	109.5	H17	C17	H19	109.5
H18	C17	H19	109.5	C18	C19	H20	120.0
C18	C19	H21	120.0	H20	C19	H21	120.0
C18	C20	H22	109.5	C18	C20	H23	109.5
C18	C20	H24	109.5	H22	C20	H23	109.5
H22	C20	H24	109.5	H23	C20	H24	109.5

Table 7. Torsion Angles(°)

atom	atom	atom	atom	angle	atom	atom	atom	atom	angle
O1	C1	O2	C4	-177.1(2)	O1	C1	C2	C3	178.5(2)
O1	C1	C2	C15	-8.5(3)	O2	C1	C2	C3	-1.8(2)
O2	C1	C2	C15	171.1(2)	O2	C4	C3	C2	2.1(2)
O2	C4	C5	C6	109.5(2)	O3	C6	C5	C4	68.5(2)
O3	C6	C7	C8	21.6(3)	O4	C11	C10	C9	-167.9(2)
O4	C11	C10	C17	10.5(3)	O4	C11	C12	O5	50.5(2)
O4	C11	C12	C8	167.5(2)	O4	C11	C12	C13	-75.2(2)
O5	C12	C8	C7	-58.3(2)	O5	C12	C8	C9	124.7(2)
O5	C12	C11	C10	-125.6(1)	O5	C12	C13	C14	179.7(1)
O5	C12	C13	C18	-49.1(2)	C1	O2	C4	C3	-3.2(2)

C1	O2	C4	C5	-130.8(2)	C1	C2	C3	C4	-0.3(2)
C1	C2	C15	C14	-111.0(2)	C2	C1	O2	C4	3.2(2)
C2	C3	C4	C5	124.0(2)	C2	C15	C14	C13	63.6(2)
C3	C2	C15	C14	60.1(3)	C3	C4	C5	C6	-8.7(2)
C4	C3	C2	C15	-172.5(2)	C4	C5	C6	C7	-50.9(2)
C4	C5	C6	C16	-171.9(2)	C5	C6	C7	C8	140.4(2)
C6	C7	C8	C9	-0.1(3)	C6	C7	C8	C12	-176.3(2)
C7	C8	C9	C10	-178.2(2)	C7	C8	C12	C11	-176.9(2)
C7	C8	C12	C13	63.2(2)	C8	C7	C6	C16	-99.4(2)
C8	C9	C10	C11	-4.3(2)	C8	C9	C10	C17	177.6(2)
C8	C12	C11	C10	-8.6(2)	C8	C12	C13	C14	58.9(2)
C8	C12	C13	C18	-169.9(2)	C9	C8	C12	C11	6.1(2)
C9	C8	C12	C13	-113.8(2)	C9	C10	C11	C12	8.3(2)
C10	C9	C8	C12	-1.5(2)	C10	C11	C12	C13	108.6(2)
C11	C12	C13	C14	-54.0(2)	C11	C12	C13	C18	77.2(2)
C12	C11	C10	C17	-173.3(2)	C12	C13	C14	C15	-140.5(2)
C12	C13	C18	C19	-81.2(2)	C12	C13	C18	C20	98.0(2)
C14	C13	C18	C19	49.6(2)	C14	C13	C18	C20	-131.2(2)
C15	C14	C13	C18	88.4(2)					

Table 8. Non-bonded Contacts out to 3.75 Å

atom	atom	distance	ADC	atom	atom	distance	ADC
O1	O3	2.878(2)	54501	O1	C16	3.291(2)	54501
O1	C3	3.360(2)	54502	O1	C4	3.398(2)	54502
O1	C6	3.644(2)	54501	O2	C5	3.421(2)	44502
O2	C16	3.548(2)	44502	O2	O3	3.700(2)	54502
O3	C4	3.590(2)	2	O4	O5	2.810(2)	55603
O4	O4	3.442(3)	55603	O4	C18	3.456(2)	55603
O4	C20	3.475(3)	55603	O4	C19	3.562(3)	55603
O4	C12	3.737(2)	55603	O5	C17	3.469(2)	45501
O5	C19	3.638(3)	55603	C1	C4	3.622(3)	54502
C1	C3	3.716(3)	54502	C9	C16	3.678(3)	65501
C9	C20	3.717(3)	56501	C17	C19	3.635(3)	56501
C17	C19	3.745(3)	65603				

3.14 References and Notes

1. M. J. H. Van Oppen, J. C. Mieog, C. A. Sánchez and K. E. Fabricius, *Mol. Ecol.*, 2005, **14**, 2403.
2. A. D. Rodríguez, *Tetrahedron*, 1995, **51**, 4571.
3. J. Marrero, A. D. Rodríguez, P. Baran, R. G. Raptis, J. A. Sánchez, E. Orterga-Barria and T. L. Capson, *Org. Lett.*, 2004, **6**, 1661.
4. P. Roethle and D. Trauner, *Nat. Prod. Rep.*, 2008, **25**, 298.
5. B. Doroh and G. A. Sulikowski, *Org. Lett.*, 2006, **8**, 903.
6. R. Miao, S. G. Gramani and M. J. Lear, *Tetrahedron Lett.*, 2009, **50**, 1731.
7. (a) M. T. Crimmins, *Chem. Rev.*, 1988, **88**, 1453. (b) J. Iriondo-Alberdi and M. F. Greaney, *Eur. J. Org. Chem.*, 2007, **2007**, 4801.
8. G. Ciamician and P. Silber, *Chem. Ber.*, 1908, **41**, 1928.
9. P. E. Eaton and T. W. Cole Jr., *J. Am. Chem. Soc.*, 1964, **86**, 962, 3157.
10. K. Wiesner, V. Musil and K. J. Wesner, *Tetrahedron Lett.*, 1968, **9**, 5643.
11. E. J. Corey, R. B. Mitra and H. Uda, *J. Am. Chem. Soc.*, 1964, **86**, 485.
12. (a) M. Racamonde, R. Alibés, M. Figueredo, J. Font and P. de March, *J. Org. Chem.*, 2008, **73**, 5944. (b) M. Inoue, T. Sato and M. Hirama, *Angew. Chem. Int. Ed.*, 2006, **45**, 4843. (c) M. Tanaka, K. Tomioka and K. Koga, *Tetrahedron*, 1994, **50**, 12829. (d) B. T. B. Hue, J. Dijkink, S. Kuiper, S. van Schaik, J. H. van Maarseveen and H. Hiemstra, *Eur. J. Org. Chem.*, 2006, **2006**, 127.
13. D. I. Schuster, G. Lem and N. A. Kaprinidis, *Chem. Rev.*, 1993, **93**, 3.
14. (a) Y. Tamura, Y. Kita, H. Ishibashi and M. Ikeda, *J. Chem. Soc. D,* 1971, 1167. (b) R. M. Coates, P. D. Senter and W. R. Baker, *J. Org. Chem.*, 1982, **47**, 3598.
15. P. A. Roethle and D. Trauner, *Org. Lett.*, 2006, **8**, 345.
16. C. Ko, J. B. Feltenberger, S. K. Ghosh and R. P. Hsung, *Org. Lett.*, 2008, **10**, 1971.
17. S. Ma and E. Negishi, *J. Org. Chem.*, 1997, **62**, 784.
18. A. D. Rodríguez, J. Shi and Y. Shi, *J. Org. Chem.*, 2000, **65**, 3192.
19. D. E. Williams, R. J. Andersen, J. F. Kingston and A. G. Fallis, *Can. J. Chem.*, 1988, **66**, 2928.
20. S. C. Wang and D. J. Tantillo, *J. Org. Chem*., 2008, **73**, 1516.

Chapter 4

Progress Towards a Macrocyclic Precursor of Bielschowskysin

4.1 Introduction

Bielschowskysin (**1.38**), like the majority of furanocembranoids, possesses an acetoxy group at the C-13 position of its carbon skeleton (Figure 4.1). Undoubtedly nature uses an enzyme to oxidize this position. If a synthetic method existed to selectively functionalize this position of the furanocembranoid framework, then bielschowskysin could in principle be synthesized from bipinnatin J (**1.11**) in the laboratory. However, no such strategy has made itself evident to us. Lacking this oxidative tool, the total synthesis of bielschowskysin requires extensive synthetic replanning. Accordingly, we have developed a synthetic route to the macrocyclic precursor for bielschowskysin with the requisite C-13 acetoxy.

Figure 4.1 Bielschowskysin and bipinnatin J.

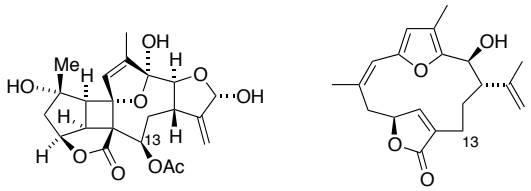

bielschowskysin (**1.38**) bipinnatin J (**1.11**)

4.2 Retrosynthesis

With our previously discussed biosynthetic hypothesis in mind, we set out to develop a retrosynthesis that places the cycloaddition at the last or next to last step. Thus, one of our first disconnections breaks the cyclobutane to give *exo*-alkylidene dihydrofuran **4.1** (Scheme 4.1). This key intermediate could potentially be obtained from epoxide **4.2** as outlined in Chapter 3. After the cycloaddition, the C8 alcohol would have to be generated by addition of water to the exocyclic alkene. Formation of the lactol ring may be accomplished through allylic oxidation of the isopropylidene. The next few disconnections follow the previously established route to bipinnatin J. A Nozaki-Hiyama-Kishi macrocyclization would close the ring, and the open-chain precursor **4.4** would be assembled via a Stille coupling. Vinyl iodide **4.5** could be obtained through a silver-catalyzed S_N1 displacement of allylic bromide **4.6** by siloxyfuran **4.7**.[1] Siloxyfuran **4.7** could be assembled through lithium-mediated addition of known TIPS-protected bromofuranol[2] **4.8** to aldehyde **4.9**. Aldehyde **4.9** could be obtained through oxidation of the corresponding alcohol, which in turn could be synthesized from known vinyl iodide[3] **4.10** via a lithium-mediated addition of oxirane (**4.11**).[4]

Scheme 4.1 Retrosynthesis of bielschowskysin.

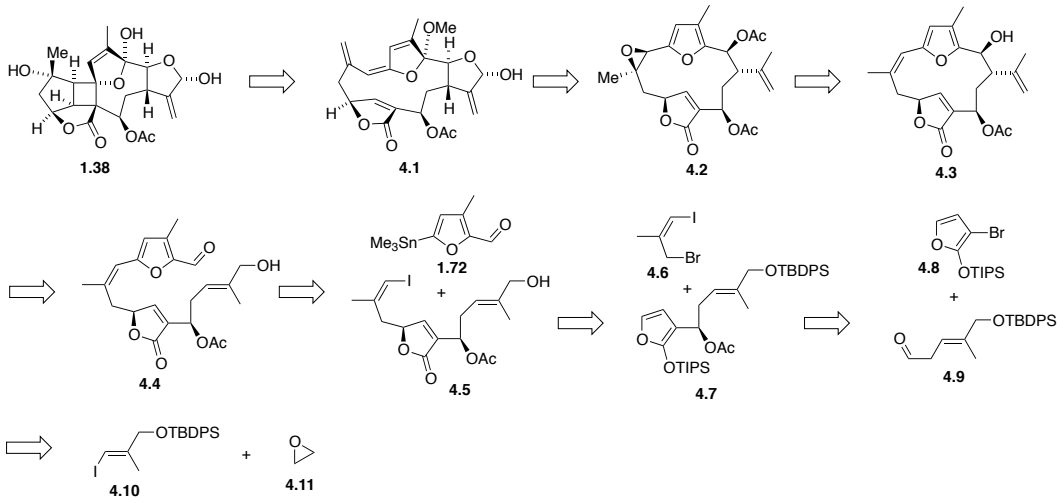

The primary advantage of this route is the utilization of established methods for a rapid assembly and functionalization of the macrocycle. A major disadvantage would be the generation of a diastereomeric mixture after the silver-catalyzed displacement step. The route would also require additional tailoring to render it asymmetric.

4.3 Synthetic Progress

Following our retrosynthesis, the first goal was the preparation of aldehyde **4.9**. We commenced with its synthesis from known vinyl iodide **4.10**, which was in turn prepared from propargyl alcohol (**4.12**) by zirconation-methylation-iodination[5] followed by protection with TBDPS-chloride (Scheme 4.2). Lithiation of vinyl iodide **4.10** was followed by trapping with oxirane to give alcohol **4.13**. Oxidation of alcohol **4.13** with Dess-Martin periodinane furnished unstable aldehyde **4.9**, which was immediately used in the next reaction.

Scheme 4.2 Synthesis of aldehyde **4.9**.

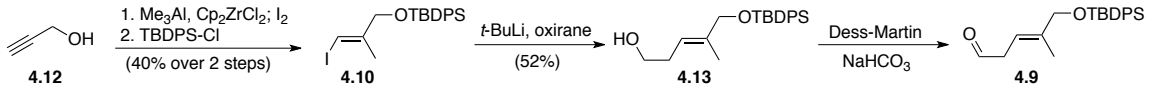

Siloxyfuran **4.8** was prepared in a two-step sequence from 2(5H)-furanone (**4.14**) via α-bromination and subsequent protection with TIPS-triflate. Lithiation of this substrate **4.8** was followed by addition into aldehyde **4.9** to give alcohol **4.16**. Alcohol **4.16** was subsequently treated with acetic anhydride under standard conditions to furnish linear substrate **4.17** (Scheme 4.3). At this point the stage has been set for the silver-catalyzed displacement with allylic bromide **4.6**. Again, this reaction would create a mixture of diastereomers that would need to be separated. Following this reaction the steps are identical to the corresponding steps in the synthesis of bipinnatin J. Further work is underway in our laboratory to explore the remainder of this promising route.

Scheme 4.3 Synthesis of linear substrate **4.17**.

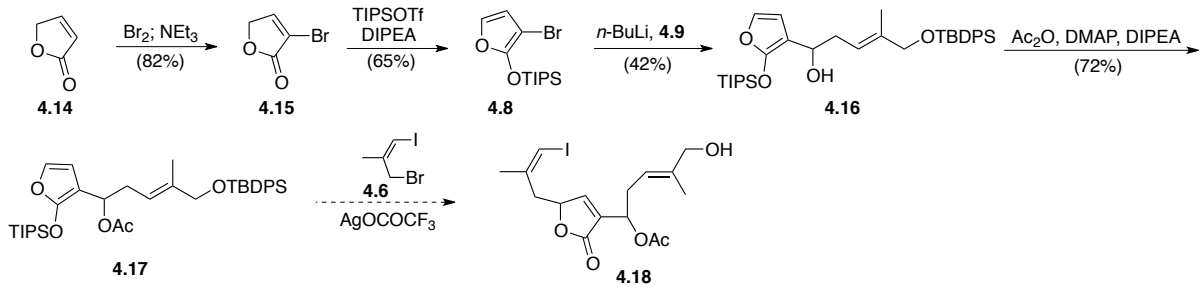

4.4 Conclusion

Although our investigation of this synthetic strategy is still in the early stages, our preliminary efforts have met with success. If the silver-catalyzed S_N1 substitution step is successful, the remaining steps up to and including the Nozaki-Hiyama-Kishi macrocyclization correspond with the equivalent steps in the synthesis of bipinnatin J. We do not anticipate that the presence of an acetoxy group should affect significantly either the Stille coupling or the macrocyclization.

Another advantage to this route is that the geometry of the $\Delta^{7,8}$ alkene is controlled at a relatively late stage in the synthesis through the geometry of allylic bromide **4.6**. By reversing the geometry of the bromide from (*Z*) to (*E*), it would be possible in theory to construct macrocycle **4.19**, which would be a precursor for the remaining bipinnatins. For example, Scheme 4.4 depicts the synthesis of bipinnatin B (**1.3**) from macrocycle **4.19**. As evident from this proposed route, the toolbox of oxidative methods we have discovered in our work with bipinnatin J would play a key role in the synthesis of these highly oxidized natural products. It is worth noting that epoxidation of butenolide **4.20** would have to take place with sodium hypochlorite when the C-13 acetoxy is present, as the Scheffer-Weitz epoxidation has been shown to fail in the presence of this group.[6]

Scheme 4.4 Proposed synthesis of bipinnatin B.

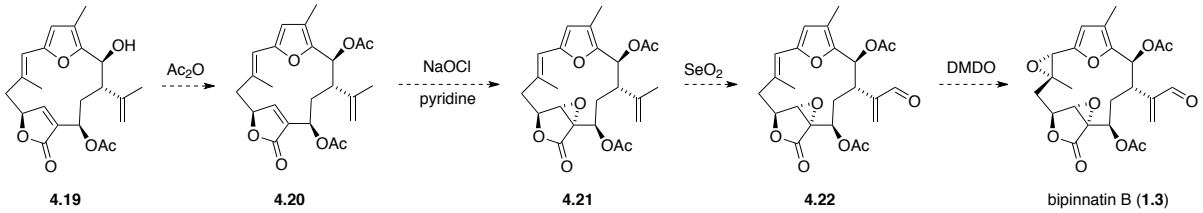

Whether or not the macrocyclization would be successful in the case of this (*E*)-double bond remains to be determined. However, if our results in the case of the (*E*)-isomer of bipinnatin J are any indication, the reaction should succeed but the yield is likely to be substantially lower. In addition, the facial selectivity for the epoxidation of macrocycle **4.22** would have to be biased towards the α-face to produce the proper configuration for the bipinnatins – a reversal of the facial selectivity from that which we determined for the (*E*)-

isomer of bipinnatin J. It may be that the presence of the C-13 acetoxy moiety is sufficient to achieve a reversal in the natural facial bias, or that nature uses an enzyme to effect the same goal.

4.5 Experimental Methods

General Experimental Details: All reactions were carried out under an inert N_2 atmosphere in oven-dried glassware. Flash column chromatography was carried out with EcoChrom ICN SiliTech 32-63 D 60 Å silica gel. Reactions and chromatography fractions were monitored with Merck silica gel 60 F_{254} plates and visualized with potassium permanganate, ceric ammonium molybdate, and vanillin. Tetrahydrofuran (THF) and methylene chloride (CH_2Cl_2) were dried by passage through activated alumina columns. Benzene (PhH) and diisopropylamine (*i*-Pr_2NH) were distilled from CaH_2 prior to use. DMSO was stored over 3 Å molecular sieves. *n*-Butyllithium was titrated with diphenylacetic acid prior to use. All other reagents and solvents were used without further purification from commercial sources. Organic extracts were dried over $MgSO_4$ unless otherwise noted.

Instrumentation: FT-IR spectra were obtained on NaCl plates with an ATI Mattson Gemini spectrometer. Proton and carbon NMR spectra (^{1}H NMR and ^{13}C NMR) were recorded in deuterated chloroform ($CDCl_3$) unless otherwise noted on a Varian VXR 400 S, Bruker AXR-300 or Bruker AMX 600 spectrometer and calibrated to residual solvent peaks. Multiplicities are abbreviated as follows: s = singlet, d = doublet, t = triplet, q = quartet, br = broad, m = multiplet. High-resolution (HR-MS) and low resolution (MS) mass spectra were recorded on a Finnigan MAT 95 instrument. Melting points were determined with an electrothermal apparatus and are uncorrected.

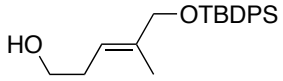

Alcohol (4.13). To a solution of (*E*)-1-*tert*-butyldiphenylsilyloxy-3-iodo-2-methylprop-2-ene (**4.10**) (2.79 g, 6.40 mmol) in THF (21 mL) at -78 °C was added dropwise a 1.5M solution of *t*-BuLi in pentane (4.27 mL, 6.40 mmol). After 20 min, oxirane (2.20 g, 49.1 mmol) was added. After 1 hr, the solution was warmed to rt. After 1 hr, the solution was cooled to 0 °C and quenched carefully with 15 mL saturated NH_4Cl. The layers were separated, and the aqueous phase extracted with CH_2Cl_2 (2 X 15 mL). The combined organic extracts were dried, filtered, and concentrated *in vacuo*. The crude oil was purified by flash chromatography (17% EtOAc/hexanes) to give 1.18 g (52%) of **4.13** as a clear oil.

R_f 0.20, 17% EtOAc/hexanes. ^{1}H NMR (600 MHz): δ 7.67 (m, 4 H), 7.39 (m, 6 H), 5.43 (tq, 1 H, *J* = 7.5, 1.5 Hz), 4.08 (s, 2 H), 3.63 (q, 2 H, *J* = 6.0 Hz), 2.32 (q, 2 H, *J* = 6.9 Hz), 1.63 (s, 3 H), 1.28 (t (OH), 1 H, *J* = 5.7 Hz), 1.07 (s, 9 H). ^{13}C (150 MHz): δ 137.5, 135.5, 133.8, 129.6, 127.6, 119.6, 68.7, 62.4, 31.1, 26.8, 19.3, 13.7. HRMS $(ESI)^+$ calcd for $C_{22}H_{31}O_2Si$ $(M+H^+)^+$ 355.2093, found 355.2089.

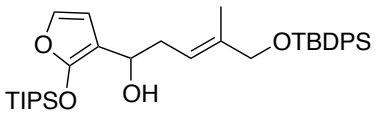

Siloxyfuran (4.16). To a solution of alcohol **4.13** (200 mg, 0.56 mmol) in CH_2Cl_2 (5 mL) was added $NaHCO_3$ (235 mg, 2.80 mmol) followed by Dess-Martin periodinane (310 mg, 0.73 mmol). After 20 min, a 1:1:1 solution (3.5 mL) of saturated $Na_2S_2O_3$, saturated $NaHCO_3$, H_2O was added. The resulting biphasic solution was stirred vigorously for 20 min. The layers were separated, and the aqueous layer was extracted with CH_2Cl_2 (2 X 8 mL). The combined organic extracts were dried, filtered, and concentrated *in vacuo* to give 199 mg (100%) of aldehyde **4.9** as a yellow oil. The crude unstable aldehyde was taken up in THF (5 mL) and used immediately in the next reaction without further purification or full characterization. Meanwhile, to a solution of TIPS-protected bromofuran **4.8** (150 mg, 0.47 mmol) in THF (5 mL) at -78 °C was added dropwise a 2.5M solution of *n*-BuLi in hexanes (0.21 mL, 0.52 mmol). After 30 min, the solution of crude aldehyde **4.9** (199 mg, 0.56 mmol) in THF (5 mL) was added via cannula. The solution turned yellow. After 1 hr, a saturated solution of NH_4Cl (5 mL) was added. The reaction was warmed to rt and diluted with Et_2O (10 mL). The layers were separated, and the aqueous phase extracted with Et_2O (2 X 5 mL). The combined organic extracts were dried, filtered, and concentrated *in vacuo*. The crude oil was purified by flash chromatography (5% EtOAc/hexanes) to give 117 mg (42%) of **4.16** as a light-yellow oil.

R_f 0.50, 17% EtOAc/Hexanes. ^{1}H NMR (300 MHz): δ 7.67 (m, 4 H), 7.38 (m, 6 H), 6.76 (d, 1 H, J = 2.3 Hz), 6.31 (d, 1 H, J = 2.4 Hz), 5.48 (t, 1 H, J = 7.4 Hz), 4.62 (m, 1 H), 4.06 (s, 2 H), 2.56 (m, 1 H), 2.41 (m, 1 H), 1.66 (d (OH), 1 H, J = 3.5 Hz), 1.63 (s, 3 H), 1.07 (m, 30 H). ^{13}C (100 MHz): δ 152.9, 137.0, 135.6, 133.8, 131.2, 129.6, 127.6, 120.1, 110.0, 99.3, 68.9, 65.7, 35.7, 26.9, 19.3, 17.6, 13.7, 12.3. HRMS $(ESI)^+$ calcd for $C_{35}H_{53}O_4Si_2$ $(M+H^+)^+$ 593.3482, found 593.3487.

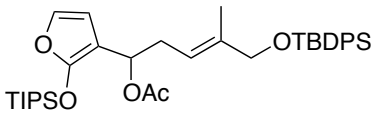

Acetylated siloxyfuran (4.17). To a solution of siloxyfuran **4.16** (55.0 mg, 0.093 mmol) in CH_2Cl_2 (0.18 mL) at 0 °C was added N*i*Pr_2Et (28.2 mg, 0.279 mmol) and DMAP (1.1 mg, 0.009 mmol) followed by acetic anhydride (11.4 mg, 0.112 mmol). After 1 hr the solution was diluted with Et_2O (5 mL) and H_2O (5 mL). The layers were separated, and the aqueous phase extracted with Et_2O (5 mL). The combined organic extracts were dried, filtered, and concentrated *in vacuo*. The crude material was purified by flash chromatography (3% EtOAc/hexanes) to give 42.2 mg (72%) of **4.17** as an off-white oil.

R_f 0.20, 3% EtOAc/Hexanes. ^{1}H NMR (600 MHz): δ 7.65 (m, 4 H), 7.38 (m, 6 H), 6.74 (d, 1 H, J = 2.2 Hz), 6.30 (d, 1 H, J = 2.2 Hz), 5.72 (t, 1 H, J = 7.1 Hz), 5.43 (m, 1 H), 4.00 (s, 2 H), 2.67 (m, 1 H), 2.52 (m, 1 H), 1.98 (s, 3 H), 1.60 (s, 3 H), 1.08 (m, 20 H), 1.03 (s, 10 H). HRMS $(ESI)^+$ calcd for $C_{37}H_{55}O_5Si_2$ $(M+H^+)^+$ 635.3588, found 635.3583.

4.6 Appendix

Characterization Data for 4.13, 4.16 and 4.17.

4.13

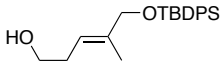

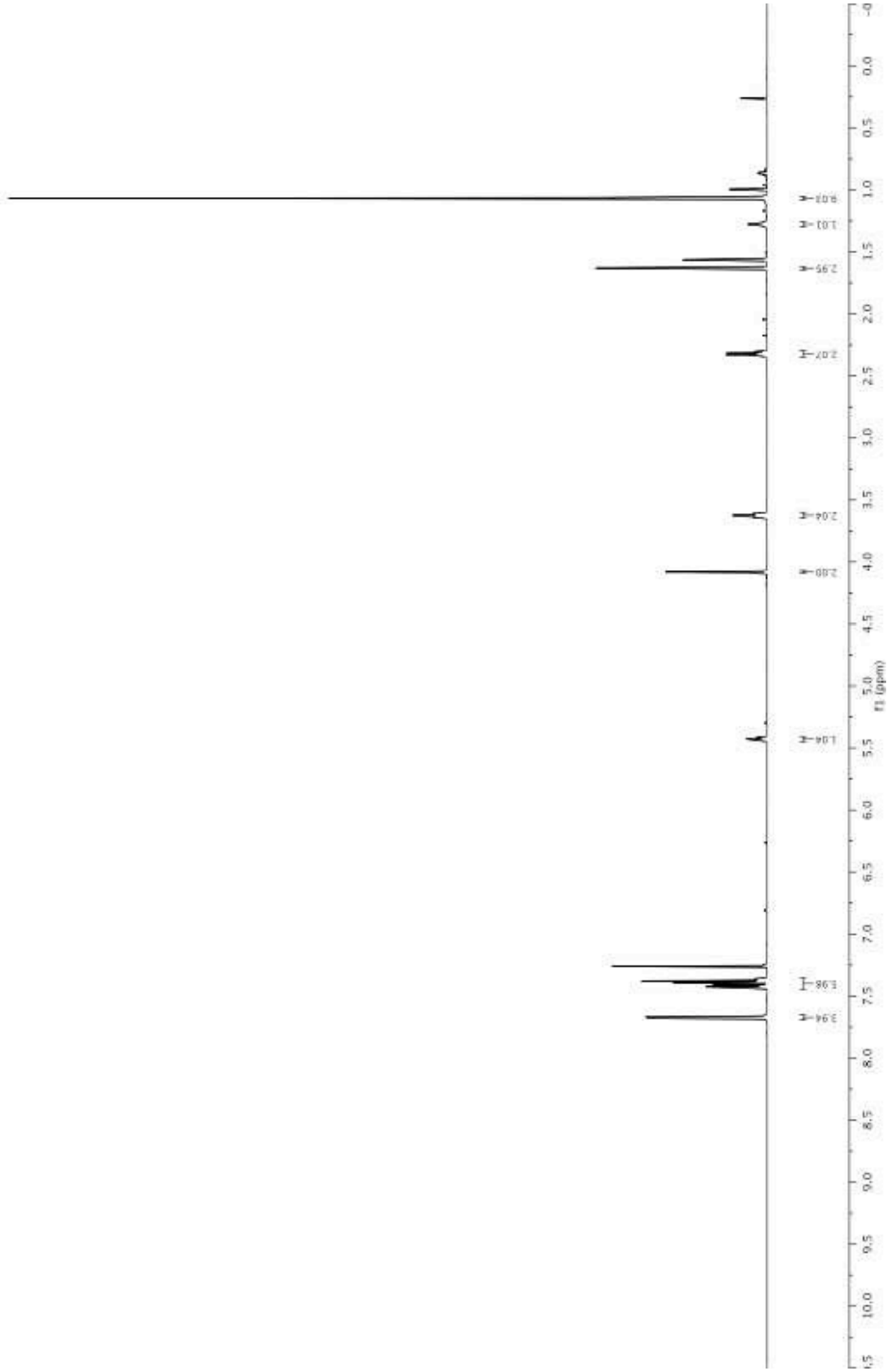

4.16

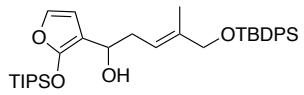
O
OTBDPS
TIPSO
OH

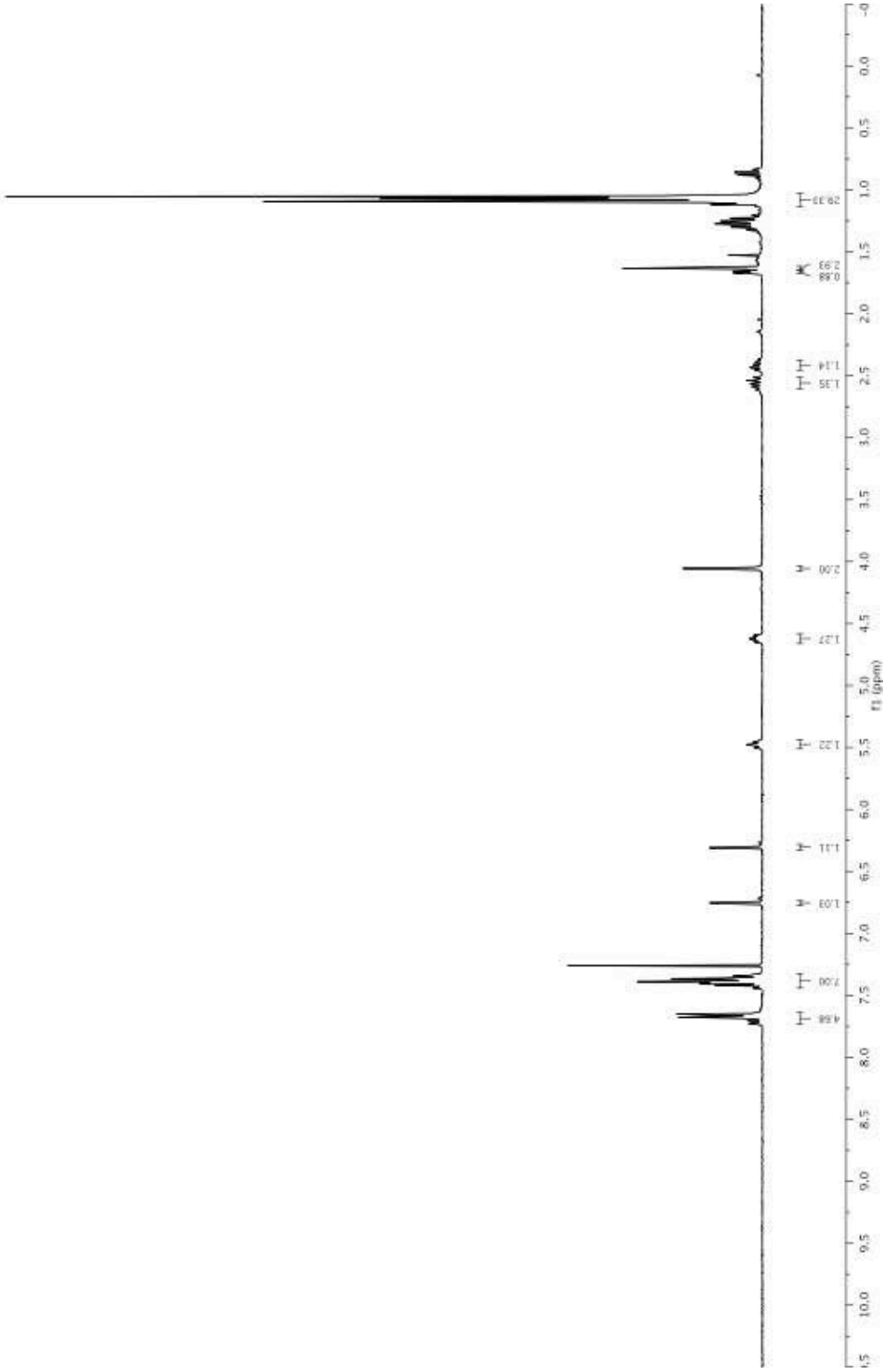
29.33
0.88
2.93
1.14
1.35
2.00
1.27
1.22
1.11
1.03
2.00
4.58
f1 (ppm)

4.17

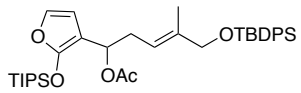

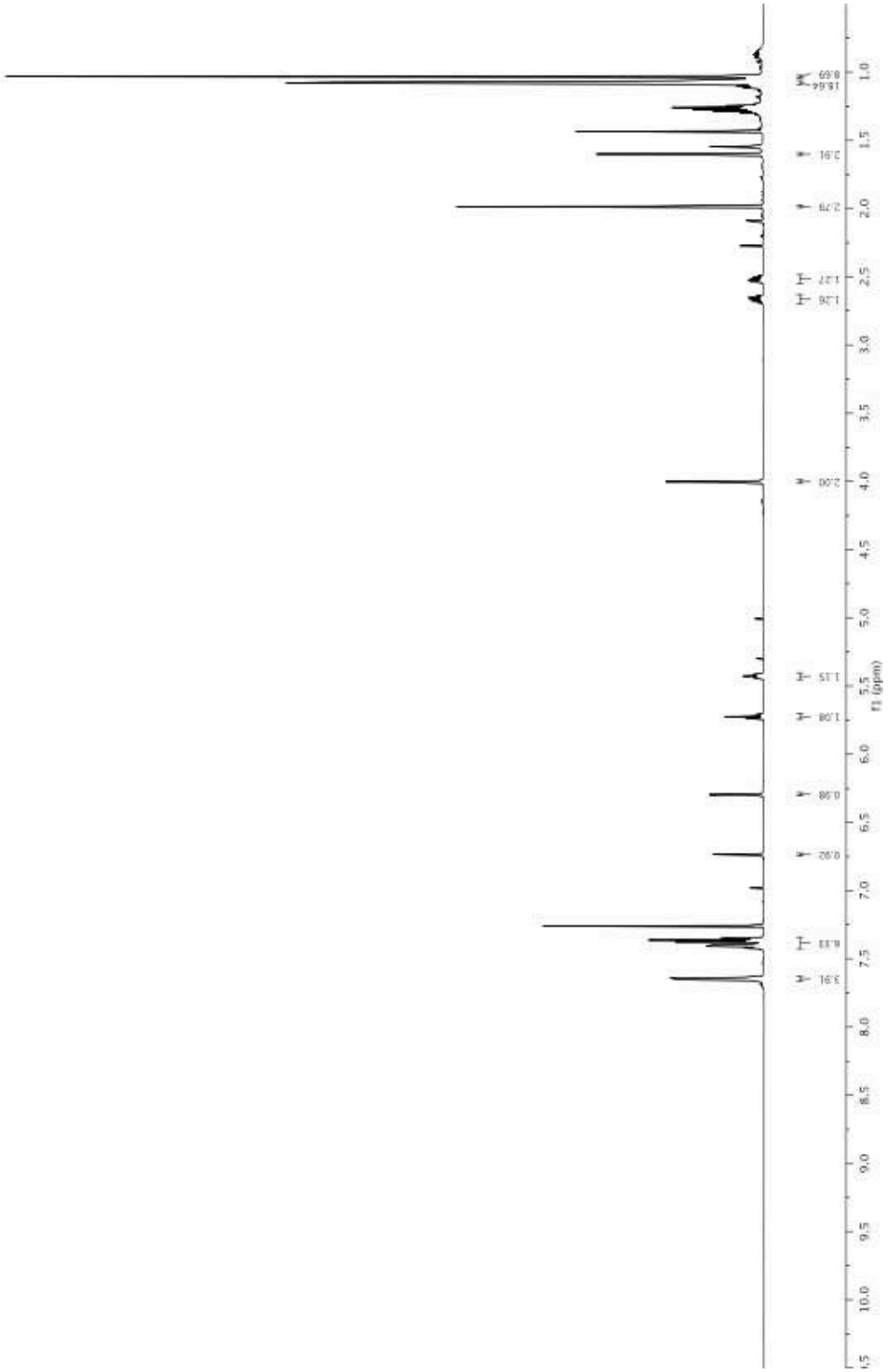

4.7 References and Notes

1. (a) C. W. Jefford, A. W. Sledeski, J. Rossier and J. Boukouvalas, *Tetrahedron Lett.*, 1990, **31**, 5741. (b) Q. Huang and V. H. Rawal, *Org. Lett.*, 2006, **8**, 543.
2. J. Boukouvalas and O. Marion, *Synlett*, 2006, **2006**, 1511.
3. S. Marumoto, H. Kogen and S. Naruto, *Tetrahedron*, 1999, **55**, 7145.
4. G. Andresen, A. B. Eriksen, B. Dalhus, L. Gundersen and F. Rise, *J. Chem. Soc., Perkin Trans. 1*, 2001, **2001**, 1662.
5. F. Liu and E. Negishi, *J. Org. Chem.*, 1997, **62**, 8591.
6. T. Gaich, H. Weinstabl and J. Mulzer, *Synlett*, 2009, **2009**, 1357.